

# The Bioaccumulation of Ionizable Organic Compounds in Fish Cell Lines

Présentée le 20 octobre 2023

Faculté de l'environnement naturel, architectural et construit  
Laboratoire de toxicologie de l'environnement  
Programme doctoral en génie civil et environnement

pour l'obtention du grade de Docteur ès Sciences

par

**Fabian Gerhard Peter BALK**

Acceptée sur proposition du jury

Prof. A. Meibom, président du jury  
Prof. K. Schirmer, Prof. J. Hollender, directrices de thèse  
Prof. C. Schlechtriem, rapporteur  
Prof. M. McLachlan, rapporteur  
Prof. R. Eggen, rapporteur



## Acknowledgements

First, I would like to thank my supervisors, Kristin Schirmer and Juliane Hollender for giving me the opportunity to work on this exciting project and their generous support throughout my journey. Their knowledge and advice was invaluable and I would not be where I am today without it. In this respect, I also want to thank Julita Stadnicka-Michalak, who greatly supported this work in its initial phase with her knowledgeable advice and expertise.

Further, I thank my thesis committee, Prof. Anders Meibom, Prof. Rik Eggen, Prof. Christian Schlechtriem and Prof. Michael McLachlan for their review of my thesis and feedback.

This work would not have been successful without the indispensable support by the people in the laboratory. René and Severin, your help with sample preparation of hundreds and hundreds of samples for chemical analysis and the concurrent entertainment and company was much appreciated. Melanie, your help with cell culture and cytotoxicity assays were of extreme value to me and I thank you for it. Bastian, your dedication to the experimental work was admirable and with your help the overall progress in my thesis would not have been nearly as fast. I also want to explicitly thank Philipp Longree, Birgit Beck and Bernadette Vogler for their assistance and advice with the mass spectrometers, I learned a lot from you.

Additionally, I would like to thank the Utox and the Uchem department for being such an excellent bunch of people with whom it was a pleasure to work with. The atmosphere, openness and supportive environment I encountered were outstanding and helped me through the daily challenges of PhD life. Especially, I would like to thank my colleagues and friends Sarah, Jenny, Johannes S., Christoph, Johannes R., Alena, William, Roman, Ann-Sophie, Nicole and Jagannath. No matter what the situation, it was always apt to talk non-sense with you, loved it.

Finally, I want to thank my family for their unwavering belief and support on this journey. And one person I would like to thank in particular. Jenny, your belief in me, unconditional support and love were more than I could have hoped for, thank you.



## Abstract

Bioaccumulation is defined as the enrichment of a compound in an organism relative to the surrounding water or its food, and is an important endpoint in chemical risk assessment. Under laboratory conditions, bioaccumulation is measured as bioconcentration factor (BCF) or biomagnification factor (BMF) in fish, which represents compound exposure via the respiratory (water) and dietary (food) pathway, respectively. Such tests are resource intense, costly and ethically questionable, due to the sacrifice of large numbers of fish. A potential *in vitro* alternative for the bioaccumulation assessment with fish are permanent fish cell lines. Cell tests have the advantage that the cells conserve many important processes for bioaccumulation in fish. Most prominent fish cell lines are the rainbow trout (*Oncorhynchus mykiss*) gill and liver-derived cell lines, RTL-W1 and RTgill-W1, which have successfully been used to predict the BCF of a neutral model compound in fish. However, application of fish cell lines for bioconcentration predictions has not yet been assessed for ionizable organic compounds (IOC). IOC are frequently detected in natural water bodies and aquatic organisms, yet, their assessment for environmental hazard assessment is not well covered in international regulation to date. Motivated to fill this knowledge gap, this thesis set out to assess the bioconcentration potential of IOC in RTL-W1 and RTgill-W1 cells, and predict IOC bioconcentration in fish. For this purpose, three cationic IOC and four anionic IOC, which are ionized at biologically relevant pH, were selected.

Firstly, a method was developed which enabled the derivation of full mass balances of the tested IOC in the experimental set up with fish cell cultures. Bioconcentration assays were then conducted with non-toxic exposure concentrations, which were previously determined in acute cytotoxicity assays with RTgill-W1 cells. From measured compound concentrations in the medium and cells, *in vitro* BCF were determined and compared to *in vivo* BCF and BMF. In combination with *in vitro* biotransformation assays and partition coefficients to biological matrices, the derived *in vitro* BCF may serve as a line of evidence for conservative estimates of the bioconcentration potential of IOC in fish. This highlights the potential of this method as a future screening tool for environmental risk assessment. The pH-dependent octanol-water partitioning and membrane lipid-water partitioning best predicted the measured *in vitro* BCF for anionic and cationic IOC, respectively.

The experimental mass balances and *in vitro* BCF were compared to different model approaches, to gain insights into the relevant cellular accumulation mechanisms and to

evaluate the applicability of a novel screening approach that uses the human volume of distribution,  $V_D$  and the blood water partition coefficient,  $K_{BW}$ . The model outcomes were that the test compounds' affinity to membrane lipid and protein are most influential for compound accumulation. The prediction of bioconcentration in fish and cells using human  $V_D$  and  $K_{BW}$  showed to be a promising read across to screen the bioconcentration potential of IOC in fish, where availability of reliable  $K_{BW}$  remains the main challenge.

This thesis highlights key areas to aid in the efforts towards the replacement of animal experimentation in bioaccumulation assessments of organic compounds. Additionally, it emphasizes the value of *in vitro* assays for environmental risk assessment.

### **Keywords**

RTL-W1, RTgill-W1, permanent fish cell lines, bioconcentration, biotransformation, ionizable organic compounds, HPLC HRMS/MS, *in vitro* mass balance modelling, phase partitioning

## Zusammenfassung

Bioakkumulation beschreibt die Anreicherung eines Stoffes in einem Organismus im Verhältnis zum umgebenden Wasser oder seiner Nahrung und ist ein wichtiger Endpunkt in der Umweltrisikobewertung. Unter Laborbedingungen wird die Bioakkumulation in Form des Biokonzentrationsfaktors (BCF) oder des Biomagnifikationsfaktors (BMF) in Fischen gemessen, welche die Anreicherung eines Stoffes über die Atemwege (BCF) bzw. die Nahrung (BMF) darstellen. Solche Tests sind materialaufwendig, kostspielig und ethisch fragwürdig, da eine große Anzahl von Fischen geopfert werden muss. Eine mögliche *in vitro* Alternative für die Bewertung der Bioakkumulation in Fischen sind permanente Fischzelllinien. Zelltests haben den Vorteil, dass in den Zellen viele wichtige Prozesse für die Bioakkumulation erhalten bleiben. Die bekanntesten Fischzelllinien sind die von der Regenbogenforelle (*Oncorhynchus mykiss*) stammenden Kiemen- und Leberzelllinien RTL-W1 und RTgill-W1, die erfolgreich zur Vorhersage des BCF eines neutralen Stoffes in Fischen verwendet wurden. Die Anwendung von Fischzelllinien für Biokonzentrationsvorhersagen wurde jedoch noch nicht für ionisierbare Stoffe (IS) bewertet. IS werden häufig in natürlichen Gewässern und aquatischen Organismen nachgewiesen, doch ihre Umweltrisikobewertung ist bisher in internationalen Vorschriften nicht ausreichend berücksichtigt. Um diese Wissenslücke zu schließen, wurde in dieser Arbeit das Biokonzentrationspotenzial von IS in RTL-W1- und RTgill-W1-Zellen untersucht und die Biokonzentration von IS in Fischen vorhergesagt. Zu diesem Zweck wurden drei kationische IS und vier anionische IS ausgewählt, welche bei biologisch relevanten pH-Werten geladen vorliegen.

Zunächst wurde eine Methode entwickelt, die die Ableitung von Massenbilanzen der getesteten IS im Versuchsaufbau mit Fischzellkulturen ermöglichte. Anschließend wurden Biokonzentrationsversuche mit nicht-toxischen Expositionskonzentrationen durchgeführt, die zuvor in akuten Zytotoxizitätstests mit RTgill-W1-Zellen bestimmt wurden. Aus den gemessenen Konzentrationen im Medium und den Zellen wurden die *in vitro* BCF bestimmt und mit den *in vivo* BCF und BMF verglichen. Daraus konnte geschlossen werden, dass die *in vitro* BCF als ein Endpunkt für die konservative Abschätzung der Bioakkumulation von IS in Fischen genutzt werden können, vor allem in Kombination mit *in vitro* Biotransformationstests und Verteilungskoeffizienten zu biologischen Matrices. Der pH-abhängige Octanol-Wasser- und Membranlipid-Wasser-Verteilungskoeffizient sagten die gemessenen *in vitro* BCF für anionische bzw. kationische IS am besten voraus.

Die Massenbilanzen und *in vitro* BCF wurden mit verschiedenen Modellansätzen verglichen, um Einblicke in die relevanten zellulären Akkumulationsmechanismen zu gewinnen und die Anwendbarkeit eines neuartigen Screening-Ansatzes zu bewerten, der das menschliche Verteilungsvolumen ( $V_D$ ) und Blut-Wasser Verteilungskoeffizienten,  $K_{BW}$ , in Fisch verwendet. Die Modellergebnisse führten zu dem Ergebnis, dass die Affinität der getesteten IS zu Membranlipiden und -proteinen den größten Einfluss auf die Akkumulation der Stoffe hat. Die Vorhersage der Biokonzentration in Fischen und Zellen unter Verwendung des menschlichen  $V_D$  und des  $K_{BW}$  von Fischen erwies sich als vielversprechender Ansatz für das Screening des Biokonzentrationspotenzials von IS in Fischen, wobei die Verfügbarkeit von akkuraten  $K_{BW}$  die grösste Herausforderung stellt.

Diese Arbeit weist Schlüsselbereiche der Forschung aus, welche die Bemühungen um den Ersatz von Tierexperimenten in der Bioakkumulationsforschung weiter vorantreibt. Darüber hinaus unterstreicht sie den Wert von *in vitro* Tests für die Umweltrisikobewertung.

### **Schlüsselwörter**

RTL-W1, RTgill-W1, permanente Fischzelllinien, Biokonzentration, Biotransformation, ionisierbare Stoffe, HPLC HRMS/MS, *in vitro* Massenbilanzmodellierung, Partitionierung



## Table of Content

Abstract.....	iv
Zusammenfassung.....	vi
List of Figures.....	xi
List of Tables.....	xiii
1. Introduction .....	1
1.1. Bioaccumulation in the environment .....	1
1.2. Bioaccumulation in chemical hazard assessment .....	2
1.3. <i>In silico</i> methods to predict bioconcentration in fish .....	3
1.4. <i>In vitro</i> methods to support bioconcentration predictions.....	4
1.5. Permanent fish cell lines as alternative to animal experimentation.....	5
1.6. Ionizable organic compounds .....	6
1.7. Bioaccumulation of ionizable organic compounds.....	7
1.8. Ionizable organic compounds in cell culture test systems .....	9
1.9. Research objectives .....	11
2. Investigating the bioaccumulation potential of anionic organic compounds using a permanent rainbow trout liver cell line .....	14
2.1. Abstract .....	15
2.2. Introduction.....	15
2.3. Methods.....	18
2.3.1. Test Compound Selection.....	18
2.3.2. Preparation of stock solutions of test compounds .....	19
2.3.3. Cell culture.....	20
2.3.4. Determination of non-toxic exposure concentrations.....	21
2.3.5. Experimental procedure for bioaccumulation assessment .....	22
2.3.6. Cell seeding and exposure start.....	22
2.3.7. Bioaccumulation experiments .....	22
2.3.8. Derivation of <i>in vitro</i> -based bioconcentration factors .....	24
2.3.9. Chemical analysis.....	25
2.3.10. Data analysis and visualization .....	26
2.4. Results and Discussion.....	26
2.4.1. General observations.....	26
2.4.2. Impact of chemicals on cell viability .....	26
2.4.3. Bioaccumulation experiments .....	29

2.4.3.1.	Mass balances and biotransformation activity .....	29
2.4.3.2.	Prediction of cell internal concentrations .....	32
2.4.4.	Comparison of <i>in vitro</i> and <i>in vivo</i> bioaccumulation.....	34
2.5.	Conclusions and outlook.....	36
2.6.	Acknowledgements.....	37
3.	Bioaccumulation of cationic surfactants in permanent fish cell lines .....	38
3.1.	Abstract .....	39
3.2.	Introduction.....	39
3.3.	Methods.....	41
3.3.1.	Test compound selection .....	41
3.3.2.	Routine cell culture .....	42
3.3.3.	Determination of non-toxic exposure concentrations.....	42
3.3.4.	Cell densities and seeding of RTgill-W1 and RTL-W1 for bioaccumulation experiments .....	43
3.3.5.	Bioaccumulation experiments .....	43
3.3.6.	Bioaccumulation experiments with re-equilibration.....	44
3.3.7.	Mass balances and <i>in vitro</i> bioconcentration factors .....	44
3.3.8.	Chemical analysis.....	45
3.3.9.	Data analysis .....	46
3.4.	Results and Discussion.....	46
3.4.1.	Cytotoxicity elicited by test compounds.....	46
3.4.2.	Bioaccumulation experiments .....	47
3.4.3.	Biotransformation activity in bioaccumulation experiments .....	50
3.4.4.	Comparison to <i>in vivo</i> BCF and $D_{MLW}$ -predicted BCF .....	51
3.5.	Outlook .....	54
3.6.	Acknowledgements.....	54
4.	Model comparison to refine bioconcentration prediction of ionizable organic compounds. ....	55
4.1.	Abstract .....	56
4.2.	Introduction.....	56
4.3.	Methods.....	60
4.3.1.	Dataset of <i>in vitro</i> BCF.....	60
4.3.2.	Literature search for $V_D$ comparison .....	62
4.3.3.	Principal model considerations .....	62
4.3.4.	Simple partitioning-based models .....	63

4.3.5.	Kinetic cell model.....	64
4.3.6.	<i>In vitro</i> mass balance model .....	66
4.3.7.	Sensitivity analysis.....	67
4.3.8.	Data analysis .....	67
4.4.	Results and Discussion.....	67
4.4.1.	$V_D$ comparison .....	67
4.4.2.	BCF prediction by the kinetic cell model .....	70
4.4.3.	Predictions by the <i>in vitro</i> mass balance model IV MBM EQP.....	73
4.5.	Concluding remarks.....	75
4.6.	Acknowledgements.....	76
5.	Conclusions and Outlook.....	77
5.1.	Extension and optimization of the bioconcentration assay with RTL-W1 and RTgill-W1 cells.....	77
5.2.	Characterization of RTgill-W1 and RTL-W1 to understand accumulation mechanisms.....	79
5.3.	Improvements for <i>in silico</i> prediction of bioconcentration .....	81
5.4.	RTL-W1 and RTgill-W1 as predictors for bioconcentration in fish? .....	83
	Supporting Information Chapter 2.....	86
	Supporting Information Chapter 3.....	123
	Supporting Information Chapter 4.....	147
	Bibliography .....	163
	Glossary .....	182
	Curriculum Vitae.....	185

## List of Figures

Figure 1.1: Most common ionizable chemical groups in IOC. ....	7
Figure 1.2: Principal partitioning processes relevant to IOC bioaccumulation. ....	8
Figure 1.3: Compound distribution and loss processes in a cell-based <i>in vitro</i> assay. ....	10
Figure 1.4: Graphical abstract for Chapter 2. ....	12
Figure 1.5: Graphical abstract for Chapter 3. ....	12
Figure 1.6: Graphical abstract for Chapter 4. ....	13
Figure 2.1: Work flow from exposure concentration determination to bioaccumulation experiments. ....	23
Figure 2.2: Acute cytotoxicity of the test compounds to RTgill-W1 cell cultures over 48h exposure. ....	27
Figure 2.3: Distribution of the compounds in the test system during bioaccumulation experiments. ....	30
Figure 2.4: Comparison of observed and partition coefficient-based accumulation in RTL-W1 cells. ....	32
Figure 2.5: Comparison of different prediction methods for bioaccumulation in fish. ....	35
Figure 3.1: Mass balances of test compounds in exposed RTL-W1 and RTgill-W1 cells exposed over 48 h/72 h. ....	49
Figure 3.2: Comparison of <i>in vitro</i> BCFs with DMLW-based predictions and <i>in vivo</i> BCFs. ..	53
Figure 4.1: Comparison of measured human and fish $V_D$ ( $L\ kg^{-1}$ ). ....	69
Figure 4.2: $V_D$ predicted BCF relative to observed <i>in vivo</i> and <i>in vitro</i> BCF. ....	70
Figure 4.3: Comparison of kinetic cell model predictions ( $BCF_{cell\ model}$ ) and observed <i>in vivo</i> and <i>in vitro</i> BCF. ....	73
Figure 4.4: Comparison of mass balance model predicted BCF and observed <i>in vivo</i> and <i>in vitro</i> BCF. ....	75
Figure S2.1: pH influence on the degree of ionization of the test compounds. ....	86
Figure S2.2: Acute cytotoxicity of the final exposure concentrations after 72 h exposure in RTL-W1. ....	89
Figure S2.3: Varied RTL-W1 cell densities in cell culture flasks at seeding and over 48 h experimental duration. ....	91
Figure S2.4: Cell numbers in bioaccumulation experiments. ....	92

Figure S2.5: Test compound in cell samples of exposed cells and the cell-free control in the 24 well plate format after 48 h. ....	98
Figure S2.6: Bioaccumulation experiments with DCF at different exposure concentrations. ....	116
Figure S2.7: pH changes in the bioaccumulation experiments at 0, 24 and 48 hours. ....	117
Figure S3.1: Absorption experiment of test compounds to glass or plastic vials in varying water-methanol mixtures. ....	128
Figure S3.2: Cell numbers of RTgill-W1 in two tested densities over 48 h. ....	129
Figure S3.3: Percent cell viability relative to unexposed control as measured by alamarBlue™, CFDA-AM and Neutral Red upon 24 h exposure of the test compounds to RTgill-W1. ....	130
Figure S3.4: Impact on cell viability of the exposure concentrations used in bioaccumulation assessments after 72 h. ....	133
Figure S3.5: pH measurements of exposed cells and controls over the experimental duration. ....	135
Figure S3.6: Comparison of <i>in vitro</i> BCF with $K_{OW}$ - and $D_{OW}$ -based BCF predictions in the cells.....	143
Figure S3.7: Detection of demethylated T10 in medium samples. ....	145
Figure S3.8: Detection of demethylated T10 in cell samples.....	146
Figure S3.9: Detection of demethylated T10 in plastic samples. ....	146
Figure S4.1: Comparison of predicted BCF and observed <i>in vivo</i> and <i>in vitro</i> BCF using predicted $D_{MLW}$ and $D_{PW}$ .....	151
Figure S4.2: Comparison of predicted BCF and observed <i>in vivo</i> and <i>in vitro</i> BCF using predicted $D_{MLW}$ , while protein sorption was excluded. ....	152
Figure S4.3: Sensitivity of input parameters of the kinetic cell model. ....	153
Figure S4.4: Sensitivity of input parameters of the IV MBM EQP model to predict compound accumulations in the cells.....	154
Figure S4.5: Input system parameters. ....	158

## List of Tables

Table 2.1: Overview of test compounds with usage and key physico-chemical properties....	20
Table 2.2: Results of acute cytotoxicity assay with RTgill-W1 cells.....	28
Table 3.1: Relevant structural and physico-chemical properties of the test compounds.....	42
Table 3.2: EC <sub>50</sub> values of acute cytotoxicity assays performed with RTgill-W1 cells. ....	47
Table 4.1: Test compounds with available <i>in vitro</i> BCF from experiments with RTL-W1 cells. .....	61
Table 4.2: Partition coefficients used in the model predictions.....	65
Table S2.1: Supplementary information on test compounds and internal standards. ....	86
Table S2.2: Nominal and measured exposure concentrations of the test compounds in acute cytotoxicity assays with RTgill-W1 along with resulting cell viability values for alamarBlue (AB).....	87
Table S2.3: Measured exposure concentrations of acute cytotoxicity assay with RTL-W1 cells.....	88
Table S2.4: Fractions of quantifiable cell samples in the well plate and cell culture flask format.....	90
Table S2. 5: Absolute amount of test compound in bioaccumulation experiments with treated RTL-W1 cells.....	92
Table S2.6: Absolute amount of test compound in bioaccumulation experiments with cell-free control. ....	95
Table S2. 7: Absolute test compound amounts in cell samples after 48 h.....	98
Table S2.8: Derived RTL-W1 BCF per replicate and chemical based on intracellular and exposure medium concentration.....	99
Table S2.9: Bioaccumulation studies of the test compounds in rainbow trout. ....	100
Table S2.10: Collision energies of test compounds and formed fragment ions. ....	101
Table S2.11: Analytical performance of sample measurements from bioaccumulation experiments.....	102
Table S2.12: Relative and absolute Recoveries of the test compounds in the bioaccumulation experiments.....	103
Table S2.13: Reference LC <sub>50</sub> values of Pentachlorophenol taken from Fischer et al. 2019.	104
Table S2.14: Symbol Explanation for Equation S2.2 and S2.3. ....	113
Table S2.15: Time to steady state in RTL-W1 cells. ....	114

Table S2.16: Mass balances in bioaccumulation experiments with exposed cells and cell-free control. ....	115
Table S2.17: Settings in Compound Discoverer for biotransformation product screening. ...	118
Table S2.18: Linear regression analysis according to OECD TG319A for detection of biotransformation activity. ....	118
Table S2.19: Input data for partition exercise. ....	121
Table S2.20: Calculated log BCF based on the test compound's $K_{OW}$ , $D_{OW}$ and $D_{MLW}$ . ....	121
Table S2.21: Reference BCF values of Pentachlorophenol (PCP) in different fish species.	122
Table S3.1: Detail on the test compounds and their respective internal standards (CDN isotopes). ....	123
Table S3.2: Test compound's m/z and collision energies. ....	126
Table S3.3: Compound Discoverer settings for peak detection of suspected biotransformation products. ....	127
Table S3.4: Limit of quantification of test compounds and comparison of intended vs. measured exposure concentration in bioaccumulation experiments. ....	127
Table S3.5: Matrix specific relative recoveries of the test compounds. ....	128
Table S3.6: Cell numbers per test compound and cell line. ....	129
Table S3.7: Nominal and measured exposure concentrations of the acute cytotoxicity assays. ....	131
Table S3.8: Percent cell viability and corresponding nominal exposure concentrations of the acute cytotoxicity assays after 24 h exposure. ....	132
Table S3.9: Measured concentrations ( $C_{0h}$ and $C_{72h}$ ) of the cytotoxicity assay with final exposure concentrations for bioaccumulation experiments. ....	134
Table S3.10: Mass balances of RTgill-W1 and RTL-W1 cells and cell-free controls exposed to S12 in bioaccumulation experiments. ....	136
Table S3.11: Mass balances of RTgill-W1 and RTL-W1 cells and cell-free controls exposed to T10 in bioaccumulation experiments. ....	138
Table S3.12: Mass balances of RTgill-W1 cells and cell-free controls exposed to Q14 in one bioaccumulation experiment. ....	140
Table S3.13: Mass balances of RTL-W1 cells and cell-free controls exposed to Q14 in bioaccumulation experiments containing a re-equilibration phase. ....	141
Table S3.14: Predicted and measured BCFs of the test compounds. ....	142

Table S3.15: Analysis for biotransformation activity of the experiments with S12 following OECD TG criteria in RTL-W1 (top) and RTgill-W1 (bottom) cell lines. ....	143
Table S3.16: Analysis for biotransformation activity of the experiments with T10 following OECD TG criteria in RTL-W1 (top) and RTgill-W1 (bottom) cell lines. ....	144
Table S3.17: Analysis for biotransformation activity of the experiments with Q14 following OECD TG criteria in RTL-W1 (top) cell lines.....	144
Table S4.1: Substance descriptors of the neutral test compounds. ....	147
Table S4.2: $V_D$ derivation from literature. ....	148
Table S4.3: Weight-based tissue composition in rainbow trout and catfish. ....	150
Table S4.4: Variations in $BCF_{cell\ model}$ dependent on the volume fraction of phospholipid in cells.....	150
Table S4.5: Comparison of measured and predicted mass distribution at steady state.....	155
Table S4.6: Comparison of predicted BCF using the <i>in vitro</i> mass distribution model IV MDM EQP and measured BCF.....	156
Table S4.7: Input chemical data. ....	157
Table S4.8: Input well plate characteristics.....	158
Table S4.9: Calculation ionic strength in L15 medium. ....	159
Table S4.10: Model output of mass fractions in the test system. ....	161
Table S4.11: Model output of concentrations in the test system. ....	162



---

## 1. Introduction

The present thesis focuses on 2D *in vitro* cell models and their applicability to support bioconcentration predictions in fish. It provides insight into the processes that govern accumulation in the *in vitro* models and discusses the potential to predict bioconcentration in fish using cell cultures. This research complements the application portfolio of *in vitro* models for chemical hazard assessment. In addition, it explores computational model approaches and evaluates read across methods to support bioaccumulation assessments.

This introductory chapter provides the background on which the thesis research builds. It first concentrates on the phenomenon of bioaccumulation, the role of bioaccumulation in current chemical hazard assessment schemes and the resources it takes to follow these schemes using traditional animal tests. It then sheds light on computational and *in vitro* methods to predict bioconcentration, i.e. the uptake of chemicals from the water phase, without the need for animal experimentation, focusing on fish. Finally, mechanisms are explained that are thought to govern the bioconcentration of ionizable organic compounds, which are the specific focus in this thesis research.

### 1.1. Bioaccumulation in the environment

Bioaccumulation describes the enrichment of any substance in a living organism. For example, organisms accumulate nutrients from their food to maintain their body integrity. Substances which are of no use to the organism are usually excreted from the body. However, especially for human-made substances, many organisms have no mechanisms in place to preempt an enrichment of this substance in their bodies. The enrichment may occur because the organism cannot actively prevent the substance's uptake and/or effectively eliminate it from its body <sup>1</sup>. This is where bioaccumulation may pose a threat to the organism's well-being.

Human ingenuity brought enormous technological advancement and concurrent improvement of human life. Along with this development, humans synthesized a rapidly increasing number of chemical compounds for different applications. To date, about 204 million chemical compounds are known <sup>2</sup> of which 40 000 to 60 000 compounds are in commerce <sup>3</sup>. However, along with the production, use and disposal of chemical compounds, many of them are

released to the environment, where they can have unintended effects on exposed organisms, whole populations or even ecosystems <sup>4</sup>.

After the Second World War, it was discovered that neutral organic compounds, in this case Dichlorodiphenyltrichloroethane (DDT), can enrich in organisms via the food web and lead to sharp population declines of raptors <sup>5</sup>: DDT concentration in organisms increased along the food chain from phytoplankton up to raptors. Apex predators were mainly exposed to DDT via their prey and showed highest DDT concentrations in their body tissue compared to organisms in lower trophic levels <sup>5</sup>. This discovery and many more studies formed the basic understanding that neutral hydrophobic compounds tend to accumulate in organisms, where they enrich in the lipid rich tissues. In line with this understanding, current international legislation regulates the prevention of bioaccumulation of potentially harmful substances as outlined in the following chapter.

## **1.2. Bioaccumulation in chemical hazard assessment**

The bioaccumulation potential of an organic compound is a central piece of information in international legislation <sup>6</sup>. In the European Union, regulation of industrial chemicals for their safe use and the protection of human and environmental health falls under the Registration, Evaluation, Authorization and Restriction of Chemicals – REACH. Under REACH, a compound needs to undergo bioaccumulation assessment if its production or import equals or exceeds 100 t/year <sup>7</sup>. Currently, the most commonly used organism for bioaccumulation assessment in the aquatic environment is fish, representing an ecologically and economically important organism group.

Bioaccumulation is defined as the enrichment of an organic compound in an organism. It results when the compound uptake via respiratory, dermal and dietary pathways from the environment outcompetes the elimination of the compound from the organism <sup>8</sup>. Under laboratory conditions, bioaccumulation can be measured as either the bioconcentration factor (BCF) or the biomagnification factor (BMF). The BCF results from exclusively aquatic exposure and respiratory and potentially dermal compound uptake. It is calculated as the ratio of the compound concentration in the organism over the compound concentration in the water at steady state. The BMF results from the dietary exposure of an organism and is calculated as the ratio of the compound concentration in the organism over the concentration in the food.

The BCF is commonly measured in standardized experiments, as defined in the OECD Test Guideline (TG) 305<sup>9</sup>, where rainbow trout (*Oncorhynchus mykiss*) are among one of the most frequently used fish species. In such an experiment, fish are exposed to a chemical via the water for several weeks to measure the increase of the chemical in the fish over time. When the assumed maximum concentration in the fish was reached, the remaining animals are transferred to compound-free water and the decrease of the chemical load in the fish is measured. Beside the measured concentrations in fish, the kinetic uptake and elimination rates can be determined from the corresponding experimental phases to calculate a kinetic BCF from the ratio of uptake and elimination rate. On the one hand, such animal experiments have the advantage that all possible exposures and accumulation mechanisms are accounted for. On the other hand, these type of experiments are costly, resource intense and ethically questionable due to the sacrifice of animals. According to OECD TG 305<sup>9</sup>, bioaccumulation assessment of a single compound requires at least 108 fish<sup>10</sup>. Above all, it is unrealistic to test the high number of compounds potentially requiring bioaccumulation assessment in fish exposures<sup>11, 12</sup>. Therefore, less resource-demanding, and ideally animal-free, alternatives to assess bioaccumulation are being sought.

### **1.3. *In silico* methods to predict bioconcentration in fish**

One alternative to animal experimentation are computational models which simulate the bioaccumulation of an organic compound in fish. The complexity of such models varies as well as the approach they take to simulate bioaccumulation. On one end of the spectrum are empirical models, termed linear free-energy relationships and quantitative structure activity relationships<sup>13, 14</sup>. They relate physicochemical properties<sup>13, 14</sup> or molecular structures<sup>13</sup> of a compound to a measured BCF to predict bioaccumulation. Other models attempt to explain observed bioaccumulation by the compounds diffusion through membranes<sup>15</sup> and their affinity for constituents inside the organism, such as storage lipid, membrane lipid or different protein types<sup>16, 17</sup>. On the other end of the spectrum are complex models, termed physiology-based toxicokinetic (PBTk) models. They base the bioaccumulation process on putative mechanisms and physiological processes<sup>11, 18</sup>. In the most complex designs, the fish is compartmentalized into its organs and tissues, which are linked to each other via the blood stream, e.g. by means of differential equations and subsequent compound partitioning into the tissue, using linear free energy relationships. The resulting models can help to understand the fate of an organic compound in the simulated organism and predict endpoints such as the BCF.

The octanol-water partition coefficient,  $K_{OW}$ , of the neutral compound, or the pH-dependent octanol-water partition coefficient,  $D_{OW}$ , ( $pK_a$ -dependent weighting of the partitioning of the neutral and charged compound fraction) have been used as chemical property for BCF prediction<sup>14, 19</sup>. In this context,  $K_{OW}$  and  $D_{OW}$  are used as surrogates to describe the lipid affinity of a compound<sup>19</sup>. The use of  $K_{OW}$  or  $D_{OW}$  assumes that the neutral fraction of the compound is mainly responsible for the bioaccumulation in organisms and that it enriches exclusively in storage lipid-rich tissues. Resulting overestimations of octanol-water partition based predictions can be refined to result in more realistic bioconcentration estimations by the inclusion of *in vitro* measured biotransformation rates (see Chapter 1.4). However, the assumption of octanol-water partition based bioaccumulation ignores that compounds, which are largely charged at environmental and physiological relevant pH (~7-8), may not follow this accumulation pattern and tend to result in erroneous BCF prediction<sup>14, 20, 21</sup>. Consequently, several adaptations were suggested to better address the bioaccumulation of compounds that do not follow the  $K_{OW}$  concept. Such adaptations comprise the inclusion of compound elimination via biotransformation in the organism (as it is done for neutral organic compounds as well)<sup>22</sup>, active uptake and elimination processes<sup>16</sup>(less relevant for neutral compounds) and the partitioning to other tissue constituents than storage lipid<sup>17, 21</sup>. Among these processes, biotransformation is currently considered the most important to account for the differences in predicted versus measured BCF. Biotransformation is defined as the enzymatic conversion of an organic compound in an organism. This process leads to the formation of biotransformation products (BTPs) that are usually eliminated from the fish. As a result, models, which neglect this process, frequently overestimate the BCF<sup>14, 18</sup>. Biotransformation rates of an organic compound in fish can be either estimated, albeit still with considerable uncertainties<sup>22</sup>, or measured by *in vitro* test systems<sup>23, 24</sup>. The *in vitro* measured biotransformation rates are scaled by In vitro-In vivo extrapolation (IVIVE) to whole-body biotransformation rates and incorporated into simple as well as the complex PBTK models to refine BCF predictions<sup>18, 25, 26</sup>.

#### **1.4. *In vitro* methods to support bioconcentration predictions**

Most common *in vitro* methods to support *in silico* BCF prediction are liver S9-fractions<sup>24</sup>, microsomes<sup>27</sup> and primary hepatocytes<sup>28</sup>, all of which are obtained from freshly isolated fish liver tissue. While the S9-fraction and microsomes are obtained by tissue homogenization and centrifugation<sup>27, 28</sup>, the primary hepatocytes are obtained by dispersion of a liver sample and

may be used directly or after cryopreservation. Liver S9-fractions and cryopreserved hepatocytes were evaluated for the repeatability and reproducibility of measured biotransformation rate constants in an international ring trial<sup>28</sup>. As a result, two OECD TG have been adopted<sup>23, 24</sup>. However, these test systems still rely on the sacrifice of animals and batch-to-batch variations may hamper reproducibility. In addition, liver S9-fractions and microsomes lack cellular structures, such as cell membranes, and instead comprise only a mixture of active biotransforming enzymes.

### 1.5. Permanent fish cell lines as alternative to animal experimentation

Permanent fish cell lines are alternative biological models that help to overcome the outlined deficits of other *in vitro* methods, since they represent intact cells and are a homogenous resource without the need to sacrifice more fish<sup>29, 30, 31</sup>. Most prominent in the literature are three rainbow trout cell lines, namely the RTL-W1<sup>29</sup>, the RTgill-W1<sup>30</sup> and the RTgutGC<sup>31</sup> cell line. All three cell lines were isolated from healthy rainbow trout tissues representing the liver (RTL-W1), gill (RTgill-W1) and gut (RTgutGC) and have been successfully cultured and cryopreserved over several years<sup>29, 30, 31</sup>. Thanks to continuous research efforts, these cell lines have been tested in many applications and have great potential to inform environmental hazard assessment. The three cell lines express chemical efflux transporters<sup>32</sup> as well as a diverse range of biotransforming enzymes<sup>29, 33, 34, 35</sup> and appear to well biotransform neutral organic compounds<sup>35</sup>. These properties were successfully exploited to measure biotransformation rates of a neutral model compound, benzo[a]pyrene, with the rates being used to predict the fish BCF in combination with a PBTK model<sup>35</sup>. Other applications comprise the transfer of organic compounds, particles and metals across intact RTgutGC epithelia to inform the *in vivo* functionality of the fish intestine<sup>36, 37, 38, 39</sup> or the prediction of acute toxicity in fish<sup>40, 41, 42</sup>. The latter research efforts resulted in the adaption of the OECD TG 249<sup>43</sup>, which derives an *in vitro* effective concentration affecting 50 % of the exposed RTgill-W1 cells (EC<sub>50</sub>) via concentration-response curves. The EC<sub>50</sub> was shown to correlate well with the lethal compound concentration killing 50 % of exposed fish (LC<sub>50</sub>)<sup>40</sup> in an acute exposure scenario and can therefore replace experimentation with fish for LC<sub>50</sub> determination<sup>44</sup>. It is noteworthy that these relationships were mainly established for neutral compounds and that a deliberate focus on charged compounds was lacking<sup>40, 42</sup>. For cell-based assays beyond acute toxicity, it is recommended to establish concentration-response curves of a test compound to ensure appropriate selection of exposure concentrations for non-acute subsequent assays<sup>45</sup>. Despite

these successful applications of rainbow trout cell lines, they were not deliberately tested in the context of bioaccumulation assessment of ionizable organic compounds (IOC), a topic, which gained increasing attention in the last years <sup>46, 47</sup>.

### 1.6. Ionizable organic compounds

IOC can be either permanently charged or undergo pH- and  $pK_a$ -dependent speciation into a neutral and a charged fraction (Figure 1.1) <sup>21</sup>. This implies that IOC can be acids and bases. Zwitterions and amphoteric chemicals, which act as base or acid, are also IOC, but are not considered in the present work. The big group of IOC comprises many compounds of different functionality, such as pesticides, pharmaceuticals, surfactants and additives in personal care products <sup>48</sup>. For example, a sample analysis of 1510 compounds out of ~143,000 preregistered industrial chemicals at the European Chemicals Agency in 2010, estimated that 27 % are acids, 14 % bases, and 8 % zwitterions or amphoteric <sup>48</sup>. Another study examined 907 active pharmaceutical ingredients and found that the majority of them were ionizable (64 %) <sup>49</sup>.

Typically, ionizable structures in IOC are carboxylic acids, phenols, sulfonates and amines, while typical permanently charged structures without an exchangeable hydrogen are quaternary ammonium and phosphonium compounds <sup>21</sup> Figure 1.1. It is noteworthy that in certain compound groups, such as perfluoroalkyl acids, the functional carboxylic acid and sulfonate groups can have very low  $pK_a$  values, which means that the charged species dominate over a wide pH range <sup>21</sup>.

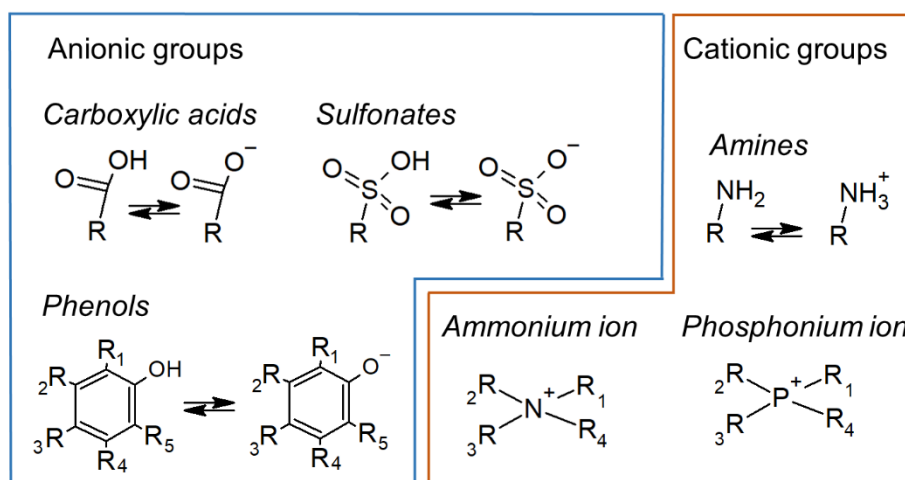


**Figure 1.1: Most common ionizable chemical groups in IOC.** Rx represent any organic structure, which may be associated with the respective functional group. Chemical structures created with Chemschetch 2021.1.2 (ACD/Labs) <sup>50</sup>

### 1.7. Bioaccumulation of ionizable organic compounds

Due to their broad range of applications, IOC are released into the aquatic environment <sup>51, 52, 53</sup>, where they may bioaccumulate in aquatic organisms. As opposed to neutral compounds that mainly bioaccumulate in the lipid fraction of organisms, IOC can have several relevant sorption phases <sup>21, 46</sup> as depicted in (Figure 1.2). While the neutral fraction of an IOC may still sorbs to the neutral lipid fraction, the sorption of the charged fraction to lipids is usually deemed negligible <sup>54</sup>, due to the low octanol affinity of the ionic species <sup>55 56 57</sup>. Instead, the charged IOC fraction may sorb to proteins <sup>58, 59, 60</sup> and cell membranes <sup>57, 61, 62, 63, 64</sup>, as these bear charges themselves.

The sorption to cell membranes is caused by the structure of the building blocks of cell membranes, i.e. the phospholipids. Phospholipids consist of a hydrophobic aliphatic tail and a charged (often zwitterionic) head group, which arranges to a phospholipid bilayer in cell membranes with a hydrophobic core and a negatively charged outer layer. This gives cell membranes a high IOC absorption capacity, especially for compounds that have a similar molecular structure as phospholipids, such as ionic surfactants <sup>63, 64, 65</sup>. Therefore, the pH-dependent membrane lipid-water partitioning coefficient,  $D_{MLW}$ , has been suggested as a screening parameter for the bioaccumulation potential of IOC <sup>65</sup>. Current estimation methods,

experimentally as well as computational, exist and appear to provide reliable  $D_{MLW}$  estimations, which can be used for BCF prediction<sup>63, 66</sup>.

To date, protein sorption is distinguished in sorption to structural protein<sup>60</sup> and serum albumin<sup>59</sup>, where the latter can be a very site-specific interaction<sup>67 68 69 70</sup>. Protein sorption is dependent on the molecular structure and the surrounding pH, which influences protein conformation as well as the degree of ionization of the IOC. In terms of overall sorption capacity, the albumin fraction in organisms is thought to be around 0.4 % while the structural protein fraction is much larger with 11 %<sup>17</sup>. Although the importance of this phase for IOC bioaccumulation has been recognized for certain IOC groups<sup>71</sup>, there are only a small number of methods to estimate the protein partition coefficients of IOC<sup>59, 60</sup>. In addition, such estimation methods do have a limited applicability domain, which may result in considerable uncertainty of estimations for compounds, which are outside this applicability domain<sup>59, 60, 72, 73</sup>.

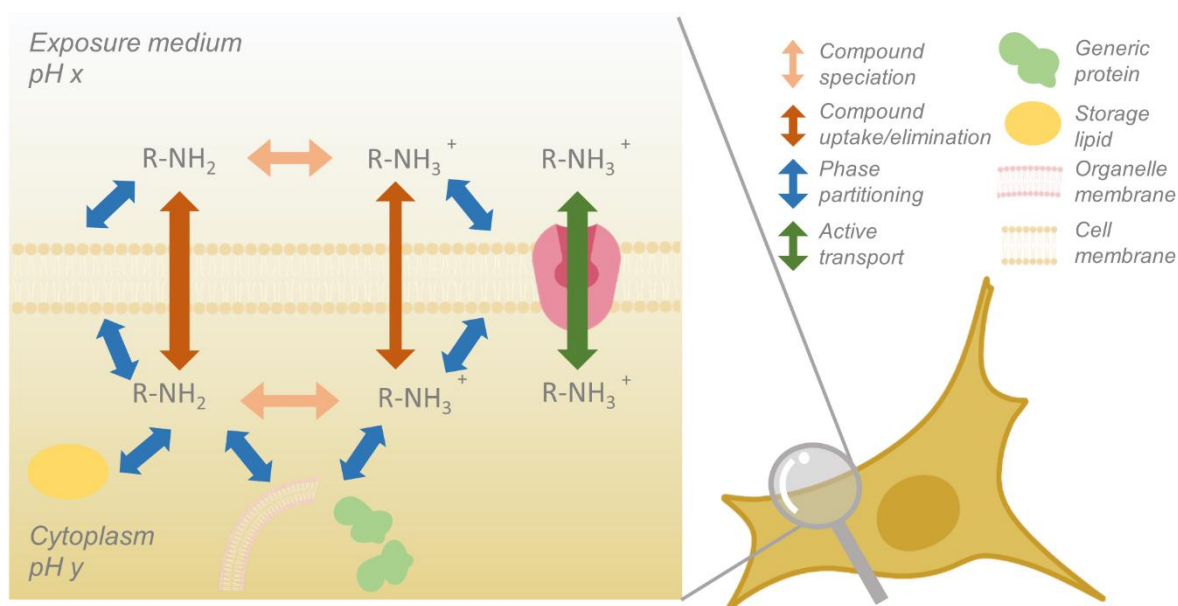


**Figure 1.2: Principal partitioning processes relevant to IOC bioaccumulation.** “R” represents a generic organic compound with a primary amine as an ionizable functional group. pH x and y can be identical or different, which, in combination with the compound’s pKa, determines the speciation of the compound to a neutral and a charged fraction. Those fractions have varying affinities to the diverse phases inside an organism. This figure was partly created with BioRender.com.

The bioaccumulation of IOC is thought to be mainly driven by the passive uptake of the neutral fraction of an IOC at a given pH (Figure 1.2)<sup>26, 46, 74</sup>. Passive uptake and elimination describes the permeation of a compound through a cell membrane driven by the concentration



difference. However, passive uptake and elimination of the charged IOC fraction is considered to be orders of magnitude smaller and therefore negligible<sup>21, 46</sup>. Another way for the charged IOC fraction to cross the cell membrane is the active transport facilitated by cell membrane integrated transporter proteins, which belong to the ATP binding-cassette (ABC) transporter family<sup>75</sup> and the solute carrier family<sup>76 77</sup>. To date, research efforts in fish were mainly focused on ABC transporters<sup>78</sup>, which were shown to exist in the above discussed rainbow trout cell lines<sup>32</sup>. Another pathway that organic compounds may take not depicted in Figure 1.2, is the paracellular pathway<sup>79</sup>. It may become relevant when the above partitioning processes, which can be summarized under the transcellular pathway, is negligibly small for an organic compound<sup>39</sup>.

### 1.8. Ionizable organic compounds in cell culture test systems

Since the neutral and charged species of an IOC have intrinsic affinities for different matrices (see 1.6), the effect concentration applied in a cell-based *in vitro* assay is dependent on the sorption of the compound to plastic, medium constituents or the cells themselves. Another potential loss process is evaporation from the medium<sup>72, 80, 81</sup> (Figure 1.3). This means that an initial exposure concentration may be reduced as a result. Only the resulting freely dissolved aqueous concentration,  $C_{\text{free}}$ , is assumed to be available for cellular uptake and exert an effect on the exposed cells (Figure 1.3). Moreover,  $C_{\text{free}}$  was demonstrated to be more useful for *in vitro* to *in vivo* comparisons of effective concentrations such as the median effect concentration,  $EC_{50}$ <sup>80, 81</sup>.

Proteins present in the exposure medium are assumed to act as reservoir to replenish  $C_{\text{free}}$ , since the sorption to typical protein types in media may be reversible<sup>82 83</sup>. The most common protein supplement for cell culture media is fetal bovine serum, which contains serum albumin as the main protein type<sup>84</sup>. Anionic compounds are expected to interact at specific sites with albumin, while cationic compounds are limited to hydrophobic and nonspecific interactions<sup>68, 69, 85</sup>. In modelling studies, bovine serum albumin served as surrogate of the protein phase in organisms and the partitioning of organic compounds (neutral and IOC) to serum albumin has often been studied<sup>59, 68, 69, 85, 86, 87, 88</sup>.

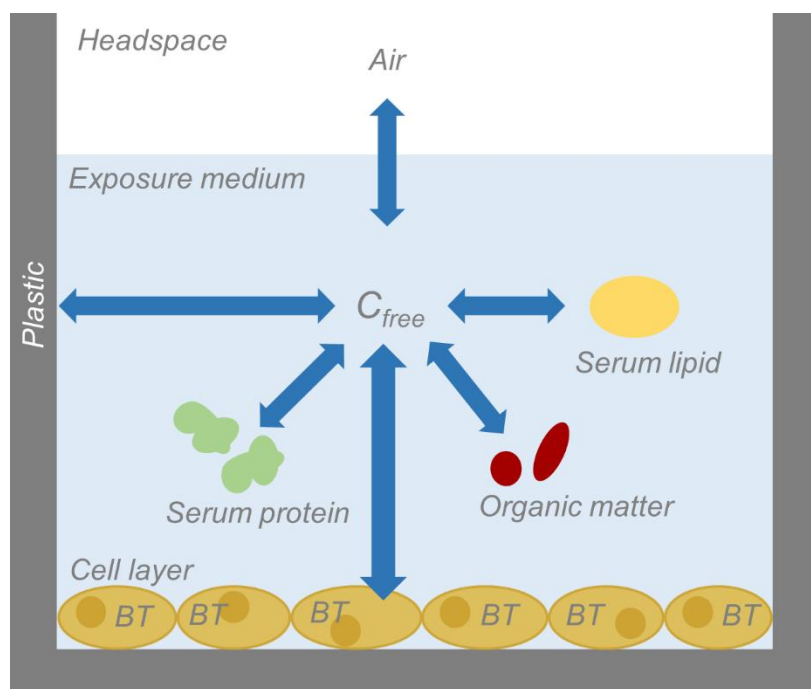


**Figure 1.3: Compound distribution and loss processes in a cell-based *in vitro* assay.** The principal assumption is that only  $C_{free}$  is available for partitioning to the cells. Organic matter represents other proteins than serum protein but also smaller molecules, such as amino acids. For IOC, the described processes of compound distribution pertain to both, the neutral and the charged species. Note that inside the cell biotransformation (BT) of the test compound can occur and influence the mass balance.

There are two principal approaches to determine  $C_{free}$  <sup>72</sup>. One approach experimentally determines  $C_{free}$  using solid-phase microextraction (SPME) fibers, which is assumed to directly correspond to  $C_{free}$  <sup>80</sup>. The other approach applies *in vitro* mass balance models to predict  $C_{free}$  in the exposure medium at chemical equilibrium <sup>72, 89, 90</sup>. For neutral compounds, this approach may give acceptable predictions of  $C_{free}$  <sup>90</sup>, while for IOC greater variations in model performance were found <sup>90</sup>. The main challenge for the model approaches is the limited availability of measured full mass balances from *in vitro* assays for model evaluation as well as uncertainties in the partition coefficient estimations <sup>89, 90</sup>. However, for the purpose of full mass balance derivation of an *in vitro* system and detection of biotransformation activity, the medium concentration should be measured <sup>35, 41</sup>. The medium concentration includes  $C_{free}$  and all bound compound fractions in the medium.

### 1.9. Research objectives

This introductory chapter (Chapter 1) summarizes the current knowledge on the replacement of animal experimentation in bioaccumulation assessments using permanent fish cell lines and the relevant knowledge on IOC bioaccumulation with associated experimental challenges. With my research I aim to complement our understanding of IOC bioaccumulation in permanent fish cell lines and the extrapolation to fish. The following chapters report on the bioaccumulation assessment of IOC in fish using the permanent fish cell lines, RTL-W1 and RTgill-W1. For this purpose, I selected seven IOC, based on availability of high quality *in vivo* data for reference and used them in cell exposure protocols to quantify cellular accumulations. I specifically addressed the following questions:

- Can non-toxic concentrations of the tested IOC in RTgill-W1 and RTL-W1 be determined for bioaccumulation experiments and effective concentrations predict acute toxicity in fish?
- Can cell-based bioconcentration predict the bioconcentration in fish and do differences exist for anionic and cationic IOC?
- Do the exposed cells biotransform IOC and can biotransformation rates be determined for IVIVE?
- Are the accumulation mechanisms in the cell cultures and in fish predictable with simple or/and complex *in silico* approaches?

My thesis research spans from experimental approaches with cell cultures and state-of-the art chemical quantification to the application of *in silico* methods to advance the use of *in vitro* alternatives for bioaccumulation assessment. The results of my research are presented in three chapters, which are briefly summarized in the following. In the last chapter, I draw general conclusions and discuss future research directions.

## Chapter 2: Investigating the bioaccumulation potential of anionic organic compounds using a permanent rainbow trout liver cell line

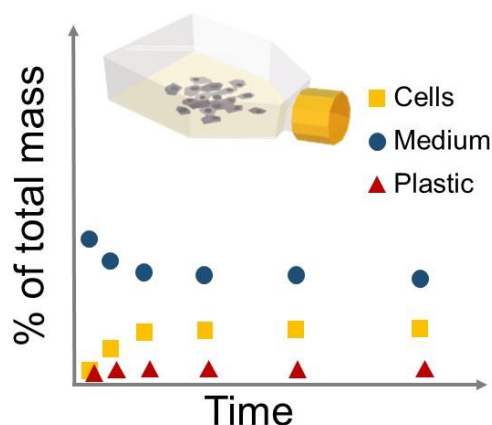


**Figure 1.4: Graphical abstract for Chapter 2.**

Mass balances of *in vitro* test systems are indispensable for the detection of biotransformation activity by the exposed cells and to understand measured cellular accumulation of the test compound. With the established method, mass balances of RTL-W1 cells, exposed to non-toxic exposure concentrations of four anionic compounds, were obtained and used to derive *in vitro* BCF. Those cell-based BCF were compared to *in vivo* BCF or BMF values and simple partition coefficient-based predictions. From the comparisons, it could be concluded that the established protocol can be used as conservative estimate to predict bioconcentration in fish as one line of evidence. Further, the mass balances gave insights into the fate of the four tested anionic compounds. A valuable side outcome was that the acute cytotoxicity assay with RTgill-W1 implied that it can predict acute toxicity of anionic organic compounds in fish.

## Chapter 3: Bioaccumulation of cationic surfactants in permanent fish cell lines

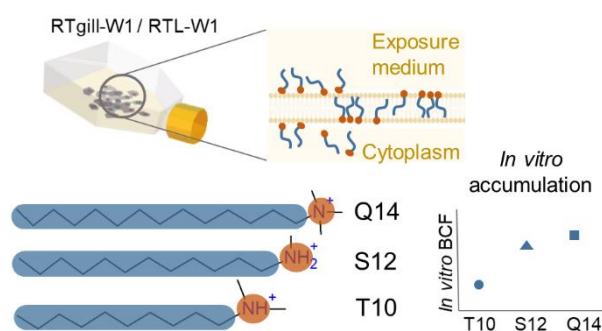


**Figure 1.5: Graphical abstract for Chapter 3.**

The established method to measure anionic compounds in fish cell cultures was extended to cationic surfactants in exposures with RTL-W1 and RTgill-W1. Specifically, the role of cell

surface bound compound was scrutinized. Observed cellular accumulations of the three tested cationic surfactants closely followed the compound's affinity to membrane lipid and was well predictable by the  $D_{MLW}$ . It could be demonstrated that measured *in vitro* BCF in both cell lines were dependent on the alkyl chain-length and independent of the exposed cell type. *In vitro* BCF of the non-permanently charged test compounds were well comparable to BCF measured in fish.

#### Chapter 4: Model comparison to refine bioconcentration prediction of ionizable organic compounds

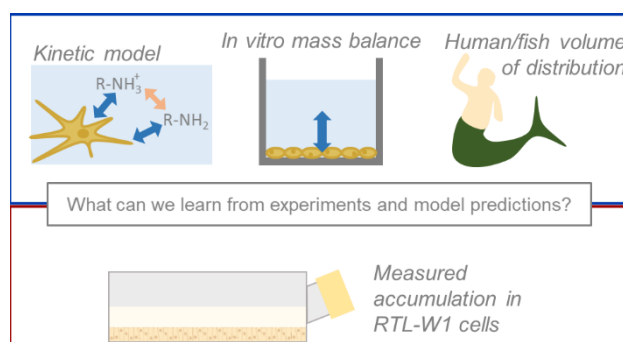


**Figure 1.6: Graphical abstract for Chapter 4.**

Computational models are useful to investigate and validate putative accumulation mechanisms inside an organism or cells. In this chapter, cell-based BCF and *in vivo* BCF were compared to two different model approaches: a typical *in vitro* mass balance model and a kinetic model, which combines kinetic membrane permeation with a mass balance inside the cell. The models' assumptions for bioconcentration were evaluated and their relevance discussed in context with the experimental bioconcentration data. The comparison of the computational and experimental *in vitro* data revealed that a mass balance sufficed for the prediction of cellular compound accumulations and that kinetic considerations of charge-dependent permeation in models can be neglected. Further, the models revealed that the influence of  $C_{free}$  in the medium was dependent on the compound class. Important factors determining the experimental accumulations were the test compound affinity to membrane lipid and protein as well as the medium and cellular pH. Additionally, a novel approach to screen for bioconcentration potential in fish and cells using human volume of distribution and the blood water partition coefficient from fish was evaluated. Human and fish  $V_D$  were largely similar for a set of IOC from the literature. The combination of the human  $V_D$  with the blood water partition coefficient from fish for BCF prediction implied potential for screening the bioconcentration potential in fish. However, predictions of  $K_{BW}$  require refinements to be more accurate and measured  $K_{BW}$  values are not readily available. Therefore, this read across approach is limited by the use of accurate  $K_{BW}$ .

---

## **2. Investigating the bioaccumulation potential of anionic organic compounds using a permanent rainbow trout liver cell line**

Fabian Balk<sup>1,2</sup>, Juliane Hollender<sup>1,3</sup>, Kristin Schirmer<sup>1,2,3</sup>

<sup>1</sup> Eawag, Swiss Federal Institute of Aquatic Science and Technology, 8600 Dübendorf, Switzerland

<sup>2</sup> EPF Lausanne, School of Architecture, Civil and Environmental Engineering, 1015 Lausanne, Switzerland

<sup>3</sup> ETH Zürich, Department of Environmental Systems Science, 8092 Zürich, Switzerland

### **Credit author statement**

Fabian Balk: Conceptualization, Experimental work, Formal analysis, Visualization, Writing of original draft, Review and Editing

Juliane Hollender: Conceptualization, Review and Editing

Kristin Schirmer: Conceptualization, Review and Editing

Reprinted with permission from Balk, F.; Hollender, J.; Schirmer, K., Investigating the bioaccumulation potential of anionic organic compounds using a permanent rainbow trout liver cell line. *Environment International* 2023, 174, 107798.

## 2.1. Abstract

Permanent rainbow trout (*Oncorhynchus mykiss*) cell lines represent potential *in vitro* alternatives to experiments with fish. We here developed a method to assess the bioaccumulation potential of anionic organic compounds in fish, using the rainbow trout liver-derived RTL-W1 cell line. Based on the availability of high quality *in vivo* bioconcentration (BCF) and biomagnification (BMF) data and the substances' charge state at physiological pH, four anionic compounds were selected: pentachlorophenol (PCP), diclofenac (DCF), tecloftalam (TT) and benzotriazol-*tert*-butyl-hydroxyl-phenyl propanoic acid (BHPP). The fish cell line acute toxicity assay (OECD TG249), was used to derive effective concentrations 50% and non-toxic exposure concentrations to determine exposure concentrations for bioaccumulation experiments. Bioaccumulation experiments were performed over 48 h with a total of six time points, at which cell, medium and plastic fractions were sampled and measured using high resolution tandem mass spectrometry after online solid phase extraction. Observed cell internal concentrations were over-predicted by  $K_{OW}$ -derived predictions while pH-dependent octanol-water partitioning ( $D_{OW}$ ) and membrane lipid-water partitioning ( $D_{MLW}$ ) gave better predictions of cell internal concentrations. Measured medium and cell internal concentrations at steady state were used to calculate RTL-W1-based BCF, which were compared to  $D_{OW}$ - or  $D_{MLW}$ -based model approaches and *in vivo* data. With the exception of PCP, the cell-derived BCF best compared to  $D_{OW}$ -based model predictions, which were higher than predictions based on  $D_{MLW}$ . All methods predicted the *in vivo* BCF for diclofenac well. For PCP, the cell-derived BCF was lowest although all BCF predictions underestimated the *in vivo* BCF by  $\geq 1$  order of magnitude. The RTL-W1 cells, and all other prediction methods, largely overestimated *in vivo* BMF, which were available for PCP, TT and BHPP. We conclude that the RTL-W1 cell line can supplement BCF predictions for anionic compounds. For BMF estimations, however, *in vitro-in vivo* extrapolations need adaptation or a multiple cell line approach.

## 2.2. Introduction

Bioaccumulation is an important parameter for environmental risk assessment of organic compounds as the accumulated compounds potentially endanger environmental and human health. Bioaccumulation occurs as bioconcentration from the surrounding environment, expressed as bioconcentration factor (BCF), or as biomagnification from dietary uptake, expressed as biomagnification factor (BMF). Most commonly fish, and more specifically, rainbow trout (*Oncorhynchus mykiss*), are used for bioaccumulation assessments concerned with the aquatic environment<sup>9</sup>. Such assessments are standardized according to OECD Test

Investigating the bioaccumulation potential of anionic organic compounds using a permanent rainbow trout liver cell line  
Guideline (TG) 305, where enrichment and depuration of a compound are measured in week-long exposures of over 100 fish in a resource-intensive and ethically questionable manner<sup>9</sup>.

One alternative method to assess bioaccumulation in fish are modelling approaches, which predict bioaccumulation with varying degrees of complexity and, most commonly, on the bases of the compound's octanol-water partition coefficient,  $K_{OW}$ <sup>18</sup>. The octanol phase is used as surrogate of the organisms' lipid phase, which is assumed to drive the bioaccumulation of neutral compounds. However, such  $K_{OW}$  – based models often overestimate bioaccumulation relative to the *in vivo* reference, since depuration processes, such as biotransformation, are not considered<sup>14, 91</sup>.

*In vitro* methods have been developed to obtain information about the capacity of fish liver to biotransform chemicals. OECD TG319a/b detail the use of freshly isolated and cryopreserved hepatocytes or of S9-fractions from fish to determine biotransformation rates<sup>23, 24</sup>. Via *In vitro* - *In vivo* Extrapolations (IVIVE), these biotransformation rates aid in the refinement of bioaccumulation models<sup>18, 23, 24</sup>. Yet, these *in vitro* methods still require the sacrifice of fish; as well, the activity of the hepatocytes and S9-fractions may vary depending on the health status and strain of the fish, the season of isolation and the isolation procedure itself.

Another *in vitro* alternative, which avoids experimentation with fish altogether, are permanent fish cell lines<sup>35, 41</sup>. Two approaches for the prediction of bioaccumulation in fish were tested with permanent fish cell lines to date using cell lines from rainbow trout, which stem from gill (RTgill-W1,<sup>30</sup>), liver (RTL-W1,<sup>29</sup>) and intestinal tissue (RTgutGC,<sup>31</sup>). The simpler of the two approaches derives a BCF directly from measured cellular concentrations in an IVIVE procedure: the cellular concentration of a compound at steady state, expressed as per cell mass, divided by the exposure medium concentration<sup>41</sup>. This was done using the RTgill-W1 cell line in Stadnicka-Michalak et al. (2014), though the focus of that study was on extrapolation of internal effect concentrations and not a comparison to *in vivo* bioaccumulation. In the second approach, the measured *in vitro* biotransformation rate of the test compound serves as input parameter for physiology-based toxicokinetic (PBTK) models, enabling IVIVE and BCF prediction<sup>92</sup>. This approach was successfully demonstrated for all three above mentioned rainbow trout cell lines for the polycyclic aromatic hydrocarbon, benzo[a]pyrene<sup>35</sup>.

Cell line-based approaches operate on a small scale, which has advantages in terms of test material needs and waste produced. Yet, the small scale makes quantifying test compounds in cell samples challenging due to the minute amounts added to these test systems. Stadnicka-Michalak et al. (2014, 2018) addressed this challenge by using radiolabeled test compounds<sup>35, 41</sup>. More recently, fish cell-internal concentrations have also been determined in a mass balance-type approach for non-radiolabeled compounds<sup>38, 39, 81, 93, 94</sup>. One of these studies



Investigating the bioaccumulation potential of anionic organic compounds using a permanent rainbow trout liver cell line examined the formation of biotransformation products (BTP) in the RTgill-W1 and RTL-W1 cell lines upon test compound exposure and found a putative BTP, a hydroxy-metabolite in RTL-W1 cells, which implies the activity of phase I biotransformation enzymes<sup>94</sup>. Other studies, which examined the transfer of volatile and hydrophobic organic compounds across an RTgutGC epithelium, demonstrated biotransformation activity and suggested to use the test system for different cell lines and for the identification of BTPs of test compounds<sup>38, 39</sup>. These advances in applications of fish cell lines and analytical methods provide impetus to expand these types of investigations to a wider chemical space.

Ionizable organic compounds (IOC) are a group of chemicals for which the mechanisms and extent of bioaccumulation is little understood. IOC are distinct from neutral compounds by having a charged fraction, either permanently or depending on the pH of the surrounding milieu, which results in organic anions, cations or zwitterions. IOCs comprise a great number of chemical classes<sup>48, 95</sup> and are used as, for example, surfactants<sup>96, 97, 98</sup>, pharmaceuticals<sup>99</sup> and pesticides<sup>100</sup>, with the concurrent release into the aquatic environment<sup>51, 52, 53</sup>. The bioaccumulation of IOCs strongly depends on their molecular structure. For example, pharmaceuticals, such as the anionic diclofenac, express a low bioaccumulation in fish compared to neutral compounds despite a log  $K_{OW}$  of  $> 4$ <sup>101, 102</sup>. However, certain anionic surfactants, such as perfluoroalkyl substances and long chained alkyl sulfonates (alkyl chain  $\geq 14$ )<sup>26, 103, 104</sup>, exert a high bioaccumulation in fish relative to other anionic compounds<sup>105 106 107</sup>. Anionic compounds that lack the typical surfactant-like structure but have a largely hydrophobic surface, such as pentachlorophenol, also show high bioaccumulation in fish<sup>7, 108</sup>. Thus, it seems that the neutral and charged fraction of an IOC determine bioaccumulation<sup>46</sup>. In accordance with this observation, the  $K_{OW}$  was found to be an inappropriate descriptor for the bioaccumulation of IOCs that are mainly or permanently charged<sup>14</sup>. The pH-dependent octanol-water distribution ratio,  $D_{OW}$  ( $K_{OW}$  corrected for the neutral and charged fraction at a specific pH), appeared more suitable for bioaccumulation prediction<sup>14, 22</sup>. Recent investigations found that the compound's pH-dependent membrane lipid-water distribution ratio,  $D_{MLW}$ , describes the accumulation in fish for surfactants well, since the cell membranes appear to be the main sink for surfactants in fish<sup>16, 17, 26, 61, 65, 66</sup>. Beside the cell membranes' phospholipid, the interaction with proteins can pose another significant matrix for bioaccumulation<sup>109 110 111 58 54</sup> as shown for perfluorooctanoic acid<sup>71</sup>. Further, membrane integrated proteins, can play an important role in the uptake and efflux of IOC, which would otherwise permeate the cell membrane in negligible amounts<sup>46</sup>. Comprising functional entities with phospholipids and proteins in place, it is reasonable to assume that fish cell lines possess all the relevant matrices to assess the bioaccumulation potential of IOC in fish.

We therefore set out in this study to assess the potential of the RTL-W1 fish cell line to predict the bioaccumulation of four purposefully selected anionic organic compounds in fish. The RTL-W1 cell line was selected for testing because it represents the liver as primary organ for biotransformation and is among the best studied fish cell lines with regard to its biotransformation capabilities<sup>29, 33, 34, 35</sup>. Indeed, the expression of cytochrome CYP1A, glutathione-S-transferase, sulfotransferase and UDP-glucuronosyltransferase have been confirmed in this cell line<sup>29, 33, 34, 35</sup>. We hypothesized that the RTL-W1 cell line possesses the principal ability to accumulate and biotransform IOC and that derived *in vitro*-based BCF are comparable to *in vivo* bioaccumulation. To test this hypothesis, we 1) determined non-toxic exposure concentrations for bioaccumulation experiments based on the established RTgill-W1 cell viability assay following OECD TG249<sup>43, 45</sup>; 2) established a method to measure cell-internal concentrations of anionic organic compounds in RTL-W1 cell cultures over time for mass balance analysis; and 3) derived *in vitro* BCF from measured concentrations in cells and exposure medium and compared these with *in vivo* data and common BCF prediction methods.

## 2.3. Methods

### 2.3.1. Test Compound Selection

Detailed information on the test compounds is documented in the supporting information (SI): CAS registry number, structural formula, vendor and purity in SI Table S2.1, and influence of pH on degree of ionization in SI Figure S2.1. Three criteria were applied to select the four test compounds. The first criterion was that high quality, in line with OECD TG305<sup>9</sup>, bioaccumulation data in rainbow trout are available for reference. The second criterion was that the compounds are largely negatively charged at physiologically relevant pH (7-8) while the third criterion was environmental relevance. Based on these criteria, the selected anionic compounds were: benzotriazol-*tert*-butyl-hydroxyl-phenyl propanoic acid (BHPP), diclofenac (DCF), pentachlorophenol (PCP) and tecloftalam (TT). BHPP belongs to a group of ultraviolet stabilizers, which are most prominently used as additive in plastic polymers and car paints<sup>112, 113</sup>. DCF is a well-known pharmaceutical used for its pain relieving and anti-inflammatory properties<sup>114, 115</sup>. PCP is a pesticide disinfectant that was used in the past as a preservative in wood, leather, agricultural seeds and in paper mill systems<sup>116</sup>, but has been listed in Annex A of the Stockholm Convention due to its high toxicity and environmental persistence since 2015<sup>117</sup>. TT is a pesticide used to control bacterial leaf blight (*Xanthomonas oryzae*) in rice<sup>118, 119</sup>. It is expected to end up in the aquatic environment, although this has not been addressed in the accessible scientific literature. In contrast, BHPP, DCF and PCP have been ubiquitously found in surface waters and in aquatic organisms<sup>120, 121, 122, 123, 53</sup>.

Investigating the bioaccumulation potential of anionic organic compounds using a permanent rainbow trout liver cell line

For BHPP and TT, only BMF from rainbow trout exposure studies were available. A comparison of BCF and BMF is fundamentally difficult because of the different exposure matrices used for normalization (water concentration for BCF, concentration in prey/feed for BMF). Therefore, we transformed the BMF value to a tentative BCF,  $BCF_{BMF}$ , calculated as the ratio of the measured elimination rate,  $k_e$  ( $d^{-1}$ ), from the BMF study<sup>107</sup>, over an estimated chemical uptake rate,  $k_u$  ( $L\ kg^{-1}\ d^{-1}$ )<sup>9</sup>. Whole body measured  $k_e$  values from the BMF study for BHPP and TT were  $1.24\ d^{-1}$  and  $2.96\ d^{-1}$ , respectively<sup>107</sup>. For PCP, *in vivo* BCF and BMF were available and the  $BCF_{BMF}$  ( $k_e = 1.79\ d^{-1}$ ) was calculated to estimate the accuracy of the transformation method. Since the charged fraction of the studied IOC is dominant at neutral pH (7-8), the gill uptake is likely smaller compared to a neutral compound, assuming that active uptake of the charged fraction is minor<sup>124</sup>. For this reason, the approach from Armitage et al.<sup>16</sup> was chosen for chemical uptake rate calculation to account for the lowered uptake efficiency of the tested IOC:

$$\text{Equation 2.1} \quad k_u = ((R_w + \mu R_o / K_{OW})^{-1} + \beta) \times \frac{V}{W}$$

The left factor in Equation 2.1 represents the chemical absorption efficiency, where  $R_w$  (1.85) and  $R_o$  (155) are resistances through the aqueous and organic diffusion layer at and in the gill, respectively. The  $\mu$  represents the pH-dependent dissociation of the tested IOC (for acids:  $1 + 10^{pH-pK_a}$ ),  $K_{OW}$  is the octanol-water partition coefficient of the neutral IOC species,  $V$  the gill ventilation rate ( $L\ day^{-1}$ ) and  $W$  the fish weight (kg). The  $\beta$  describes the mass transfer of the charged IOC fraction across the organic gill layers and passive uptake via the paracellular transport. Since the mechanisms for  $\beta$  are poorly characterized, we applied two different values to reflect the resulting uncertainty of this parameter (0.005 and 0.0005) on the BCF estimation (mean and standard deviations Table S2. 9). For a detailed discussion on the uncertainties of  $\beta$ , see<sup>16</sup>. Required information from the BMF studies for  $k_u$  calculation were the water temperature ( $11\ ^\circ C$ ), water pH (7.35), mean fish weight (5.42 g), and dissolved oxygen concentration ( $9.29\ mg\ L^{-1}$ )<sup>107</sup>, while the required information on the tested IOC is shown in Table 2.1. The calculation of  $k_u$  was conducted with the BIONIC model v3 available as spreadsheet<sup>16</sup>, where all input data kept their default values, if not mentioned differently above.

### 2.3.2. Preparation of stock solutions of test compounds

The test compounds Table 2.1 were delivered via dimethyl sulfoxide (DMSO, CAS 67-68-5, Sigma Aldrich) stock solutions in concentrations that resulted in a DMSO concentration of 0.5% (v/v) in the final exposure medium of the fish cell line acute cytotoxicity assays (OECD TG249<sup>43</sup>), while it was 0.1% (v/v) for the bioaccumulation experiments (same as in OECD TG 319b

Investigating the bioaccumulation potential of anionic organic compounds using a permanent rainbow trout liver cell line

<sup>24</sup>). The same DMSO stock solution per test compound, stored at -20 °C in between experiments, was used for all biological replicates for each cytotoxicity or bioaccumulation experiment. The computation of the compound's  $K_{OW}$  values (of the neutral species) has been attempted with the software COSMOtherm but was not successful for some of the substances. Therefore, the  $K_{OW}$  and  $D_{OW}$  were taken from other estimation programs as detailed in Table 2.1.

**Table 2.1: Overview of test compounds with usage and key physico-chemical properties.** Partition coefficient estimations were taken from the same source to keep uncertainties comparable.

Test compound	Abbreviation	CAS	Category/ Usage	$pK_a$ <sup>1</sup>	log $K_{OW}$ <sup>2</sup>	log $D_{OW}$ (pH 7.4) <sup>3</sup>	log $D_{MLW}$ <sup>4</sup>
Benzotriazol- <i>tert</i> -butyl-hydroxyl-phenyl propanoic acid	BHPP	84268-36-0	UV stabilizer in plastics and paints <sup>112, 113</sup>	4.65	4.23	1.75	2.2
Diclofenac	DCF	15307-79-6	Pharmaceutical <sup>114, 115</sup>	4.18	4.04	1.37	1.4
Pentachloro phenol	PCP	87-86-5	Pesticide Disinfectant <sup>116, 117</sup>	4.68	4.76	2.45	2.9
Tecloftalam	TT	76280-91-6	Pesticide <sup>118, 119</sup>	1.07	5.48	3.13	2
<sup>1</sup> : ACD/Labs prediction, <sup>2</sup> : Mean of EPI Suite and ACD/Labs predictions, <sup>3</sup> : ACD/Labs, <sup>4</sup> : Prediction method in Armitage et al. 2013 <sup>16</sup>							

### 2.3.3. Cell culture

RTL-W1 <sup>29</sup> and RTgill-W1 cell lines <sup>30</sup> were routinely cultured in cell culture flasks with 150 cm<sup>2</sup> growth area (Techno Plastic Product AG) at 19 ± 1 °C in the dark at normal atmosphere in 20 mL routine cell culture medium, i.e. Leibovitz's medium (L-15, Invitrogen), supplemented with 5% (v/v) fetal bovine serum (FBS, Eurobio Scientific). When a cell culture reached approximately 95% confluency, the cells were diluted in a 1:1 (v/v) ratio to obtain two new cell culture flasks or seeded for an experiment. To detach the cells, the medium was removed, the cell layer rinsed twice with 1.4 mL Versene solution (Gibco™ Versene Solution, Thermo Fisher Scientific Inc.) and 0.7 mL trypsin (Pan Biotech) added. When the cell layer visibly detached from the plastic bottle, the trypsin reaction was stopped by the addition of routine cell culture medium, after which cells were brought into suspension. For the acute cytotoxicity assays with RTgill-W1 cells, cell passages 62 to 74 were used; for confirmation of non-toxic concentrations and the bioaccumulation experiments with RTL-W1 cells, cell passages were 80 to 94.

#### **2.3.4. Determination of non-toxic exposure concentrations**

It was crucial to use non-toxic exposure concentrations of the test compounds in the bioaccumulation experiments to avoid that toxic effects mask the accumulation behavior of the exposed cells. RTL-W1 cells cannot easily be transferred to the test conditions of the standardized acute cytotoxicity assay, due to the absence of FBS in the exposure medium in this test <sup>43</sup>. Therefore, acute cytotoxicity assays were conducted with RTgill-W1 cells according to OECD TG249, assuming an overall comparability in the acute cytotoxicity between rainbow trout cell lines, as it was demonstrated for RTgill-W1 vs. RTgutGC cells by Schug et al. (2020). In brief, RTgill-W1 cells were exposed in a 24 well plate format to a range of six exposure concentrations of a single test compound dissolved in DMSO <sup>43</sup> with a 48 h exposure duration. For the exposures, the protein-free type of Leibovitz's medium, L-15/ex, was applied <sup>43</sup>. At the start and termination of exposure ( $C_{0h}$  and  $C_{48h}$ ), the exposure medium, was sampled for later chemical analysis (SI section S2.2, Table S2.2). After exposure, cell viability was quantified based on a set of three fluorescent indicator dyes. These were alamarBlue™, 5-carboxyfluorescein diacetate acetoxymethyl ester (CFDA-AM) and Neutral Red, indicating cell metabolic activity, cell membrane integrity and lysosomal membrane integrity, respectively <sup>43</sup>. The raw fluorescent data were expressed as % of control and corrected for the actual measured exposure concentrations based on the geometric mean, which was calculated with  $C_{0h}$  and  $C_{48h}$  of the respective exposure concentrations of the biological replicates. These data were used to produce sigmoidal concentration-response curves of cell viability <sup>43</sup> and calculate the effective concentrations causing 50% decline of cell viability ( $EC_{50}$ ). Moreover, the non-toxic concentrations were calculated in an online application <sup>126</sup>, according to Stadnicka-Michalak et al. (20), which applies an algorithm on the toxicity data to determine a reproducible and conservative estimate.

The exposure concentrations for the bioaccumulation experiments were chosen based on three criteria: 1) the exposure concentration should be as low as possible and not exceed the non-toxic concentrations (see above); 2) to avoid enzyme inhibition in the exposed cells, the exposure concentration should be  $\leq 1 \mu\text{M}$  <sup>23</sup>, and 3) the chosen concentration should be at least 10 times above the method limit of quantification (LOQ). Final exposure concentrations for the bioaccumulation experiments were confirmed to be non-toxic upon exposure of RTL-W1 cells over 72 h (SI section S2.2, Table S2.3, Figure S2.2), i.e. the longest time span foreseen for the bioaccumulation studies (see below). For this purpose, the same fluorescence-based cytotoxicity assay was applied as outlined above, but with 5% FBS supplementation of the exposure medium to sustain the viability and metabolic activity of the RTL-W1 cells.

### **2.3.5. Experimental procedure for bioaccumulation assessment**

The presented experimental procedure was inspired by previous studies that focused on IVIVE using rainbow trout cell lines to predict bioaccumulation in fish <sup>41</sup>. Initially, two formats were considered, all using RTL-W1 cells: 24 well plates (1.9 cm<sup>2</sup> growth area/well, Greiner Bio-One) holding 2.5×10<sup>5</sup> cells/well in a volume of 1 mL and cell culture flasks (25 cm<sup>2</sup> growth area/flask, Techno Plastic Product AG) holding 3.3×10<sup>6</sup> cells/flask in a volume of 6 mL. Cell internal concentrations were better measurable in the flask format (SI section S2.3); it hence was decided to conduct the bioaccumulation experiments in the 25 cm<sup>2</sup> cell culture flasks.

### **2.3.6. Cell seeding and exposure start**

For each experimental run, ten 25 cm<sup>2</sup> cell culture flasks were seeded with 3.3×10<sup>6</sup> RTL-W1 cells per flask in a volume of 6 mL routine cell culture medium. This cell density ensured a confluent monolayer with minimal fluctuation of cell number during the experimental duration (SI section S2.4, Figure S2.3). Cells from routine culture at about 95% confluency were detached and suspended as described above for cell counting, using the electronic cell counting system CASY TCC (BIOVENDIS Products GmbH). A 10 µL sample of the cell suspension was diluted in 10 mL CASY solution and the cell number, viability and cell diameter measured in two technical replicates, aiming for no more than ± 10% variability to be valid. The seeding density was calculated and the cell suspension appropriately prepared in routine cell culture medium. Seeded cells were incubated for 48 h to 72 h under routine cell culture conditions (see above) to obtain the confluent monolayers for experimentation. The experiments were started by the removal of the cell culture medium and the addition of 3 mL of L-15 medium with test compound solved in DMSO and 5% FBS (v/v) to sustain the cells <sup>29</sup>.

### **2.3.7. Bioaccumulation experiments**

Figure 2.1 depicts the experimental set up and all subsequent sampling and extraction steps. Two flasks were sampled at each sampling time point, which were 0 h, 4 h, 8 h, 16 h, 24 h and 48 h of exposure: the flask with exposed cells (A, Figure 2.1) and the cell-free negative control (B). At experimental onset and termination, the cell count control (C) and the process control (D) were sampled additionally. The process control contained cells but no test compound and was used to account for potential chemical background contamination, while the cell count control contained cells and test compound and was used to monitor changes in cell number. For the latter, cells were sampled and numbers determined with the CASY TCC as described above. Cell numbers of all bioaccumulation experiments are reported in the SI (section S2.5, Figure S2.4). Finally, the prepared exposure medium was stored at 19 °C during the experiment and sampled at the onset and termination of each experiment to monitor the test

Investigating the bioaccumulation potential of anionic organic compounds using a permanent rainbow trout liver cell line compound's stability. These samples served as reference to account for potential abiotic degradation of the test compounds. Each bioaccumulation experiment was done in two independent experiments per test compound with one sample per treatment and sampling time point (i.e. one cell culture flask). We considered two independent experiments sufficient, because neither opposing trends nor unreasonable variations in cell internal concentrations were observed in the two replicates (SI, section S2.5, Table S2.5 and S2.6).

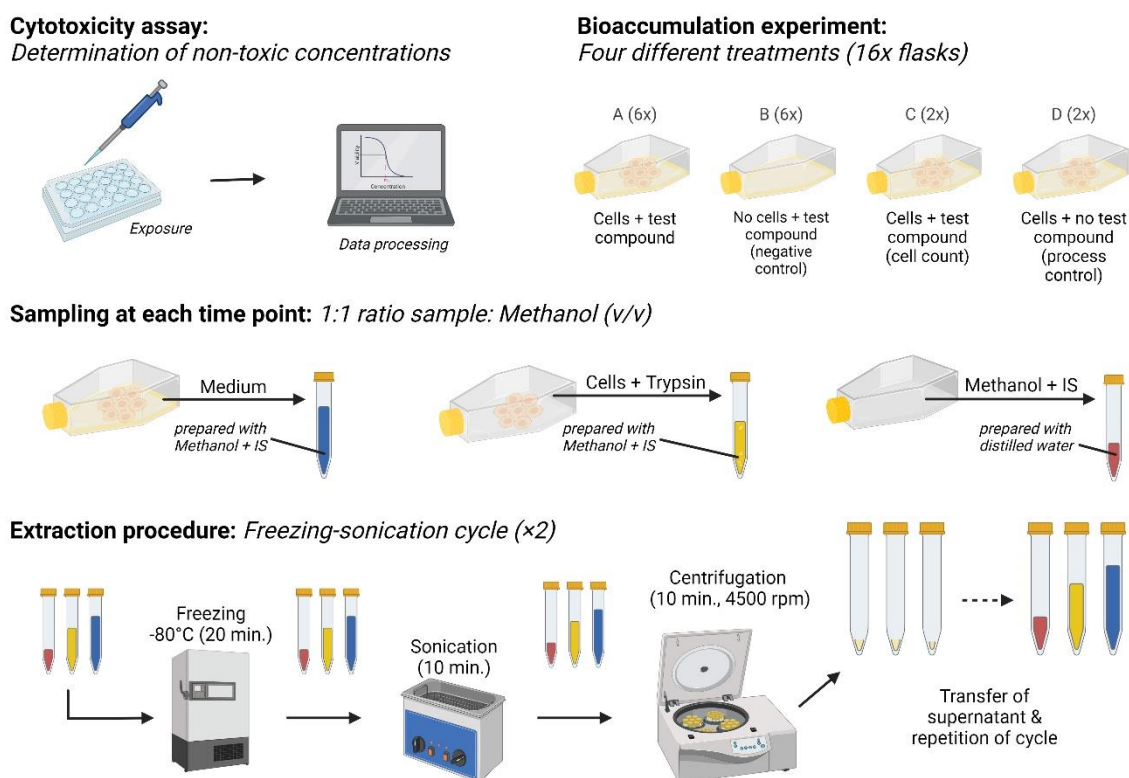


**Figure 2.1: Work flow from exposure concentration determination to bioaccumulation experiments.** In a first step, a suitable non-toxic exposure concentration was determined for each compound. Each bioaccumulation experiment had four different treatment types to (A) measure test compound accumulation in cells, (B) to monitor abiotic loss, such as sorption to plastic, (C) count the cell number over the experimental duration, and (D) monitor background contaminations of test compound during exposure and sampling. IS = Internal Standard

Three fractions of the test system were considered relevant for sampling: the exposure medium, the cell monolayer and the plastic, i.e. test compound adsorbed to it (Figure 2.1). In contrast, since IOCs are not volatile in their charged state, the air-filled headspace was not considered. All samples were collected in 15 mL centrifuge tubes (91015, TPP Techno Plastic Products AG). To obtain the three fractions, the medium was sampled first. A volume of 1 mL was sampled for pH measurement by means of a small pH probe (microFET, Welling) to account for potential pH differences, which might affect the IOC ionization state. The remaining 2 mL were then sampled for chemical quantification in the medium fraction. Next, the cell surface was rinsed for 30 seconds with 3 mL of test compound-free cell culture medium. 2 mL

Investigating the bioaccumulation potential of anionic organic compounds using a permanent rainbow trout liver cell line

of this rinse solution were pooled with the initial 2 mL of exposure medium and the remaining rinse medium was discarded. Cells were harvested by the addition of 1 mL trypsin solution followed by incubation until the cell monolayer visibly detached and further dislodged by use of a cell scraper (Techno Plastic Products AG) to ensure complete capture of cells. The trypsin solution was sampled and an additional 1 mL of trypsin solution added to the flask to collect all remaining cells. This second trypsin application was combined with the first trypsin sample. The rinsing steps for exposure medium and cells were necessary to clearly distinguish the test compounds associated with each sample fraction and reduce carry over across the different sample matrices (SI section S2.6, Figure S2.5). At last, the test compound sorbed to plastic was sampled by the addition of 2 mL methanol, containing internal standard. The flask, now only containing methanol, was shaken on a plate shaker for 5 min at 200 rpm, after which the methanol was transferred to a 15 mL centrifuge tube and diluted with distilled water (CAS 7732-18-5) in a 1:1 (v/v) ratio. The medium and cell samples were each diluted with methanol in a 1:1 ratio (v/v), to assure sufficient extraction of test compounds and aid protein precipitation. The applied trypsin and methanol solutions were sampled and extracted in the same manner and measured to account for background contaminations.

For sample extraction and matrix removal, all samples were frozen for 20 min at -80 °C, and sonicated for 15 min at room temperature thereafter (Figure 2.1). Then, the samples were centrifuged for 10 min at 4347 m/s<sup>2</sup> to precipitate the protein and cell debris. The supernatant was transferred into a new 15 mL centrifuge tube. The samples went through the extraction process twice to remove the matrix and were stored at -20 °C until chemical analysis. Mass balances were derived at each sample time point according to Equation 2.2:

$$\text{Equation 2.2} \quad \% \text{ of total amount} = \frac{Y_t}{\sum Y_t},$$

where the compound amount in fraction  $Y_t$  (ng) was either taken from the exposure medium, the cells or the plastic and sum of total compound amount in test system,  $\sum Y_t$  (ng), both present at a sample time point  $t$ . Further, the total summed up amounts at each time point,  $\sum Y_t$ , were compared to the initially added amount at the experimental start  $\sum Y_{0h}$ , to detect potentially occurring biotransformation activity or uncontrolled losses:

$$\text{Equation 2.3} \quad \% \text{ of total initial amount} = \frac{\sum Y_t}{\sum Y_{0h}}$$

### 2.3.8. Derivation of *in vitro*-based bioconcentration factors

Using the mean cell number ( $C$ , Figure 2.1), the mean cell diameter,  $d$  (16.6 μm), and the calculated absolute amount of test compound in the cell samples,  $cell_t$ , (SI,



Investigating the bioaccumulation potential of anionic organic compounds using a permanent rainbow trout liver cell line (section S2.5, Table S2.5), the internal cellular concentration,  $C_{cell}$ , at steady state was determined, assuming that the cell volumes can be approximated as being spherical <sup>35</sup>:

$$\text{Equation 2.4: } C_{cell} \left[ \frac{ng}{L} \right] = \frac{cell_t [ng]}{\text{mean cell number of experiment} \times \left( \frac{1}{6} \times \pi \times d^3 \right) [L]}$$

The *in vitro* BCF (RTL-W1 BCF, Equation 2.5) was calculated as the ratio of  $C_{cell}$  over the measured exposure medium concentration,  $C_{medium}$ , per biological replicate and the mean of those was used for presentation (SI, section S2.7, Table S2.8):

$$\text{Equation 2.5: } RTL - W1 \text{ BCF} = \frac{C_{cell}}{C_{medium}}$$

The obtained RTL-W1 BCF values were compared to other common prediction methods, including *in vivo* data (SI, section S2.7, Table S2.9), to assess the RTL-W1 cell's suitability for bioaccumulation prediction. The prediction methods covered empirical regression-based models that use the compound's  $D_{OW}$ , (<sup>127</sup>,  $BCF_{DOW}$ ) or the compound's  $D_{MLW}$  (<sup>65</sup>,  $BCF_{DMLW}$ ). Further, a more refined prediction tool that applies the compound's  $D_{OW}$  in a one-compartment PBTK model was applied (<sup>18</sup>, PBTK with  $K_{OW}/D_{OW}$ ). The  $BCF_{DOW}$  and the  $BCF_{DMLW}$ , together with the PBTK model predictions, are referred to as "numerical predictions" in the following.

### 2.3.9. Chemical analysis

For quantification, 1 mL of sample extract was added to 19 mL distilled water and enriched via online solid phase extraction prior to measurement using a high performance liquid chromatography - electrospray ionization - tandem high resolution mass spectrometry system (HPLC-ESI-HRMS/MS, QExactive or QExactive Plus, Thermo Fisher Scientific)<sup>128</sup>. The chromatographic separation on the column (XBridge C18, 3.5  $\mu$ m, 2.1 x 50 mm) was achieved by a methanol/water gradient (SI section S2.8), both containing formic acid (0.5% (v/v)). In addition to the target screening of the test compounds, a suspect screening for known and suspected biotransformation products of the test compounds was performed and evaluated using Compound Discoverer 3.3 (Thermo Fisher Scientific). For further details on the analysis set-up, see SI section S2.8 to S2.9.

Target screening for all test compounds was performed by taking full scan MS (resolution of 70 000 at  $m/z$  200) with subsequent data-dependent MS2 acquisition (resolution of 17 500, isolation window of 1  $m/z$ ) in positive mode for BHPP and DCF, while TT and PCP were measured in negative mode. Quantification was done by standard calibration in ultrapure water (with equivalent percentage of methanol as in sample) using internal standards. The Software Tracefinder 4.1 (Thermo Fisher Scientific) was used to analyze the obtained MS data. The limits of quantification were determined by the peak shape with at least five mass scans

Investigating the bioaccumulation potential of anionic organic compounds using a permanent rainbow trout liver cell line forming the peak and a signal to noise ratio greater than ten. Isotope labeled homologs were only available for DCF (DCF-D<sub>4</sub>) and PCP (PCP-<sup>13</sup>C<sub>6</sub>) and used as internal standards. For BHPP and TT, the best fitting internal standard was mefenamic acid-D<sub>4</sub>, as it showed closest retention time and structural similarity to the test compounds. For samples, in which a detection of test compound was possible but below LOQ, half of the LOQ ( $0.5 * LOQ$  (ng/L)) was used to approximate the test compound amount. To correct for potential matrix effects and compound losses during the extraction process (Figure 2.1), a known amount of each test compound was spiked into exposure medium, harvested cell solution and pure methanol from the plastic fraction, (relative recovery, SI, section S2.8, Table S2.11). These samples went through the same extraction process as outlined above (section 2.3.7) and the recovery was determined (SI, section S2.9, Table S2.12). Table S2.11 in the SI (section S2.8) contains the method LOQ for the different matrices as well as the final exposure concentrations per compound, the matrix-dependent relative recoveries and the comparison of measured and nominal exposure concentrations in the bioaccumulation experiments.

### **2.3.10. Data analysis and visualization**

Obtained sample concentrations were further analyzed and visualized using the programming language R <sup>129</sup> and the packages openxlsx, tidyr, dplyr, ggplot and patchwork <sup>130 131 132 133 134</sup>. Software Graphpad Prism 9.4.0 (GraphPad Software, US) and Biorender (BioRender.com, Toronto) were also used for visualization.

## **2.4. Results and Discussion**

### **2.4.1. General observations**

The goal of this study was to assess the potential of a fish liver cell line, RTL-W1, to predict the bioaccumulation potential of anionic organic compounds in rainbow trout. This required careful method set-up, including determination of non-toxic exposure concentrations and chemical quantification for mass balance analysis. The results were finally put into the context of bioaccumulation predictions in fish.

### **2.4.2. Impact of chemicals on cell viability**

All test compounds were toxic to RTgill-W1 cells, following the OECD TG249 acute toxicity assay procedure, with the only variation being a 48 h rather than 24 h exposure duration to account for the prolonged exposures for bioaccumulation assessment. Cell toxicity data were corrected for the geometric mean ( $C_{0h}/C_{48h}$ ) of measured compound concentrations (Figure 2.1, SI section S2.2, Table S2.2). PCP was the most toxic test compound with its EC<sub>50</sub> of

Investigating the bioaccumulation potential of anionic organic compounds using a permanent rainbow trout liver cell line

72 µg/L (60 – 90 µg/L, 95% confidence interval) being about 100-fold lower relative to the other test compound's EC<sub>50</sub> values (Table 2.2). Cell metabolic activity, as measured by alamarBlue, and lysosomal membrane integrity, assessed by Neutral Red, responded more sensitively to compound exposure than cell membrane integrity based on CFDA-AM. This order in sensitivity is commonly observed <sup>42</sup>.

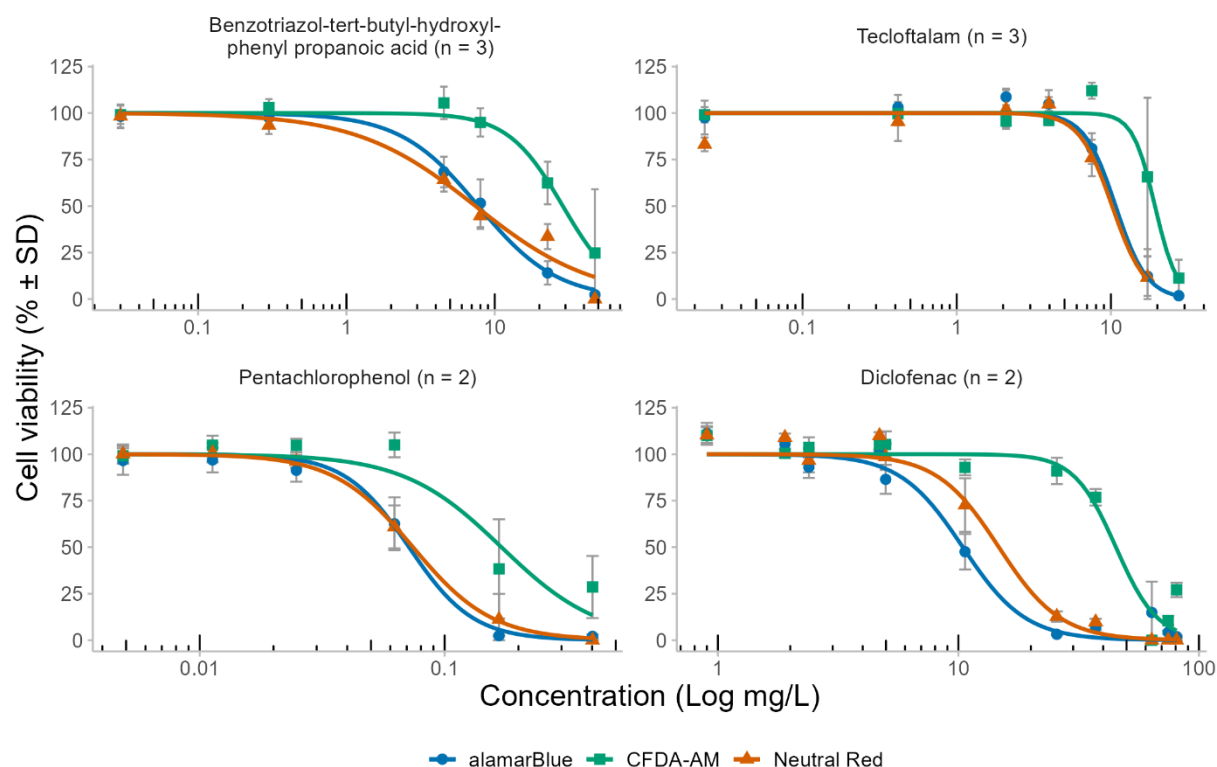


**Figure 2.2: Acute cytotoxicity of the test compounds to RTgill-W1 cell cultures over 48h exposure.** alamarBlue = indicates for cell metabolic activity, CFDA-AM for cell membrane integrity and Neutral Red for lysosomal membrane integrity., Errors bars = standard deviation. For more information, consult Table S2.2 and SI section S2.2. n = number of independent replicates.

The EC<sub>50</sub> values from the most sensitive RTgill-W1 acute cytotoxicity assay, i.e. cell metabolic activity in all cases, were compared with available *in vivo* LC<sub>50</sub> values and found to be in good agreement (Table 2.2) <sup>40, 42, 43, 125, 135</sup>. The difference for DCF is largest if the EC<sub>50</sub> is compared to the LC<sub>50</sub> in juvenile zebrafish, being 166 mg/L <sup>136</sup> compared to 10.4 mg/L in RTgill-W1, indicating that the cell line is more sensitive to DCF exposure than the juvenile stage in fish, which was observed elsewhere for non-polar chemicals <sup>40, 42</sup>. A similar observation can be made for the PCP EC<sub>50</sub> relative to LC<sub>50</sub> from species other than rainbow trout: on average, LC<sub>50</sub> were 0.19 mg/L in bluegill (*Lepomis macrochirus*) to 0.87 mg/L in guppy (*Poecilia reticulata*) compared to EC<sub>50</sub> of 0.072 mg/L in RTgill-W1. The LC<sub>50</sub> for rainbow trout with 0.14 mg/L, however, was only 2-fold higher than the RTgill-W1-based EC<sub>50</sub>. Species differences in sensitivity may be the reason for the observed discrepancies between *in vivo* and RTgill-W1-based values <sup>42, 91, 137</sup>.

**Table 2.2: Results of acute cytotoxicity assay with RTgill-W1 cells.** EC<sub>50</sub> = Concentration causing 50% reduction in cell viability, CI = confidence interval, LC<sub>50</sub> = Concentration causing 50% mortality in tested fish batch, SD = standard deviation, BHPP = benzotriazol-tert-butyl-hydroxyl-phenyl propanoic acid, DCF = diclofenac, PCP = pentachlorophenol, TT = tecloftalam.

Test Compound	EC <sub>50</sub> of cell metabolic activity (mg/L [95% CI])	LC <sub>50</sub> (mg/L, <i>in vivo</i> )	Reference
BHPP	7.4 [2.9 - 14.5]	not available	-
DCF	10.4 [8.4-13.4]	6.9 ± 1.2*, 166**	*mean of 72h <sup>138</sup> and 144h exposure <sup>136</sup> in zebra fish embryo, **in juvenile zebra fish (96h exposure) <sup>136</sup>
PCP	0.072 [0.06-0.09]	0.14 ± 0.03, 0.19 ± 0.05, 0.28 ± 0.12 , 0.87 ± 0.45	mean (± SD) in various stages of rainbow trout, bluegill, fat head minnow and guppy respectively at 96h exposure (SI section S2.10, Table S2.13 for references)
TT	10.7 [8.9 - 13.0]	30	in common carp <sup>139</sup>

For PCP, literature EC<sub>50</sub> values were available for comparison from identical RTgill-W1 acute cytotoxicity assays. The studies reported EC<sub>50</sub> values of 10 µg/L (10 – 20 µg/L 95% confidence interval) <sup>40</sup> and 163 µg/L ± 46 µg/L (mean of interlaboratory study ± standard deviation) <sup>42</sup> after 24 h exposure. Our EC<sub>50</sub>, with 72 µg/L (61 – 92 µg/L 95% confidence interval) after 48 h exposure, lies in between this range despite the extended exposure duration. This fits the observation that toxicity generally develops well within 24 h <sup>43</sup> and therefore supports the notion that exposure durations >24 h appear to often have a negligible influence on cytotoxicity in the RTgill-W1 cell line. This is the first report on the acute cytotoxicity of test compounds in RTgill-W1 with a deliberate focus on the compound's charge. Although only four anionic compounds were tested here, the results add to the growing evidence that the acute cytotoxicity assay with RTgill-W1 cells also predicts acute fish toxicity of negatively charged compounds <sup>40, 42, 125, 135</sup>.

The concentration-response curves were used to derive the non-toxic exposure concentrations <sup>45</sup>, which served as one base to set the exposure concentrations for bioaccumulation assessment (section 2.3.4 and SI section S2.2). The such chosen exposure concentrations (Figure 2.3) were confirmed to be non-toxic in the RTL-W1 cell line under the exposure conditions applied for bioaccumulation assessment, i.e. monolayer exposure in the presence of 5% FBS, over a period of ≤ 72 h (SI, section S2.2). These final exposure concentrations were therefore then used to run the bioaccumulation experiments.

### **2.4.3. Bioaccumulation experiments**

#### **2.4.3.1. Mass balances and biotransformation activity**

Based on the optimization of cell sampling and analytical procedures, all test compounds were recoverable from all sampled test compartments, i.e. medium, cells and plastic (Figure 2.3). Comparison between cell-containing flasks and cell-free flasks (negative control; B, Figure 2.1) allowed to differentiate compound amounts truly taken up by the cells (SI, section S2.5, Table S2.5 and S2.6). The calculated steady state of accumulated compound in the cells was reached within 14 h (BHPP, PCP and TT) to 24 h (DCF) of experimental duration (for calculation see SI section S2.11). Up to  $4 \pm 0.7\%$  of BHPP,  $1.2 \pm 0.9\%$  of TT,  $0.34 \pm 0.03\%$  of PCP and  $0.24 \pm 0.15\%$  DCF of the initially added compound mass accumulated in the RTL-W1 cells at steady state (Figure 2.3). The by far largest amounts of test compound,  $\geq 93\%$ , were found in the medium, while amounts sorbed to plastic were only minor and well below 1% or < LOQ (Figure 2.3). The mass balances indicate little influence of compound loss due to biotransformation in the cells: total amounts were on average over all time points around  $94 \pm 15\%$  for BHPP (mean  $\pm$  standard deviation),  $72 \pm 29\%$  for TT,  $106 \pm 11\%$  for DCF and  $99 \pm 2\%$  for PCP (SI section S2.5, Table S5, S6 and section S2.12, Table S2.16). In an attempt to improve quantification of chemical distribution and test concentration dependency of bioaccumulation, DCF exposure was explored at different concentrations tested in the same way. These experiments demonstrated an independence of bioaccumulation from the initial exposure concentration and showed that exposure concentrations of 200  $\mu\text{g/L}$  and 400  $\mu\text{g/L}$  were better quantifiable in the cell samples than the initially chosen exposure concentration of 20  $\mu\text{g/L}$  (Figure 2.3 and SI section S2.13, Figure S2.6). The pH decreased from 7.4 to 7.0 over the experimental duration irrespective of the compound exposure (SI section S2.14, Figure S2.7), i.e. solely due to the presence of cells. This change in pH only marginally changed the large charged fraction of the test compounds (SI, section S2.1, Figure S2.1) but changed the neutral fraction of BHPP, DCF and PCP by approximately 2.5-fold. Under the assumption that the neutral fraction at least partly drives the bioconcentration, an influence of the observed pH changes on test compound accumulation cannot entirely be ruled out.

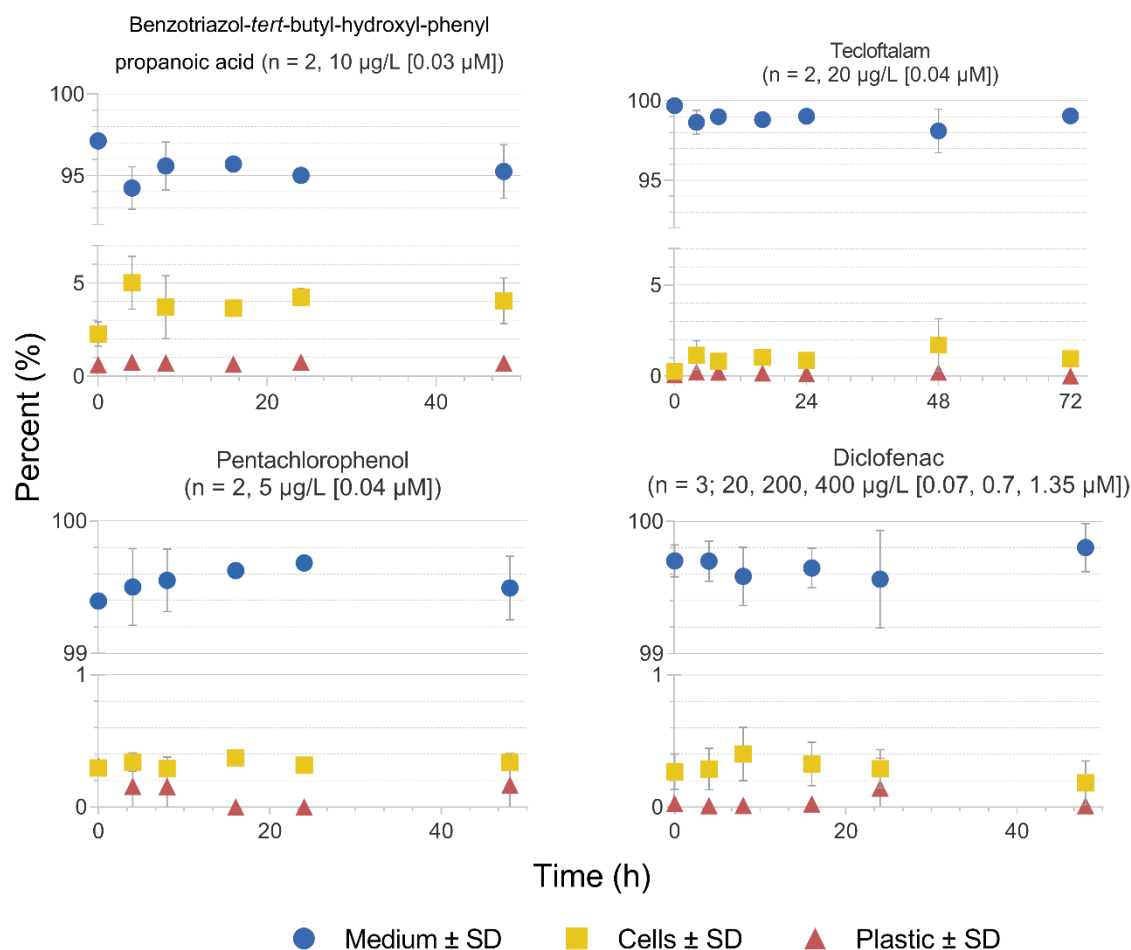


**Figure 2.3: Distribution of the compounds in the test system during bioaccumulation experiments.** Note that for diclofenac the average of three biological replicates with three different exposure concentrations is depicted. In the second replicate of tecloftalam, the time point 72 h was sampled rather than the 16 h time point. Exposure concentrations given as  $\mu\text{g/L}$  and as  $\mu\text{M}$  in brackets. SD = Standard Deviation,  $n$  = number of biological replicates.

Stadnicka-Michalak et al. (2014) conducted similar experiments in 24 well plates with RTgill-W1 cells and observed comparable accumulation, i.e. from 0.5 to 2.5% of added mass, of 8 neutral compounds (3 partly charged) with low to moderate  $K_{\text{OW}}$  from 0.57 to 4.05<sup>41</sup>. One exception was PCP, for which an apparent higher accumulation was found in the RTgill-W1 cells, about 6% of added mass<sup>41</sup>, compared to 0.4% in the present study. This difference might stem from the different analytical methods. Stadnicka-Michalak et al. (20) used radiolabeled compounds and liquid scintillation counting without HPLC for sample measurement, while here unlabeled compounds were used in an HPLC-HRMS/MS method. The liquid scintillation counting method without HPLC separation does not differentiate between parent compound and its biotransformation products so that the fraction measured in the cells reflects the sum of those. Interestingly, tetrachlorohydroquinone (THQ), a PCP biotransformation product, was found in low amounts in the exposure medium of PCP-exposed RTL-W1 cells<sup>93</sup>, which has

Investigating the bioaccumulation potential of anionic organic compounds using a permanent rainbow trout liver cell line  
been confirmed in only one *in vivo* study with striped bass to date <sup>140</sup>. In our measurements, this biotransformation product could not be detected. A possible reason is that Pietsch et al. (20) applied high (and toxic) PCP-exposure concentrations, which may have facilitated a sufficiently high and detectable production of THQ.

Another reason for the different amounts of accumulated PCP in Stadnicka-Michalak et al.'s work (20) and the present study may be differing biotransformation capabilities of RTgill-W1 and RTL-W1 cells. For example, biotransformation of benzo[a]pyrene was faster in the RTL-W1 compared to the RTgill-W1 cell line <sup>35</sup>. Yet, the presented mass balances in the current study neither indicate a measurable loss attributable to biotransformation activity (SI section S2.12, Table S2.16), nor were biotransformation products detected (SI, section S2.15). Further, the criteria for biotransformation activity of the test guidelines for *in vitro* biotransformation were not met with the exception of a significant slope in the case of PCP (<sup>23</sup>, SI section 2.16, Table S2.18). This latter finding can be seen as an indication that RTL-W1 perform PCP biotransformation, albeit at a low extent, in line with the finding by Pietsch et al. (20) and the proposal by Stadnicka-Michalak et al. (20) for RTgill-W1. Amounts of formed PCP biotransformation products in the RTL-W1 cells may have been too low to be detectable by the applied analytical method. Another reason for the failure to observe biotransformation activity and formed biotransformation products in our experiments may be the uncertainty of the quantification of test compound and the resulting variation in the mass balance. This could mask small biotransformation activity, as discussed above for PCP (SI section S2.12, Table S2.16).

While the removal of xenobiotics in fish via biotransformation, or rather general elimination, has been extensively studied knowledge on the responsible biotransformation enzymes in fish and their cell lines is limited <sup>46</sup>. The phase I enzymes CYP1A and CYP3A <sup>141, 142</sup> were shown to be expressed in fish and DCF exposure in rainbow trout was demonstrated to induce cytochrome CYP1A1 gene expression <sup>142</sup>. On a genetic bases, several subfamilies of the cytochrome 450 family were found in rainbow trout (1A, 3A, 2K and 2N), along with Flavin-containing monooxygenases, nitroreductase, alcohol and aldehyde dehydrogenases, peroxidases and uridine diphosphate glucuronosyltransferase <sup>141</sup>. RTL-W1 cells are known to have an inducible activity of CYP1A1 <sup>29, 35</sup> and basal activities of 17 $\beta$ -HSD (dehydrogenation), 5 $\alpha$ -reductase, UDP-glucuronosyltransferase isoforms, phenol sulfotransferase isoforms <sup>34</sup> and glutathione-S-transferase <sup>33</sup>. Thus, RTL-W1 cells express enzymes that are involved in phase I (addition of functional group) and II (conjugation) of biotransformation.

DCF and PCP are known to biotransform in rainbow trout <sup>143 116 108 144 121 145 146 147 142 148 149</sup>, while there is no information available on the biotransformation of BHPP and TT in fish. PCP

Investigating the bioaccumulation potential of anionic organic compounds using a permanent rainbow trout liver cell line was found to be biotransformed in rainbow trout to dechlorinated congeners<sup>146</sup> and its glucuronide and sulfate conjugates<sup>116, 143, 144, 145, 147</sup>, while DCF was biotransformed to hydroxylated DCF isomers and a variety of their conjugate isoforms, such as glucuronide, sulfate and glutathione conjugates<sup>148, 149, 150, 151</sup>. However, *in vitro* clearance of DCF in different assays, which used rainbow trout liver tissue, was relatively low (but significantly different from controls)<sup>151, 152, 153</sup> and we could not detect the formation of DCF BTPs in RTL-W1 cells. Both, the low DCF clearance previously documented *in vitro* and our observations, confirm the general difficulty to detect BTPs in *in vitro* systems. However, it appears that the formation of BTPs by the RTL-W1 cells might not be relevant to predict *in vivo* bioaccumulation as discussed below (section 2.4.4).

#### 2.4.3.2. Prediction of cell internal concentrations

When considering the differences of the test compounds'  $K_{OW}$  and  $D_{OW}$ , the compounds' pH-dependent speciation probably played a role in the observed accumulation in RTL-W1 cells. A simple partitioning exercise, which assumes an accumulation into RTL-W1 cells according to the compounds'  $K_{OW}$ ,  $D_{OW}$  or  $D_{MLW}$ , and the cells' approximated fractional volume of lipid and membrane lipid, was conducted to gain an insight into the partitioning of the test compounds (Figure 2.4, SI section S2.17).

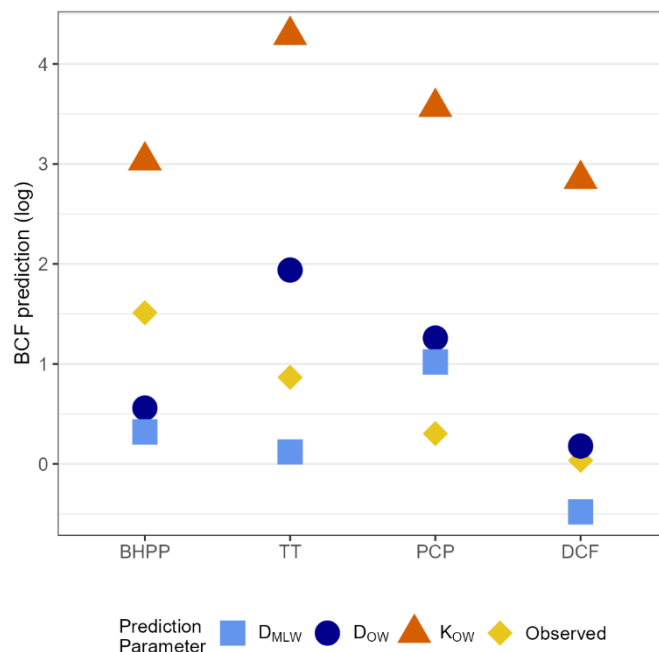


**Figure 2.4: Comparison of observed and partition coefficient-based accumulation in RTL-W1 cells.** Under the assumption of 4% (v/v) lipid and 1% membrane lipid content in RTL-W1 cells, the test compound's  $K_{OW}$ ,  $D_{OW}$  or  $D_{MLW}$  were applied to predict test compound accumulation in RTL-W1 cells. The RTL-W1 BCF values showed little variation among all replicates per test compound (SI section S2.7, Table S2.8). For more information see SI section S2.17. BHPP = benzotriazol-tert-butyl-hydroxyl-phenyl propanoic acid, TT = tecloftalam, PCP = pentachlorophenol, DCF = diclofenac.



This exercise revealed that the  $K_{OW}$  consistently overestimates the accumulation in RTL-W1 cells by about two orders of magnitudes. In contrast, the  $D_{OW}$  and  $D_{MLW}$ -based predictions are mostly within one order of magnitude of the observed accumulation in RTL-W1 cells (SI section S2.17, Table S2.20). It stands out that the  $D_{OW}$  and  $D_{MLW}$  predictions lie close to each other for all compounds, between 0.2 to 0.7 log units, except for TT. For PCP and DCF, the partition-based prediction appears to suffice to predict the accumulation in RTL-W1 cells, since observed and predicted values were within one order of magnitude. For BHPP, however, the predicted values were about one order of magnitude lower than what was observed in the cells while the observed value lay between the  $D_{OW}$  and  $D_{MLW}$  predictions for TT.

The discrepancies between observed and predicted accumulation may be caused by two reasons. First, the applied input values — partition coefficients and volumetric fractions in cells — are approximations, which could be refined if measured values or refined estimation methods became available. For TT for example,  $D_{OW}$  values range between -0.76 to 3.13 depending on which estimation software is applied, which results in very different cellular TT accumulations. However, an extensive discussion on the uncertainties of parameter estimations is beyond the focus of the present study. The volumetric cell fraction is calculated from experimental cell counts (section 2.3.8 and SI section S2.17) and reflects variations in handling that may influence the partition predictions in terms of cell mass. Second, facilitated transmembrane flux of charged compounds via transport proteins in membranes could modulate the observed accumulation in RTL-W1 cells relative to the partition-based predictions<sup>75 154 155 156 46</sup>. There is evidence, that RTL-W1 cells do possess such transporter proteins, either because they were studied in the cell line or in rainbow trout and other fish<sup>32 157 78 158</sup>. It can be assumed that some of the test compounds are substrates of such transporters in the RTL-W1 cells, contributing to the accumulation behavior. For example, organic anion transporting polypeptides may be responsible for xenobiotic uptake<sup>157 158</sup>, while some members of the ATP binding cassette transporter family may contribute to xenobiotic efflux<sup>32 78</sup>.

Another influencing factor, applying to all compounds studied here, is their charge. The neutral as much as the ionized fraction of an IOC may permeate the phospholipid bilayer of the cell membrane although the charged species diffuses considerably slower through the cell membrane compared to the neutral species<sup>14, 159</sup>. The permeation of the ionized species depends on favorable interactions between the test compound's charge and electrostatic charges of the phospholipid bilayer, steric effects, as well as pH gradients across membranes<sup>14, 26, 160</sup>. As summarized in Fu et al. (2009), acidic organic compounds, which are largely charged at pH 7, show a low BCF, due to their repulsion caused by the negative electrical potential of a cell<sup>14, 160</sup>. On the opposite, strong basic compounds (positively charged,  $pK_a > 7$ ) accumulate in cells, because of the attraction from the negative cell potential<sup>14</sup>. Further, Fu et

Investigating the bioaccumulation potential of anionic organic compounds using a permanent rainbow trout liver cell line al. (2009) report that a higher BCF for anionic organic compounds along increasing  $pK_a$  values from 3 to 6<sup>14</sup> is caused by the ion trap effect. The ion trap mechanism was shown to be present in rainbow trout cell lines<sup>161 162</sup> and is relevant for bioconcentration in fish<sup>163</sup>. On a cellular level, it occurs especially when the neutral species permeate the lysosomal membrane and, due to pH differences between cytoplasm (pH ~7) and inside the intralysosomal space (pH ~5), dissociates inside the lysosome. However, a correlation of  $pK_a$  and BCF was not found in the present study, although the  $pK_a$  values fall within the range where ion trapping may be observed (Table 2.1). Testing of compounds with a broader range of  $pK_a$  values in RTL-W1 cell exposures would give more insight into the relevance of this effect for IOC uptake into RTL-W1 cells.

It is possible that the charged fraction of test compound sorbed to the cell surface, specifically to positively charged head groups of some phospholipid species<sup>26, 74</sup> or proteins. However, under the consideration that the overall cell surface charge is negative, the sorption of anionic compounds to the external cell surface is likely small. Rather, we predict that the association of cationic compounds with the cell membrane would be more relevant, due to opposing charges of the cell membrane and the compound<sup>63</sup>. A validated mechanism, which describes the compound-dependent sorption to cell surfaces, has not been developed to date. Therefore, cell surface sorption could not be considered in the presented partition exercise.

Dedicated experiments and model approaches are needed to scrutinize the effect and contribution of each phenomenon to the overall observed accumulation in RTL-W1 cells<sup>164 37 38 165 166</sup>. In the larger context of IOCs, it would be interesting to test a set of anionic organic compounds with similar molecular structures that resemble the structure of the cell membranes' phospholipids, such as surfactants<sup>26</sup>, or cationic organic compounds, which bear positive charges<sup>167</sup>.

#### 2.4.4. Comparison of *in vitro* and *in vivo* bioaccumulation

Figure 2.5 compares the RTL-W1 BCF to the available *in vivo* bioaccumulation data and several common numerical predictions that focus on the chemical accumulation predictions in fish. Overall, the use of RTL-W1 cells to directly predict the bioaccumulation in fish performs in a similar manner as the numerical BCF predictions. With the exception of PCP, this is particularly true for  $D_{OW}$ -based BCFs (PBTK  $D_{OW}$  and  $BCF_{DOW}$ ), which are higher and more consistent with RTL-W1-derived BCF than BCF predicted based on  $D_{MLW}$ . This finding again supports the notion that uptake of chemicals into living cells involves a multitude of interactions, as discussed above. It moreover is apparent that the RTL-W1 BCF, along with the numerical BCF predictions, cannot account for *in vivo* BMFs, which were all <-1 log BMF (Table S2. 9).

Investigating the bioaccumulation potential of anionic organic compounds using a permanent rainbow trout liver cell line

Indeed, the comparison of the RTL-W1 BCFs with *in vivo* BCF or BCF<sub>BMF</sub> deviates considerably and needs to be discussed as per test compound with the caveat that no *in vivo* BCF information exists for TT and BHPP.

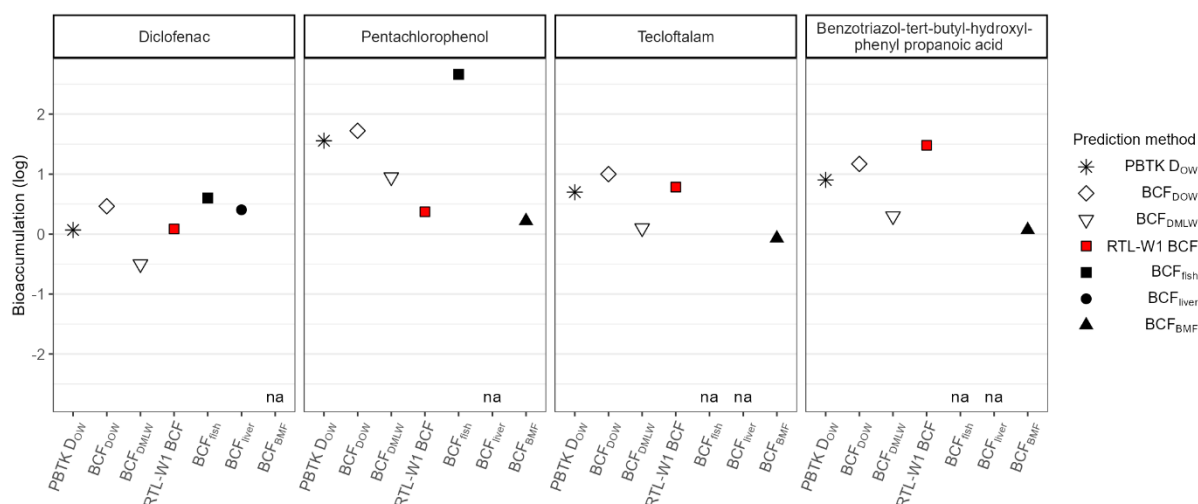


**Figure 2.5: Comparison of different prediction methods for bioaccumulation in fish.** The RTL-W1 BCF values showed little variation among all replicates per test compound (SI section S2.7, Table S2.8) and thus are not shown. All *in vivo* values (Fish/Liver BCF<sub>fish/liver</sub>/BCF<sub>BMF</sub>) were taken from rainbow trout (SI section S2.7, Table S2.9).  $\log BCF_{DMLW} = \log D_{MLW} - 1.9$ ,  $\log BCF_{DOW} = 0.85 \times \log D_{OW} - 0.7$ ,  $\log \text{RTL-W1 BCF} = \text{derived cell-based } in vitro \text{ BCF}$ , PBTk model DOW: Nichols et al. 2013<sup>18</sup> using DOW instead of KOW and neglect of biotransformation, BCF = Bioconcentration factor in whole fish, BCF<sub>BMF</sub> = Bioconcentration factor obtained from BMF conversion, see 2.3.1 and Table S2. 9. BCF<sub>liver</sub> = BCF based on sampled liver tissue<sup>102</sup>, na = not available, \*Droge et al. (2021)<sup>65</sup> \*\*EU Commission Technical Guidance Document (2004)<sup>127</sup>

DCF is the only test compound, where all accumulation predictions and the *in vivo* BCF studies lie within an order of magnitude from each other (Figure 2.5). It is notable that the RTL-W1 BCF agrees well with the *in vivo* BCF values in whole fish and liver. This indicates that the RTL-W1 cells contain the relevant accumulation mechanisms that govern the DCF accumulation in the whole fish.

For PCP, the RTL-W1 BCF is at least half an order of magnitude lower than the numerical predictions of BCFs and more than two orders of magnitude lower than the *in vivo* BCF. The difference to the numerical predictions may be caused by the suggested, although albeit small, biotransformation of PCP in the RTL-W1 cells, which reduces the RTL-W1 BCF relative to the numerical predictions that do not consider biotransformation or elimination in general. Apparently, neither RTL-W1 bioaccumulation nor numerical predictions reflect well what was measured in the one *in vivo* study using rainbow trout. BCFs of PCP in fish species other than rainbow trout indicate varying accumulations with values ranging from log BCF of 0.7 to 3.7, with a geometric mean of log BCF of 2.1 (median at 2.3) (SI section S2.18, Table S2.21).

For both, DCF and PCP, the lack of BTP identification appears to be irrelevant for the *in vivo* bioaccumulation prediction. Our RTL-W1 BCF for DCF compares well with the *in vivo* BCF despite the absence of detecting BTPs, while for PCP, the *in vivo* BCF was much higher than the RTL-W1 BCF, which appears to be independent of potential BTP formation. Biotransformation activities vary in *in vitro* as well as in *in vivo* experiments<sup>13, 101, 102</sup> and depend on tissue type as well as prior and ongoing exposure of test animals. These aspects require consideration when discussing the role of BTPs in BCF determinations.

In general all  $BCF_{BMF}$  values were lower than the numerical prediction methods, the RTL-W1 BCF and the *in vivo* BCF (Figure 2.5). In the case of PCP and TT  $\log BCF_{BMF}$  were 0.2 and -0.07 respectively and were within one order of magnitude of the *in vitro* BCF (0.37 and 0.81 respectively). However, the  $BCF_{BMF}$  may bear high uncertainties. We applied here the only established estimation method for  $k_u$  of IOC. It was derived from a method that bases  $k_u$  prediction on a combination of  $K_{OW}$ , fish weight and resistances of relatively hydrophobic compounds<sup>16</sup>. The limited number of compounds used for defining the resistances in the aqueous and organic layers (see Equation 2.1) suggest that the true compound-specific resistances may differ. Further, the original  $K_{OW}$ /fish weight-based method for  $k_u$  was found to be as imprecise as other estimation methods<sup>168</sup>. For example, the application of two different  $k_u$  models and subsequent  $BCF_{BMF}$  derivation (see 2.3.1) resulted in a  $\log BCF_{BMF} \sim -3.3$  for BHPP<sup>169 170</sup>, which is more than three orders of magnitudes higher than the value in Figure 2.5. Our chosen  $k_u$  model does consider IOC specific accumulation mechanisms, such as species-dependent resistance in the organic layer ( $R_o$ ). But certain processes, such as the passive uptake of the charged IOC species are poorly quantified (i.e. the parameter  $\beta$  see 2.3.1) and should be refined if measured values (such as passive uptake of charged species) become available. The measured *in vivo* BCF of PCP relative to the corresponding  $BCF_{BMF}$  reflects the uncertainty that is associated with the  $k_u$  estimation. Therefore, the observation that the *in vitro* BCF is either accurate or overestimates the *in vivo* BCF needs careful consideration of the limitations, if estimated  $BCF_{BMF}$  are used as reference. Biomagnification strongly depends on the xenobiotic entry via the intestines and associated residence times and depuration mechanisms, which contrast the entry via the gill<sup>163</sup>. A combination of cell lines may instead aid in BMF predictions in the future, such as a first exposure of the rainbow trout intestinal cell line, RTgutGC, followed by exposure of the RTL-W1 liver cell line.

## 2.5. Conclusions and outlook

We here developed a procedure using a permanent fish cell line, RTL-W1, to enable the measurement of intracellular amounts of IOC for bioaccumulation assessment in fish. This complements the set of assays that use fish cell lines for diverse endpoints in risk assessment,

Investigating the bioaccumulation potential of anionic organic compounds using a permanent rainbow trout liver cell line

---

such as the measurement of biotransformation rate constants for IVIVE, prediction of acute cytotoxicity in fish and the study of trans-epithelial transport. The results imply that our developed method is suitable to test diverse groups of chemicals, including anionic compounds. In the future, it would be relevant to study other structures of anionic organic compounds as well as cationic organic compounds to further evaluate the role of chemical structure and charge on bioaccumulation mechanisms that base on the structure and charge of the compound. The measured cell internal concentrations could also be used in a PBTK-based model approach to back-calculate to the exposure concentration and derive a BCF.

From a regulatory perspective, both the RTL-W1-based as well as the numerical bioaccumulation predictions indicate that the bioaccumulation of the test compounds does not surpass regulatory thresholds ( $\log \text{BMF} > 1$ ,  $\log \text{BCF} > 3.3$ )<sup>7</sup>. Despite the inability to observe biotransformation in RTL-W1 cells for the test compounds investigated here, they may be an experimental alternative to experimentation with fish if combined with other lines of evidence, such as *in vitro* biotransformation assays and/or the estimation/measurement of sorption affinities to different phases (i.e. membrane lipid etc.). The latter are based on surrogates of cellular membranes, particularly phospholipids, whereas the cells retain accumulation mechanisms that may not be reflected well by the compounds'  $D_{\text{OW}}$  or  $D_{\text{MLW}}$ . Fish cell lines should therefore be further explored as part of gathering weight of evidence and in tiered testing strategies where bioaccumulation assessments in fish remain as a last resort.

## 2.6. Acknowledgements

The authors thank Julita Stadnicka-Michalak and Andreas Buser for valuable discussions, Juliane Glüge for computations of  $K_{\text{OW}}$  values with COSMOtherm and René Schönenberger, Severin Ammann, Philipp Longree and Birgit Beck for support in the chemical analysis.

---

### 3. Bioaccumulation of cationic surfactants in permanent fish cell lines

Fabian Balk<sup>1,2</sup>, Bastian Hüsser<sup>1</sup>, Juliane Hollender<sup>1,3,§</sup>, Kristin Schirmer<sup>1,2,3,§</sup>

<sup>1</sup>Eawag, Swiss Federal Institute of Aquatic Science and Technology, 8600 Dübendorf, Switzerland

<sup>2</sup>EPF Lausanne, School of Architecture, Civil and Environmental Engineering, 1015 Lausanne, Switzerland

<sup>3</sup>ETH Zürich, Department of Environmental Systems Science, 8092 Zürich, Switzerland

§ Both senior authors contributed equally to this work

#### Credit author statement

Fabian Balk: Conceptualization, Experimental work, Formal analysis, Visualization, Writing of original draft, Review and Editing

Bastian Hüsser: Experimental work and review

Juliane Hollender: Conceptualization, Review and Editing

Kristin Schirmer: Conceptualization, Review and Editing

Reprinted with permission from Balk, F. G. P.; Hüsser, B.; Hollender, J.; Schirmer, K., Bioaccumulation of cationic surfactants in permanent fish cell lines. *Environmental Science & Technology* **2023**, (submitted).

### 3.1. Abstract

Cationic surfactants are used in many industrial processes and in consumer products with concurrent release into the aquatic environment, where they have the potential to accumulate in aquatic organisms to regulatory relevant thresholds. Here, we aimed to better understand the bioconcentration behavior of this class of compounds and set out to assess the accumulation of three selected cationic surfactants, namely *N,N*-dimethyldodecylamine (T10), *N*-methyldodecylamine (S12) and *N,N,N*-trimethyltetradecylammonium (Q14), in the cells of a fish liver (RTL-W1) and gill (RTgill-W1) cell line. We conducted full mass balances for bioaccumulation tests with the cell cultures, in which the medium, the cell surface, the cells themselves and the plastic compartment were sampled and quantified for each surfactant by HPLC MS/MS. Accumulation in/to cells correlated with the surfactants' alkyl chain lengths and their membrane lipid-water partitioning coefficient,  $D_{MLW}$ . Cell-derived bioconcentration factors (BCF) of T10 and S12 were close to *in vivo* BCF, while for Q14 the cell-derived BCF were  $\sim \log_2$  higher than the *in vivo* BCF. As a proof of concept, rainbow trout cell lines appear to be a suitable conservative *in vitro* screening method for the bioaccumulation assessment of cationic surfactants, since *in vitro* BCF were similar or higher than *in vivo* BCF.

### 3.2. Introduction

Ionizable organic compounds (IOC) are a large group of compounds with diverse structures, which are charged under environmental conditions. About 41 to 49 % of industrial chemicals preregistered at the European Chemicals Agency and substances already registered under the REACH legislation are IOC, which comprise anionic, cationic, amphoteric or permanently charged compounds <sup>48, 95</sup>. They are produced in high numbers because of their manifold applications. Cationic surfactants, for example, are being used as biocides and surfactants in consumer products, personal care products and numerous industrial processes <sup>96, 98, 171, 172</sup>. Most common cationic surfactants consist of one hydrophobic alkyl chain, which is linked to a positively charged amine or ammonium head group. Kierkegaard et al. <sup>167</sup> found 29 cationic surfactants among the registered dossiers within REACH with substantial production volumes  $\geq 1000$  tonnes/year, which necessitates an assessment of their bioaccumulative potential according to international guidance documents <sup>7</sup>. Traditionally, these bioaccumulation tests are done in experimentation with fish following OECD Test Guideline (TG) 305 <sup>9</sup>, leading to the determination of either a biomagnification factor (BMF, dietary exposure) or bioconcentration factor (BCF, aqueous exposure). The latter is more relevant for IOC bioaccumulation in fish, as IOC are expected to be mainly present in the water phase <sup>46</sup>. Therefore, the term bioaccumulation is used synonymous for bioconcentration henceforth. The animal tests are resource intense and ethically questionable due to the sacrifice of fish.

Moreover, due to their strong tendency to sorb to surfaces, cationic surfactants, just like anionic surfactants, prove experimentally difficult to assess <sup>172, 173</sup>.

Only recently, several ionic surfactants were systematically tested for their bioaccumulation potential in rainbow trout (*Oncorhynchus mykiss*) to derive BCF <sup>26, 74, 167</sup>. The measured BCF of the cationic surfactants ranged from 2.2 to 8200 L kg wet weight<sup>-1</sup> <sup>167</sup>. Seven out of twelve tested surfactants exceeded regulatory thresholds for classification as bioaccumulative (>2000 L kg<sup>-1</sup>) <sup>167</sup>. The bioaccumulation of the surfactants was found to be influenced by electrostatic interactions, causing them to sorb to surfaces, as well as their affinity to cell membranes, described by the pH-dependent membrane lipid-water distribution coefficient,  $D_{MLW}$  <sup>26, 63, 74, 167</sup>. The underlying bioaccumulation mechanism is thought to base on the structural similarity of the tested surfactants and phospholipids, which results in energetically favorable intercalations of ionic surfactants in cell membranes <sup>65, 174</sup>. Therefore, the octanol-water partition coefficient,  $K_{OW}$ , and the coefficient corrected for speciation at the pH of interest,  $D_{OW}$ , have been considered inadequate to estimate the bioaccumulation of ionic surfactants in fish <sup>63</sup>, which also pertains to IOC in general <sup>14</sup>.

Along with the bioaccumulation assessment, several cationic surfactants were tested for their biotransformation potential in hepatic S9-fractions of rainbow trout <sup>25, 175</sup>. Measured biotransformation products (BTP) were mainly demethylations of the amine group (*N*-demethylation) and the responsible enzymes were thought to belong to the CYP family <sup>25</sup>. Despite a considerable biotransformation activity of the amines in the S9 assay, and detection of some demethylation products of amines but not of the ammonium compounds (*in vivo* and in S9), the role of biotransformation in the bioaccumulation assessment in fish could not be clearly determined <sup>74, 167</sup>. Besides the S9 assays, the bioaccumulation assessment of ionic surfactants using *in vitro* cell systems as a new approach methodology has thus far found little attention <sup>26, 81</sup>. While the S9 assay represents the proteome available for biotransformation, intact cells, such as of permanent fish cell lines, combine a membrane boundary with biotransforming enzymes, which is a more realistic exposure scenario compared to the S9 assay.

Permanent fish cell lines represent an alternative to support the bioaccumulation prediction of IOC in fish. As opposed to experimentation with fish, permanent fish cell lines enable more controlled exposures, highly standardized compound testing and a mechanistic understanding of uptake and toxicity <sup>42, 94, 125, 176</sup>. The rainbow trout cell lines, RTgill-W1 (gill, <sup>30</sup>), RTL-W1 (liver, <sup>29</sup>) and RTgutGC (intestines, <sup>31</sup>) were successfully used to predict the bioaccumulation of the neutral organic compound, benzo[a]pyrene, in rainbow trout <sup>35</sup>. Recently, we used RTL-W1



cells to predict the bioaccumulation of anionic organic compounds in fish <sup>176</sup> and concluded that RTL-W1 cells can be used to predict *in vivo* bioconcentration.

In the present study, we applied a fish cell line protocol for the *in vitro* bioaccumulation assessment of cationic surfactants and assess the predictability of bioconcentration in fish. The selected cell lines were RTgill-W1 and RTL-W1. The RTgill-W1 cell line represents an important environment-organism interface for compound uptake from water while the RTL-W1 cell line represents the best-studied tissue for xenobiotic clearance in fish, i.e. the liver. As smallest units of life, we assume the cells to contain the structures and processes necessary for chemical uptake: the cell membrane as the presumably most relevant sorption matrix for surfactants, including possible static interactions with the overall negatively charged outer cell surface, and biotransformation enzymes inside the cell. We therefore hypothesized that the tested cationic surfactants will accumulate in the cells in quantifiable amounts and that derived *in vitro* BCFs are likely to follow the test compounds'  $D_{MLW}$ . We conducted the bioaccumulation tests with previously determined non-toxic exposure concentrations with both cell lines and derived mass balances for the experiments. Further, we investigated if the surfactants could desorb from the cells in two ways: 1) by the application of a rinse of the cells with ethylenediaminetetraacetic acid (EDTA) solution and 2) in a depuration-type experiment that contained a re-equilibration phase in test compound-free medium. Finally, we compared *in vitro*-based BCFs with the respective *in vivo* BCF from rainbow trout <sup>167</sup> and BCFs derived from  $D_{MLW}$  ( $D_{MLW}$  BCF).

### 3.3. Methods

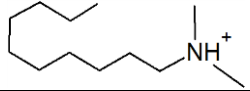
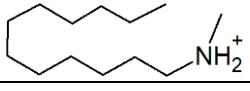
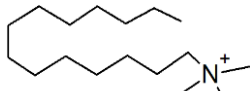
#### 3.3.1. Test compound selection

The three test compounds were selected in line with four criteria. The first criterion was that a large fraction of the test compound had to be positively charged at environmentally relevant pH (7-8) with smaller fractions of the neutral species. The second criterion was the availability of high quality BCF, following OECD TG305 <sup>9</sup>. Third, the selected compounds should have structural similarities but subtle differences, which may influence their bioaccumulation behavior. As last criterion, the test compounds should be of environmental relevance.

In line with these criteria, the three test compounds selected for testing were: *N*-methyldodecylamine (S12), *N,N*-dimethyldecylamine (T10) and *N,N,N*-trimethyltetradecylammonium (Q14). Detailed information about the test compounds can be found in Table 3.1 and Section S3.1 (Purity, vendor, CAS registry number) in the supporting information (SI). These three test compounds have an alkyl chain of different lengths with a nitrogen head. Each of the test compounds bears a different number of methyl substituents at

the nitrogen, which makes the test compounds a secondary amine (S12, one methyl substituent), a tertiary amine (T10 two methyl substituents) and a permanently charged quaternary ammonium ion (Q14, three methyl substituents).

**Table 3.1: Relevant structural and physico-chemical properties of the test compounds.** Please be aware that the depicted alkyl chains would be linear under experimental conditions.

Structure (charged species)	Compound	Acro- nym	Formula	pK <sub>a</sub> <sup>1</sup>	Log D <sub>MLW</sub> <sup>2</sup>	Log D <sub>OW</sub> <sup>3</sup> (pH 7)	Log K <sub>OW</sub> <sup>3</sup>
	<i>N,N</i> -dimethyldecyl-amine	T10	C <sub>12</sub> H <sub>27</sub> N	9.79	3.65	2.53	6.13
	<i>N</i> -methyldodecyl-amine	S12	C <sub>13</sub> H <sub>29</sub> N	10.78	5.16	4.77	6.57
	<i>N,N,N</i> -trimethyltetradecyl ammonium	Q14	C <sub>17</sub> H <sub>38</sub> N	n/a	5.54	n/a	n/a

<sup>1</sup>Taken from ACD/Labs, <sup>2</sup>average of three methods <sup>63</sup>, <sup>3</sup>calculated using COSMOtherm version 2022 and Henderson-Hasselbalch equation for D<sub>OW</sub>, n/a = not available

### 3.3.2. Routine cell culture

RTgill-W1 <sup>30</sup> and RTL-W1 <sup>29</sup> cells were cultured in cell culture flasks (150 cm<sup>2</sup> growth area, Techno Plastic Product AG) at 19 ± 1 °C in the dark and atmospheric pressure in 20 mL of cell culture medium, which consisted of Leibovitz's medium (L-15, Invitrogen) and a 5 % (v/v) fetal bovine serum (FBS) supplement (termed from here on L-15/FBS). Cell cultures with an approximately 95 % confluency were used for seeding of an experiment (see below). For acute cytotoxicity assays with RTgill-W1 cells, cell passages 67 to 70 were used; for confirmation of non-toxic concentrations and bioaccumulation experiments, passages 73 to 85 of the RTgill-W1 cell line and 79 to 88 of the RTL-W1 cell line were used.

### 3.3.3. Determination of non-toxic exposure concentrations

A detailed description of the procedure for determination of non-toxic exposure concentrations is available in Balk et al. <sup>176</sup>. In brief, fluorescence-based acute cytotoxicity assays, in line with OECD TG249 <sup>43</sup>, were conducted with RTgill-W1 cells over 24 h to obtain concentration-response curves for each test compound. These assays apply the fluorescent dyes alamarBlue<sup>TM</sup>, 5-carboxyfluorescein diacetate acetoxymethyl ester (CFDA-AM) and Neutral Red, which indicate metabolic activity, cell membrane integrity and lysosomal membrane integrity, respectively <sup>43</sup>. RTL-W1 cells do not sustain the conditions of this assay, but we

assumed that the observed cytotoxicity in RTgill-W1 is representative also for RTL-W1. The concentration-response curves were corrected for measured exposure concentrations and served to calculate effective concentrations of 50 % reduction in cell viability ( $EC_{50}$ ) and non-toxic exposure concentrations (SI section S3.9 and S3.10) <sup>45</sup>. The exposure concentrations of the test compounds were determined in line with three criteria: 1) The chosen exposure concentration should be as low as possible and not cause toxicity in exposed cell cultures; 2) it should be  $\leq 1 \mu\text{M}$  to avoid enzyme inhibition in the exposed cells and 3) it should be at least 10 times above the method limit of quantification (LOQ). The chosen exposure concentrations were confirmed as non-toxic in exposures of RTgill-W1 and RTL-W1 cells over 72 h (SI section S3.10) by the application of the fluorescence-based cytotoxicity assays. The only difference in the exposure of the two cell lines to assess cytotoxicity was the supplementation of the exposure medium of RTL-W1 cells with 5 % (v/v) FBS to sustain the liver cells for the assay duration.

#### **3.3.4. Cell densities and seeding of RTgill-W1 and RTL-W1 for bioaccumulation experiments**

In our previous work, a procedure for bioaccumulation assessment of minute amounts of organic compounds in RTL-W1 cells has been established in cell culture flasks <sup>176</sup>. Optimal seeding densities were determined to obtain confluent monolayers within 2 days. For RTL-W1 and RTgill-W1 cells in the cell culture flasks (25 cm<sup>2</sup> growth area, Techno Plastic Product AG), this number was  $3.3 \times 10^6$  cells/flask and  $4.6 \times 10^6$  cells/flask, respectively, each in 6 mL of cell culture medium. Both seeding densities showed minimal fluctuations in cell number over the experimental duration (SI section S3.8 and <sup>176</sup>). The cell suspensions were prepared based on cell counts using the electronic cell counting system CASY TCC (BIOVENDIS Products GmbH, see <sup>176</sup>). Before starting a bioaccumulation experiment, the seeded cell cultures were incubated for 48 h to 72 h under routine culture conditions to reach confluency.

#### **3.3.5. Bioaccumulation experiments**

The detailed description of the bioaccumulation experiments can be found in the SI section S3.2 and in Balk et al <sup>176</sup>. To start an experiment, the routine cell culture medium was removed from a flask and replaced with 3 mL of the L-15/FBS exposure medium. Exposed cells and cell-free negative control flasks were sampled at 0 h, 4 h, 8 h, 24 h, 48 h and 72 h, whilst a cell count control and a test compound-free control were sampled at experimental onset and termination. Every 24 h, the medium pH was measured using a small pH probe (microFET, Welling) or indicator strips (Macherey-Nagel). At each sampling time point, medium, cell surface, the cells themselves and the plastic were sampled. Unlike in our previous experiments

<sup>176</sup>, we sampled the cell surface by rinsing with 400  $\mu$ L Versene solution for 30 seconds. Versene contains the cell dissociation agent ethylenediaminetetraacetic acid (EDTA), which chelates with divalent metal ions <sup>177</sup>, due to its four carboxylic acid groups with strong dissociation constants ( $pK_a$  0.26 to 2.76 <sup>178</sup>). Thus, any test compound loosely associated with the cell surface would have been sampled with the EDTA upon the rinse with Versene. Between sampling of different fractions, we introduced washing steps to minimize carryover of test compound. For test compound extraction and protein precipitation, samples were cooled to -80 °C, centrifuged and subsequently sonicated in a water bath <sup>176</sup>.

Initial trial measurements showed considerable background contamination of all test compounds in the materials used for experimentation, as well as the material used for chemical analysis. Therefore, all glassware used for experimentation and sample measurement was heated to 500 °C for 150 min to destruct any organic contaminants. Reusable plastic containers were rinsed twice with acetone and subsequently once with methanol and left to dry.

### 3.3.6. Bioaccumulation experiments with re-equilibration

In an attempt to assess association of test compound with the exposed cells, a re-equilibration phase was introduced in experiments with Q14, where the exposure medium was exchanged after 24 h with 3 mL of test compound-free medium. This time point was selected because a trial experiment with RTgill-W1 cells at 100  $\mu$ g L<sup>-1</sup> exposure concentration showed that the test compound distribution reached steady state well within 24 h and the acute cytotoxicity assays indicated no cytotoxicity at this concentration (SI section S3.10). However, in acute cytotoxicity assays over 72 h in the absence of FBS, RTgill-W1 cells indicated cytotoxicity at this concentration (SI section S3.10). Therefore, we used a lower exposure concentration of 20  $\mu$ g/L in experiments including a re-equilibration phase with RTL-W1 cells. Nevertheless, we included the initial trial experiment with 100  $\mu$ g/L of Q14 in RTgill-W1 in our discussions, since the supplemented FBS in the exposure medium likely protected the cells from toxic effects, as indicated by the stable cell counts in the trial experiment (0 h : 6.9x10<sup>6</sup> cells/flask, 72 h: 7.2x 10<sup>6</sup> cells/flask, SI section S3.8). During the exposure phase, the experimental onset (0 h) and end of the exposure phase (24 h) were sampled, while the re-equilibration phase was sampled more often (1 h, 3 h, 6 h, 24 h post medium exchange). The sampling of all compartments was done as described above.

### 3.3.7. Mass balances and *in vitro* bioconcentration factors

The calculations are detailed in the SI section S3.3. In brief, at each time point x, the test compound distribution (%) in the bioaccumulation experiments was calculated as the sample

type of interest over the total amount of the sample types (medium, cells, etc.) at time point x. The *in vitro* BCF was calculated as the quotient of the cell concentration and the medium concentration at apparent steady state (incl. all times points  $\geq 24$  h), while the  $D_{MLW}$ -based BCF was derived using the approximated cellular phospholipid volume fraction (0.01)<sup>179</sup> and the test compound's  $D_{MLW}$ .

### 3.3.8. Chemical analysis

For compound quantification, a high performance liquid chromatography electrospray ionization tandem high resolution mass spectrometry system was used (HPLC-ESI-HRMS/MS, QExactive, QExactive Plus or Exploris, Thermo Fisher Scientific). After injection of 25  $\mu$ l of sample, separation was achieved using an XBridge C18 column (3.5  $\mu$ m, 2.1 x 50 mm) and a methanol/water gradient, both containing formic acid (0.1% (v/v)) and 1 mM ammonium acetate. Commercial ultrapure water was used as eluent for chemical analysis to avoid contamination from the Millipore water production unit. The samples were measured in plastic auto sampler vials (8004-WM-PP, infochroma ag) to minimize potential adsorption to the glass vial walls. For more details on the chemical analysis, see SI section S3.4. In addition, especially where biotransformation activity was indicated by the calculated mass balances and OECD TG319 criteria, a suspect screening was conducted with Compound Discoverer v3.3 (Thermo Fisher Scientific Inc.) for biotransformation products (SI section S3.5). The peak shape with at least five mass scans comprising one peak and a signal to noise ratio greater than ten were used to set the limit of quantification (LOQ). Tetradecyl- $d_{29}$ -trimethylammonium was used as internal standard for Q14. For S12 and T10, no isotope labelled homologs were available. Therefore, decyl- $d_{21}$ -trimethylammonium was selected as internal standard based on its comparable retention time and structural similarity. For peak detections below the LOQ, half of the LOQ ( $0.5 \cdot \text{LOQ}$  ( $\text{ng L}^{-1}$ )) was used to calculate the test compound amount. This assumption only became relevant for one re-equilibration experiment with Q14, where the exposure medium samples of the last two time points were  $< \text{LOQ}$ . Resulting uncertainties are discussed below in section 3.4.2. A relative recovery was calculated for each sample matrix by spiking a known amount of test compound in exposure medium, harvested cell solution, Versene and pure methanol from the plastic fraction (SI section S3.6). Quantified sample concentrations of test compound without isotope-matching internal standards were corrected with the relative recovery.

### 3.3.9. Data analysis

Processed data were analyzed and visualized using the programming language R<sup>129</sup>, the R packages openxlsx, tidyr, dplyr, ggplot and patchwork<sup>130 131 132 133 134</sup>, GraphPad Prism 9.4.0 (GraphPad Software) and ChemsSketch 2021.1.2 (ACD/Labs)<sup>50</sup>.

## 3.4. Results and Discussion

### 3.4.1. Cytotoxicity elicited by test compounds

EC<sub>50</sub> values were derived for all test chemicals in acute cytotoxicity assays with RTgill-W1 over 24 h (Table 3.2). Measured exposure concentrations at 0 h and 24 h of exposure in the medium and respective concentration-response curves can be found in the SI section S3.9. The fluorescence response of alamarBlue™ (measuring metabolic activity) was the most sensitive, with the sequence of toxicity from highest to lowest being Q14 > S12 > T10 (Table 3.2). It stands out that the EC<sub>50</sub> values derived from measured medium concentrations are consistently lower than the EC<sub>50</sub> based on nominal concentrations, which we attribute to a reduced availability of test compounds over the duration of the assay, mainly due to sorption processes.

Due to the poor characterization of the *in vivo* studies and the limited number of available LC<sub>50</sub> values (Table 3.2), only a partial comparison of the LC<sub>50</sub> and our cell-derived *in vitro* EC<sub>50</sub> could be made. For T10, the EC<sub>50</sub> was ~16-fold higher than the LC<sub>50</sub> in fish. Other tertiary amines with longer alkyl chains exhibited LC<sub>50</sub> that ranged from 0.62 mg L<sup>-1</sup> (mix of 12 to 14 alkyl chained tertiary amines) to 0.26 mg L<sup>-1</sup> (16 alkyl chained tertiary amine), indicating that the LC<sub>50</sub> was dependent on alkyl chain length<sup>180</sup>. A similar finding of chain-length dependent toxicity (EC<sub>50</sub>) was found for quaternary ammonium surfactants in cytotoxicity assays with RTgill-W1<sup>181</sup>. Our EC<sub>50</sub> of Q14 (0.08 mg L<sup>-1</sup>) was well within the range of EC<sub>50</sub> of similarly structured quaternary ammonium surfactants, such as benzyldimethyltetradecylammonium (EC<sub>50</sub>: 0.02 mg L<sup>-1</sup> in RTgill-W1)<sup>181</sup> and hexadecyltrimethylammonium (EC<sub>50</sub>: 0.83 mg L<sup>-1</sup> in PLHC-1C cell line)<sup>182</sup>. The comparison is limited, however, by the few tested compounds in the cytotoxicity assay as well as the limited availability of *in vivo* data in fish (Table 3.2). OECD TG249 is based on a correlation of the EC<sub>50</sub> after 24 h exposure of RTgill-W1 cells with the LC<sub>50</sub> after 96 h of the acute toxicity assessment in fish (OECD TG203, Table 3.2). Table 3.2 For T10, it was unclear whether exposure concentrations were documented as measured or nominal<sup>180</sup>. For Q14, the documented *in vivo* exposure concentration was nominal and measured over only 24 h, which implies that the actual LC<sub>50</sub> was likely lower.

**Table 3.2: EC<sub>50</sub> values of acute cytotoxicity assays performed with RTgill-W1 cells.** Determination based on alamarBlue™ fluorescence responses. The fluorescence responses of all dyes and test compounds can be found in SI section S3.9, Table S3.8. 95% CI = 95% confidence interval, S12 = N-methyldodecylamine, T10 = N,N-dimethyldodecylamine, Q14 = N,N,N-trimethyltetradecylammonium

Test compound	Nominal EC <sub>50</sub> [95% CI] (mg L <sup>-1</sup> )	Measured EC <sub>50</sub> [95% CI] (mg L <sup>-1</sup> )	LC <sub>50</sub> (mg L <sup>-1</sup> )
S12	2.3 [2.2 - 2.4]	1.3 [1.2 - 1.4]	not available
T10	39.9 [37 - 49]	18.1 [16.8 - 19.5]	1.13 <sup>1</sup>
Q14	0.5 [0.48 - 0.52]	0.08 [0.08 - 0.1]	1.92 <sup>2</sup>

<sup>1</sup> acute fish toxicity 96 h in unknown fish species in line with OECD TG203. More information on exposure conditions and whether concentrations were measured was not accessible <sup>180</sup>, <sup>2</sup> 24 h acute toxicity in rainbow trout in line with OECD TG203 (1993) under static exposure conditions, nominal concentrations reported <sup>183</sup>

The obtained concentration-response curves were used to derive non-toxic exposure concentrations <sup>45</sup>, which were applied for the determination of exposure concentrations for later use in the bioaccumulation experiments. Additionally, the determined exposure concentrations were used in acute cytotoxicity assays with RTgill-W1 and RTL-W1 and a cell-free control, which confirmed that the exposure concentrations were non-toxic over the time periods up to 72 h (SI section S3.10).

### 3.4.2. Bioaccumulation experiments

The test compounds showed a drastic redistribution from the exposure medium to the cells over the experimental duration (Figure 3.1, SI section S3.12). On average, 31±2 % of T10, 83±2 % of S12 and 92±3 % of Q14 of the initial compound mass was found associated with the cells within 24 h. The RTL-W1 and RTgill-W1 cell lines accumulated similar amounts of the cationic surfactants in the cell fraction (within 10 %, SI section S3.12), indicating that the accumulation mechanism in both cell lines is similar. The observed accumulations appear to depend on the alkyl chain length of the test compound: the longer the alkyl chain, the higher the accumulation in the cells of the test system. The same trend was found for an *in vivo* study on the bioaccumulation of cationic surfactants in rainbow trout <sup>167</sup>.

Another study, which derived mass balances of experiments with RTgill-W1 cells exposed to a cationic quaternary ammonium compound, benzyldimethyldodecyl-ammonium (nominal 150 µg L<sup>-1</sup> exposure), measured ~35 % of test compound in the cells <sup>81</sup>. This is in agreement with our reported accumulation range between 31 % to 92 % of total compound. Other studies

that tested anionic and neutral compounds with RTL-W1 cells show contrasting accumulations<sup>35, 41, 176</sup>. For example, anionic organic compounds of diverse molecular structure accumulated to a maximum of  $4 \pm 0.7$  % in RTL-W1 cells<sup>176</sup>. A neutral compound, benzo[a]pyrene, was rapidly biotransformed, thus showed little accumulation in RTL-W1 cells<sup>35</sup>. Similar low accumulations were also found for other neutral compounds with a wide range of hydrophobicity and volatility, where accumulations in RTgill-W1 cells ranged between <1 to ~10 %.

To be able to distinguish whether the test compounds were truly taken up by cells or merely adsorbing to their surface, a rinse with EDTA solution was conducted prior to sampling the cell fraction. This rinse revealed 0-3 % of the initial test compound mass, i.e. very little loosely, surface-bound compound. In comparison, 1-12 % was extracted with methanol from the plastic. These results indicate that there is negligible loose binding on the outer cell surface (Figure 3.1).

To investigate if the chemical with the greatest association with cells, i.e. Q14, would establish a new equilibrium between cell and medium compartment, experiments were carried out in which RTL-W1 cells were further incubated after the Q14 had been removed and replaced once with chemical-free complete medium. We observed that  $94 \pm 1$  % of the Q14 associated with the cell fraction remained associated with the cells during the re-equilibration phase (Figure 3.1) and minimal Q14 amounts re-distributed to the medium. However, it appears that this re-distribution of Q14 between cells and Q14-free medium during the re-equilibration phase was driven by Q14's cell membrane affinity, described by its  $D_{MLW}$ . On average over all time points, medium concentrations of Q14 in the re-equilibration phase (steady state assumed) were  $\sim 1300$  ng L<sup>-1</sup> relative to a  $D_{MLW}$ -predicted medium concentration of 129 ng L<sup>-1</sup> (derived from average cellular concentrations of the re-equilibration phase divided by  $D_{MLW}$ ). However, the concentration in the medium was likely lower than our measured value, since some samples were <LOQ (SI section S3.12) and control samples contained slightly higher amounts of Q14. Considering only quantifiable samples, our measured medium concentrations would be 480 ng L<sup>-1</sup>, which compares better to the predicted 129 ng L<sup>-1</sup>. An identical experiment including a re-equilibration phase conducted with T10 and RTL-W1 cells resulted in better comparable measured and  $D_{MLW}$ -predicted concentrations (measured: 19.7 µg L<sup>-1</sup>,  $D_{MLW}$ -predicted: 15.5 µg L<sup>-1</sup>). This suggests that cell accumulation of Q14 and T10 follow their  $D_{MLW}$ . Further experiments should repeatedly exchange the medium during the re-equilibration phase to measure the continuous re-equilibration between the cell and medium fraction.



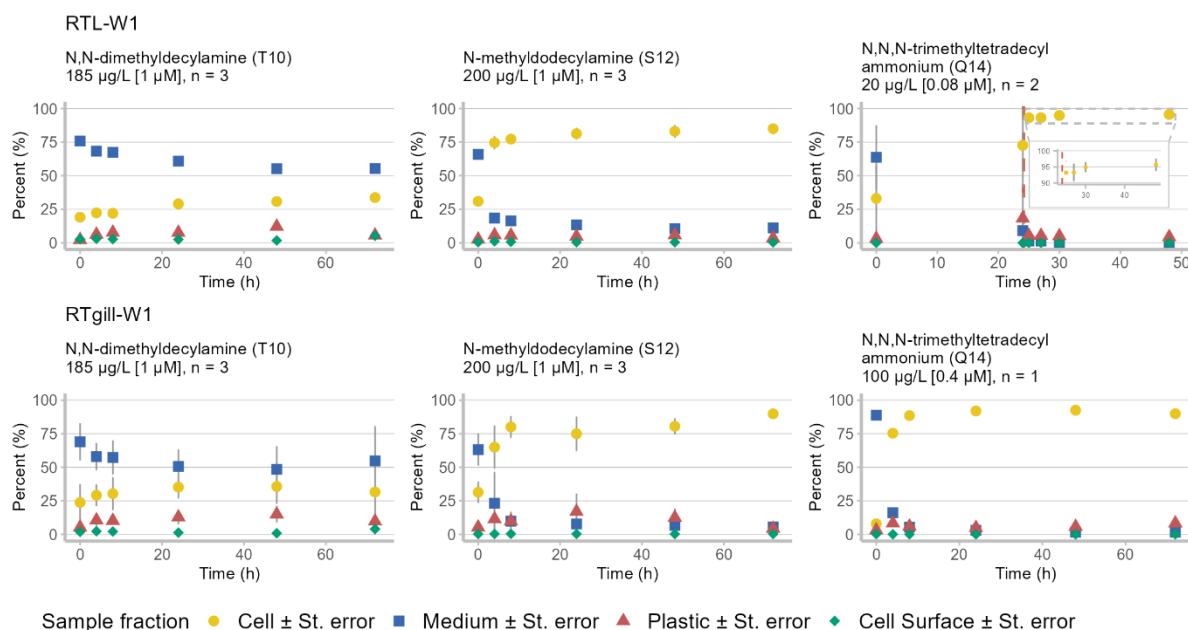


**Figure 3.1: Mass balances of test compounds in exposed RTL-W1 and RTgill-W1 cells exposed over 48 h/72 h.** The top row depicts experiments with RTL-W1, the bottom row experiments with RTgill-W1. The applied nominal exposure concentrations are given below the compound names, the total found was set to 100% at each time point. In addition, one trial experiment containing a re-equilibration phase was conducted with T10 in RTL-W1, which is not shown here. The red dashed line indicates the onset of the re-equilibration phase for Q14 (after 24 h of exposure). Please note that for Q14 (RTL-W1), the data points for the medium concentrations are partly covered by other data points. The experiments with Q14 were conducted in duplicate since previous experiments with T10 and S12 showed good reproducibility across the biological replicates. Further, because we did not see considerable differences in the accumulation behavior between RTgill-W1 and RTL-W1, the experiment with Q14 in RTgill-W1 was conducted only once. n = number of biological replicates, error bars mark = standard deviation

Measured pH values ranged from 7 to 7.5 with no clear trends for changes dependent on compound exposure or the presence of cells (SI section S3.11). A caveat was the use of pH strips, which could only give a resolution of 0.5 pH units. A variation by 0.5 pH meant a potential 2.6-fold change of neutral T10 and 2-fold change of neutral S12, which may have influenced the accumulation. It was shown that varying water pH in *in vivo* studies with rainbow trout (pH 6.2 and 7.6) lead to different BCF values of T10 while it had no influence on the permanently charged Q14<sup>167</sup>. However, our experiments were not designed to study the impact of pH; all experiments were conducted at the same starting pH of ~7.5. It is likely that RTgill-W1 and RTL-W1 cells withstand a broad pH range of 6 - 8.5 at which they retain full functionality, as it has been shown for RTgill-W1<sup>184</sup>. Therefore, it would be feasible to conduct experiments with varying pH of the exposure medium to study pH-dependent accumulation in the rainbow trout cell lines.

### 3.4.3. Biotransformation activity in bioaccumulation experiments

The derived mass balances, together with the screening for biotransformation products (BTP) were used to assess the biotransformation activity in RTgill-W1 and RTL-W1 cells. In a first step, we applied the criteria of OECD TG319 to the mass balances of the bioaccumulation experiments<sup>23, 24</sup>. In brief, the total test compound masses per sample time point of all replicates were set against time to determine if there was a significant loss of parent compound as determined via linear regression (slope significantly different from 0, and  $R^2 \geq 0.85$ ) to detect biotransformation activity (SI section S3.14). The slope of the linear regression was significantly different from 0 for experiments with S12 and RTL-W1, but the  $R^2$  (0.45) was below the cut-off value of 0.85 (SI section S3.14). For T10 and Q14, the above mentioned criteria for parent compound loss were not met (SI section S3.14). For Q14, this is in agreement with depuration studies in liver S9-fractions, which neither observed the formation of any BTP of Q14 nor significant Q14 losses applying the criteria from OECD test guidelines<sup>23, 24</sup>.

Our findings for T10 contrast hepatic S9 studies, where T10 depuration fulfilled the OECD criteria for biotransformation activity (significant slope from 0, negative control <20 % loss relative to activate S9,  $R^2 = 0.92$ )<sup>25, 175</sup>. In our experiments with RTL-W1 cells exposed to T10, the slope of the linear regression was significantly different from 0, as was for the cell-free control. It seems that biotransformation activity in our experiments was too low to cause parent compound loss to meet the OECD criteria. Due to the significant loss in the cell-free control of T10 experiments with RTL-W1, biotransformation activity could have been masked by potential abiotic loss. To obtain more information on biotransformation activity in the RTL-W1 cells, we screened the experiments with significant slope for suspected BTPs (SI section S3.5 and S3.15). Specifically, we screened for demethylated products, as shown in depuration studies with hepatic S9-fractions from rainbow trout<sup>25, 175</sup>. Demethylated T10 was indeed found although the amounts were below the limit of quantification (SI section S3.15). Further, the cell-free controls and other quality controls also contained demethylated T10, potentially originating from an impurity in the stock solution, which was not found in the reported hepatic S9 studies<sup>25</sup>. Therefore, it was not possible to distinguish the formation of the demethylated BTP of T10 from a potential impurity. Interestingly, demethylated T10 (S10) formation decreased over time in the S9 experiments with concurrent slight increase of the secondary BTP, namely the twice demethylated T10 (P10)<sup>25</sup>. Our experiments, however, only indicate an increase of demethylated T10 formation with no clear decrease over time and no formation of twice demethylated products. Thus, it appears that the S9 studies are not directly comparable to our experiments with intact RTL-W1 cells, which might be due to different

accessibilities of biotransformation enzymes. For S12 and Q14, no BTPs could be detected in any of the experiments.

The detection of demethylated T10 below LOQ and the significant loss of S12 imply slow biotransformation as it has been suggested in our previous work with pentachlorophenol exposed RTL-W1 cells <sup>176</sup>. In contrast, benzo[a]pyrene, a neutral compound, was found to be quickly biotransformed by RTL-W1 with concurrent increase in CYP1A activity <sup>35</sup> and RTgill-W1 cells in the absence of an induction of CYP1A <sup>35</sup>. The RTL-W1 cell line has thus far received more focus on its biotransformation capabilities than RTgill-W1 and the expression of several phase I and II biotransformation enzymes has been described <sup>29, 33, 34, 35, 94</sup>. However, there is clear indication that RTgill-W1 cells likewise contain biotransformation capacity <sup>35</sup>.

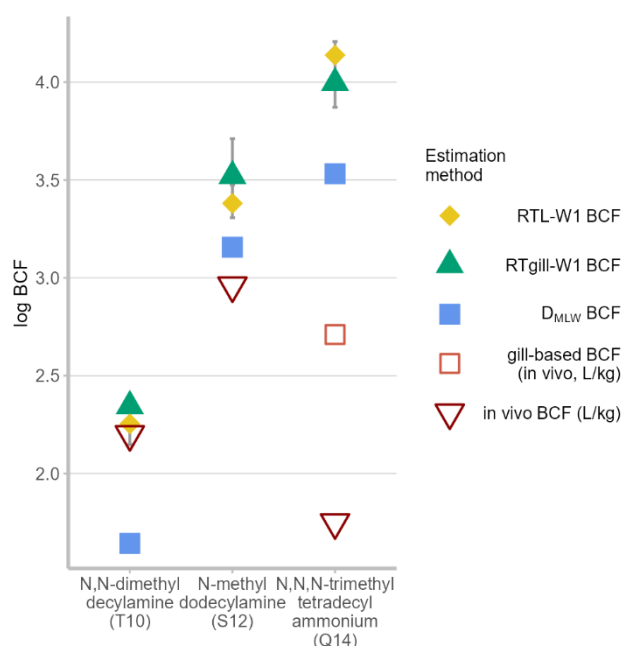
#### 3.4.4. Comparison to *in vivo* BCF and D<sub>MLW</sub>-predicted BCF

Figure 3.2 shows the comparison of cell-based, *in vivo* and D<sub>MLW</sub>-based BCFs (D<sub>MLW</sub> BCF: assuming 0.01 volume fraction of phospholipid in cells <sup>179</sup>, SI section S3.13). We assumed that the medium concentration was analogous to the total water concentration for BCF calculations (see methods). This assumption is well justified, since the mass balances, which demonstrate immense uptake by the cells, indicate that the impact on bioavailability by the medium constituents of our test compounds is small or at least that desorption and replenishment of the neutral bioavailable fractions was not lowered. Longer chain surfactants, however, might show decreased bioavailability in the medium, due to sorption processes, in which case a freely dissolved concentration could be measured <sup>185</sup> or approximated <sup>90</sup>. The cell line-derived *in vitro* BCFs increase with longer alkyl chain of the test compounds. As a result from the similar extent of accumulation in both cell lines (Figure 3.1), the *in vitro* BCF of all test compounds only marginally differed between the cell lines (Figure 3.2). The *in vitro* BCFs were also comparable to the D<sub>MLW</sub>-based predictions of accumulation, where the differences were maximally 0.7 log units (T10). We varied the relevant phospholipid volume fraction according to measurements done in mammalian cell lines <sup>89</sup> from 0.01 to 0.034 to get an insight into the resulting variation of the D<sub>MLW</sub> BCF, which was maximal 0.6 log BCF (T10: 1.6 - 2.2, S12: 3.2 - 3.7, Q14: 3.5 - 4.1) units higher than the presented D<sub>MLW</sub> BCF (Figure 3.2, based on 0.01 phospholipid volume fraction). For future studies, it would be relevant to determine the phospholipid content in the fish cells to refine associated predictions. Similar predictions that use the test compounds' D<sub>OW</sub> or K<sub>OW</sub> were not consistently accurate or overestimated the cellular accumulation (assuming 0.04 lipid fraction as in whole fish, SI section S3.13). It is noteworthy that the K<sub>OW</sub> of the neutral and ionic species were modelled with a quantum-chemical based software (COSMOtherm). Yet, they seem to be at least partly inaccurate as measured fish oil-water distribution ratios for surfactants are considerably lower compared to our reported predictions <sup>65</sup>. Overall our results

imply that the underlying mechanism for accumulation is similar in both cell lines and is likely driven by the test compound's affinity to phospholipid membranes. This mechanism has previously been suggested to be the main driving force of the cationic surfactants' bioaccumulation in rainbow trout, which supports our observations<sup>63, 65, 74, 167</sup>. Yet, all  $D_{DMLW}$  BCF were lower compared to the *in vitro* BCF suggesting that other sorption phases, such as cellular protein, or active uptake processes may contribute to the cellular accumulations.

It is noteworthy that the RTL-W1 BCF and RTgill-W1 BCF of Q14 are well comparable, despite the differing exposure concentrations in each experiment (RTgill-W1: 100  $\mu\text{g L}^{-1}$ , RTL-W1: 20  $\mu\text{g L}^{-1}$ , Figure 3.1 and Figure 3.2). This demonstrates that the bioaccumulation of Q14 was independent of the exposure concentration, which is according to the theory<sup>186</sup>. Strikingly, for T10 and S12, the *in vivo* BCF from rainbow trout studies were very close to the *in vitro* BCFs, being within factor 1.3 and 3.5 for T10 and S12, respectively (Figure 3.2 and SI section S3.13).

The increases in BCF per carbon atom in the alkyl chain of non-permanently charged amines were similar for *in vitro* and *in vivo* BCF. Our *in vitro*-derived BCFs for T10 and S12 increased by  $\sim 0.6$  log units per carbon atom, while it was  $\sim 0.4$  log units per carbon for the different secondary and tertiary alkyl amines in *in vivo* experiments with rainbow trout<sup>167</sup>. However, the small number of test compounds may bear uncertainty regarding the observed chain length-dependency of the *in vitro* BCF. Different to the *in vivo* study<sup>167</sup>, in our experiments with three compounds, the alkyl chain impact could not be differentiated from the influence of the degree of methylation at the functional head group<sup>167</sup>. Notably, the cell lines gave consistently higher, thus more conservative, BCF estimations than the  $D_{MLW}$ -derived BCF. The consistently higher *in vitro* BCF led to considerable differences for Q14 *in vitro* and *in vivo* BCFs.



**Figure 3.2: Comparison of *in vitro* BCFs with DMLW-based predictions and *in vivo* BCFs.** Error bars represent the variations in cell number and test compound quantification across biological replicates, data points represent the mean. Q14's RTgill-W1 BCF was conducted at  $100 \mu\text{g L}^{-1}$  while Q14's RTL-W1 BCF at  $20 \mu\text{g L}^{-1}$  (Figure 3.1). *In vivo* BCF in rainbow trout <sup>167</sup>,  $D_{MLW}$  BCF =  $D_{MLW}$ -based prediction of the BCF in cells, gill-based BCF = tissue-normalized BCF <sup>74</sup>

The *in vivo*-derived BCF of Q14 is up to 2.4 orders of magnitude lower than the *in vitro* BCFs or the  $D_{MLW}$  BCF (Figure 3.2). Kierkegaard et al. <sup>167</sup> argued in their *in vivo* study that the permanent charge of Q14 considerably limits the compounds uptake into fish <sup>167</sup>. Indeed, most of the Q14's body burden in fish was associated with the gill tissue (70 %) <sup>74, 167</sup>, which is reflected in the gill tissue-normalized BCF (Figure 3.2). The distribution into the remaining body was suggested to be limited by the slow diffusion of Q14 across the gill membrane <sup>25</sup>. The fact that only very small amounts of Q14 partition from cell tissue into other compartments can be seen in our re-equilibration study with RTL-W1 cells exposed to Q14 (Figure 3.1). A similar partitioning behavior might have occurred in the fish's gill-blood stream interface *in vivo*, which then resulted in the low *in vivo* BCF with most of the body burden in the gill tissue. Interestingly, the low BCF of Q14 *in vivo* was also not explained by a high elimination rate. Q14's elimination rate of  $0.0020 \text{ h}^{-1}$  was among the lowest rates in the study, where elimination rates ranged from  $0.0020$  to  $0.129 \text{ h}^{-1}$  for cationic surfactants <sup>167</sup>. However, our experiments of single cell culture exposures cannot simulate the partitioning of Q14 into different compartments as seen *in vivo* <sup>74, 167</sup>. An insert test system with one cell line seeded in the apical chamber could be applied to address the question whether significant partitioning of Q14 across the cell layer into the basal chamber occurs <sup>37, 184</sup>.

Apart from Q14, the cell exposures and  $D_{MLW}$ -based predictions suffice to predict bioaccumulation of T10 and S12 in rainbow trout. This is particularly interesting considering the fact that biotransformation appears to be irrelevant for the bioaccumulation of all test compounds in our work. This finding raises the question whether the test compounds were accessible for biotransforming enzymes in fish *in vivo* as well as in our cell cultures. It is possible that the test compounds strongly sorb to phospholipid membranes and therefore are little accessible for biotransforming enzymes, which is not the case in S9 substrate depletion assays where no cellular boundaries exist. A subcellular fractionation of exposed cells could give more insight into the location of cationic surfactants inside the fish cells. Another approach might be the application of visualization techniques, which could be used to localize chemicals in subcellular compartments<sup>187</sup>. In this context, extended exposure times may result in increased availability of the cationic surfactants to organelles harboring biotransformation enzymes inside the cells.

### 3.5. Outlook

The presented work presents a proof of concept, in which the rainbow trout cell lines, RTgill-W1 and RTL-W1, were used as *in vitro* alternative to predict the bioconcentration of alkyl amines in fish. In comparison to a simple  $D_{MLW}$ -based BCF prediction, the cells provide the additional potential of biotransformation, which deserves more investigation. In this regard, the RTL-W1 cell line may be preferred over RTgill-W1, since RTL-W1 represents an important organ for biotransformation, i.e. the liver. However, biotransformation cannot be scaled 1:1 across different tissues and a single cell line. Therefore, inclusion of other cell lines, as also demonstrated by Stadnicka-Michalak et al.<sup>35</sup> would be prudent. The RTgill-W1 may represent a valuable NAM to study the transepithelial transport of cationic surfactants, especially to better understand the accumulation behavior of Q14 observed *in vivo*. Additionally, it will be valuable to test more cationic surfactants to further evaluate the approach's applicability.

### 3.6. Acknowledgements

The authors thank Andreas Buser for valuable discussions, Juliane Glüge for COSMOtherm calculations and Philipp Longree, René Schönenberger and Severin Ammann for support in the chemical analysis.

---

## **4. Model comparison to refine bioconcentration prediction of ionizable organic compounds**

Fabian Balk <sup>1,2</sup>, Christoph Aeppli <sup>1,3</sup>, Juliane Hollender <sup>1,4</sup>, Kristin Schirmer<sup>1,2,4</sup>

<sup>1</sup> Eawag, Swiss Federal Institute of Aquatic Science and Technology, 8600 Dübendorf, Switzerland

<sup>2</sup> EPF Lausanne, School of Architecture, Civil and Environmental Engineering, 1015 Lausanne, Switzerland

<sup>3</sup> Bigelow Laboratory for Ocean Sciences, Marine Environmental Chemistry Laboratory, Maine 04544, United States

<sup>4</sup> ETH Zürich, Department of Environmental Systems Science, 8092 Zürich, Switzerland

### **Credit author statement**

Fabian Balk: Conceptualization, Experimental work, Formal analysis, Visualization, Writing of original draft, Review and Editing

Christoph Aeppli: Experimental work, Formal analysis and review

Juliane Hollender: Conceptualization, Review and Editing

Kristin Schirmer: Conceptualization, Review and Editing

#### 4.1. Abstract

In this study we used different computational approaches to examine which experimental and physicochemical parameters influence cellular accumulation of ionizable organic compounds (IOC) in a liver-derived permanent fish cell line, RTL-W1. Experimental accumulation data of eleven IOC, comprising anionic and cationic compounds and one permanently charged quaternary ammonium ion, and two neutral compounds, were available for comparison to model predictions. Three different model approaches were applied: One *in vitro* mass balance model, termed IV MBM EQP, one kinetic model, considering IOC flux across cell membranes, and one model which applies the human volume of distribution,  $V_D$ , for read across to predict bioconcentration in fish and RTL-W1 cells. The comparison of human  $V_D$  to estimated fish  $V_D$  of ten IOC were comparable with deviations being on average ~2-fold for 8 compounds and accurately predicted the bioconcentration in fish as well as in RTL-W1 cells. Although the comparison of human  $V_D$ -based BCF predictions was limited to four anionic compounds, this read across from human clinical data is a promising screening parameter for bioconcentration assessment of IOC in fish. The kinetic model predicted cell-derived bioconcentration factors unsatisfactory with absolute mean deviations of 4.3 orders of magnitude relative to measured accumulations in RTL-W1 cells. Consideration of protein sorption in the kinetic model lead to large overestimations of cellular accumulations. The IV MBM EQ model, however, gave accurate BCF values for 8 out of the 13 test compounds with deviations below one order magnitude. Most important parameters determining bioconcentration in the two models, whose experimental determination could lead to better model performance were the test compound affinity to membrane lipid and structural protein. The model results also implied that kinetic rates can be neglected in the prediction of cellular compound accumulations and that partitioning-based approaches suffice.

#### 4.2. Introduction

Current international chemical regulation requires the bioaccumulation assessment of organic compounds if import or production volumes are above a certain threshold<sup>7, 10</sup>. Bioaccumulation assessments are conducted in standardized experiments with fish<sup>9</sup>, from which a bioconcentration factor (BCF) is derived. The BCF describes the enrichment of the tested organic compound in the fish or specific tissues relative to the water concentration. Besides the ethically questionable sacrifice of at least 108 fish per typical compound assessment<sup>9, 10</sup>, these tests are resource intense and costly.

One group of chemicals, which is experimentally challenging to test in bioaccumulation assessments, are ionizable organic compounds (IOC). IOC bear at least one positive or



negative charge (or both) at biologically relevant pH (6-8) and are used in (among others) pesticides, pharmaceuticals, surfactants and as additives in personal care products<sup>48</sup>. Due to this broad range of applications and uses, it is not surprising that many IOC are released into the environment and have been measured in biota<sup>123</sup> and environmental matrices<sup>188 189 190 191 192</sup>.

In general, IOC can interact with proteins<sup>59</sup> as well as membranes, i.e. phospholipids<sup>26, 46, 74</sup>, within an organism. As a result, their bioaccumulation potential in fish is not reliably describable by the octanol-water partition coefficient,  $K_{OW}$ , which assumes principal compound accumulation in the storage lipid of an organism<sup>65</sup>. The pH-dependent octanol-water partition coefficient,  $\log D_{OW}$ , has as well been suggested for bioaccumulation assessment of IOC<sup>14</sup>. However, a compound's  $D_{OW}$  does not address the sorption to membrane lipid or protein accurately<sup>64 65</sup>. Consequently, the pH-dependent membrane lipid-water partition coefficient,  $D_{MLW}$ , has been suggested as a more appropriate descriptor for the regulatory risk assessment of surfactants<sup>65</sup>.

Permanent fish cell lines are a potential alternative to animal experimentation that supports bioaccumulation assessment of organic compounds in fish. By means of In vitro-In vivo extrapolation (IVIVE), it is possible to use *in vitro* measured biotransformation rates in physiology-based toxicokinetic models to predict bioconcentration in fish<sup>35</sup>. This has been demonstrated in a proof-of concept study with the neutral compound, benzo[a]pyrene, and the use of the permanent cell lines RTL-W1<sup>29</sup>, RTgill-W1<sup>30</sup> and RTgutGC<sup>31</sup> from rainbow trout (*Oncorhynchus mykiss*). Further, by means of measuring cellular and exposure medium concentrations in such cell lines, the ratio of the concentrations has been used to derive *in vitro*-based BCF for screening the bioconcentration potential of test compounds<sup>176</sup>.

Our recent work investigated the bioconcentration potential of a selection of IOC in RTL-W1 and RTgill-W1 cells and tested the suitability of the pH-dependent membrane-water partition coefficient,  $D_{MLW}$ , to predict the observed *in vitro* bioaccumulation<sup>193</sup>. For non-permanently charged cationic surfactants, the predictions of cellular accumulation closely followed the compounds'  $D_{MLW}$ -based BCF prediction as well as the *in vivo* BCF<sup>193</sup>. For anionic compounds, however,  $D_{MLW}$ -based predictions of cellular accumulation partly deviated from the measured cellular accumulations and  $D_{OW}$ -based predictions were more accurate<sup>176</sup>. In the associated *in vitro* experiments, we measured the total medium concentration and assumed that 100 percent of this measured exposure concentration was bioavailable for cellular uptake, which, specifically for IOC, may not be the case<sup>72</sup>. This is because IOC are known to sorb to exposure medium constituents, which is assumed to reduce the freely dissolved concentration,  $C_{free}$ , available for cellular uptake<sup>72, 181, 185</sup>. The measured or approximated  $C_{free}$  is expected to be

closer to the bioavailable chemical concentrations of *in vivo* experimentation and therefore potentially more suitable for IVIVE.

Indeed, many experimental and computational approaches have been proposed which attempt the determination of compound distributions inside *in vitro* test systems and  $C_{\text{free}}$ <sup>72, 81, 185</sup>. Most commonly, compound sorption to exposure medium and cell constituents are considered as well as sorption to the plastic of the test vessel<sup>16, 90, 185, 194</sup>. In theory, generic models, which are adjustable to one's own experimental conditions and test system, can simulate the *in vitro* BCF and help to understand which parameters and partition processes are relevant for *in vitro* accumulations. One such generic model, termed IV-MBM EQP ("*in vitro* mass balance model equilibrium partitioning"), predicts the compound mass distribution in an adjustable *in vitro* test system at chemical equilibrium<sup>90</sup>. The model considers the pH-dependent speciation of IOC in the extracellular and intracellular space and their affinities for medium and cell constituents, comprising storage lipid, membrane lipid and bulk protein as well as sorption to plastic. To date, the model has been evaluated with experimental data from different assays, in which rainbow trout cell lines<sup>40, 125</sup>, algae<sup>195</sup> and human cell lines<sup>196</sup> were exposed to a range of different compounds, including neutral compounds, volatile compounds and IOC<sup>90</sup>. Overall, model performance of IV MBM EQP was deemed acceptable ( $R^2 \geq 0.7$ )<sup>90</sup>.

Another type of mass balance model considers the permeation of both, neutral and charged species, through the cell membrane<sup>14, 15</sup>. This simulation considers the realistic scenario that not only the neutral species of a compound penetrates a cell membrane but also the charged species, although with a much slower diffusion relative to the neutral compound species<sup>197 198</sup>. Such models have been used to predict IOC accumulation in bacteria<sup>199</sup>, mammalian cells and fish<sup>14</sup> and zebrafish embryos<sup>15</sup>. Similar to the IV-MBM EQP it also considers the partitioning of both compound species inside the cell to protein and membrane lipid phases as well as pH differences between extra and intracellular space. So far, simple mass balance models were sufficient to explain the accumulation of cationic compounds in RTL-W1 and RTgill-W1 cells<sup>193</sup>, whereas the accumulation of anionic compounds in RTL-W1 cells showed larger deviations from observed accumulations<sup>176</sup>. Here, it would be interesting to find out, whether the kinetic cell model is more accurate in its predictions of the cellular accumulations of anionic compounds than simple mass balance models.

Opposite to the frequently applied strategy of mass balance models<sup>16, 17, 72</sup>, another approach for BCF prediction has received little attention to date<sup>15, 200, 201</sup>: the prediction of bioconcentration via the compound's volume of distribution,  $V_D$  and the blood-water partition coefficient,  $K_{\text{BW}}$ . The  $V_D$  is defined as the total body burden of a compound relative to its blood or plasma concentration ( $\text{L kg}^{-1}$ ) in the respective organism. At steady-state, it describes the

absorption capacity of the organism's tissue relative to the organism's blood without the need of a mechanistic explanation of the measured distribution. Recently, Zhang et al.<sup>201</sup> found that the human  $V_D$  predicted the accumulation of a range of pharmaceuticals in zebrafish embryos. Further, Nichols et al.<sup>200</sup> found that the  $V_D$  of diphenhydramine in fathead minnow (*Pimephales promelas*) was well within the range of the human  $V_D$ . Both findings corroborate the potential for read across from human pharmacological data to fish<sup>202</sup>. However, Nichols et al.'s derivation of the fish  $V_D$  (BCF divided by the blood-water partition coefficient,  $K_{BW}$ ) and the  $K_{BW}$  has not been assessed for its potential to predict BCF beyond that one compound, diphenhydramine. The application of  $K_{BW}$  as a partition coefficient is only valid under the condition that concentrations in blood and water were measured at steady state or estimated based on compound-specific knowledge of the bioaccumulation behavior. If these conditions were not met, Nichols et al.'s estimation approach is only applicable to compounds that are exclusively eliminated via the gills and by no other elimination process, e.g. biotransformation or fecal egestion.

In the present study, we set out to predict IOC accumulation in RTL-W1 cells and fish using different model approaches to gain insight into the model parameters that influence the predictability of measured accumulations. First, we compared available human  $V_D$  to fish  $V_D$  of compounds to estimate similarities and dissimilarities of sorption capacities. Then we used the  $V_D K_{BW}$  -relation to predict BCF in fish and fish cells, to conclude whether the comparison is viable. Second, we applied the above outlined kinetic cell model and the IV-MBM EQP model to predict BCF in fish and fish cells. These predicted BCF were compared to *in vitro*-based BCF from experiments with RTL-W1 and *in vivo* BCF from fish. With the model predictions we intend to answer the following questions: 1) Is the human  $V_D K_{BW}$  approach a suitable predictor of bioaccumulation in fish and fish cell lines? 2) Where are refinements in model predictions necessary to accurately predict accumulations in RTL-W1 cells? 3) What can we learn from the models to improve the bioconcentration test with RTL-W1 cells?

## 4.3. Methods

### 4.3.1. Dataset of *in vitro* BCF

The *in vitro* BCF were taken from as of yet unpublished and published experiments conducted in the permanent fish cell line, RTL-W1<sup>176, 193</sup>, which represents the liver tissue of rainbow trout. Except for three compounds, the tested IOC are nearly fully ionized at the experimental pH of 7 to 7.4 (Table 4.1).

**Table 4.1: Test compounds with available *in vitro* BCF from experiments with RTL-W1 cells.** Test compounds with available *in vitro* BCF from experiments with RTL-W1 cells. The *in vivo* BCF were taken from studies with rainbow trout, with the exception of FOSA, which was measured in common carp (*Cyprinus carpio*)<sup>203</sup>. DCF, PCP, TT and BHPP *in vitro* data taken from Balk et al.<sup>176</sup>, T10, S12 and Q14 *in vitro* data from Balk et al.<sup>193</sup>, PFOA, PFOS, EtFOSAA, FOSA, EtFOSA and EtFOSE taken from *in vitro* data unpublished yet. pK<sub>a</sub> = values taken either from literature or estimated using MarvinSketch (Chemaxon, v 23.7), \*Except for EtFOSA (0.01 % charged) and EtFOSE (0 % charged), all compounds are nearly 100 % charged at pH 7, n/a = not available

Compound	Acronym	CASRN	Type	pK <sub>a</sub>	log <i>in vitro</i> BCF	log <i>in vivo</i> BCF
Diclofenac	DCF	15307-79-6	acid	4.15	0.035	0.6 <sup>102</sup>
Pentachlorophenol	PCP	87-86-5	acid	4.68	0.3	2.7 <sup>108</sup>
Tecloftalam	TT	76280-91-6	acid	1.07	0.7	n/a
Perfluorooctanoic acid	PFOA	335-67-1	acid	0.3	0.8	0.8 <sup>103</sup>
Benzotriazol-tert-butyl-hydroxyl-phenyl propanoic acid	BHPP	84268-36-0	acid	4.65	1.4	n/a
Perfluorooctanesulfonic acid	PFOS	1763-23-1	acid	-3.32	1.6	3.2 <sup>103</sup>
N-Ethylperfluorooctanesulfonamidoacetic acid	EtFOSAA	2991-50-6	acid	0.064	1.8	n/a
Perfluorooctanesulfonamide	FOSA	754-91-6	acid	3.37	1.9	2.4 <sup>203</sup>
N,N-dimethyldodecylamine	T10	1120-24-7	base	9.79	2.3	2.1 <sup>167</sup>
N-Ethylperfluorooctanesulfonamide	EtFOSA	4151-50-2	neutral	9.5 <sup>+</sup>	2.7	n/a
N-Ethyl-N-(2-hydroxyethyl)perfluorooctylsulphonamide	EtFOSE	1691-99-2	neutral	12.52 <sup>+</sup>	2.9	n/a
N-methyldodecylamine	S12	7311-30-0	base	10.78	3.4	2.9 <sup>167</sup>
N,N,N-trimethyltetradecylamine	Q14	4574-04-3	base	n/a	4.1	1.7 <sup>167</sup>

#### 4.3.2. Literature search for $V_D$ comparison

The comparison of human and fish  $V_D$  was limited to compounds for which  $V_D$  values for human and fish were available. For better comparability of the human and fish  $V_D$ , we only considered  $V_D$  measured at steady state. We based our literature search for human steady state  $V_D$  on published databases<sup>204 205</sup> and compounds that were studied because of their health concern to humans, such as perfluoroalkyl substances (PFAS) or illicit drugs.

For most of the fish studies, no volume of distribution was directly available and was estimated from either tissue concentrations or tissue-specific BCF. For all compounds included, we obtained at least 3 values, typically concentrations or BCF in blood, liver and remaining body, which sufficed to approximate  $V_D$  as follows:

- If tissue specific concentrations were documented, the whole body concentrations were derived by the multiplication of the tissue concentration with the reported tissue weight (SI Table S4.2) and divided by the measured blood or plasma concentrations to obtain  $V_D$ .
- If only tissue specific BCF were documented instead of tissue concentrations, they were weighted according to their weight fraction and summed up to obtain an approximated total body BCF. This total body BCF was then divided by the BCF measured in blood or plasma.

We found tissue-based BCF for rainbow trout, brown trout (*Salmo trutta*), fathead minnow (*Pimephales promelas*) and catfish (*Ictalurus punctatus*) (SI Table S4.2), but weight-based tissue fractions were found only for rainbow trout<sup>6</sup> and catfish<sup>40</sup> (SI Table S4.2). Therefore, the weight fractions of tissues in rainbow trout were used as default for BCF-based  $V_D$  calculations of brown trout and fathead minnow. Measurements of blood and plasma concentrations or respective BCF values, i.e.  $BCF_{Plasma}$  or  $BCF_{Blood}$ , were regarded as synonymous. For more information on  $V_D$  derivation, see SI Table S4.2.

#### 4.3.3. Principal model considerations

For the derivation of the pH-dependent membrane-water and protein-water partition coefficients, the partition coefficient of the ionic and the neutral species were needed (Table 4.2). These were calculated from polyparameter linear free energy relationships (PP-LFER)<sup>60, 87, 206, 207</sup>. The required substance descriptors were calculated using the UFZ-LSER database

<sup>208</sup> (four perfluorosulfonamides) or the ACD/Percepta v14.50.0 software using the ABSOLV module (ACD/Labs) <sup>209</sup>. For data summary, see SI Table S4.1. To derive the pH-dependent partition coefficients to membrane lipid or structural protein, the partition coefficient of each species (Table 4.2) was weighted according to its neutral fraction,  $\alpha_n$ , estimated by the Henderson-Hasselbalch equation:

For basic species

$$\text{Equation 4.1} \quad \alpha_n = (1 + 10^{pK_a - pH})^{-1}$$

For acidic species

$$\text{Equation 4.2} \quad \alpha_n = (1 + 10^{pH - pK_a})^{-1}$$

The charged fraction of the compound (index 'i') was calculated as

$$\text{Equation 4.3} \quad \alpha_i = 1 - \alpha_n$$

A pH of 7.4 was assumed for the cellular water, i.e. the cytosol <sup>14</sup>, while the medium pH (7) was taken from experimental measurements <sup>176</sup>. Where relevant in the below model approaches, the cells were assumed to consist of protein, membrane lipid, i.e. phospholipids, and water.

#### 4.3.4. Simple partitioning-based models

For reference, the simplest prediction applied here was the mass balance model, termed,  $BCF_{DMLW}$ , which follows the compound's  $D_{MLW}$  (Table 4.2) multiplied by the phospholipid volume fraction in the cells <sup>176</sup>,  $f_{PL}$ :

$$\text{Equation 4.4} \quad BCF_{DMLW} = f_{PL} \times D_{MLW}$$

$f_{PL}$  was taken as mean ( $0.021 \pm 0.011$ ) from measurements of lipid content in different mammalian cell lines <sup>89</sup> and is assumed to be representative of the cellular membrane lipid content. The fish  $V_D$  was used to predict the BCF by the relation in Equation 4.5:

$$\text{Equation 4.5} \quad BCF_{VD\text{fish or human}} = K_{BW} \times V_D$$

Equation 4.5 was initially used to derive the fish  $V_D$  by Nichols et al. <sup>200</sup>. As noted in 4.2  $K_{BW}$  is defined as a partition coefficient for the application in Equation 4.5. Therefore,  $K_{BW}$  were taken from fish studies, where blood and plasma concentrations were taken as synonymous and

assuming that the measurements were taken at steady state (SI Table S4.2). It should be noted that, naturally, there are no  $K_{BW}$  in humans available. The  $BCF_{VD}$  was once calculated with the fish  $V_D$  ( $BCF_{VDfish}$ ) and once with the human  $V_D$  ( $BCF_{VDhuman}$ ).

### 4.3.5. Kinetic cell model

The cell model was applied in the scenario where neutral and charged species contribute to the flux across the cell membrane in proportion to their fractions at a given pH and the compound's  $pK_a$ <sup>15</sup>. For this purpose, the Nernst-Planck equation was applied, which describes the motion of a charged compound considering electrostatic forces. The central equation of this kinetic model was taken from Bittner et al.<sup>15</sup>:

$$\text{Equation 4.6} \quad BCF_{cell\ model} = \frac{k_{up}}{k_{elimination}} = \frac{\gamma_{medium,n} \alpha_{medium,n} + 10^{-3.5} \frac{N}{e^N - 1} \gamma_{medium,i} \alpha_{medium,i}}{\gamma_{cell,n} \alpha_{cell,n} + 10^{-3.5} \frac{N}{e^N - 1} \gamma_{cell,i} \alpha_{cell,i}} \times \frac{f_w}{F_{w,cell}}$$

Where  $\gamma$  is the activity coefficient of the neutral or charged compound in the medium or cell and, the term  $10^{-3.5} \frac{N}{e^N - 1}$  the permeability of the charged compound<sup>15</sup>.  $N$  was calculated as the term  $\frac{zEF}{RT}$  where  $z$  is the charge of monoprotic bases (+1) or acids (-1),  $E$  the membrane potential,  $F$  the Faraday constant (96485 C mol<sup>-1</sup>),  $R$  the universal gas constant (8.314 J mol<sup>-1</sup> K<sup>-1</sup>) and  $T$  the absolute experimental temperature in Kelvin (19 °C = 292.15 K). Since  $E$  is not known in the fish cell cultures, we assumed -0.11 V<sup>210</sup>, which is in the range of typical values for mammalian cells (-0.02 to -0.120 V)<sup>211</sup>.  $f_w$  is the cellular water fraction (0.886) and  $F_{w,cell}$  is the substance fraction in the water phase of the cell and was calculated according to Equation 4.7:

$$\text{Equation 4.7} \quad F_{w,cell} = \left( 1 + D_{MLW} \frac{f_{PL}}{f_w} + D_{PW} \frac{f_P}{f_w} \right)^{-1}$$

Where  $D_{MLW}$  and  $D_{PW}$  are the pH-dependent membrane-water or structural protein-water partition coefficients and  $f_{PL}$  and  $f_P$  the volume fractions of membrane lipid and structural protein, respectively ( $f_{PL} = 0.021 \pm 0.011$ ,  $f_P = 0.093 \pm 0.013$  (mean  $\pm$  standard deviation) from mammalian cell lines<sup>89</sup>, no values for RTL-W1 known). The absorption to muscle protein was assumed to be representative of the structural protein in the cells<sup>17</sup>, since the partitioning to



bovine serum albumin (BSA) was found to be unsuitable to describe the partitioning to structural protein <sup>59, 89</sup>.

$\gamma$  was calculated following the Setchenov equation for the neutral species (index “n”) and the Davies approximation for charged species (“i”) <sup>15</sup>:

$$\text{Equation 4.8} \quad \gamma_n = 10^{0.3 I}$$

$$\text{Equation 4.9} \quad \gamma_i = 10^{0.5 |z| \left( \frac{\sqrt{I}}{1} + \sqrt{I} - 0.3I \right)}$$

Where  $z$  is +1 for monoprotic bases and -1 for acids,  $I$  the ionic strength of the cell lumen (0.3 M, taken from zebrafish embryos <sup>15</sup>) or the exposure medium (calculated as 1.91 M for Leibovitz’s medium, see SI Table S4.9).

**Table 4.2: Partition coefficients used in the model predictions.** Acronyms shown in Table 4.1. Measured  $D_{MLW}$  are listed as well as the PP-LFER estimations of the neutral (n) and charged (i) compound. For some of the compounds, fish  $V_D$  were available. For sources, detail and derivation of the different parameters, see SI Table S4.1 and SI Table S4.2.  $K_{PW}$ : Protein-water partition coefficient of the charged (i) or neutral (n) species, used to calculate the pH-dependent  $D_{PW}$ . \*estimated value using substance descriptors as listed in SI Table S4.1, no measured  $D_{MLW}$  available, %  $D_{MLW}$  were measured at pH 7.4 except for two values, which were measured at pH 7 \*own TRANSIL<sup>XL</sup> experiments (not published), for method see <sup>212</sup>.

Compound	log $K_{MLWn}$	log $K_{MLWi}$	log $D_{MLW}$	log $K_{PWn}$	log $K_{PWi}$	$V_D$ (fish log L kg <sup>-1</sup> )	$K_{BW}$ (fish, log L kg <sup>-1</sup> )
DCF	4.8	3.1	2.6 <sup>61</sup>	3.7	5.4	0.8 <sup>102</sup>	0.7 <sup>149, 213</sup>
PCP	5.1	5.9	3.8 <sup>57</sup>	3.8	8.7	2.0 <sup>108</sup>	2.1 <sup>108</sup>
TT	5.8	8.4	8.4 <sup>+</sup>	4.8	17.1	n/a	n/a
PFOA	4.1	1.2	3.5% <sup>64</sup>	3.1	2.8	0.2 <sup>103</sup>	1.4 <sup>103</sup>
BHPP	4.3	2.3	2.4 <sup>+</sup>	3.5	5.5	n/a	n/a
PFOS	3.0	-0.3	4.9% <sup>64</sup>	2.3	1.9	0.4 <sup>103</sup>	3.5 <sup>103</sup>
EtFOSAA	8.4	6.6	4.9*	6.5	9.5	n/a	n/a
FOSA	6.0	3.9	5.1*	4.4	7.0	n/a	n/a
T10	4.4	3.8	3.6 <sup>63</sup>	3.3	3.6	1.0 <sup>74</sup>	1.4 <sup>74</sup>
EtFOSA	6.6	4.5	5.3*	4.9	7.8	n/a	n/a

Compound	log $K_{MLWn}$	log $K_{MLWi}$	log $D_{MLW}$	log $K_{PWn}$	log $K_{PWi}$	$V_D$ (fish log L kg <sup>-1</sup> )	$K_{BW}$ (fish, log L kg <sup>-1</sup> )
EtFOSE	8.0	6.2	5.3*	6.2	9.3	n/a	n/a
S12	5.0	4.9	5.4 <sup>63</sup>	3.9	4.0	1.5 <sup>74</sup>	1.8 <sup>74</sup>
Q14	8.3	7.6	5.5 <sup>63</sup>	6.8	5.8	n/a	n/a

#### 4.3.6. *In vitro* mass balance model

We applied the IV-MBM EQP model to our test system-specific conditions<sup>176</sup> to gain insight into the relevance of different absorbing matrices in the cell as well as the medium. In the model, the cells consist of storage lipid, membrane lipid, water and bulk protein, i.e. structural protein, while the medium consists of water, dissolved organic matter (mostly amino acids, see Table S4.9), albumin and lipids. All those constituents were set to our experimental conditions as detailed in section S4.1. Most importantly, the RTL-W1 cells were assumed to have an identical composition as reported above in the kinetic cell model, i.e. the storage lipid fraction was neglected. Membrane lipid-water partition coefficients reported for the neutral and the ionic compound species in Table 4.2 were used as input to the model as well as the  $K_{OW}$  and the serum albumin-water partition coefficients of the neutral and ionic species. Other compound specific inputs were the  $pK_a$ , molecular weight, melting temperature, the air-water partition coefficient, water solubility and exposure concentrations<sup>176</sup>. Medium<sup>214</sup> and serum composition (albumin: 16.92 g L<sup>-1</sup>, lipid: 0.84 g L<sup>-1</sup>, eurobio scientific, Fr) was taken from the suppliers. For more details on derivation of parameters or used software for estimation, see SI section S4.1.

Besides the compound inputs, the cell number (3.3x10<sup>6</sup> cells flask<sup>-1</sup>), weight (2.4x10<sup>-3</sup> ng cell<sup>-1</sup>)<sup>176</sup> and test system specific information were used as input. Here, it is important to mention that the cell culture flasks used in our experiments are not applicable in the model, as it is limited to well-plate formats. Therefore, we assumed that the used cell flasks (25 cm<sup>2</sup> growth area, 66.6 mL total volume, 3 mL medium volume) represent one hypothetical well with identical metrics for volumes and growth area as the flasks in our experiments. Additional, test system specific inputs were the pH in the exposure medium (7) and inside the cells (7.4). The model output, i.e. mass fractions and concentrations in the compartments of the test system,

were used to calculate predicted *in vitro* BCF by taking the cellular concentration over the medium concentration. Here, either the total medium concentration was used, including the aqueous free and the bound compound fraction in the medium ( $\text{BCF}_{\text{bulk}}$ ), or only the estimated aqueous free concentration,  $C_{\text{free}}$  ( $\text{BCF}_{\text{Cfree}}$ ).

#### 4.3.7. Sensitivity analysis

Sensitivity analyses of the kinetic cell model and the *in vitro* mass balance model were conducted to determine which input parameters influence the output most for the different compound classes (anion, cation, quaternary ammonium ion, neutral). For this purpose, the input parameters were changed, one at a time, by a fixed percentage, i.e. 0.1 %, and the change in the output (*in vitro* BCF predictions) was determined. The sensitivity,  $S$ , was calculated as <sup>215</sup>:

$$\text{Equation 4.10} \quad S = \frac{O_{\Delta}/O}{I_{\Delta}/I}$$

Where  $I_{\Delta}/I$ , is the change in the model input, i.e. 0.001, and  $O$  and  $O_{\Delta}$  the default model output and the change in model output, respectively.

#### 4.3.8. Data analysis

Data were analyzed and visualized using the programming language R <sup>129</sup>, the R packages openxlsx, tidyr, dplyr, ggplot and patchwork <sup>130 131 132 133 134</sup>, GraphPad Prism 9.4.0 (GraphPad Software) and ChemsSketch 2021.1.2 (ACD/Labs) <sup>50</sup>.

### 4.4. Results and Discussion

#### 4.4.1. $V_D$ comparison

Figure 4.1 shows the comparison of human and fish  $V_D$  of IOC ranked from smallest to greatest fish  $V_D$ . Maximum deviations were observed for atenolol with a factor 25 greater for fish  $V_D$  than human  $V_D$  and a factor of 15 for methamphetamine. Excluding these two largest deviations (atenolol and methamphetamine), the absolute mean difference between human and fish  $V_D$  was 0.93 ( $\text{L kg}^{-1}$ ) or factor 2.1.

For most of the compounds (8 out of 10), the fish  $V_D$  was estimated from tissue specific BCF, which were weighted according to the organ weight fraction (see SI Table S4.3) to derive a whole body BCF. This derivation method likely came with greater uncertainties in the fish  $V_D$  estimation compared to  $V_D$  derivation from measured tissue concentrations. The reason is that the BCF represents all processes that influence the compound's fate in fish, while the  $V_D$  merely describes a fish's sorption capacity of a compound. Therefore, the big differences between fish and human  $V_D$  of atenolol and methamphetamine may have several reasons (uptake efficiency into fish, biotransformation and sorption capacity). However, these reasons are impossible to delineate for their contributions to the observed differences, since there is no knowledge on the actual fish  $V_D$  of these compounds. The low measured  $BCF_{\text{plasma}}$  in fish of both compounds is an indicator that the uptake efficiency, i.e.  $K_{BW}$  (steady-state assumed) is low. However, this does not reflect the  $V_D$  in the fish then. Despite those differences and uncertainties, the remaining human and fish  $V_D$  are similar, which means that for the majority of the compounds, fish and humans appear to have comparable sorption capacities in blood and body tissue. This encourages the BCF prediction in RTL-W1 and fish via the human  $V_D$  and measured  $K_{BW}$  (Equation 4.5).

No clear differences in fish  $V_D$  of different fish species were found though this analysis was hampered by insufficient data to compare  $V_D$  in different fish species for the same compound. Nevertheless, interestingly, the derivation of fish  $V_D$  using tissue-based BCF and  $K_{BW}$  from different fish species for ibuprofen (Table S4.2) coincided with a very comparable human  $V_D$ . A comparison of  $V_D$  in different fish species for a larger set of compounds would give valuable insights into relative differences in  $V_D$  and whether the observed close correspondence of  $V_D$  in fish and human of ibuprofen was coincidental or not.

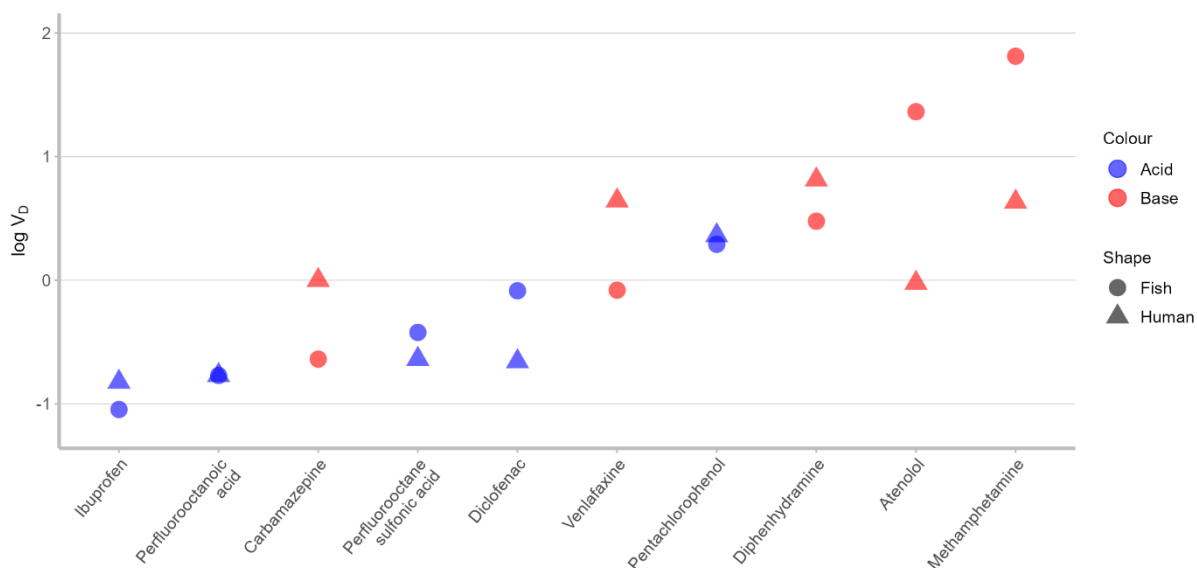


**Figure 4.1: Comparison of measured human and fish  $V_D$  ( $L\ kg^{-1}$ ).** Only those compounds are shown for which a  $V_D$  in human and fish was available from literature. For  $V_D$  derivation, see SI Table S4.2.

Where available, derived  $V_D$  together with measured  $K_{BW}$  in fish were used to calculate  $BCF_{VDfish}$  or  $BCF_{VDhuman}$  (Equation 4.5) for the test compounds and compared to *in vitro* and *in vivo* BCF (Figure 4.2). Interestingly, the  $BCF_{VDhuman}$  for DCF, PCP, PFOA and PFOS were within 4-fold to fish *in vivo* BCF, which supports that this approach can be used as an additional or alternative avenue to predict bioconcentration fish. The caveat is that a measured  $K_{BW}$  (at steady-state) or detailed knowledge on the bioaccumulation behavior of a compound for  $K_{BW}$  prediction is necessary to make accurate predictions. Also, the *in vitro* BCF for DCF and PFOA was within 10-fold of the *in vivo* BCF and the predicted BCF. The lower *in vitro* BCF of PFOS and PCP compared to the other BCF estimations is discussed below.

An *a priori* hazard assessment of a compound would be a challenging case, since the compound likely lacks the human as well as the fish data to make BCF predictions by  $V_D$  and  $K_{BW}$ . Here, it would be valuable to have robust modelling approaches, which can estimate  $V_D$  and  $K_{BW}$  values. Current methods for  $V_D$  and  $K_{BW}$  apply the  $K_{OW}$  as the central parameter<sup>216, 217</sup> under the assumption of chemical equilibrium. However, the  $K_{OW}$  does not well represent the sorption behavior of IOC in fish and is only applicable when the state of chemical equilibrium is not violated or the processes influencing steady-state are well quantifiable. For pharmaceuticals and a range of other compounds of human and environmental concern, however, it is likely that human  $V_D$  and measured  $K_{BW}$  in fish are available from clinical and

monitoring studies. In this context, this information could serve as read across for BCF prediction, without the need for a computational prediction.

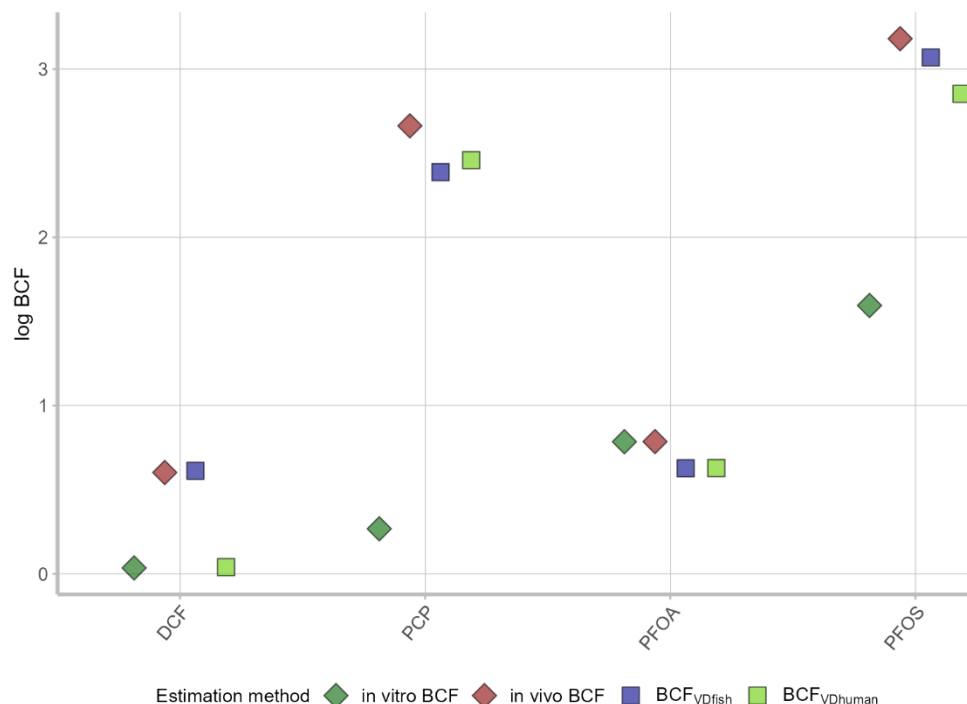


**Figure 4.2:  $V_D$  predicted BCF relative to observed *in vivo* and *in vitro* BCF.** Only those compounds are shown for which a  $V_D$  in human and fish was available from literature as well as *in vitro* BCF.

#### 4.4.2. BCF prediction by the kinetic cell model

Figure 4.3 shows the comparison of the *in vitro*, the *in vivo* BCF, the BCF<sub>DMLW</sub> ( $D_{MLW}$ -based prediction) and the BCF<sub>cell model</sub> (kinetic cell model, Equation 4.6). The consideration of protein partitioning in the kinetic cell model lead to large overestimations of BCF<sub>cell model</sub>, which were on average log3.7-fold (taking out DCF with a 135-fold difference) greater than the *in vitro* BCF (SI Figure S4.1). Therefore, we excluded the sorption to protein in the cell model predictions presented in Figure 4.3. This means that BCF<sub>DMLW</sub> and BCF<sub>cell model</sub> mainly differ through the incorporation of the charge-dependent permeation of the compound in Equation 4.6 and the different assumptions for bioavailability in the exposure media: the kinetic cell model relates bioavailability to the pH dependent speciation in the exposure medium without consideration of sorption processes inside the medium, while the IV MBM EQP model considers additional sorption processes to medium constituents and plastic inside the *in vitro* test system.

Despite that some IOCs are well known to sorb to proteins, such as certain PFAS<sup>218, 219</sup>, it appears to play a minor role for bioaccumulation in RTL-W1 cells, since inclusion of protein sorption worsened the model accuracy (Figure S4.1 and S4.2). It also possible that the applied PP-LFER for protein partitioning (Table 4.2) simply do not well represent the sorption to cellular protein. Total protein content of the fish cell cultures can be measured photometrical<sup>41, 89</sup>. However, the precise quantification of protein content likely does not improve model predictions, since we expect that the protein content of RTL-W1 cells won't differ considerably from the values we used from mammalian cells<sup>89</sup>. It is likely more useful to experimentally determine protein-water partition coefficients as discussed below.

For most compounds, the  $BCF_{\text{cell model}}$  was not a reliable predictor of the *in vitro* and *in vivo* BCF with absolute mean deviations of log4.3 and log1.2, respectively. Notably,  $BCF_{\text{cell model}}$  generally followed the  $BCF_{\text{DMLW}}$ , which implies that simple partition-based prediction still has a big influence in the kinetic cell model. Therefore, the permeation calculations in the kinetic cell model, could be neglected and a simple partitioning-based approach may be applied instead. This agrees with a previous study, which concluded that the IOC kinetics in cell culture test systems are sufficiently fast to be negligible in computational models<sup>194</sup>. Predictions of the kinetic cell model were considerably more accurate if measured  $D_{\text{MLW}}$  were applied instead of estimated  $D_{\text{MLW}}$  using PP-LFER (Table 4.2, Figure 4.3, Figure S4.1 and S4.2). Therefore, experimentally determined partition coefficients should be preferred over *in silico* estimation methods.

The sensitivity analysis of the kinetic cell model showed that the medium and cell pH, volume fractions of cell constituents and corresponding partition coefficients were the most influential factors in the model and associated uncertainty have the highest influence on the model performance (Figure S4.3). This is in agreement with our observation that the use of measured or predicted  $D_{\text{MLW}}$ , and the inclusion or exclusion of protein sorption, resulted in contrasting BCF predictions (Figure 4.3, Figure S4.2 and S4.1). As stated above, we do not expect a considerable model improvement, if protein content was quantified in the RTL-W1 cells, since they likely do not deviate much from those in mammalian cell lines. The same pertains to the quantification of membrane or storage lipid in the cells. To estimate the importance of the membrane lipid content on the overall *in vitro* BCF, the membrane lipid volume fraction was varied by 0.01 to 0.034 (measured in mammalian cell lines<sup>89</sup>), which resulted in a maximal variation of log0.5 in  $D_{\text{MLW}}$ -based BCF predictions<sup>193</sup>. This is a rather small variation compared

to our observed variations when estimated or measured  $D_{MLW}$  were used in the kinetic model (Figure 4.3, Figure S4.2 and S4.1). Even bigger deviations resulted from the inclusion of  $D_{PW}$  in the model. Therefore, it seems more important to refine the  $D_{MLW}$  and  $D_{PW}$  values.  $D_{PW}$  values for this model are based on PP-LFER equations that used chicken muscle as surrogate for structural protein, which may not be representative of the structural protein in the fish cells<sup>60</sup>. In this context, the partitioning to total extracted protein from the cell cultures is most suitable to minimize uncertainties in the partition coefficient estimation<sup>87</sup>.

With the exception of PFOS and PCP, all *in vivo* BCF were either below or within factor 10 of the *in vitro* BCF, which supports the suggestion to use the RTL-W1 cell line as a conservative screening approach for bioaccumulation potential. However, PCP and PFOS's bioaccumulation potential in fish is underestimated by the RTL-W1 cells (Figure 4.3). In our previous study we found indications that PCP was possibly biotransformed to a low degree in RTL-W1 cells, which might cause the reduction of the *in vitro* BCF relative to the *in vivo* BCF<sup>176</sup>. It is also possible that PCP and PFOS sorbed stronger to the serum albumin present in the exposure medium than the other test compounds, which could have reduced  $C_{free}$ <sup>59, 194</sup>. BSA is considered the main sorptive protein in cell culture media<sup>72, 84</sup>. Albumin was shown to have two cavities with positively charged amino acids, which can interact with anionic compounds<sup>68, 69</sup>, while other binding sites were shown to be hydrophobic or nonspecific<sup>68, 85</sup>. Another reason may be that fish have sorption phases which are underrepresented in fish cell cultures of specific tissues. For example, serum albumin is the main constituent in blood plasma<sup>17, 220</sup> and likely has different sorption properties compared to, e.g., structural or catalytic protein in of RTL-W1 cell cultures. For PCP and PFOS, high binding affinities to serum albumin are known in mammals and fish<sup>59, 71, 86, 103, 221</sup>. With a measured BSA-water partition coefficient of 5.3 for PCP ( $\log L\ kg^{-1}$ ) and 4.7 for PFOS ( $\log L\ kg^{-1}$ )<sup>222</sup> they are on average  $\log 2.1$  to  $\log 1.5$  larger, respectively than the mean for other anionic compounds ( $\log 3.2\ L\ kg^{-1}$ )<sup>59</sup>. This high BSA affinity of the two compounds might be the cause for the higher *in vivo* BCF compared to the corresponding *in vitro* BCF.

It finally should be noted that six compounds (Q14, EtFOSE, EtFOSA, FOSA and PFOS, PFOA) were outside the applicability domain of the PP-LFER used for partition coefficient estimation (Table 4.2), which increases uncertainty in the estimated parameters and subsequent application in model predictions. However, PP-LFER are assumed to be more accurate than other estimation methods, such as single parameter-LFER or the correction with



single constants. The correction with single constants applies one compound class-specific constant on the partition coefficient of the neutral species to estimate the partitioning of the charged species<sup>17, 223</sup>. The experimental determination of partition coefficients, such as the membrane lipid-water partition coefficients of neutral and charged species for individual compounds is cumbersome<sup>57</sup>. Nevertheless, experimentally determined values are preferable over *in silico* estimations, as they imply better model performance.

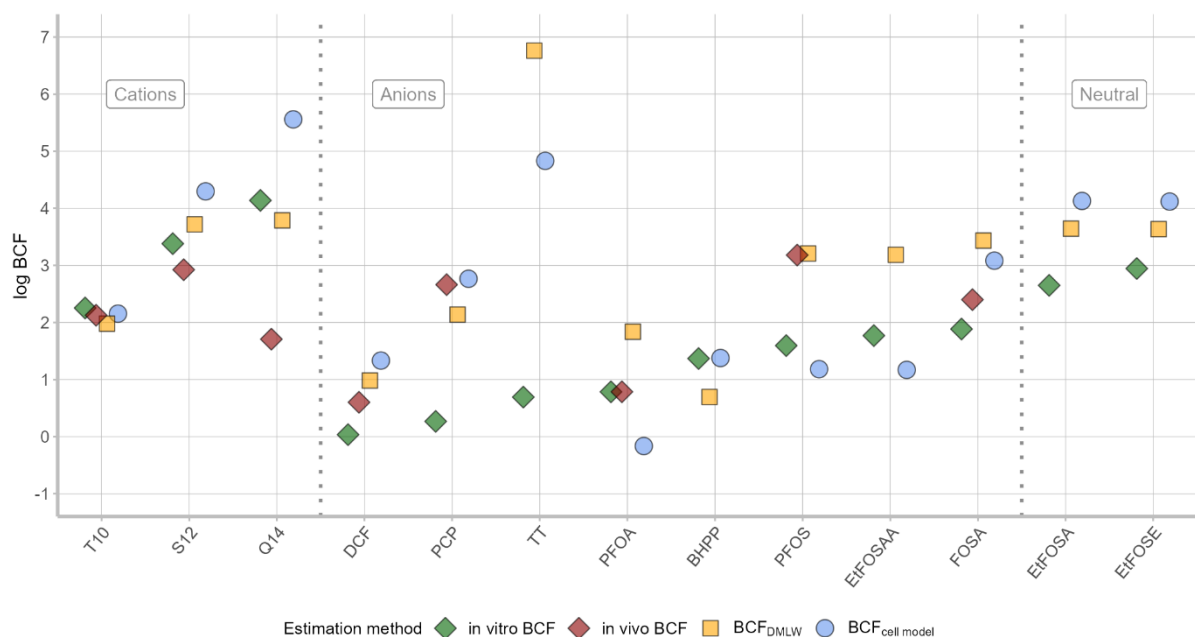


**Figure 4.3: Comparison of kinetic cell model predictions ( $BCF_{cell\ model}$ ) and observed *in vivo* and *in vitro* BCF.** Instead of estimated  $D_{MLW}$  measured  $D_{MLW}$  were used for the modelled BCF.  $BCF_{DMLW} = f_{PL} \times D_{MLW}$  (Equation 4.4),  $BCF_{cell\ model}$  = considers kinetics of neutral and ionic species (Equation 4.6)

#### 4.4.3. Predictions by the *in vitro* mass balance model IV MBM EQP

Figure 4.4 shows the BCF predictions from the IV MBM EQP model<sup>90</sup> based on medium concentrations ( $BCF_{bulk}$ ) or the estimated free aqueous concentration in the medium  $C_{free}$  ( $BCF_{Cfree}$ ). Since the medium in our experiments was supplemented with 5 % (v/v) fetal bovine serum, a fraction of the compounds likely sorbed to the serum albumin in the medium. This was considered in the model predictions, which consequently lowered  $C_{free}$ , hence increased the predicted BCF (Figure 4.4). The model predicted accurate *in vitro* BCF for 8 (T10, S12, PFOA, BHPP, PFOS, FOSA, EtFOSA and EtFOSE) of the 13 compounds, if  $BCF_{bulk}$  was considered (within factor 10 of *in vitro* BCF), while  $BCF_{Cfree}$  systematically overpredicted *in vitro* BCFs by, on average, 3.7 orders of magnitude (excluding DCF). However, the BCF predictions

of  $C_{\text{free}}$  may not be reliable, since the predicted overall mass distributions of the model were partly flawed (Table S4.5). For example, the cell mass fraction of cationic surfactants (T10, S12 and Q14) ranged from 0.3 % to 6 % in the model, while experimental mass balances gave a range of 34 % to 96 %. In general, the measured cellular mass fractions of the test compound were higher than those predicted by IV MBM EQP (Table S4.5). Yet, the comparison of  $\text{BCF}_{C_{\text{free}}}$  and  $\text{BCF}_{\text{bulk}}$  gives valuable insights into the deviations between *in vitro* BCF and *in vivo* BCF of PCP and PFOS (Figure 4.4). As mentioned above, both compounds show high serum albumin affinities. This may result in the sorption of these compounds to the serum albumin present in the exposure medium, thus lowering  $C_{\text{free}}$ . *In vivo* tests likely measure water concentrations closer to  $C_{\text{free}}$ , because they have less sorbents present in the water relative to exposure medium of *in vitro* tests. This explains the good agreement of  $\text{BCF}_{C_{\text{free}}}$  of PCP and PFOS and their *in vivo* BCF. This implies that the bioavailable fraction in the exposure medium of our *in vitro* test system is overestimated by the use of the bulk medium concentration, due to the neglect of sorption to medium constituents. A possible refinement for future bioconcentration testing with RTL-W1 would be the additional sampling of  $C_{\text{free}}$  via solid-phase microextraction fibers<sup>185</sup> to estimate the true extent of its influence on bioavailability. However, the fact that  $\text{BCF}_{\text{bulk}}$  gave better predictions of the *in vitro* BCF (and tended to be closer to *in vivo* BCF as well) implies that the sampling of the bulk medium in our experiments is appropriate for BCF derivation.

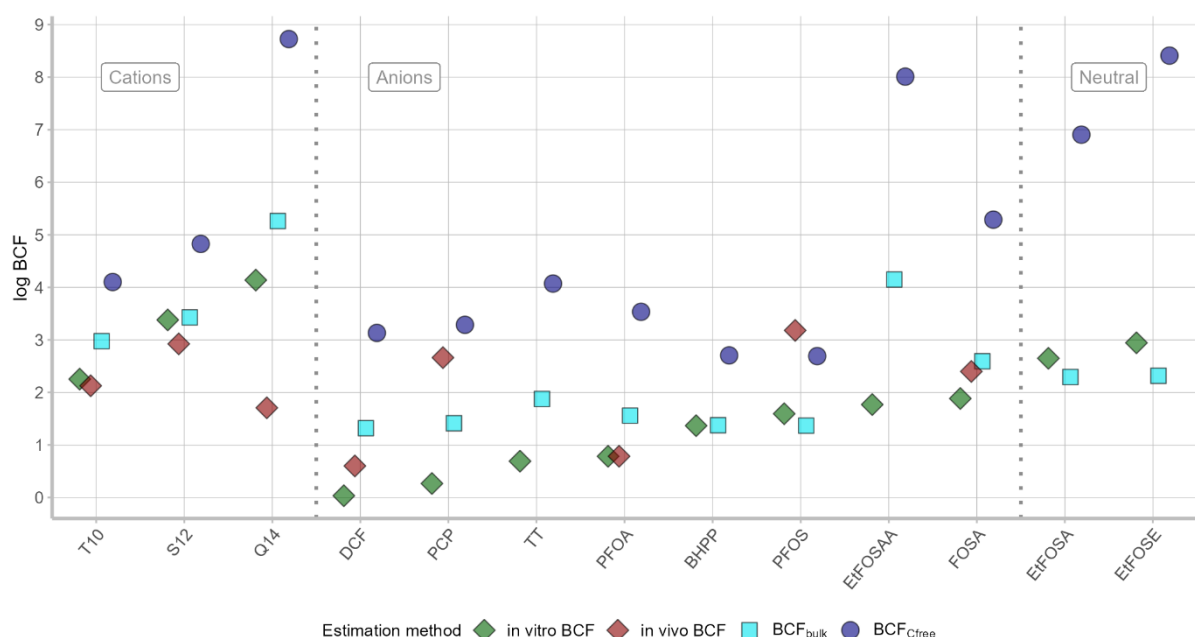


**Figure 4.4: Comparison of mass balance model predicted BCF and observed *in vivo* and *in vitro* BCF.** Model predictions were made with the IV-MBM EQP model with system specific settings from the experimental set up <sup>176</sup>, except for cell internal fractions of protein and lipid (taken from other studies, see methods).

The sensitivity analysis of the IV MBM EQP model gave similar results as for the kinetic cell model. pH in medium and cells and the partition coefficients to membrane lipid and protein were most influential on the model result (Figure S4.4). It is important to note, that the protein partitioning in the IV MBM EQP model refers to the serum albumin-water partitioning and not to the partitioning to structural protein as in the kinetic cell model. Due to the medium supplementation with FBS, which contains BSA, the corresponding partition coefficient ( $K_{SaW}$ ) was important for the determination of  $C_{free}$  and subsequent partitioning processes into the cell. Similar to the kinetic model the relative high sensitivity of the IV MBM model to the partition coefficients compared to other input parameters, accurate estimation methods or experimental determination of the partition coefficients will most likely result in better model performance.

#### 4.5. Concluding remarks

With our experimental *in vitro* BCF in RTL-W1 and the *in vivo* BCF in fish as reference, the *in vitro* mass balance model was more accurate compared to the kinetic cell model. The consideration of compound species-dependent permeation appeared irrelevant for our cellular exposures and the incorporation of protein sorption led to large overestimations in the kinetic

cell model. Interestingly, the consideration of protein in the *in vitro* mass balance model did not lead to overestimations of the *in vitro* BCF ( $BCF_{bulk}$ ), but it was rather predicted  $C_{free}$  that was associated with greater uncertainties. Despite the very limited data availability, the  $V_D$  and the  $K_{BW}$  as predictor for bioconcentration in fish was most accurate from all presented computational approaches, which was mainly the result of measured  $K_{BW}$  values. However, the estimation of these predictors will likely introduce greater variability in prediction accuracy. This pertains especially to the estimation of  $K_{BW}$  as it ultimately determines how much compound is taken up by the fish, while the  $V_D$  describes the distribution between blood and body tissue inside the fish.

Despite the consideration of different sorption matrices and mechanistic explanations, the cell's membrane lipid fraction appears to be the most relevant sorption matrix for cellular bioconcentration of IOC. Experimental determination of the partition coefficients of the test compounds to membrane lipid and protein could refine predictions of the different model approaches applied here. If available,  $V_D$  from clinical studies in humans and measured  $K_{BW}$  from fish can give a first approximation for bioaccumulation potential of a compound in cells as well as in whole fish. A central question that remains is the influence of  $C_{free}$  on bioaccumulation in the cells. Both models, the kinetic cell model and the *in vitro* mass balance model, consider  $C_{free}$  implicitly (kinetic cell model) or explicitly (*in vitro* mass balance model) as driver for bioaccumulation in the cells. For compounds that strongly accumulate in cells,  $C_{free}$  appears to be less relevant and the bulk medium concentration gives a better approximation for the bioavailability of such compounds. These were the cationic and neutral compounds. For compounds with high affinity to albumin and other medium constituents such as lipids and amino acids,  $C_{free}$  should be measured additionally in future cell-based bioaccumulation experiments to assess the impact on bioavailability for cellular uptake and accumulation<sup>185</sup>

#### 4.6. Acknowledgements

The authors thank Michael McLachlan and Beate Escher for fruitful discussions.

---

## 5. Conclusions and Outlook

In my thesis research, I assessed whether permanent fish cell lines can be used to predict the bioconcentration potential of IOC in fish. For this purpose, I developed an experimental method with fish cell lines to quantify cellular concentrations of IOC. Further, I used different model approaches to gain insight into relevant accumulation mechanisms and evaluated the usability of a novel read across method. The most prominent conclusions and findings from this thesis are:

- Effective concentrations of IOC in an acute fish cell viability assay according to OECD TG249 correlated well with *in vivo* fish acute toxicity though for cationic compounds comparability was hampered by the quantity and quality of available *in vivo* data.
- *In vitro* bioconcentration assessment may be a conservative screening approach and one line of evidence to test the bioconcentration potential of IOC in fish.
- Biotransformation of the tested IOC is not an important elimination pathway in the studied cell lines.
- IOC accumulation in cells appears to be dominated by simple partitioning to membrane lipid, represented by the  $D_{MLW}$ .
- In combination with reliable  $K_{BW}$  values, the human  $V_D$  is a useful read across parameter to screen IOC for their bioconcentration potential in fish.

This thesis is a valuable contribution to advance *in vitro* alternatives to animal experimentation in the field of bioaccumulation science. However, new findings also raise new questions and ideas for future research. In this concluding chapter, therefore, the main outcomes of my thesis are discussed in the context of future investigations.

### 5.1. Extension and optimization of the bioconcentration assay with RTL-W1 and RTgill-W1 cells

Chapter 2 and 3 dealt with setting up a cell-based bioconcentration assay and the testing of a diverse range of cationic and anionic compounds for their accumulation in RTL-W1 and RTgill-W1 cell cultures. This application expands the portfolio of assays that use permanent fish cell lines to predict different outcomes of relevance for chemical risk assessment. However, compared to other cell-based assays, such as the acute cytotoxicity assay, where one 75 cm<sup>2</sup> cell culture flask is used for one exposure plate and test compound, a larger biomass is

needed, hence requiring more time for cell culture preparation. With at least 24 h of exposure, our established bioconcentration assay also takes more time than the depletion assays with primary hepatocytes or S9-fractions (typically 2 h) <sup>23, 24</sup>. A few measures may, however, offer high potential for optimization of the assay and enable the testing of more compounds: 1) Limiting the number of sampling time points, and 2) miniaturization of the assay format. Limiting the number of sampling time points to experimental onset and termination at steady-state <sup>72</sup> could reduce the number of samples and required biomass. This measure is justified because cellular uptake of compounds appeared to be fast – a true uptake phase could not be monitored with the implemented sampling scheme, where the first sample time point after onset of exposure was 4 h. Such practice would also be supported by prior cell accumulation experimentation for compounds with medium hydrophobicity ( $4 > K_{OW}$ ) <sup>41</sup>. In this way, throughput and robustness of the assay could be improved.

A miniaturization of the assay format from cell culture flasks to a well plate format (e.g. 6-well plate) could also be considered. We applied state-of-the-art chemical analysis methods, used exposure concentrations well below the proposed 1  $\mu\text{M}$  <sup>24</sup> and were able to quantify minute anionic compound amounts in exposed cells. In other words, we successfully attempted the quantification on the lower limit of current analytical possibilities. Therefore, it would require even lower detection and quantification limits of the chemical analysis method to enable the quantification in the cell samples of the downsized test system. Considering the continuous advancement of analytical methods it may be possible to miniaturize the test system in the future <sup>224</sup>.

Application of an *in vitro* mass balance model, as demonstrated in Chapter 4, indicated that the majority of the tested anionic compound masses likely sorbed to the FBS constituents in the medium. This sorption may effectively have reduced the bioavailable concentration for cellular uptake,  $C_{\text{free}}$ , thus influenced the cellular compound accumulation and the *in vitro* BCF. However, the use of  $C_{\text{free}}$  likely will not improve predictions of *in vivo* bioconcentration, due to the large overestimation when using  $C_{\text{free}}$  for BCF derivation in fish and cells. Additional sampling of  $C_{\text{free}}$  in the medium using SPME fibers <sup>185</sup> could help to understand the effect of reduced bioavailability due to compound sorption to medium constituents. If  $C_{\text{free}}$  was sampled over several time points, the true extent of the replenishment of  $C_{\text{free}}$  by compound desorption from medium constituents could be evaluated. An even simpler test, avoiding additional SPME fiber sampling, may be a comparison of two bioconcentration assays of the same test

compound, which differ only in the supplementation of FBS in the exposure medium. For example, FBS concentration could differ by factor 10 (e.g. 5 % FBS and 0.5 %) in the bioconcentration assays. If the serum albumin served as a reservoir to replenish  $C_{\text{free}}$ , no difference in  $C_{\text{free}}$  and the cellular compound amounts of the two bioconcentration assays would be discernable. Differing cellular accumulations of the compound and  $C_{\text{free}}$  could give a clear indication whether FBS presence affected cellular compound accumulations.

The main question of the presented thesis is whether permanent fish cell lines can predict the bioconcentration potential of IOC in fish and therefore replace the common bioaccumulation assessment with animals. However, this replacement of animal experimentation with an *in vitro* alternative would still use the animal test as benchmark. Since there are little *in vivo* data on IOC bioaccumulation in fish relative to neutral compounds, the question raises to what benchmark the *in vitro* data could be compared to, if little or no *in vivo* data of the respective substance class were available. Therefore, the established cell-based bioconcentration assay could help prioritize additional animal experimentation by testing the influence of molecular structure and charge on bioaccumulation in the cell cultures. A simple approach would be to test more compounds with similarly structured backbones, but different functional groups, resulting in either a positive or negative charge or no charge. Particularly suitable for such experiments are surfactants because of their simple molecular structure, the wide spectrum of chain lengths and the diversity of functional head groups <sup>65</sup>.

In addition to testing more IOC, it would be valuable to conduct bioconcentration assays at different medium pH in order to shed light on the influence of IOC speciation. Such experiments were conducted in rainbow trout with anionic surfactants recently and could serve as reference <sup>26</sup>. The equivalent experiment in rainbow trout cell cultures would give a deeper insight into the role of pH-dependent speciation and the associated accumulation mechanism that governs the cellular IOC uptake.

## **5.2. Characterization of RTgill-W1 and RTL-W1 to understand accumulation mechanisms**

Except for tecloftalam and benzotriazol-tert-butyl-hydroxyl-phenyl propanoic acid, the tested compounds in Chapter 2 and 3 are known to be biotransformed in hepatic S9-fractions <sup>25, 175</sup> or in bioaccumulation studies with fish to different degrees <sup>108, 148</sup>. For example, diclofenac ( $9.5 \text{ mL h}^{-1} \text{ g liver}^{-1}$ ) <sup>152</sup> was modestly biotransformed in rainbow trout liver S9-fractions relative

to N-methyldodecylamine ( $162 \text{ mL h}^{-1} \text{ g liver}^{-1}$ )<sup>175</sup>. Obtained mass balances from the bioconcentration assays in Chapter 2 and 3 revealed that biotransformation activity in the cells was negligible for the test compound's fate in the experiments despite the known biotransformation capacities in the cells<sup>35</sup>. The three cell lines were shown to biotransform a neutral model compound to the extent that derived biotransformation rates, when applied to IVIVE, led to an accurate BCF prediction in fish<sup>35</sup>. As discussed in Chapter 2, RTL-W1 and RTgill-W1 possess a repertoire of biotransformation enzymes, although their activity may be low compared to primary cell cultures<sup>34</sup>. However, biotransformation activity by the permanent fish cell lines may be modified. One approach could be to alter the cell culture conditions to which the RTgill-W1 and RTL-W1 cells were shown to adapt<sup>32</sup>. For example, one suggestion is to expose cell cultures to low non-toxic concentrations of compounds known to increase activity of phase I and II biotransformation enzymes, either over extended periods under routine culture conditions or as pre- or co-exposure during bioaccumulation assessment. Compounds that could be used to induce such biotransformation activity are high molecular weight polycyclic aromatic hydrocarbons<sup>225</sup>, dioxins<sup>225</sup> and beta-naphthoflavone<sup>226 227</sup>.

In Chapter 2, we concluded that the measured cellular accumulations were may be a result of processes beyond simple partitioning-based accumulation following  $D_{ow}$ . Responsible mechanisms may be active transport processes, which facilitate compound flux across the cell membrane or the membranes of organelles. The presence and activity of such transporter processes in RTL-W1 and RTgill-W1 cells is still rather poorly characterized and deserves further investigation<sup>46</sup>. So far, ABC transporters and one subfamily of the Solute Carrier transporters have been studied in the rainbow trout cell lines<sup>32, 228</sup>. In general, research efforts were mainly focused on ABC-transporters in fish<sup>78</sup>, due to their function as efflux (phase III) pumps of xenobiotics, which is part of the cellular detoxification mechanism. However, the importance of single transporter types for the overall bioconcentration of an IOC may be small. Therefore, it may be more useful to assess the importance of active transport more globally comprising the collective activity of all present transporters. In the context of IOC bioconcentration in the permanent fish cell lines, it would be useful to apply a two-compartment system separated by an insert with cultivated cells, as it has been done with RTgutGC cells and primary gill cells of rainbow trout<sup>36, 37, 38, 164</sup>. It was demonstrated that with the help of such systems, *in vitro* transfer rates across epithelia could be measured, which may proof valuable for PBTK-model approaches that simulate dynamic compound distributions in fish<sup>229</sup>.



With the advent of microfluidic systems, also new innovative experimental set ups for bioaccumulation assessment of organic compounds using fish cell lines become technically feasible <sup>230</sup>. Among many other applications, flow-through chips that offer space for the cultivation of an intact cell layer are particularly interesting for bioconcentration assessment of IOC with fish cell cultures. Especially multiple cell line exposures of microfluidic systems with different cell types in a serial or more complex set up are thinkable to simulate interaction of fish tissue *in vitro*. The set up could realistically mimic the IOC uptake via the fish gill, using RTgill-W1 cells, as primary entry into fish. Subsequent distribution to other cell cultures, for example from the liver and intestine, to represent different organs, could be achieved through interacting multiple channels or chips.

Closing the outlined knowledge gaps would advance permanent fish cell lines as experimental platform for bioaccumulation assessment of IOC and their predictive capacity for bioconcentration in fish. Further, the acceptance of cell lines for environmental risk assessment would benefit from a deeper knowledge that comes with the above suggested experiments.

### 5.3.Improvements for *in silico* prediction of bioconcentration

The outcomes of Chapter 4 indicate which parameters were most relevant for the prediction of cellular compound accumulation as well as for bioconcentration in fish. Greatest parameter sensitivities of the models were associated with the assumed pH in the cells and compound affinities to membrane lipid and protein, represented by  $D_{MLW}$  and  $D_{PW}$ , respectively. The uncertainty in partition coefficient estimation became especially clear when measured  $D_{MLW}$  values led to considerable improvements in the kinetic cell model (Chapter 4). This emphasized that the partition coefficient of both IOC species, i.e. the neutral and the charged species, should be determined experimentally, if possible <sup>57</sup>. Current PP-LFER for partition coefficient prediction of IOC have limited applicability domains, which results in greater uncertainties if used for extrapolation to compounds that are not structurally similar to compounds in the PP-LFER training set <sup>73</sup>.

One potentially erroneous assumption might be that protein sorption in fish cell cultures is comparable to that in mammals and birds <sup>231 232</sup>. Therefore, it should be investigated if partitioning to BSA and chicken muscle are indeed representative surrogates for cellular protein in fish. This could be assessed with dialysis experiments that apply protein extracts from the fish cell cultures <sup>59 60</sup>. In such an experiment, the protein extracts are dissolved in one

chamber and the equilibration with a second chamber, which is separated by a dialysis membrane, is used to derive  $D_{PW}$ . Such experimentally determined values with the actual matrix are likely most useful to improve future model attempts.

To refine the model predictions, the quantification of protein and lipid content (storage lipid and membrane lipid) in RTL-W1 and RTgill-W1 cell cultures could be one option. For example, the dye-based Lowry assay has been used to measure protein content in RTgill-W1 cells in the past <sup>233 41</sup>. The lipid content could be measured via extraction <sup>234</sup> and the spectrophotometric sulfo-phosphovanillin method <sup>235</sup>, using different calibration standards for storage lipid and phospholipid <sup>89</sup>.

The current literature provides a principal understanding of mechanisms behind IOC accumulation in fish and their cells, although not all processes are well described and usable for mechanistic incorporation in computational models <sup>236 46 21 72</sup>. The most prominent process is transporter mediated flux across cell membranes (see above). To date, no PBTK model for fish has implemented measured compound transport rates because such rates are not readily available and little studied <sup>39</sup>. The above mentioned two compartment system to measure epithelial transfer rates could be an experimental set up to measure such rates *in vitro*. In general, more efforts in the research of transporter activity in fish promise valuable contributions to our understanding of their importance and role in bioaccumulation of IOC in fish.

#### 5.4. RTL-W1 and RTgill-W1 as predictors for bioconcentration in fish?

The question may be raised whether the cells actually accumulate the tested IOC and whether the observed accumulation may not be also achieved by dead cell material. Essentially, this question is about the location of the IOC in the exposed cells and to what extent the presented bioaccumulation processes in living cells can account for actual uptake and internal distribution inside the cells. Several reasons speak for the need to have live cells.

First, the determination of non-toxic exposure concentrations via the acute cytotoxicity assay with RTgill-W1<sup>43</sup> ensured that no toxic exposure concentrations were applied in the subsequent bioaccumulation assays (see 2.4.2 and 3.4.1). Therefore, it can be excluded that the exposed cells in the presented bioaccumulation assays were experiencing measurable cytotoxicity, which would have impacted or killed the cells. This was also confirmed via visual inspection of the exposed cell cultures during the bioaccumulation assay. Further, the fact that a concentration-dependent accumulation was measurable in the cytotoxicity assays with RTgill-W1 imply that the tested compounds were taken up into the cells, not merely associated with the cell surface.

Second, the negative controls as well as the intermittent rinse steps between sampling the different fractions of the *in vitro* test system ensured that indeed only IOC associated with the cells was sampled. Admittedly, the sampling scheme and design of the bioaccumulation assay did not allow for the determination of detailed compound location within the cell or how the tested IOC were taken up. Both aspects were secondary in this research project. Nevertheless, as a first step toward finding the IOC location in the cell fraction was taken in Chapter 3. In experiments with cationic surfactants, a rinse of the cell surface with EDTA was intended to assess the extent of loosely cell surface bound IOC. Further experiments to narrow down the compound location in the cells and mode of uptake into the cells could be conducted as described next.

The question on IOC location in the cells and whether active uptake or cell metabolism played a role in the overall IOC accumulation could be answered in two principal approaches. The first approach concerns temperature and transporter-dependent uptake processes, while the second one would be the visualization of IOC location in the cells. As for the first approach, the temperature during the bioaccumulation assay could be lowered from 19 °C down to 4 °C to slow down the cells' metabolism<sup>36</sup>. A lower accumulation at 4 °C would proof that a protein mediated, thus temperature-dependent, uptake process is involved in the IOC accumulation in RTL and RTgill-W1 cells. A similar accumulation between the two temperature regimes and comparison with partition-based accumulation predictions could answer the question whether the measured compound concentration in the cell samples resulted from passive uptake

through diffusion or protein-mediated active uptake processes. Here it should be noted though that the chosen partition coefficient is also temperature dependent, which requires further assessment. Similar effects could also be observed by blocking specific membrane integrated transporters with strongly binding substrates <sup>32</sup>, which may lead to lower uptake into the intracellular space and thus an overall lower bioaccumulation in the exposed cells. It should be noted though that the results of these experiments likely differ dependent on the tested IOC class. For example, while cationic surfactants may appear to be accumulating via passive uptake into the cell membranes, this may not be the case for anionic IOC, such as diclofenac. The second approach attempts the compound location in the cell using fluorescence microscopy. A cell culture would be exposed to either a model IOC labelled with a fluorescent marker or an intrinsically fluorescent compound. The accumulation in the cells and precise location in organelles could then be measured using different microscopy techniques that also allow for detection of time-dependent accumulation patterns <sup>194, 237</sup>. Further suggestions on how to improve the bioaccumulation assay with rainbow trout cell lines and close critical knowledge gaps concerning bioaccumulation in the studied cell lines are discussed in Chapter 5.2 and 5.3.

So far, bioaccumulation has been assumed to be measured as the concentration within an organism or tissue relative to the exposing medium concentration. In organisms, this definition is challenged by the fact that certain IOC classes, such as charged surfactants, may not accumulate within an organism but on its surface. This has been shown for cationic surfactants in rainbow trout, where large parts of the tested surfactants were associated with mucus, skin and gills <sup>74</sup>. In our *in vitro* test, a similar situation may be encountered, where IOC may not accumulate within the cell. This raises interesting regulatory questions of protection aims for environmental protection. A conservative regulation may require the avoidance of any compound accumulation on any body part or associated compartment (e.g. mucus) of a fish. This however, may not be relevant for protection of human health, since the fish consumption usually only concerns the muscle tissue, where potentially only marginal compound amounts accumulated in the fish. A detailed discussion of this matter goes beyond the present work but may be taken as an initial thought for further discussions.

In Chapters 2 to 4, I presented derived *in vitro* BCF in RTL-W1 and RTgill-W1 cells and their simulation by different model approaches. All these parts of my research give valuable arguments for why these fish cell lines may serve as one line of evidence to screen the bioaccumulation potential of IOC in fish. Fish cell lines may be preferred over experimentation with fish since fish experiments do not fulfill current regulatory needs for rapid testing of many different compounds for their bioaccumulation potential. As discussed in Chapter 5.1, a high throughput method for bioaccumulation assessment with the fish cells is realistic and could

fulfil the regulatory demand for higher throughput of compound testing. Also, the use of cell lines fulfils the societal desire to reduce and/or replace animal experimentation. The cells obviously cannot represent all processes that govern IOC bioaccumulation in fish, which, under certain circumstances (i.e. novel compounds with rare combination of physicochemical properties), may requires experimentation with fish <sup>46</sup>. However, the question is whether an *in vitro* alternative to such fish experiments needs to account for all bioaccumulation relevant processes in fish. Other lines of evidence, such as *in vitro* biotransformation assays or affinities to certain biological matrices may serve as additional lines of evidence to assess the IOC bioaccumulation potential in fish. For example, if a compound was shown to have a high *in vitro* BCF above a regulatory BCF threshold, refinement of the *in vitro* BCF with biotransformation assays using primary hepatocytes or liver S9 from rainbow trout <sup>23, 24</sup> can be an option. Yet, possible underestimations by the *in vitro* BCF, as shown above for PCP and PFOS, should be avoided. This could be achieved by the estimation of the compound's affinity to medium constituents and/or the measurement of  $C_{\text{free}}$  as discussed in section 5.2. All together, these three lines of evidence, *in vitro* BCF, *in vitro* biotransformation and partition coefficient, may serve as a battery of screening tools to replace fish experimentation with several new approach methodologies. In comparison to other cell lines in general, the RTL-W1 and RTgill-W1 belong to one of the best assessed cell lines for environmental risk assessment, most prominently evidenced by the adoption of the acute fish cell line toxicity assay with the RTgill-W1 cell line as a OECD Test guideline <sup>43</sup>. Therefore, they currently represent the best choice for *in vitro* bioaccumulation assessment for regulatory risk assessment.

This work marks a first step toward the bioaccumulation assessment of IOC using permanent fish cell lines for environmental risk assessment. Continued use of this bioconcentration assay on different IOC will provide further insights into the bioconcentration mechanisms of the exposed cell cultures. With the establishment of the bioconcentration assay we expand the portfolio of fish cell lines as experimental platform. Further research based on the bioconcentration assay will improve the overall comparability of *in vitro* experimentation to fish experiments and increase the acceptance of permanent fish cell lines as *in vitro* alternative for bioaccumulation assessment.

## Supporting Information Chapter 2

### S2.1 Test Compounds

Table S2.1: Supplementary information on test compounds and internal standards.

Test compound	Abbreviation	CAS	Formula	Vendor	Purity (%)
Benzotriazol-t-butyl-hydroxyl-phenyl propanoic acid	BHPP	84268-36-0	C <sub>19</sub> H <sub>21</sub> N <sub>3</sub> O <sub>3</sub>	BOC Sciences	95
Diclofenac Sodium	DCF	15307-79-6	C <sub>14</sub> H <sub>10</sub> Cl <sub>2</sub> NNaO <sub>2</sub>	Sigma Aldrich	98
Pentachlorophenol	PCP	87-86-5	C <sub>6</sub> Cl <sub>5</sub> OH	Sigma Aldrich	97.9
Tecloftalam	TT	76280-91-6	C <sub>14</sub> H <sub>5</sub> Cl <sub>6</sub> NO <sub>3</sub>	APIChem Technology	95.3
Mefenamic D <sub>4</sub> acid	-	1216745-79-7	C <sub>15</sub> H <sub>11</sub> D <sub>4</sub> NO <sub>2</sub>	CDN-Isotopes	99
Diclofenac-D <sub>4</sub>	-	15307-86-5	C <sub>14</sub> H <sub>7</sub> D <sub>4</sub> Cl <sub>2</sub> NO <sub>2</sub>	CDN-Isotopes	99
Pentachlorophenol- <sup>13</sup> C <sub>6</sub>	-	85380-74-1	<sup>13</sup> C <sub>6</sub> HCl <sub>5</sub> O	CDN-Isotopes	98.6

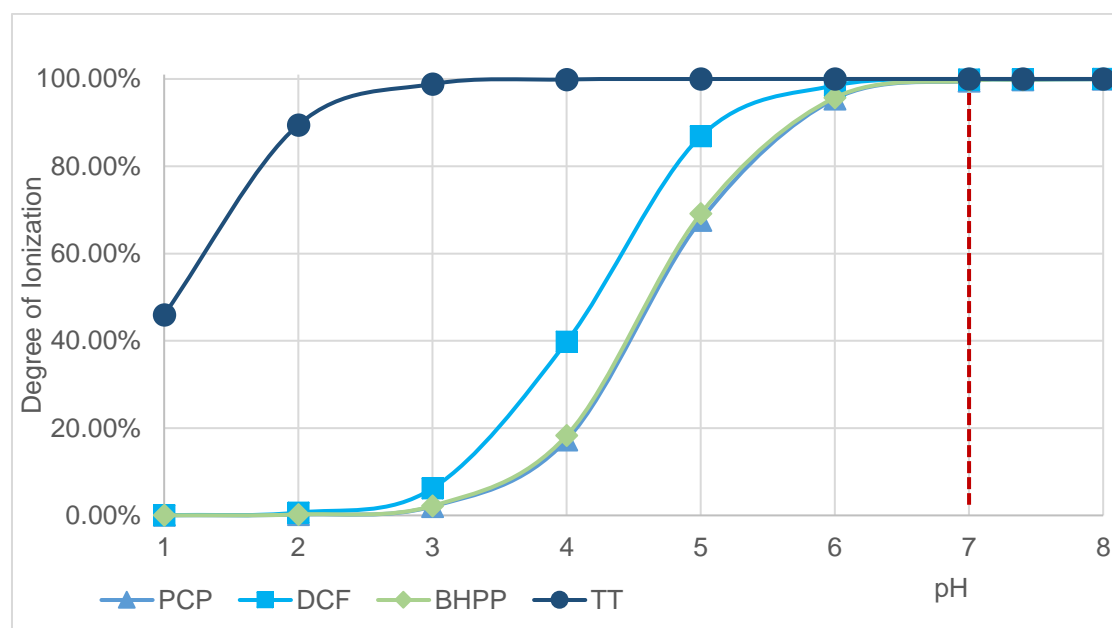


**Figure S2.1: pH influence on the degree of ionization of the test compounds.** Degree of ionization was calculated with the Henderson-Hasselbalch equation. The dashed line indicates the pH at which cytotoxicity assays and bioaccumulation experiments were conducted. PCP = Pentachlorophenol, DCF = Diclofenac, BHPP = Benzotriazol-t-butyl-hydroxyl-phenyl propanoic acid, TT = Tecloftalam

## S2.2 Acute cytotoxicity assays and confirmation of non-toxic final exposure concentrations

The acute cytotoxicity assay with RTgill-W1 served to determine the final non-toxic exposure concentration for the bioaccumulation experiments. Table S2.2 documents the intended nominal and the measured exposure concentrations of the conducted cytotoxicity assays. The exposure media were sampled at experimental onset and termination of the cytotoxicity assay, measured and the geometric mean of the two sample times calculated. For BHPP, a precipitation of BHPP could be visually observed in the highest four exposure concentrations (nominal 180,000 to 15000 µg/L), which caused the considerably lower measured exposure concentrations relative to the nominal exposure concentrations.

**Table S2.2: Nominal and measured exposure concentrations of the test compounds in acute cytotoxicity assays with RTgill-W1 along with resulting cell viability values for alamarBlue (AB).** SD = Standard Deviation, DCF = Diclofenac, PCP = Pentachlorophenol, BHPP = Benzotriazol-t-butyl-hydroxyl-phenyl propanoic acid, TT = Tecloftalam, LOQ = Limit of Quantification

Compound	Nominal (µg/L)	Measured geometric mean (µg/L)	SD (µg/L)	Measured vs. Nominal (%)	Viability (AB, %)	SD Viability (AB, %)
DCF	100000	80746	3132	81	1.9	0.6
DCF	70000	63676	1841	91	14.9	16.5
DCF	35000	25658	3175	73	3.2	0.3
DCF	14000	10661	501	76	47.5	9.5
DCF	7000	4986	203	71	86.5	7.8
DCF	3500	2389	239	68	93.1	5.8
PCP	476	401	19	84	2.1	1.0
PCP	200	167	9	83	2.4	0.4
PCP	84	62	13	74	62.6	14.2
PCP	35	25	5	70	91.3	6.1
PCP	15	11	2	76	96.9	6.7
PCP	6	5	1	78	96.6	7.7
BHPP	180000	47401	40495	26	2.3	1.1
BHPP	90000	22732	70248	25	14.1	6.3
BHPP	30000	7998	32238	27	51.5	12.8
BHPP	15000	4539	15076	30	68.3	8.2
BHPP	330	165*	0	50	97.6	4.4
BHPP	33	16.5*	102	50	98.3	6.4

Compound	Nominal (µg/L)	Measured geometric mean (µg/L)	SD (µg/L)	Measured vs. Nominal (%)	Viability (AB, %)	SD Viability (AB, %)
TT	30000	27529	8924	92	1.8	0.7
TT	24000	17264	1852	72	12.3	10.6
TT	12000	7521	276	63	80.9	8.3
TT	6000	3956	155	66	104.9	3.7
TT	3000	2089	562	70	108.7	4.5
TT	300	416	223	139	103.1	6.7
TT	30	23	4	77	97.6	9.1

\*Values below LOQ: 0.5 × LOQ used

From this data set, the exposure concentrations for bioaccumulation experiments were determined and used in a cytotoxicity assay with RTL-W1 cells, to confirm that the final exposure concentrations were non-toxic to the exposed cells. Table S2.3 shows the comparison of nominal and measured exposure concentrations of the cytotoxicity assays with RTL-W1. The concurrent viability measurements, quantified via fluorescence measurements of alamarBlue, 5-carboxyfluorescein diacetate acetoxymethyl ester (CFDA-AM) and Neutral Red are shown in Figure S2.2. The geometric mean of the exposure concentrations were within the range of the nominal intended concentrations (Table S2.3), which corroborates that the determined exposure concentrations are indeed non-toxic (Figure S2.2).

**Table S2.3: Measured exposure concentrations of acute cytotoxicity assay with RTL-W1 cells.** SD = Standard Deviation, Medium control = measured exposure concentrations stored in vessel used for preparation and sampled over the experimental duration, BHPP = Benzotriazol-t-butyl-hydroxyl-phenyl propanoic acid, DCF = Diclofenac, PCP = Pentachlorophenol, TT = Tecloftalam.

Compound	Exposure Type	Nominal Exposure (µg/L)	Measured Exposure Concentration (µg/L)	SD (µg/L)	Measured/Nominal (%)	SD (%)
BHPP	No cell control	10	8.2	1.7	82	17
BHPP	RTL-W1	10	4.6	2.2	46	22
BHPP	Medium control	10	9.5	2.2	95	22
DCF	No cell control	400	416.6	116.3	104	29
DCF	RTL-W1	400	391.7	19.3	98	5



Compound	Exposure Type	Nominal Exposure (µg/L)	Measured Exposure Concentration (µg/L)	SD (µg/L)	Measured/Nominal (%)	SD (%)
DCF	Medium control	400	383.1	24.7	96	6
PCP	No cell control	5	4.8	0.2	96	3
PCP	RTL-W1	5	3.8	0.8	75	16
PCP	Medium control	5	4.5	0.6	90	12
TT	No cell control	20	21.7	3.6	109	18
TT	RTL-W1	20	22.2	4.1	111	20
TT	Medium control	20	22.1	2.7	111	14

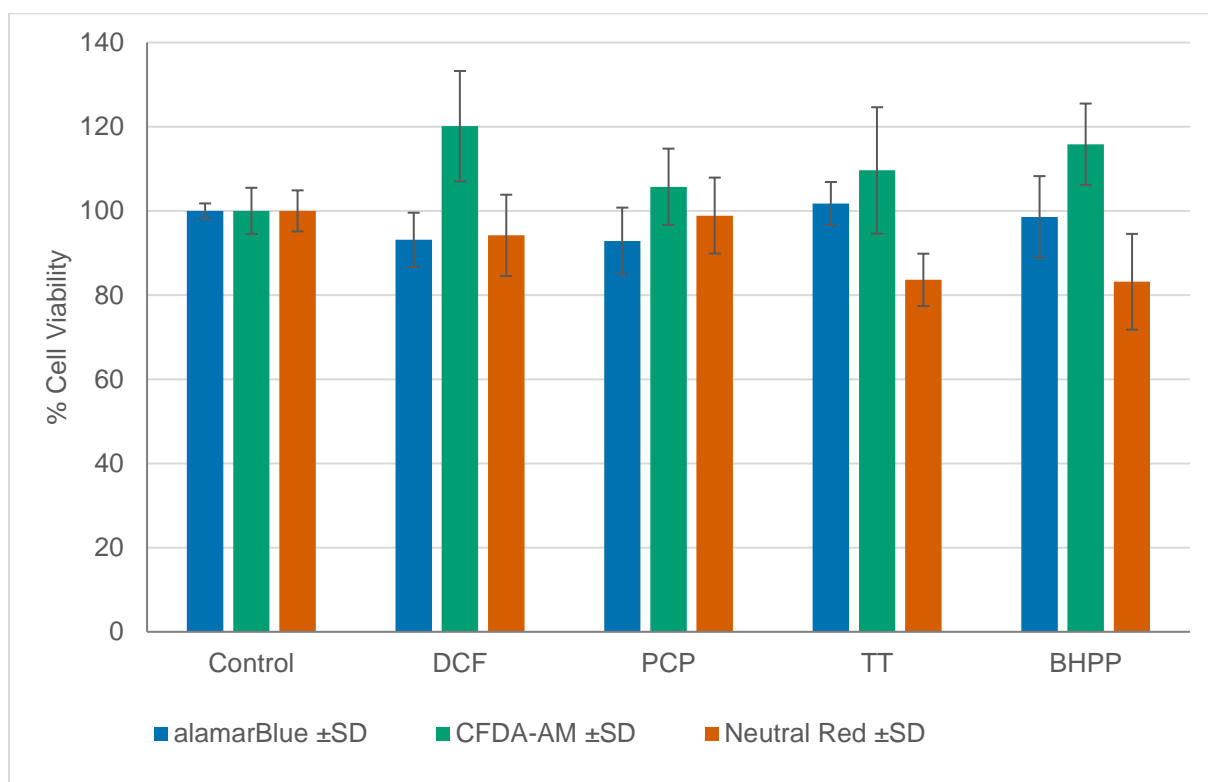


**Figure S2.2: Acute cytotoxicity of the final exposure concentrations after 72 h exposure in RTL-W1.** The tested exposure concentrations were used in the bioaccumulation experiments. alamarBlue indicates for metabolic activity, CFDA-AM for cell membrane integrity and Neutral Red for lysosomal membrane integrity. Control = test compound-free control, SD = Standard Deviation, DCF = Diclofenac (400 µg/L), PCP = Pentachlorophenol (5 µg/L), TT = Tecloftalam (20 µg/L), BHPP = Benzotriazol-t-butyl-hydroxyl-phenyl propanoic acid (10 µg/L)

### S2.3 Well plate versus cell culture flasks

To increase the number of cells in the bioaccumulation experiments, cell culture flasks were used instead of 24 well plates. This allowed all test compounds to be quantifiable in the cell samples, as shown in Table S2.4. Except for TT, the use of cell culture flasks increased the number of cell samples with quantifiable sample amounts. For example, PCP was detectable in all cell samples, of which 50 % was quantifiable. One cell sample in the TT exposure experiments was an assumed outlier.

**Table S2.4: Fractions of quantifiable cell samples in the well plate and cell culture flask format.**

If percentages do not add up to 100 %, the remainder was a none detect of test compound in the sample. The well plate experiment was conducted once with two technical replicates and two sampling time points (0 h and 48 h) (n = 4 cell samples). The bioaccumulation experiments were conducted twice with one technical replicate and the 0 h and 48 h time points were used for comparison (n = 4). For DCF, the bioaccumulation experiment in flasks with 200 µg/L exposure concentration was used for comparison (n = 2), since only this concentration was applied in the experiment in well plates (n = 4). BHPP = Benzotriazol-t-butyl-hydroxyl-phenyl propanoic acid, DCF = Diclofenac, PCP = Pentachlorophenol, TT = Tecloftalam.

Test compound	Well plate		Cell culture flask	
	Detected, not quantifiable (%)	Quantifiable (%)	Detected, not quantifiable (%)	Quantifiable (%)
BHPP	25	50	0	100
DCF	25	75	0	100
PCP	0	0	50	50
TT	0	100	25	75

### S2.4 Determination of optimal cell density in cell culture flasks

To find the optimal cell density, where the cell number of RTL-W1 cells varied as little as possible over the experimental duration, three different cell densities were tested:  $1.97 \times 10^6$  cells/flask,  $2.63 \times 10^6$  cells/flask and  $3.29 \times 10^6$  cells/flask. The flasks had the same format as used in the bioaccumulation experiments. The cell density was measured at time of seeding, after 48 h incubation under standard culture conditions, at the experimental onset (0 h) and at experimental termination (48 h). The resulting cell numbers of the three tested cell densities are depicted in Figure S2.3. The flasks seeded with  $3.29 \times 10^6$  RTL-W1 cells showed smallest variations in cell number over the experimental duration (0 h and 48 h). Therefore, the cell seeding density of  $3.29 \times 10^6$  cells/flask was used for the bioaccumulation experiments.

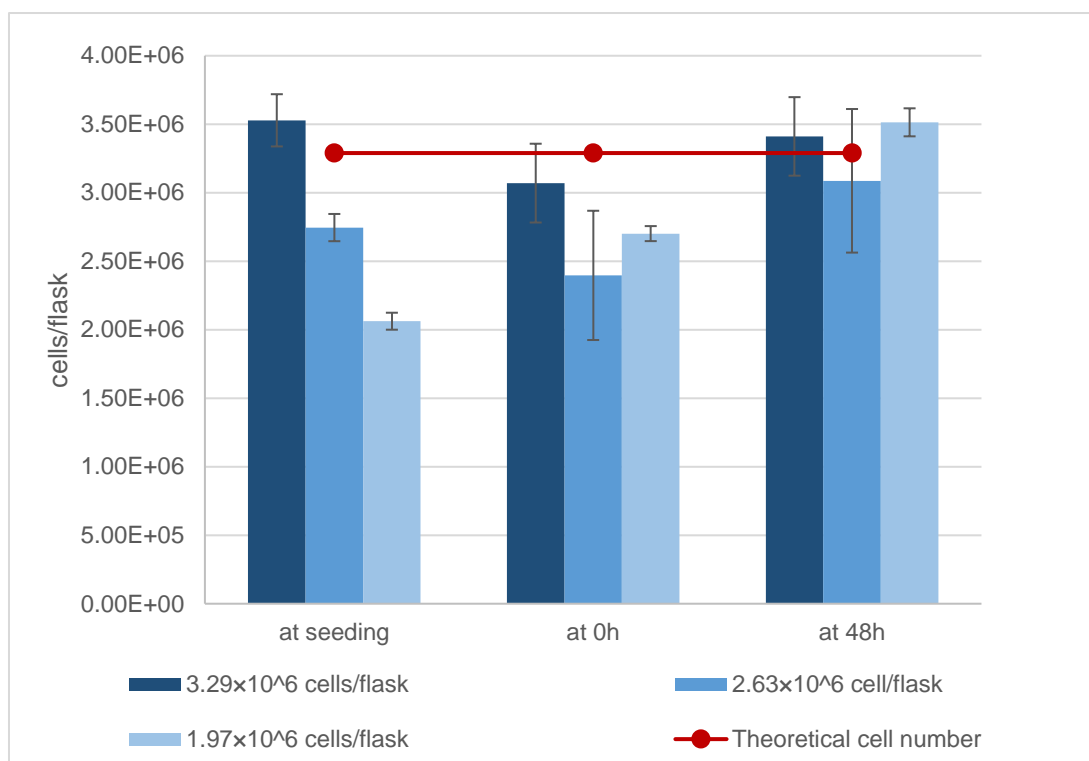


**Figure S2.3: Varied RTL-W1 cell densities in cell culture flasks at seeding and over 48 h experimental duration.** Theoretical cell number is the extrapolated cell number from 24 well plates with a seeding density of 150,000 RTL-W1 cells/well, which is known to result in stable and homogenous cell numbers <sup>43</sup>.

## S2.5 Bioaccumulation experiments

### Reported cell numbers and mass balances of bioaccumulation experiments

The RTL-W1 cells were counted in the bioaccumulation experiments at the start and termination (0 h and 48 h/72 h). The cell numbers are reported in Figure S2.4 and the mass balances of treated cells and cell-free control in Table S2.5 and Table S2.6.

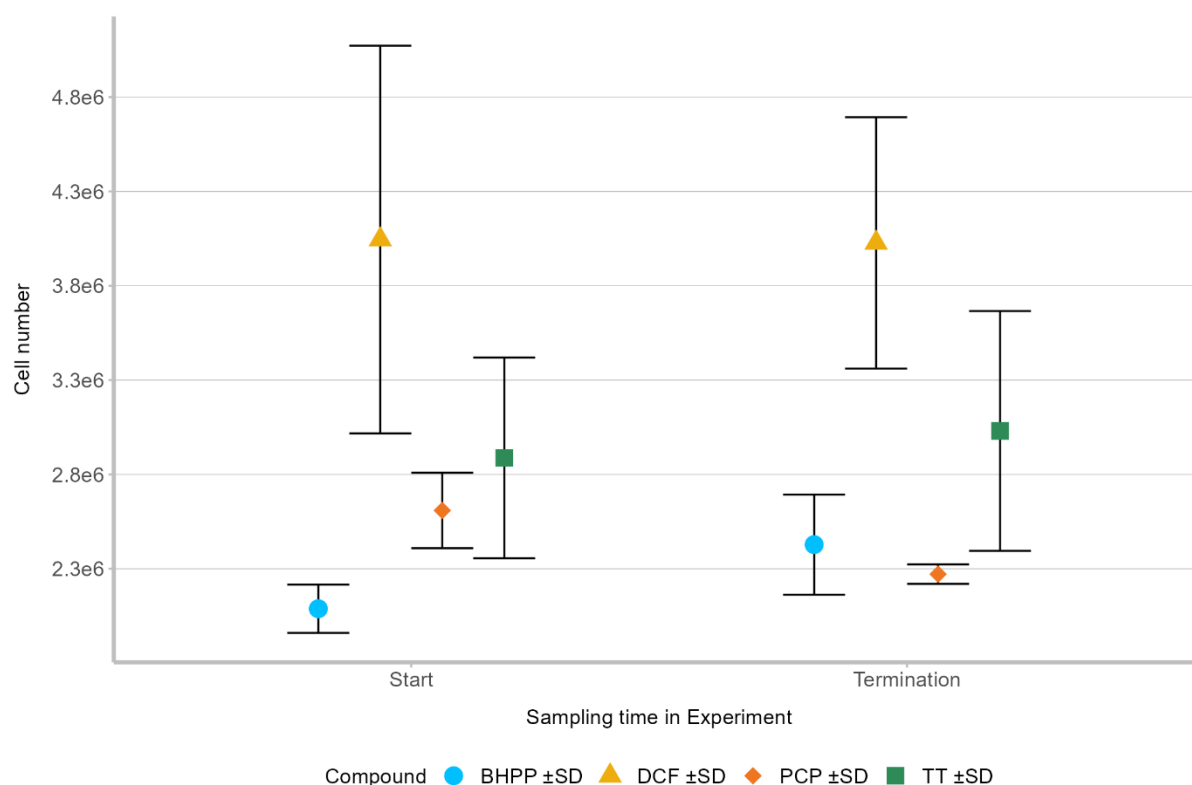


**Figure S2.4: Cell numbers in bioaccumulation experiments.** BHPP = Benzotriazol-t-butyl-hydroxyl-phenyl propanoic acid, SD = Standard Deviation, DCF = Diclofenac, PCP = Pentachlorophenol, TT = Tecloftalam

**Table S2. 5: Absolute amount of test compound in bioaccumulation experiments with treated RTL-W1 cells.** Test compounds were detected in all samples except for one\*. SD = standard deviation, BHPP = Benzotriazol-t-butyl-hydroxyl-phenyl propanoic acid, TT = Tecloftalam, na = not available (due to lacking replicates at these time points, since one replicate sampled at 72 h instead of at 16 h), DCF = Diclofenac, PCP = Pentachlorophenol

Compound	Sample type	Sample time (h)	Mean amount (ng)	SD (ng)
BHPP	CELL	0	0.4	0.1
BHPP	CELL	4	0.9	0.3
BHPP	CELL	8	0.7	0.0
BHPP	CELL	16	0.9	0.1
BHPP	CELL	24	0.8	0.2
BHPP	CELL	48	0.8	0.5
BHPP	MEDIUM	0	20.4	10.2
BHPP	MEDIUM	4	20.9	7.2
BHPP	MEDIUM	8	19.3	8.5
BHPP	MEDIUM	16	20.6	10.0
BHPP	MEDIUM	24	20.6	5.3

Compound	Sample type	Sample time (h)	Mean amount (ng)	SD (ng)
BHPP	MEDIUM	48	16.5	6.9
BHPP	PLASTIC	0	0	0
BHPP	PLASTIC	4	0	0
BHPP	PLASTIC	8	0.05	0.08
BHPP	PLASTIC	16	0.06	0.09
BHPP	PLASTIC	24	0.05	0.07
BHPP	PLASTIC	48	0.05	0.07
TT	CELL	0	0.15	0.21
TT	CELL	4	0.81	0.36
TT	CELL	8	0.70	0.11
TT	CELL	16	0.85	na
TT	CELL	24	0.79	0.08
TT	CELL	48	1.2	0.71
TT	CELL	72	0.8	na
TT	MEDIUM	0	71.0	23.3
TT	MEDIUM	4	75.8	24.6
TT	MEDIUM	8	66.5	29.3
TT	MEDIUM	16	61.1	na
TT	MEDIUM	24	76.0	25.0
TT	MEDIUM	48	76.4	26.0
TT	MEDIUM	72	81.3	na
TT	PLASTIC	0	0	0
TT	PLASTIC	4	0	0
TT	PLASTIC	8	0	0
TT	PLASTIC	16	0	na
TT	PLASTIC	24	0	0
TT	PLASTIC	48	0	0
TT	PLASTIC	72	0	na
DCF	CELL	0	1.1	1.2
DCF	CELL	4	0.9	1.6
DCF	CELL	8	1.9	3.4
DCF	CELL	16	1.3	1.3
DCF	CELL	24	1.1	1.2

Compound	Sample type	Sample time (h)	Mean amount (ng)	SD (ng)
DCF	CELL	48*	1.4	1.2
DCF	MEDIUM	0	593	550
DCF	MEDIUM	4	620	598
DCF	MEDIUM	8	543	481
DCF	MEDIUM	16	580	536
DCF	MEDIUM	24	552	498
DCF	MEDIUM	48	536	471
DCF	PLASTIC	0	0.33	0.57
DCF	PLASTIC	4	0.14	0.24
DCF	PLASTIC	8	0.14	0.24
DCF	PLASTIC	16	0.27	0.47
DCF	PLASTIC	24	0	0
DCF	PLASTIC	48	0	0
PCP	CELL	0	0.00	0
PCP	CELL	4	0.03	0.04
PCP	CELL	8	0.00	0
PCP	CELL	16	0.05	0
PCP	CELL	24	0.02	0.03
PCP	CELL	48	0.04	0
PCP	MEDIUM	0	13.5	0.4
PCP	MEDIUM	4	13.4	0.3
PCP	MEDIUM	8	13.8	0.6
PCP	MEDIUM	16	13.3	0.7
PCP	MEDIUM	24	13.0	0.1
PCP	MEDIUM	48	13.0	0.8
PCP	PLASTIC	0	0	0
PCP	PLASTIC	4	0	0
PCP	PLASTIC	8	0	0
PCP	PLASTIC	16	0	0
PCP	PLASTIC	24	0	0
PCP	PLASTIC	48	0	0

**Table S2.6: Absolute amount of test compound in bioaccumulation experiments with cell-free control.** SD = standard deviation, BHPP = Benzotriazol-t-butyl-hydroxyl-phenyl propanoic acid, TT = Tecloftalam, na = not available (due to lacking replicates at these time points, since one replicate sampled at 72 h instead of at 16 h), DCF = Diclofenac, PCP = Pentachlorophenol

Compound	Sample type	Sample time (h)	Mean amount (ng)	SD (ng)
BHPP	CELL	0	0.02	0.03
BHPP	CELL	4	0.03	0.05
BHPP	CELL	8	0.04	0.05
BHPP	CELL	16	0.03	0.05
BHPP	CELL	24	0.03	0.04
BHPP	CELL	48	0.00	0.00
BHPP	MEDIUM	0	23.1	6.8
BHPP	MEDIUM	4	20.3	9.4
BHPP	MEDIUM	8	21.6	8.8
BHPP	MEDIUM	16	23.3	7.0
BHPP	MEDIUM	24	17.0	11.6
BHPP	MEDIUM	48	21.3	3.8
BHPP	PLASTIC	0	0.1	0.2
BHPP	PLASTIC	4	0.04	0.06
BHPP	PLASTIC	8	0.05	0.07
BHPP	PLASTIC	16	0.2	0.1
BHPP	PLASTIC	24	0.05	0.07
BHPP	PLASTIC	48	0.05	0.07
TT	CELL	0	0	0
TT	CELL	4	0	0
TT	CELL	8	0	0
TT	CELL	16	0	na
TT	CELL	24	0	0
TT	CELL	48	0	0
TT	CELL	72	0	na
TT	MEDIUM	0	83.7	14.9
TT	MEDIUM	4	93.0	23.6
TT	MEDIUM	8	73.5	21.4
TT	MEDIUM	16	57.3	na

Compound	Sample type	Sample time (h)	Mean amount (ng)	SD (ng)
TT	MEDIUM	24	87.5	11.4
TT	MEDIUM	48	70.3	23.3
TT	MEDIUM	72	91.8	
TT	PLASTIC	0	0.1	0.1
TT	PLASTIC	4	0	0
TT	PLASTIC	8	0	0
TT	PLASTIC	16	0	na
TT	PLASTIC	24	0	0
TT	PLASTIC	48	0.06	0.09
TT	PLASTIC	72	0.0	na
DCF	CELL	0	0.3	0.5
DCF	CELL	4	0.4	0.6
DCF	CELL	8	0.2	0.4
DCF	CELL	16	0.2	0.3
DCF	CELL	24	0.2	0.4
DCF	CELL	48	0.8	1.4
DCF	MEDIUM	0	536	459
DCF	MEDIUM	4	554	515
DCF	MEDIUM	8	560	514
DCF	MEDIUM	16	586	542
DCF	MEDIUM	24	552	502
DCF	MEDIUM	48	556	522
DCF	PLASTIC	0	0	0
DCF	PLASTIC	4	0.3	0.4
DCF	PLASTIC	8	0.1	0.2
DCF	PLASTIC	16	0.2	0.4
DCF	PLASTIC	24	0.2	0.4
DCF	PLASTIC	48	0.3	0.6
PCP	CELL	0	0	0
PCP	CELL	4	0	0
PCP	CELL	8	0	0
PCP	CELL	16	0	0



Compound	Sample type	Sample time (h)	Mean amount (ng)	SD (ng)
PCP	CELL	24	0	0
PCP	CELL	48	0	0
PCP	MEDIUM	0	13.3	0.005
PCP	MEDIUM	4	13.7	0.3
PCP	MEDIUM	8	13.7	0.9
PCP	MEDIUM	16	13.0	0.4
PCP	MEDIUM	24	13.0	0.8
PCP	MEDIUM	48	13.0	0.1
PCP	PLASTIC	0	0.0	0.0
PCP	PLASTIC	4	0.0	0.0
PCP	PLASTIC	8	0.0	0.0
PCP	PLASTIC	16	0.0	0.0
PCP	PLASTIC	24	0.0	0.0
PCP	PLASTIC	48	0.0	0.0

## S2.6 Rinse step introduction

To enable the clear differentiation of distributed test compound in the fractions of the test system, the influence of a rinse step was investigated. This meant that in between the sampling of fractions, the system was rinsed to reduce the carry-over of test compound from one fraction to the subsequent sampled fraction. These experiments were conducted in 24 well plates (Greiner Bio-One VACUETTE Schweiz GmbH), as it has been done in previous studies<sup>35, 41</sup>. Each of these preliminary studies was conducted once.

Figure S2.5 depicts the logarithmic absolute test compound amounts in the cell fractions, where the rinse step was left out (“without rinse”) and where the rinse step was included (“with rinse”). Table S2.7 gives the original values, depicted in Figure S2.5. In the experiments “without rinse” (Figure S2.5, left) the test compound amounts between the cell-free and the exposed cells were comparable. This indicates that the intracellular test compound amount was indistinguishable from the cell-free control, due to large carry over from the medium. The introduction of a rinse step enabled to clearly distinguish between cell-free and exposed cells (Figure S2.5, right), which suggests that the rinsing in between the sampling of fractions reduced the carry over of test compound. However, with the introduction of a rinse step PCP was not detectable anymore, which implied that a greater amount of cells was necessary.

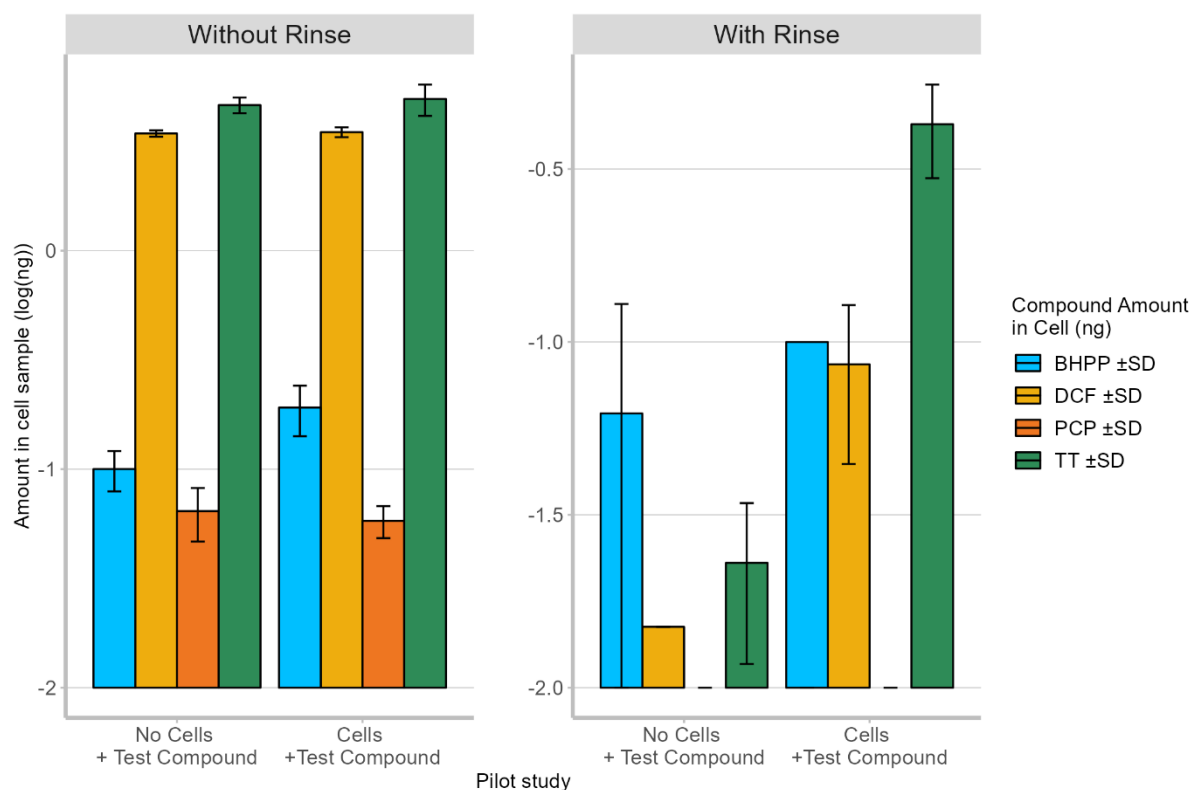


**Figure S2.5: Test compound in cell samples of exposed cells and the cell-free control in the 24 well plate format after 48 h.** Without Rinse = Sampling conducted without the application of a rinse step, With Rinse = Sampling with the application of a rinse step. Bars that lack error bars are caused by technical replicates with no detections of the test compound. BHPP = benzotriazol-t-butyl-hydroxyl-phenyl propanoic acid, SD = Standard Deviation, DCF = diclofenac, PCP = pentachlorophenol, TT = tecloftalam

**Table S2. 7: Absolute test compound amounts in cell samples after 48 h.** SD = Standard Deviation, Without Rinse = Sampling conducted without the application of a rinse step, With Rinse = Sampling with the application of a rinse step, DCF = diclofenac, PCP = pentachlorophenol, BHPP = benzotriazol-t-butyl-hydroxyl-phenyl propanoic acid, TT = tecloftalam

Compound	Experiment	Treatment	Absolute amount in cells (ng)	SD
DCF	Without Rinse	Exposed Cells	3.5	0.2
DCF	Without Rinse	Cell-free	3.4	0.1
DCF	With Rinse	Exposed Cells	0.09	0.04
DCF	With Rinse	Cell-free	0.02	0
PCP	Without Rinse	Exposed Cells	0.06	0.001
PCP	Without Rinse	Cell-free	0.06	0.02
PCP	With Rinse	Exposed Cells	na	na
PCP	With Rinse	Cell-free	na	na
BHPP	Without Rinse	Exposed Cells	0.2	0.05
BHPP	Without Rinse	Cell-free	0.10	0.02

Compound	Experiment	Treatment	Absolute amount in cells (ng)	SD
BHPP	With Rinse	Exposed Cells	0.1	na
BHPP	With Rinse	Cell-free	0.06	0.07
TT	Without Rinse	Exposed Cells	4.9	0.8
TT	Without Rinse	Cell-free	4.6	0.4
TT	With Rinse	Exposed Cells	0.4	0.1
TT	With Rinse	Cell-free	0.02	0.01

### S.2.7 Derived RTL-W1 BCF and *in vivo* data

The bioaccumulation experiments served to calculate steady-state BCFs in RTL-W1 and were compared to *in vivo* bioaccumulation data (Table S2.8 and Table S2.9).

**Table S2.8: Derived RTL-W1 BCF per replicate and chemical based on intracellular and exposure medium concentration.** The standard deviation is given after the mean. BHPP = benzotriazol-t-butyl-hydroxyl-phenyl propanoic acid, DCF = diclofenac, PCP = pentachlorophenol, TT = tecloftalam

Compound	Replicate	BCF
BHPP	1	30.28
	2	30.26
	Mean	30.27 ± 0.013
DCF	1	1.32
	2	1.74
	3	0.79
	Mean	1.28 ± 0.48
PCP	1	2.28
	2	2.44
	Mean	2.36 ± 0.12
TT	1	8.2
	2	4.5
	Mean	6.4 ± 2.6

**Table S2.9: Bioaccumulation studies of the test compounds in rainbow trout.** DCF = Diclofenac, PCP = Pentachlorophenol, TT = Tecloftalam, BHPP = Benzotriazol-t-butyl-hydroxyl-phenyl propanoic acid

Study	Chemical (CAS)	Exposure concentration	Bioaccumulation	Bioaccumulation metric unit	Bioaccumulation metric type (steady state if not indicated otherwise)
Memmert et al. 2013 <sup>102</sup>	DCF salt (15307-79-6, radio labelled)	2.1 and 18.7 µg/L via water	5 and 3 respectively	dimensionless	BCF, Whole fish
Cuklev et al. 2011 <sup>213</sup>	DCF no CAS given	1.6 ±0.93, 11.5 ±3.98, 81.5 ±14.09 µg/L via water	2.54 ± 0.36	dimensionless	BCF, Liver-based
McKim et al. 1986 <sup>108</sup>	radiolabelled PCP, no CAS given	0.968 ±0.206 µg/L	460	L/kg	BCF, Whole fish
Mueller et al. 2020 <sup>107</sup>	PCP (87-86-5)	fed 18.6-23 mg/kg	0.00898	dimensionless	BMF, Whole fish, converted BCF 0.2 ± 0.2
Mueller et al. 2020	PCP (87-86-5)	fed 18.6-23 mg/kg	0.0351	dimensionless	BMF, Liver (kinetic), converted BCF 0.2 ± 0.2
Mueller et al. 2020 <sup>107</sup>	TT (76280-91-6)	fed 27 mg/kg	0.00169	dimensionless	BMF, Whole fish, , converted BCF - 0.07 ± 0.3
Mueller et al. 2020 <sup>107</sup>	TT (76280-91-6)	fed 27 mg/kg	NA	-	BMF, Liver (kinetic), converted BCF not available
Mueller et al. 2020 <sup>107</sup>	BHPP (84268-36-0)	fed 31.63 mg/kg	0.03952	dimensionless	BMF, Whole fish, converted BCF 0.07 ± 0.4
Mueller et al. 2020 <sup>107</sup>	BHPP (84268-36-0)	fed 31.63 mg/kg	0.0779	dimensionless	BMF, Liver (kinetic), converted BCF 0.2 ± 0.4

## S2.8 Mass spectrometry settings and chromatographic gradient

The set up of the online SPE LCMS/MS system is described elsewhere and was identical for the present study<sup>128</sup>. Chromatographic separation was conducted with a C18 column (XBridge C18, 3.5 µm, 2.1 x 50 mm) and an eluent gradient of water and methanol as specified elsewhere. Electrospray ionization (ESI) was used for target analyte ionization with a spray voltage of + 4 kV in positive mode and - 3.5 kV in negative mode. The ion transfer capillary

was kept at a temperature of 320 °C. The target analytes were measured in switch mode on the MS. Further, full scan acquisitions were performed with a  $m/z$  range of 100 to 710 and a resolution of 70'000 at  $m/z$  200. Data-dependent top5 MS/MS were conducted in positive mode, while top2 MS/MS were conducted in negative mode, which was based on an inclusion list that contained all test compounds along with their suspected and known biotransformation products. The collision energies of the test compounds for the MS/MS are listed in Table S2.10. Tecloftalam lost a carboxyl group during the ionization process, which caused approximately 70 % of the detected Tecloftalam signals to be present in the fragmented form (Tecloftalam fragment  $m/z$  401.84, Table S2.10). Consequently, the quantified concentrations of both forms were summed up for the mass balances presented in the main text and everywhere else.

**Table S2.10: Collision energies of test compounds and formed fragment ions.**

Compound	Mode	Mass ( $m/z$ )	Normalized Collision Energy	Fragment Ions ( $m/z$ )
Diclofenac	positive	296.024	20	278.0132, 250.0185, 215.0498
Benzotriazol-t-butyl-hydroxyl-phenyl propanoic acid	positive	340.1656	20	284.1031, 224.0819
Pentachlorophenol	negative	264.8543	80	215.87087, 199.87596
Diclofenac	negative	294.0094	20	278.0132, 250.0185, 215.0498
Benzotriazol-t-butyl-hydroxyl-phenyl propanoic acid	negative	338.151	20	294.1612, 266.1298
Tecloftalam*	negative	445.8298	20	401.840, 214.8808
Tecloftalam fragment*	negative	401.8403	20	214.8808, 212.8838

\*Tecloftalam fragmented during the ionization from  $m/z$  445.8298 to 401.840.

The samples obtained from the cytotoxicity assay presented in section 2.4.2 were measured in offline mode (100  $\mu$ L injection volume) with the only difference to the above described analysis being the applied water/methanol gradient. The eluent flow was kept at 200  $\mu$ L/min throughout sample measurement. For the first 3 min, the methanol fraction was kept at 10 % and was gradually increased to 95 % over the following 11 min. The methanol was kept at 95 % for 3 min, after which it was brought down to 10 % again within 1 min and reconditioned at this gradient for 2 min until the next data acquisition.

**Table S2.11: Analytical performance of sample measurements from bioaccumulation experiments.** LOQ = limit of quantification, conc. = concentration, SD = Standard Deviation, BHPP = Benzotriazol-t-butyl-hydroxyl-phenyl propanoic acid, DCF = Diclofenac, PCP = Pentachlorophenol, TT = Tecloftalam

Test Compound	LOQ in medium, cell and plastic samples (ng per flask) [% of initial mass]	Exposure conc. in experiments (µg/L, [µM])	Relative recovery (medium, cell and plastic, %)	Measured vs. Nominal Medium conc. (% ± SD)
BHPP	1.3, 0.2, 0.2 [4.2, 0.7, 0.8]	10 [0.03]	88, 117, 99	68 ± 34
DCF	12, 1, 0.2 [2, 0.4, 0.4]	20, 200, 400 [0.07, 0.7, 1.35]	103, 101, 100	95 ± 1
PCP	0.2, 0.04, 0.04 [1, 0.3, 0.3]	5 [0.04]	95, 99, 95	90 ± 3
TT	0.6, 0.2, 0.2 [1, 0.3, 0.4]	20 [0.04]	92, 126, 99	118 ± 39

## S2.9 Relative recoveries

Table S12.2 summarizes the relative recoveries of the tested compounds in the different sample matrices across all replicates of the bioaccumulation experiments (left column) and in a spike experiment that was used to determine the relative recoveries (right column). The relative recovery was calculated as detailed in Equation S2.1:

$$\text{Equation S2.1:} \quad \text{Relative Recovery} = \frac{(C_{\text{spiked}} - C_{\text{unspiked}}) * 100 \%}{\text{theor. spiked amount}}$$

Where  $C_{\text{spiked}}$  is the test compound concentration of the spiked sample,  $C_{\text{unspiked}}$  the sample with no spike and *theor. spiked amount* is the theoretical amount of test compound that should have been spiked into the sample. The dedicated relative recovery experiment was performed by the spike of test compound to a test compound-free sample, which was compared to an identical spiked sample containing no matrix, i.e.  $C_{\text{unspiked}}$  was not used.

As presented in Table S2.12, the determined relative recoveries of the spike experiment for all matrices (right column) do not indicate a strong influence of the matrix. In the bioaccumulation experiment, however, the relative recoveries for each experiment varied considerably, except for PCP (Table S2.12, “Mean relative recovery (%) in bioaccumulation experiments). This is likely a result of the quantification for BHPP and TT, for which no isotope-labelled homologs were available. The larger deviations for DCF were attributable to errors in sample spiking, i.e.

unintendedly greater amounts of test compound were spiked. Consequently, the sample quantification was conducted with no correction for matrix effects.

**Table S2.12: Relative and absolute Recoveries of the test compounds in the bioaccumulation experiments.** SD = Standard Deviation

Compound	Sample Matrix	Mean relative recovery (%) in bioaccumulation experiments	SD (%)	Relative recovery (%) in spike experiment
Benzotriazol-t-butyl-hydroxyl-phenyl propanoic acid	Medium	132	71	88
Benzotriazol-t-butyl-hydroxyl-phenyl propanoic acid	Cell	120	6	117
Benzotriazol-t-butyl-hydroxyl-phenyl propanoic acid	Plastic	141	27	99
Diclofenac	Medium	161	104	103
Diclofenac	Cell	128	37	101
Diclofenac	Plastic	97	21	100
Pentachlorophenol	Medium	97	13	95
Pentachlorophenol	Cell	110	22	99
Pentachlorophenol	Plastic	84	41	95
Tecloftalam	Medium	139	100	92
Tecloftalam	Cell	74	3	126
Tecloftalam	Plastic	95	16	99

## S2.10 LC<sub>50</sub> data of PCP in fish

Table S2.13 summarizes the *in vivo* studies that were used for comparison of EC<sub>50</sub> and LC<sub>50</sub> of PCP, since data availability was much greater than for any of the other test compounds. The selection of studies based on the quality of experiments, in accordance with OECD TG305<sup>9</sup>, and state-of-the-art analytical methods, i.e. use of gas chromatography or liquid chromatography coupled to mass spectrometry.

**Table S2.13: Reference LC<sub>50</sub> values of Pentachlorophenol taken from Fischer et al. 2019.** Only measured exposure concentrations were selected. PCP was the only chemical with extensive documentation of LC50 data while data availability for the other test compounds was considerably smaller or not existent, as it was the case for BHPP.

Species	Organism Age	Organism Life stage	Exposure Type	Concentration Type	96 h LC <sub>50</sub>		Chemical Analysis	Reference Number	Author	Title	Source	Publication Year
Fathead Minnow	not reported	Juvenile	Flow-through	Active ingredient	0.564	mg/L	Measured	15031	Broderius, S.J., M.D. Kahl, and M.D. Hoglund	Use of Joint Toxic Response to Define the Primary Mode of Toxic Action for Diverse Industrial Organic Chemicals	Environ. Toxicol. Chem.14(9): 1591-1605	1995
Fathead Minnow	44 d	not reported	Flow-through	Active ingredient	0.237	mg/L	Measured	12447	Geiger, D.L., C.E. Northcott, D.J. Call, and L.T. Brooke	Acute Toxicities of Organic Chemicals to Fathead Minnows (Pimephales promelas), Volume II	Center for Lake Superior Environmental Studies, University of Wisconsin, Superior, WI:326 p.	1985
Fathead Minnow	not reported	Adult	Flow-through	Active ingredient	0.12	mg/L	Measured	11958	Hedtke, S.F., C.W. West, K.N. Allen, T.J. Norberg-King, and D.I. Mount	Toxicity of Pentachlorophenol to Aquatic Organisms Under Naturally Varying and Controlled Environmental Conditions	Environ. Toxicol. Chem.5(6): 531-542	1986
Fathead Minnow	not reported	Juvenile	Flow-through	Active ingredient	0.35	mg/L	Measured	15031	Broderius, S.J., M.D. Kahl, and M.D. Hoglund	Use of Joint Toxic Response to Define the Primary Mode of Toxic Action for Diverse Industrial Organic Chemicals	Environ. Toxicol. Chem.14(9): 1591-1605	1995



Species	Organism Age	Organism Life stage	Exposure Type	Concentration Type	96 h LC <sub>50</sub>		Chemical Analysis	Reference Number	Author	Title	Source	Publication Year
Fathead Minnow	not reported	Adult	Flow-through	Active ingredient	0.3	mg/L	Measured	11958	Hedtke, S.F., C.W. West, K.N. Allen, T.J. Norberg-King, and D.I. Mount	Toxicity of Pentachlorophenol to Aquatic Organisms Under Naturally Varying and Controlled Environmental Conditions	Environ. Toxicol. Chem. 5(6): 531-542	1986
Fathead Minnow	30 d	not reported	Flow-through	Active ingredient	0.381	mg/L	Measured	3217	Geiger, D.L., L.T. Brooke, and D.J. Call	Acute Toxicities of Organic Chemicals to Fathead Minnows (Pimephales promelas), Volume V	Center for Lake Superior Environmental Studies, University of Wisconsin, Superior, WI: 332 p.	1990
Fathead Minnow	not reported	Adult	Flow-through	Active ingredient	0.208	mg/L	Measured	11958	Hedtke, S.F., C.W. West, K.N. Allen, T.J. Norberg-King, and D.I. Mount	Toxicity of Pentachlorophenol to Aquatic Organisms Under Naturally Varying and Controlled Environmental Conditions	Environ. Toxicol. Chem. 5(6): 531-542	1986
Fathead Minnow	not reported	not reported	Flow-through	Active ingredient	0.23	mg/L	Measured	2189	Phipps, G.L., G.W. Holcombe, and J.T. Fiandt	Acute Toxicity of Phenol and Substituted Phenols to the Fathead Minnow	Bull. Environ. Contam. Toxicol. 26(5): 585-593	1981
Fathead Minnow	not reported	Adult	Flow-through	Active ingredient	0.17	mg/L	Measured	11958	Hedtke, S.F., C.W. West, K.N. Allen, T.J. Norberg-King, and D.I. Mount	Toxicity of Pentachlorophenol to Aquatic Organisms Under Naturally Varying and Controlled Environmental Conditions	Environ. Toxicol. Chem. 5(6): 531-542	1986
Fathead Minnow	not reported	not reported	Flow-through	Active ingredient	0.22	mg/L	Measured	2189	Phipps, G.L., G.W. Holcombe, and J.T. Fiandt	Acute Toxicity of Phenol and Substituted Phenols to the Fathead Minnow	Bull. Environ. Contam. Toxicol. 26(5): 585-593	1981
Fathead Minnow	30 d	not reported	Flow-through	Active ingredient	0.0986	mg/L	Measured	3217	Geiger, D.L., L.T. Brooke, and D.J. Call	Acute Toxicities of Organic Chemicals to Fathead Minnows	Center for Lake Superior Environmental	1990

Species	Organism Age	Organism Life stage	Exposure Type	Concentration Type	96 h LC <sub>50</sub>		Chemical Analysis	Reference Number	Author	Title	Source	Publication Year
										(Pimephales promelas), Volume V	Studies, University of Wisconsin, Superior, WI:332 p.	
Fathead Minnow	30 d	not reported	Flow-through	Active ingredient	0.261	mg/L	Measured	3217	Geiger,D.L., L.T. Brooke, and D.J. Call	Acute Toxicities of Organic Chemicals to Fathead Minnows (Pimephales promelas), Volume V	Center for Lake Superior Environmental Studies, University of Wisconsin, Superior, WI:332 p.	1990
Fathead Minnow	not reported	not reported	Flow-through	Active ingredient	0.233	mg/L	Measured	10775	Phipps,G.L., and G.W. Holcombe	A Method for Aquatic Multiple Species Toxicant Testing: Acute Toxicity of 10 Chemicals to 5 Vertebrates and 2 Invertebrates	Environ. Pollut. A.38(2): 141-157	1985
Fathead Minnow	30 d	not reported	Flow-through	Active ingredient	0.222	mg/L	Measured	3217	Geiger,D.L., L.T. Brooke, and D.J. Call	Acute Toxicities of Organic Chemicals to Fathead Minnows (Pimephales promelas), Volume V	Center for Lake Superior Environmental Studies, University of Wisconsin, Superior, WI:332 p.	1990
Fathead Minnow	40 d	not reported	Flow-through	Active ingredient	0.47	mg/L	Measured	15155	Cleveland,L., D.R. Buckler, F.L. Mayer, and D.R. Branson	Toxicity of Three Preparations of Pentachlorophenol to Fathead Minnows - a Comparative Study	Environ. Toxicol. Chem.1(3): 205-212	1982
Fathead Minnow	not reported	not reported	Flow-through	Active ingredient	0.244	mg/L	Measured	10775	Phipps,G.L., and G.W. Holcombe	A Method for Aquatic Multiple Species Toxicant Testing: Acute Toxicity of 10 Chemicals to 5 Vertebrates and 2 Invertebrates	Environ. Pollut. A.38(2): 141-157	1985
Fathead Minnow	32 d	not reported	Flow-through	Active ingredient	0.35	mg/L	Measured	12447	Geiger,D.L., C.E. Northcott, D.J. Call, and L.T. Brooke	Acute Toxicities of Organic Chemicals to Fathead Minnows (Pimephales promelas), Volume II	Center for Lake Superior Environmental Studies, University of	1985

Species	Organism Age	Organism Life stage	Exposure Type	Concentration Type	96 h LC <sub>50</sub>		Chemical Analysis	Reference Number	Author	Title	Source	Publication Year
											Wisconsin, Superior, WI:326 p.	
Fathead Minnow	44 d	not reported	Flow-through	Active ingredient	0.301	mg/L	Measured	12447	Geiger,D.L., C.E. Northcott, D.J. Call, and L.T. Brooke	Acute Toxicities of Organic Chemicals to Fathead Minnows (Pimephales promelas), Volume II	Center for Lake Superior Environmental Studies, University of Wisconsin, Superior, WI:326 p.	1985
Fathead Minnow	30 d	Juvenile	Flow-through	Active ingredient	0.218	mg/L	Measured	10679	Spehar,R.L., H.P. Nelson, M.J. Swanson, and J.W. Renoos	Pentachlorophenol Toxicity to Amphipods and Fathead Minnows at Different Test pH Values	Environ. Toxicol. Chem.4:389-397	1985
Fathead Minnow	44 d	not reported	Flow-through	Active ingredient	0.242	mg/L	Measured	12447	Geiger,D.L., C.E. Northcott, D.J. Call, and L.T. Brooke	Acute Toxicities of Organic Chemicals to Fathead Minnows (Pimephales promelas), Volume II	Center for Lake Superior Environmental Studies, University of Wisconsin, Superior, WI:326 p.	1985
Fathead Minnow	30 d	Juvenile	Flow-through	Active ingredient	0.261	mg/L	Measured	10679	Spehar,R.L., H.P. Nelson, M.J. Swanson, and J.W. Renoos	Pentachlorophenol Toxicity to Amphipods and Fathead Minnows at Different Test pH Values	Environ. Toxicol. Chem.4:389-397	1985
Fathead Minnow	not reported	Juvenile	Flow-through	Active ingredient	0.449	mg/L	Measured	15031	Broderius,S.J., M.D. Kahl, and M.D. Hoglund	Use of Joint Toxic Response to Define the Primary Mode of Toxic Action for Diverse Industrial Organic Chemicals	Environ. Toxicol. Chem.14(9): 1591-1605	1995
Fathead Minnow	not reported	not reported	Flow-through	Active ingredient	0.286	mg/L	Measured	10775	Phipps,G.L., and G.W. Holcombe	A Method for Aquatic Multiple Species Toxicant Testing: Acute Toxicity of 10 Chemicals to 5 Vertebrates and 2 Invertebrates	Environ. Pollut. A.38(2): 141-157	1985

Species	Organism Age	Organism Life stage	Exposure Type	Concentration Type	96 h LC <sub>50</sub>		Chemical Analysis	Reference Number	Author	Title	Source	Publication Year
Fathead Minnow	31 d	not reported	Flow-through	Active ingredient	0.24	mg/L	Measured	12447	Geiger,D.L., C.E. Northcott, D.J. Call, and L.T. Brooke	Acute Toxicities of Organic Chemicals to Fathead Minnows (Pimephales promelas), Volume II	Center for Lake Superior Environmental Studies, University of Wisconsin, Superior, WI:326 p.	1985
Fathead Minnow	not reported	Juvenile	Flow-through	Active ingredient	0.51	mg/L	Measured	11958	Hedtke,S.F., C.W. West, K.N. Allen, T.J. Norberg-King, and D.I. Mount	Toxicity of Pentachlorophenol to Aquatic Organisms Under Naturally Varying and Controlled Environmental Conditions	Environ. Toxicol. Chem.5(6): 531-542	1986
Fathead Minnow	not reported	Adult	Flow-through	Active ingredient	0.19	mg/L	Measured	11958	Hedtke,S.F., C.W. West, K.N. Allen, T.J. Norberg-King, and D.I. Mount	Toxicity of Pentachlorophenol to Aquatic Organisms Under Naturally Varying and Controlled Environmental Conditions	Environ. Toxicol. Chem.5(6): 531-542	1986
Fathead Minnow	30 d	Juvenile	Flow-through	Active ingredient	0.378	mg/L	Measured	10679	Spehar,R.L., H.P. Nelson, M.J. Swanson, and J.W. Renoos	Pentachlorophenol Toxicity to Amphipods and Fathead Minnows at Different Test pH Values	Environ. Toxicol. Chem.4:389-397	1985
Fathead Minnow	1 d	Fry	Flow-through	Active ingredient	0.314	mg/L	Measured	11958	Hedtke,S.F., C.W. West, K.N. Allen, T.J. Norberg-King, and D.I. Mount	Toxicity of Pentachlorophenol to Aquatic Organisms Under Naturally Varying and Controlled Environmental Conditions	Environ. Toxicol. Chem.5(6): 531-542	1986
Fathead Minnow	30 d	Juvenile	Flow-through	Active ingredient	0.095	mg/L	Measured	10679	Spehar,R.L., H.P. Nelson, M.J. Swanson, and J.W. Renoos	Pentachlorophenol Toxicity to Amphipods and Fathead Minnows at Different Test pH Values	Environ. Toxicol. Chem.4:389-397	1985

Species	Organism Age	Organism Life stage	Exposure Type	Concentration Type	96 h LC <sub>50</sub>		Chemical Analysis	Reference Number	Author	Title	Source	Publication Year
Fathead Minnow	not reported	Adult	Flow-through	Active ingredient	0.12	mg/L	Measured	11958	Hedtke, S.F., C.W. West, K.N. Allen, T.J. Norberg-King, and D.I. Mount	Toxicity of Pentachlorophenol to Aquatic Organisms Under Naturally Varying and Controlled Environmental Conditions	Environ. Toxicol. Chem. 5(6): 531-542	1986
Fathead Minnow	not reported	not reported	Flow-through	Active ingredient	0.266	mg/L	Measured	12004	Thurston, R.V., T.A. Gilfoil, E.L. Meyn, R.K. Zajdel, T.L. Aoki, and G.D. Veith	Comparative Toxicity of Ten Organic Chemicals to Ten Common Aquatic Species	Water Res. 19(9): 1145-1155	1985
Fathead Minnow	not reported	Juvenile	Flow-through	Active ingredient	0.396	mg/L	Measured	11958	Hedtke, S.F., C.W. West, K.N. Allen, T.J. Norberg-King, and D.I. Mount	Toxicity of Pentachlorophenol to Aquatic Organisms Under Naturally Varying and Controlled Environmental Conditions	Environ. Toxicol. Chem. 5(6): 531-542	1986
Fathead Minnow	not reported	Adult	Flow-through	Active ingredient	0.16	mg/L	Measured	11958	Hedtke, S.F., C.W. West, K.N. Allen, T.J. Norberg-King, and D.I. Mount	Toxicity of Pentachlorophenol to Aquatic Organisms Under Naturally Varying and Controlled Environmental Conditions	Environ. Toxicol. Chem. 5(6): 531-542	1986
Bluegill	not reported	not reported	not reported	Active ingredient	0.24	mg/L	Measured	4247	Samis, A.J.W., P.W. Colgan, and P.H. Johansen	Pentachlorophenol and Reduced Food Intake of Bluegill	Trans. Am. Fish. Soc. 122(6): 1156-1160	1993
Bluegill	not reported	not reported	Flow-through	Active ingredient	0.2	mg/L	Measured	11958	Hedtke, S.F., C.W. West, K.N. Allen, T.J. Norberg-King, and D.I. Mount	Toxicity of Pentachlorophenol to Aquatic Organisms Under Naturally Varying and Controlled Environmental Conditions	Environ. Toxicol. Chem. 5(6): 531-542	1986
Bluegill	not reported	not reported	Flow-through	Active ingredient	0.152	mg/L	Measured	10775	Phipps, G.L., and G.W. Holcombe	A Method for Aquatic Multiple Species	Environ. Pollut. A. 38(2): 141-157	1985

Species	Organism Age	Organism Life stage	Exposure Type	Concentration Type	96 h LC <sub>50</sub>		Chemical Analysis	Reference Number	Author	Title	Source	Publication Year
										Toxicant Testing: Acute Toxicity of 10 Chemicals to 5 Vertebrates and 2 Invertebrates		
Bluegill	not reported	not reported	Flow-through	Active ingredient	0.27	mg/L	Measured	11958	Hedtke, S.F., C.W. West, K.N. Allen, T.J. Norberg-King, and D.I. Mount	Toxicity of Pentachlorophenol to Aquatic Organisms Under Naturally Varying and Controlled Environmental Conditions	Environ. Toxicol. Chem. 5(6): 531-542	1986
Bluegill	not reported	not reported	Flow-through	Active ingredient	0.15	mg/L	Measured	10775	Phipps, G.L., and G.W. Holcombe	A Method for Aquatic Multiple Species Toxicant Testing: Acute Toxicity of 10 Chemicals to 5 Vertebrates and 2 Invertebrates	Environ. Pollut. A. 38(2): 141-157	1985
Bluegill	not reported	not reported	Flow-through	Active ingredient	0.202	mg/L	Measured	12004	Thurston, R.V., T.A. Gilfoil, E.L. Meyn, R.K. Zajdel, T.L. Aoki, and G.D. Veith	Comparative Toxicity of Ten Organic Chemicals to Ten Common Aquatic Species	Water Res. 19(9): 1145-1155	1985
Bluegill	not reported	not reported	Flow-through	Active ingredient	0.115	mg/L	Measured	10775	Phipps, G.L., and G.W. Holcombe	A Method for Aquatic Multiple Species Toxicant Testing: Acute Toxicity of 10 Chemicals to 5 Vertebrates and 2 Invertebrates	Environ. Pollut. A. 38(2): 141-157	1985
Guppy	not reported	not reported	Renewal	Active ingredient	0.4	mg/L	Measured	45297	Salkinoja-Salonen, M., M.L. Saxelin, J. Pere, T. Jaakkola, J. Saarikoski, R. Hakulinen, and O. Koistinen	Analysis of Toxicity and Biodegradability of Organochlorine Compounds Released into the Environment in Bleaching Effluents of Kraft Pulping	In: L.H. Keith (Ed.), Advances in the Identification and Analysis of Organic Pollutants in Water, Butterworth, Stoneham, MA 2:1131-1164	1981

Species	Organism Age	Organism Life stage	Exposure Type	Concentration Type	96 h LC <sub>50</sub>		Chemical Analysis	Reference Number	Author	Title	Source	Publication Year
Guppy	not reported	Young organism	not reported	Active ingredient	1.6	mg/L	Measured	15149	Adema,D.M.M., and G.J. Vink	A Comparative Study of the Toxicity of 1,1,2-Trichloroethane, Dieldrin, Pentachlorophenol, and 3,4-Dichloroaniline for Marine and Fresh Water Organisms	Chemosphere10(6): 533-554	1981
Guppy	not reported	Adult	not reported	Active ingredient	0.45	mg/L	Measured	15149	Adema,D.M.M., and G.J. Vink	A Comparative Study of the Toxicity of 1,1,2-Trichloroethane, Dieldrin, Pentachlorophenol, and 3,4-Dichloroaniline for Marine and Fresh Water Organisms	Chemosphere10(6): 533-554	1981
Guppy	not reported	Adult	not reported	Active ingredient	1.15	mg/L	Measured	15149	Adema,D.M.M., and G.J. Vink	A Comparative Study of the Toxicity of 1,1,2-Trichloroethane, Dieldrin, Pentachlorophenol, and 3,4-Dichloroaniline for Marine and Fresh Water Organisms	Chemosphere10(6): 533-554	1981
Guppy	not reported	Young organism	not reported	Active ingredient	0.72	mg/L	Measured	15149	Adema,D.M.M., and G.J. Vink	A Comparative Study of the Toxicity of 1,1,2-Trichloroethane, Dieldrin, Pentachlorophenol, and 3,4-Dichloroaniline for Marine and Fresh Water Organisms	Chemosphere10(6): 533-554	1981
Guppy	not reported	Young organism	not reported	Active ingredient	0.88	mg/L	Measured	15149	Adema,D.M.M., and G.J. Vink	A Comparative Study of the Toxicity of 1,1,2-Trichloroethane, Dieldrin, Pentachlorophenol, and 3,4-Dichloroaniline for Marine and Fresh Water Organisms	Chemosphere10(6): 533-554	1981

Species	Organism Age	Organism Life stage	Exposure Type	Concentration Type	96 h LC <sub>50</sub>		Chemical Analysis	Reference Number	Author	Title	Source	Publication Year
Rainbow Trout	not reported	not reported	Flow-through	Active ingredient	0.115	mg/L	Measured	12004	Thurston, R.V., T.A. Gilfoil, E.L. Meyn, R.K. Zajdel, T.L. Aoki, and G.D. Veith	Comparative Toxicity of Ten Organic Chemicals to Ten Common Aquatic Species	Water Res.19(9): 1145-1155	1985
Rainbow Trout	not reported	not reported	Flow-through	Active ingredient	0.159804	mg/L	Measured	10688	Hodson, P.V., D.G. Dixon, and K.L.E. Kaiser	Measurement of Median Lethal Dose as a Rapid Indication of Contaminant Toxicity to Fish	Environ. Toxicol. Chem.3(2): 243-254	1984



### S2.11 Time to steady state calculation

The steady state in the bioaccumulation experiments was determined based on a one-compartment model by Hendriks et al. (2001) that applies the compound's  $K_{OW}$ , fish lipid content, fish body weight and trophic level <sup>179</sup>. For our purposes, the fish body weight was assumed to be the total cell weight, which was obtained via extrapolation of measured cell numbers (from the bioaccumulation experiments) and the cell number per g of liver tissue in fish <sup>18</sup>. Instead of the  $K_{OW}$ , we applied the compound's  $D_{OW}$  to consider the ionized fraction. Uptake and elimination rate constant were calculated according to Equation S2.2 and Equation S2.3. The steady state was assumed to be reached when the internal concentration in the cells attained 95 % and Equation 2.4 was used to calculate this specific time point.

$$\text{Equation S2.2: } k_{in} = \frac{w_w^{-\kappa}}{\rho_{H_2O,j} + \frac{\rho_{CH_2,i}}{K_{OW}} + \frac{1}{\gamma_0}}, \quad \frac{L}{kg \times d}$$

$$\text{Equation S2.3: } k_{out} = \frac{1}{f_{lipid} \times (K_{OW} - 1) + 1} \times k_{in}, \quad \frac{kg}{kg \times d}$$

$$\text{Equation S2.4: } t_{95\%} = -\frac{\log(0.05)}{k_{out}}, \quad (\text{days})$$

**Table S2.14: Symbol Explanation for Equation S2.2 and S2.3.** Taken and edited from Hendriks et al. 2001 <sup>179</sup>

Symbol	Unit	Value	Description
$w_w$	kg	model input	body wet weight
$D_{OW}$	—	model input	octanol-water distribution ratio
$C_w$	$\mu g \cdot L^{-1}$	model input	chemical concentration in water
$i$	—	2 (for animals)	trophic level
$\kappa$	—	0.25	rate exponent
$\rho_{CH_2,i}$	$d \cdot kg^{-\kappa}$	68 (for animals)	lipid layer permeation resistance
$\rho_{H_2O,j}$	$d \cdot kg^{-\kappa}$	$2.8 \cdot 10^{-3}$	water layer diffusion resistance
$\gamma_0$	$kg^{-\kappa} \cdot d^{-1}$	200 water breathing	water absorption-excretion coefficient

Symbol	Unit	Value	Description
f_lipid	0.05	—	lipid fraction
k <sub>in</sub>	L · kg <sup>-1</sup> · d <sup>-1</sup>	—	Uptake rate constant
k <sub>out</sub>	kg · kg <sup>-1</sup> · d <sup>-1</sup>	—	Elimination rate constant
t <sub>95%</sub>	days	—	Time to steady state with 95 % attainment

**Table S2.15: Time to steady state in RTL-W1 cells.** Calculated based on compound's D<sub>ow</sub>, initial exposure concentration, total cell weight and application in Equation S2.2, S2.3 and S2.4. Since three DCF exposure concentrations were applied in the bioaccumulation experiments, the time to steady state was calculated separately for each of these replicates, BHPP = Benzotriazol-t-butyl-hydroxyl-phenyl propanoic acid, DCF = Diclofenac, PCP = Pentachlorophenol, TT = Tecloftalam

Compound	Initial exposure concentration (µg/L)	D <sub>ow</sub>	Total average cell weight (Kg)	Time to steady state (h)
BHPP	6.9	1.75	5.4E-06	15.9
DCF	189, 18.8, 386	1.37	7.8E-6, 1.1E-5, 1.2E-5	23.4, 25.3, 25.9
PCP	4.5	2.45	5.8E-06	13.2
TT	23.8	3.13	7.1E-06	14.8

## S2.12 Mass balances in bioaccumulation experiments

Absolute amounts were calculated for each sample fraction to derive the mass balance at each time point. The mass balance at each time point was compared to the initially added amount at experimental onset to detect any occurring decrease of test compound in the test system. From Table S2.16, it can be concluded that no biotransformation activity is discernable in the experiments, which would be expressed as a decrease of the total test compound amount in the test system with cells over time relative to the control.

**Table S2.16: Mass balances in bioaccumulation experiments with exposed cells and cell-free control.** The DCF replicates are shown separately, since different exposure concentrations were applied, which impacts the mass balances. SD = Standard Deviation, BHPP = Benzotriazol-t-butyl-hydroxyl-phenyl propanoic acid, TT = Tecloftalam, na = not available (due to lacking replicates at these time points, since one replicate sampled at 72h instead of at 16h), PCP = Pentachlorophenol, DCF = Diclofenac

Compound	Sample Time (h)	Mean exposed cells (ng)	SD (ng)	Mean cell-free control (ng)	SD (ng)
BHPP	0	25.0	4.5	28.1	0.3
	4	27.4	0.4	24.6	3.4
	8	25.2	1.1	28.4	0.8
	16	29.5	1.2	26.8	2.5
	24	25.2	0.3	30.0	6.7
	48	27.5	7.1	25.8	2.6
TT	0	76.1	16.1	89.4	6.7
	4	69.7	34.0	131.8	31.3
	8	73.1	20.9	72.9	22.3
	16	54.9	na	67.2	na
	24	96.2	2.5	113.5	25.3
	48	74.9	29.1	72.3	20.5
	72	82.1	na	91.8	na
PCP	0	13.5	0.4	13.3	0.0
	4	13.5	0.2	13.7	0.3
	8	13.8	0.6	13.7	0.9
	16	13.3	0.7	13.0	0.4
	24	13.0	0.0	13.0	0.8
	48	13.0	0.8	13.0	0.1
DCF1	0	56.3	-	52.9	-
	4	51.0	-	55.5	-
	8	52.3	-	53.2	-
	16	46.2	-	52.2	-
	24	52.0	-	51.3	-
	48	50.7	-	49.1	-
DCF2	0	567.9	-	586.3	-

Compound	Sample Time (h)	Mean exposed cells (ng)	SD (ng)	Mean cell-free control (ng)	SD (ng)
	4	566.1	-	524.4	-
	8	561.3	-	544.2	-
	16	577.0	-	569.6	-
	24	556.5	-	549.0	-
	48	569.0	-	527.3	-
DCF3	0	1157.9	-	968.4	-
	4	1246.5	-	1085.1	-
	8	1020.3	-	1082.8	-
	16	1120.7	-	1136.8	-
	24	1051.1	-	1057.6	-
	48	993.0	-	1095.0	-

### S2.13 Bioaccumulation of DCF in RTL-W1

In an attempt to improve quantification of chemical distribution and test concentration dependency of bioaccumulation, DCF exposure was explored at different concentrations tested in the same way (Figure S2.6).

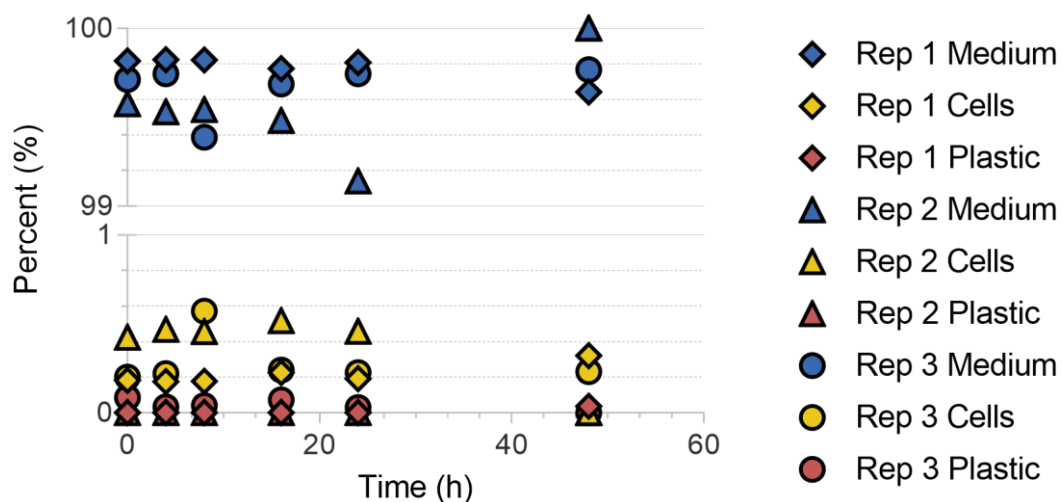


**Figure S2.6: Bioaccumulation experiments with DCF at different exposure concentrations.** Please note that the cell samples of replicate 1 were all < limit of quantification. Rep = Replicate, Rep 1 exposure concentration = 20 µg/L, Rep 2 exposure concentration = 200 µg/L, Rep 3 exposure concentration = 400 µg/L, DCF = Diclofenac

### S2.14 pH changes in the bioaccumulation experiments

During the bioaccumulation experiments, a subsample of the medium was taken every 24 h for pH measurement. The presence of RTL-W1 cells lowered the pH in the exposure medium independent of the presence of test compound (Figure S2.7). Changes in pH were, however, too small to impact the degree of ionization of the test compounds.

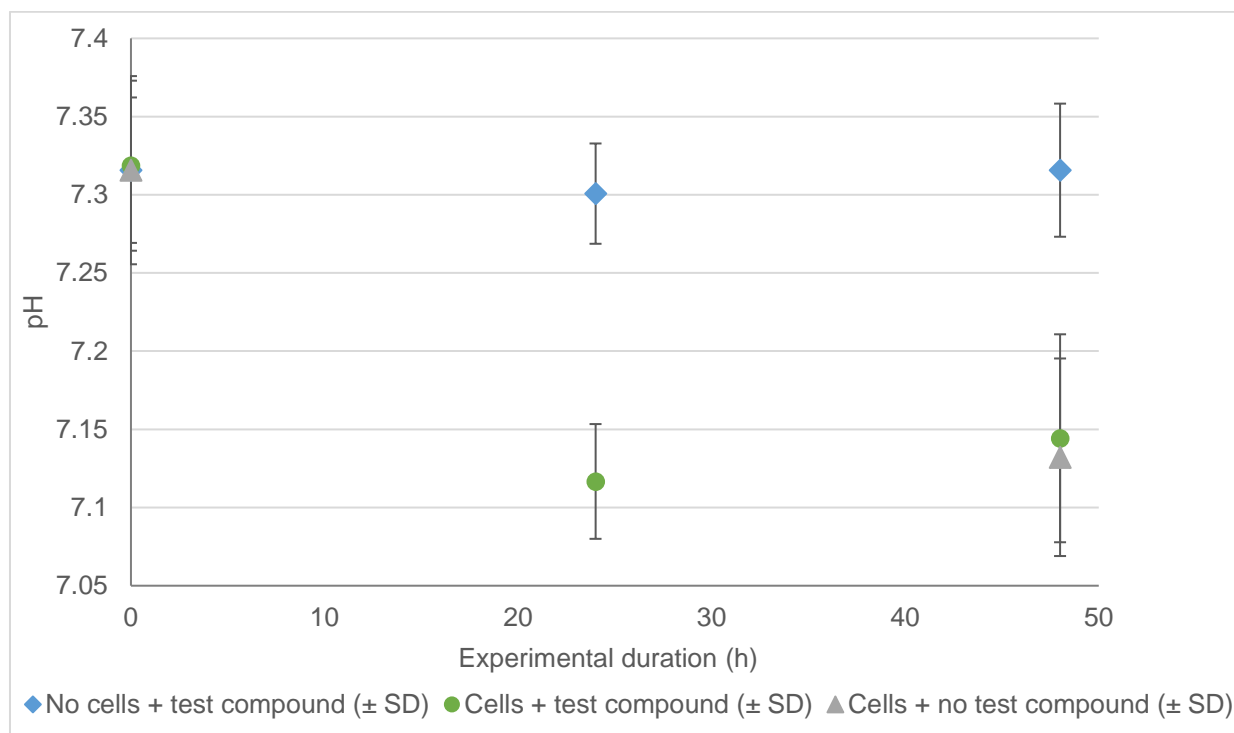


**Figure S2.7: pH changes in the bioaccumulation experiments at 0, 24 and 48 hours.** pH changes were very comparable in the bioaccumulation experiments, irrespective of the tested compound. SD= Standard Deviation

### S2.15 Screening for suspected biotransformation products

The screening of the HRMS/MS data for biotransformation products was conducted with Compound Discoverer v3.3 (Thermo Fisher Scientific Inc.). It was based on a list of suspected biotransformation products known to occur in fish (from literature) as well as a list of suspects generated *in silico* with application of common biotransformation pathways. Candidates were selected by the unique detection in the treated cells and their absence in control groups: Comparison of exposed cells with test compound-free and cell-free controls. Further settings for the analysis are listed in Table S2.17. The found candidates were searched for time dependent intensity trends over the experimental duration as well as peak intensities >0.1 % relative to the test compound.

**Table S2.17: Settings in Compound Discoverer for biotransformation product screening.**

<b>Setting for Peak detection</b>	
Minimal Peak intensity	1.00E+06
Minimal fold difference Sample/Control	5
Possible Phase I reactions for suspect generation	Dehydration; Desaturation; Hydration; Nitro Reduction; Oxidation; Oxidative Deamination to Alcohol ; Oxidative Deamination to Ketone ; Oxidative Debromination ; Oxidative Dechlorination ; Oxidative Defluorination ; Reduction ; Reductive Debromination ; Reductive Dechlorination ; Reductive Defluorination
Possible Phase II reactions for suspect generation	Acetylation ; Arginine Conjugation; Cysteine Conjugation 1; Cysteine Conjugation 2; Glucoside Conjugation ; Glucuronide Conjugation ; Glutamine Conjugation ; Glycine Conjugation ; GSH Conjugation 1 ; GSH Conjugation 2 ; Methylation ; Ornithine Conjugation ; Palmitoyl Conjugation ; Stearyl Conjugation; Sulfation ; Taurine Conjugation
Intensity Threshold relative to test compound	0.10%
m/z tolerance for detection	5 ppm
Average Peak width	0 min (automated detection)

## S2.16 Application of validity criteria of OECD TG319

According to OECD TG319 a and b, the fitted linear regression requires an  $R^2 \geq 0.85$  and the slope should be significant from 0. As seen in the below summaries for each test compound, these criteria were not met (Table S2.18). Except for the slope of PCP exposed cells, all other regressions were not significant from zero. The slope for PCP exposed cells was significant but did not meet the criteria of  $R^2 \geq 0.85$ .

**Table S2.18: Linear regression analysis according to OECD TG319A for detection of biotransformation activity.** Since the DCF replicates were conducted at different exposure concentrations, the linear regression analysis was carried out separately on them. F = F-statistic, P value = probability of significant deviation from 0 according to t-test, BHPP = Benzotriazol-t-butyl-hydroxyl-phenyl propanoic acid, DCF = Diclofenac, PCP = Pentachlorophenol, TT = Tecloftalam

<b>BHPP</b>	<b>Cell free control</b>	<b>Exposed cells</b>
<i>Goodness of Fit</i>		
R squared	0.002592	0.01638
<i>Is slope significantly non-zero?</i>		
F	0.02599	0.1666
P value	0.8751	0.6918
Deviation from zero?	Not Significant	Not Significant

Equation	$Y = -0.0003372 \cdot X + 9.123$	$Y = 0.0008839 \cdot X + 9.074$
<b>DCF1</b>	<b>Cell free control</b>	<b>Exposed cells</b>
<i>Goodness of Fit</i>		
R squared	0.1899	0.0003144
<i>Is slope significantly non-zero?</i>		
F	0.9374	0.001258
P value	0.3878	0.9734
Deviation from zero?	Not Significant	Not Significant
Equation	$Y = -0.001081 \cdot X + 12.14$	$Y = 1.227e-005 \cdot X + 12.15$
<b>DCF2</b>	<b>Cell free control</b>	<b>Exposed cells</b>
<i>Goodness of Fit</i>		
R squared	0.823	0.1167
<i>Is slope significantly non-zero?</i>		
F	18.59	0.5285
P value	0.0125	0.5075
Deviation from zero?	Significant	Not Significant
Equation	$Y = -0.002141 \cdot X + 9.806$	$Y = -0.001240 \cdot X + 9.772$
<b>DCF3</b>	<b>Cell free control</b>	<b>Exposed cells</b>
<i>Goodness of Fit</i>		
R squared	0.1731	0.5015
<i>Is slope significantly non-zero?</i>		
F	0.8373	4.024
P value	0.4119	0.1153
Deviation from zero?	Not Significant	Not Significant
Equation	$Y = 0.001278 \cdot X + 12.76$	$Y = -0.003445 \cdot X + 12.86$
<b>PCP</b>	<b>Cell free control</b>	<b>Exposed cells</b>
<i>Goodness of Fit</i>		
R squared	0.2172	0.7911
<i>Is slope significantly non-zero?</i>		
F	1.11	15.15
P value	0.3516	0.0177
Deviation from zero?	Not Significant	Significant
Equation	$Y = -0.0007747 \cdot X + 8.391$	$Y = -0.001355 \cdot X + 8.403$

TT	Cell free control	Exposed cells
<i>Goodness of Fit</i>		
R squared	0.08103	0.0001241
<i>Is slope significantly non-zero?</i>		
F	0.8817	0.001241
P value	0.3699	0.9726
Deviation from zero?	Not Significant	Not Significant
Equation	$Y = -0.005029 \cdot X + 10.39$	$Y = 0.0001813 \cdot X + 10.11$

## S2.17 Partition based bioaccumulation

A simple prediction of accumulation of test compound in the RTL-W1 cells was conducted, which based on the compound's  $K_{OW}$ ,  $D_{OW}$  or  $D_{MLW}$ . The accumulation of an organic compound in an organism can be simplified as the enrichment into a particular phase, i.e. phospholipid or lipid<sup>19</sup>, as depicted in Equation S2.5, where the bioaccumulation factor,  $K_B$ , is dependent on the compound's  $K_{OW}$  and the volume fraction of lipid in the organism,  $v_{Lipid}$ . For this exercise this concept was extended assuming that  $D_{OW}$  or  $D_{MLW}$  and the respective volume fractions  $v_{Lipid}$  and  $v_{Phospholipid}$  are usable in the same manner to predict bioaccumulation.

Equation S2.5:  $K_B = v_{Lipid} \times K_{OW}$

Based on the above assumptions, Equation S2.6 and S2.7 are the equations to calculate the BCF in the cells at steady state.  $v_{Lipid}$  was derived from the total cell weight,  $w$ , and total cell volume,  $V_{cell}$ , the weight-based lipid fraction in the cells,  $f_L$ , and the lipid density,  $\rho_L$ .  $v_{Phospholipid}$  was calculated analogous to  $v_{Lipid}$ . We derived the volume of the cell monolayer in each experiment based on the measured cell numbers. Density of lipid and phospholipid were taken from literature and assumed to be identical for the RTL-W1 cells. Input parameters are presented in Table S2.19 and the calculated BCFs in Table S2.20.

$$\text{Equation S2.6: } K_B = 10^{\log K_{OW} \text{ or } \log D_{OW}} \times v_{Lipid} = 10^{\log K_{OW} \text{ or } \log D_{OW}} \times \frac{w \times f_L}{V_{cell} \times \rho_L}$$

$$\text{Equation S2.7: } K_B = 10^{\log D_{MLW}} \times v_{Phospholipid} = 10^{\log D_{MLW}} \times \frac{w \times f_{PL}}{V_{cell} \times \rho_{PL}}$$



**Table S2.19: Input data for partition exercise.** The average total cell number was derived from measured cell numbers at experimental onset and termination of the bioaccumulation experiment, PCP = Pentachlorophenol, DCF = Diclofenac, BHPP = Benzotriazol-t-butyl-hydroxyl-phenyl propanoic acid, TT = Tecloftalam

Symbol	Value	Unit	Description
$K_B$	-	-	Bioconcentration at steady state
$\log D_{MLW}$	see table 1 main script	-	test compound's membrane-water distribution ratio
$\log K_{OW}/D_{OW}$	see table 1 main script	-	test compound's octanol-water partition ratio (K) or distribution ratio (D)
$w$	0.0058	g	average total cell weight in experiment, PCP
$w$	0.0101	g	average total cell weight in experiment, DCF
$w$	0.0054	g	average total cell weight in experiment, BHPP
$w$	0.0071	g	average total cell weight in experiment, TT
$V_{cell}$	4.37E-06	L	average total cell volume in experiment, PCP
$V_{cell}$	7.56E-06	L	average total cell volume in experiment, DCF
$V_{cell}$	4.07E-06	L	average total cell volume in experiment, BHPP
$V_{cell}$	5.33E-06	L	average total cell volume in experiment, TT
$f_{PL}$	0.01	-	weight based phospholipid fraction in fish, taken from Hendriks et al. 2001
$f_L$	0.04	-	weight based lipid fraction in fish, taken from Hendriks et al. 2001 <sup>179</sup>
$\rho_{PL}$	1013.8	g/L	Phospholipid density according to Johnson & Buttress (1973) <sup>238</sup>
$\rho_L$	830	g/L	Octanol density, representing lipid <sup>239</sup>

**Table S2.20: Calculated log BCF based on the test compound's  $K_{OW}$ ,  $D_{OW}$  and  $D_{MLW}$ .** BHPP = Benzotriazol-t-butyl-hydroxyl-phenyl propanoic acid, TT = Tecloftalam, PCP = Pentachlorophenol, DCF = Diclofenac

Compound	Observed BCF	$K_{OW}$ -based BCF	$D_{OW}$ -based BCF	$D_{MLW}$ -based BCF
BHPP	1.51	3.03	0.56	0.32
TT	0.87	4.29	1.94	0.12
PCP	0.30	3.57	1.26	1.02
DCF	0.03	2.85	0.18	-0.48

## S2.18 BCF reference values of Pentachlorophenol

Table S2.21: Reference BCF values of Pentachlorophenol (PCP) in different fish species.

Species	log BCF	Reference
Sheepshead Minnow ( <i>Cyprinodon variegatus</i> )	1.2 to 1.7	Patrick R. Parrish, et al., <i>Chronic toxicity of chlordane, trifluralin, pentachlorophenol to sheepshead minnows (cyprinodon variegatus)</i> . Ecological Research Series. 2002, Washington, D.C.: U.S. Environmental Protection Agency.DOI: EPA/600/3-78/010.
Sheepshead Minnow ( <i>Cyprinodon variegatus</i> )	0.7 to 1.4	Patrick R. Parrish, et al., <i>Chronic toxicity of chlordane, trifluralin, pentachlorophenol to sheepshead minnows (cyprinodon variegatus)</i> . Ecological Research Series. 2002, Washington, D.C.: U.S. Environmental Protection Agency.DOI: EPA/600/3-78/010.
Rainbow trout ( <i>Oncorhynchus mykiss</i> )	2.3	Stehly, G.R. and W.L. Hayton, <i>Disposition of pentachlorophenol in rainbow trout (Salmo gairdneri): effect of inhibition of metabolism</i> . Aquatic Toxicology, 1989. <b>14</b> (2): p. 131-147.DOI: <a href="https://doi.org/10.1016/0166-445X(89)90024-6">https://doi.org/10.1016/0166-445X(89)90024-6</a> .
Pink salmon ( <i>Oncorhynchus gorbuscha</i> )	2.5 to 2.9	Servizi, J.A., R.W. Gordon, and J.H. Carey, <i>Bioconcentration of Chlorophenols by Early Life Stages of Fraser River Pink and Chinook Salmon (Oncorhynchus gorbuscha, O. tshawytscha)</i> . Water Quality Research Journal, 1988. <b>23</b> (1): p. 88-99.DOI: 10.2166/wqrj.1988.007.
Longnose killifish ( <i>Fundulus similis</i> )	1.6 to 1.8	Trujillo, D.A., et al., <i>Bioaccumulation of pentachlorophenol by killifish (Fundulus similis)</i> . Chemosphere, 1982. <b>11</b> (1): p. 25-31.DOI: <a href="https://doi.org/10.1016/0045-6535(82)90085-6">https://doi.org/10.1016/0045-6535(82)90085-6</a> .
Carp ( <i>Cyprinus carpio</i> )	3.6	Sun, H., et al., <i>Enhanced bioaccumulation of pentachlorophenol in carp in the presence of multi-walled carbon nanotubes</i> . Environmental Science and Pollution Research, 2014. <b>21</b> (4): p. 2865-2875.DOI: 10.1007/s11356-013-2234-4.
Japanese Medaka ( <i>Oryzias latipes</i> )	3.3. to 3.7	Kondo, T., et al., <i>Bioconcentration factor of relatively low concentrations of chlorophenols in Japanese medaka</i> . Chemosphere, 2005. <b>61</b> (9): p. 1299-1304.DOI: <a href="https://doi.org/10.1016/j.chemosphere.2005.03.058">https://doi.org/10.1016/j.chemosphere.2005.03.058</a> .
Goldfish ( <i>Carassius auratus</i> )	2.1 to 2.8	Stehly, G.R. and W.L. Hayton, <i>Effect of pH on the accumulation kinetics of pentachlorophenol in goldfish</i> . Archives of Environmental Contamination and Toxicology, 1990. <b>19</b> (3): p. 464-470.DOI: 10.1007/BF01054993.
American flagfish ( <i>Jordanella floridae</i> )	2.3	Smith, A.D., et al., <i>Bioconcentration kinetics of some chlorinated benzenes and chlorinated phenols in American flagfish, Jordanella floridae (Goode and Bean)</i> . Chemosphere, 1990. <b>20</b> (3): p. 379-386.DOI: <a href="https://doi.org/10.1016/0045-6535(90)90068-5">https://doi.org/10.1016/0045-6535(90)90068-5</a> .

## Supporting Information Chapter 3

### S3.1 Test compound information

Table S3.1: Detail on the test compounds and their respective internal standards (CDN isotopes).

Compound	Acronym	CAS	MW g mol <sup>-1</sup>	Density (g mL <sup>-1</sup> , 20°C)	Vendor	Purity (%)
<i>N</i> -methyldecylamine	S12	7311-30-0	199.38	0.791	Sigma-Aldrich	98
<i>N,N</i> -dimethyldecylamine	T10	1120-24-7	185.35	0.792	Sigma-Aldrich	97
<i>N,N,N</i> -trimethyltetradecylammonium bromide	Q14	4574-04-3	256.49*	solid	Sigma-Aldrich	≥98
decyl-D <sub>21</sub> -trimethylammonium bromide	-	1515861-67-2	221.1*	solid	CDN Isotopes	99
Tetradecyl-D <sub>29</sub> -trimethylammonium bromide	-	95523-73-2	285.67*	solid	CDN Isotopes	99

\* w/o salt

### S3.2 Conduction of bioaccumulation experiments

In a first step, a test compound was directly dissolved in the exposure medium because all compounds were well soluble in aqueous solution without the aid of an organic solvent. The exposure medium consisted of L-15/FBS to sustain the metabolism of the cells<sup>29, 35</sup>. In a second step, the test compound stock solution was diluted to the final exposure concentration with additional L-15/FBS medium. This two-step dilution procedure was necessary to minimize variabilities in pipetting of small volumes or weighing small amounts of pure chemical (S12 and T10 liquid, Q14 solid at room temperature). To start an experiment, the routine cell culture medium was removed and replaced with 3 mL of the previously prepared L-15/FBS exposure medium.

The experimental design and sampling scheme of the bioaccumulation experiments was the same as detailed in Balk et al.<sup>176</sup> with minor adaptations. Exposed cells and cell-free negative control flasks were sampled at 0 h, 4 h, 8 h, 24 h, 48 h and 72 h, whilst a cell count control and a test compound-free control were sampled at experimental onset and termination. At each sampling time point, the medium, the cell surface, the cells themselves and test compound

sorbed to plastic were sampled. Briefly, 1 mL exposure medium was sampled and the remaining 2 mL used for pH measurement (only every 24 h) using a small pH probe (microFET, Welling) or indicator strips (Macherey-Nagel). Then, 3 mL chemical-free L-15/FBS were added and the flask gently swayed for 30 seconds to reduce the carry-over from the exposure medium to the subsequent sample fractions. A 1 mL volume of the wash medium was sampled and combined with the first sample of exposure medium. Afterwards, the cell surface was rinsed with 400  $\mu$ L Versene solution for 30 seconds. Versene contains the cell dissociation agent ethylenediaminetetraacetic acid (EDTA), which chelates with divalent metal ions<sup>177</sup>. Due to its four carboxylic acid groups with strong dissociation constants (pKa 0.26 to 2.76<sup>178</sup>), EDTA is fully dissociated at pH 7 and able to associate with positively charged test compounds. Thus, any test compound loosely associated with the cell surface would have been sampled with the EDTA upon the rinse with Versene. Afterwards, the cell layer was sampled by the addition of 400  $\mu$ L trypsin and scraping the cells with a cell scraper (Techno Plastic Products AG). An additional 400  $\mu$ L trypsin added to the flask ensured the capture of the remaining cells and minimized carry over to the subsequent sample fraction. Both trypsin samples were combined and added to methanol containing internal standard. At last, the test compound sorbed to plastic was sampled by the addition of methanol-containing internal standard and shaken for 5 min at 200 rpm on a plate shaker. Each sample fraction was collected in a 15 mL centrifuge tube (91015, TPP Techno Plastic Products AG), which contained methanol with internal standard or, in case of the plastic sampling extract, ultrapure water (Honeywell Riedel-de Haën). The sampling volumes were adapted such that the methanol fraction was 80% (v/v) in the sample, which ensured that test compound loss due to sorption to plastic or glass was minimized (SI section S3.7).

### S3.3 Mass balance derivation and *in vitro* BCF calculation

The mass balances were derived as described previously<sup>176</sup>. In brief, the % of total amount of each sample type (medium, cell surface, cells or plastic) was calculated as the quotient of the sample,  $Y_t$ , at the time point  $t$  over the sum of all sample types,  $\sum Y_t$  (ng), at time point  $t$ , as shown in Equation S3.1:

$$\text{Equation S3.1} \quad \% \text{ of total amount} = \frac{Y_t}{\sum Y_t} .$$

The total amounts measured at each time point were compared to the initial total mass at 0 h to detect biotransformation activity or other losses. The calculation of *in vitro* BCFs was identical to our previous work, except for the differences in cell volume, cell number and cell weight for RTL-W1 and RTgill-W1 (SI also Table S3.6). Equation S3.2 describes the initial derivation of the cellular concentration of test compound,  $C_{cell}$ :

$$\text{Equation S3.2} \quad C_{cell} \left[ \frac{ng}{L} \right] = \frac{cell_t [ng]}{\text{mean cell number of experiment} \times \left( \frac{1}{6} \times \pi \times d^3 \right) [L]},$$

where the absolute amount of test compound,  $cell_t$ , at time point  $t$ , is divided by the volume of the cell layer, which depends on the measured cell number in the bioaccumulation experiments and the cell diameter  $d$ . (see SI section S3.8 for metrics per chemical and cell line). We attempted to determine the time when steady state was reached in the experiments using a simple  $D_{OW}$ -based model, which, however, gave no realistic estimations. Since the model appeared to be inapplicable to cationic surfactants, we based our steady state estimations on the derived mass balances. Equation S3.3 was used to calculate the *in vitro* BCF, where  $C_{medium}$  was the averaged exposure concentration at apparent steady state of the test system (incl. all times points  $\geq 24$  h):

$$\text{Equation S3.3} \quad \textit{in vitro BCF} = \frac{C_{cell}}{C_{medium}}$$

For comparison, we calculated  $D_{MLW}$  based predictions of BCFs in cells, termed  $D_{MLW}BCF$ , which used the cells' volume fractions of phospholipid,  $v_{phospholipid}$ , the compound's  $D_{MLW}$ , averaged cell weight,  $w$  [g] (Table S3.6), the weight-based phospholipid fraction,  $f_{PL}$  (0.01)<sup>179</sup>, its density,  $\rho_{PL}$  [g L<sup>-1</sup>] (1.0138 kg L<sup>-1</sup>)<sup>238</sup>, and the cell volume multiplied by the measured cell number,  $V_{cell}$  [L] (Table S3.6):

$$\text{Equation S3.4} \quad D_{MLW}BCF = 10^{\log D_{MLW}} \times v_{phospholipid} = 10^{\log D_{MLW}} \times \frac{\frac{w \times f_{PL}}{\rho_{PL}}}{V_{cell}}$$

A detailed description of the derivation is available in the SI of our earlier work<sup>3</sup>.

### S3.4 Mass spectrometer settings

For sample quantification, an LCMS/MS system was applied. Positive full scan MS at a resolution of 140 000 at  $m/z$  200 (120 000 for Exploris) with data-dependent MS2 acquisition, with a resolution of 17 500 (30 000 for Exploris) and an isolation window of 1  $m/z$ , were recorded for all test compounds. Standard calibrations in ultrapure water containing 80% methanol and internal standards were used for quantification. Each sample run was 20 minutes long. The eluent ramp with a flow of 200  $\mu\text{L min}^{-1}$  began with 10% of methanol, which was increased to 95% after 3 minutes and kept at 95% from 14 to 17 minutes. Afterwards, the methanol fraction was decreased within a minute and brought down to 10 % from 18 minutes onward until the end of the measurement. The column temperature was set to 40°C. Ionization of the target analytes was achieved by electrospray ionization (ESI) with a spray voltage of +4kV in positive mode while the ion transfer capillary was heated to 320 °C. Full scan acquisitions were performed at a range of 50 to 630  $m/z$  and top 5 data-dependent MS/MS

conducted based on an inclusion list containing all test compounds along with their suspected and known biotransformation products. Data acquisitions were analyzed with the Software Tracefinder 4.1 (Thermo Fisher Scientific). Collision energies and  $m/z$  are listed in Table S3.2, while in Table S3.4 and Table S3.5 the limit of quantification (LOQ) and the matrix specific relative recoveries are presented, respectively.

**Table S3.2: Test compound's  $m/z$  and collision energies.** Please note that we measured samples with three different mass spectrometers, QExactive and Exploris. All targets were measured in positive mode.

Compound	Mass ( $m/z$ )	Fragment ions $m/z$	Normalized collision energy (QExactives)	Normalized collision energy (Exploris)
<i>N</i> -methyldodecylamine (S12)	200.2373	57.030, 71.0862, 85.050	60	65
<i>N,N</i> -dimethyldodecylamine (T10)	186.2216	57.0707, 71.010, 85.050	70	75
<i>N,N,N</i> -trimethyltetradecylammonium (Q14)	256.2999	57.090, 60.081, 71.000	60	65

### S3.5 Screening for biotransformation products

The mass balances of bioaccumulation experiments were used to test if criteria for biotransformation activity according to OECD TG319<sup>23, 24</sup> were met. Also, we conducted a screening for potential and known biotransformation products in the media and cell samples. A suspect list was created based on biotransformation products known from literature<sup>25, 175</sup>. Detected candidates had to be present in either media or cell samples and be absent in any of the control samples (compound-free or cell-free controls). Further, the candidates had to show temporal trends in peak intensities over the experimental duration and peak intensities had to be  $\geq 0.1$  % compared to their parent compound. The settings for detection of biotransformation products are presented in Table S3.3.

**Table S3.3: Compound Discoverer settings for peak detection of suspected biotransformation products.**

Setting	
Minimal Peak intensity	1.00E+06
Minimal fold difference Sample/Control	5
Possible Phase I reactions for suspect BTP generation	Dealkylation; Desaturation (H2 -> ); Oxidation ( -> O); Oxidative Deamination to Alcohol (H2 N -> H O); Oxidative Deamination to Ketone (H3 N -> O); Reduction ( -> H2)
Possible Phase II reactions for suspect BTP generation	Dealkylation; Acetylation (H -> C2 H3 O); Arginine Conjugation (H O -> C6 H13 N4 O2); Cysteine Conjugation 1 (H -> C3 H6 N O2 S); Cysteine Conjugation 2 ( -> C3 H7 N O2 S); Glucoside Conjugation (H -> C6 H11 O5); Glucuronide Conjugation (H -> C6 H9 O6); Glutamine Conjugation (H O -> C5 H9 N2 O3); Glycine Conjugation (H O -> C2 H4 N O2); GSH Conjugation 1 ( -> C10 H15 N3 O6 S); GSH Conjugation 2 ( -> C10 H17 N3 O6 S); Methylation (H -> C H3); Ornithine Conjugation (H O -> C5 H11 N2 O2); Palmitoyl Conjugation (H -> C16 H31 O); Stearyl Conjugation (H -> C18 H35 O); Sulfation (H -> H O3 S); Taurine Conjugation (H O -> C2 H6 N O3 S)
m/z tolerance	5 ppm
Average Peak width	automated detection

### S3.6 Performance of chemical analysis

**Table S3.4: Limit of quantification of test compounds and comparison of intended vs. measured exposure concentration in bioaccumulation experiments.**

Compound	Cell line	LOQ ( $\mu\text{g L}^{-1}$ )*	Nominal exposure C ( $\mu\text{g L}^{-1}$ )	% of nominal exposure C $\pm$ SD**
<i>N</i> -methyldodecylamine (S12)	RTgill-W1	0.050	200	112 $\pm$ 11
<i>N</i> -methyldodecylamine (S12)	RTL-W1	0.050	200	92 $\pm$ 13
<i>N,N</i> -dimethyldodecylamine (T10)	RTgill-W1	0.050	185	195 $\pm$ 86**
<i>N,N</i> -dimethyldodecylamine (T10)	RTL-W1	0.050	185	210 $\pm$ 40**
<i>N,N,N</i> -trimethyltetradecylammonium (Q14 R1)	RTgill-W1	0.050	100	86 $\pm$ 1
<i>N,N,N</i> -trimethyltetradecylammonium (Q14 R2)	RTL-W1	0.050	20	112 $\pm$ 11

\* lowest LOQ given, depending on measurement sequence it ranged from 50 to 1000 ng/L, \*\*geometric mean of stock solutions sampled at experimental onset and termination.

\*\* The doubled exposure concentration vs. nominal for T10 was thought to be caused by deviations in density documentation by the supplier and the resulting density at the temperature at which the experiments were conducted.

**Table S3.5: Matrix specific relative recoveries of the test compounds.**

Compound	relative recovery - Medium (%)	relative recovery - Surface (%)	relative recovery - Cell (%)	relative recovery - Plastic (%)
<i>N</i> -methyldodecylamine (S12)	106	102	119	110
<i>N,N</i> -dimethyldodecylamine (T10)	96	104	100	96
<i>N,N,N</i> -trimethyltetradecylammonium (Q14)	114	185	100	100

### S3.7 Compound adsorption in experimental set up

This experiment was conducted with a range of methanol percentages (v/v) to monitor the absorption of the test compounds to the walls of either glass or plastic vials (Figure S3.1). The mixtures were sampled after 24 hours, at which the system was assumed to have reached chemical equilibrium. Clear differences between absorption affinity to glass or plastic were seen for S12 for methanol percentages < 80 % (left pane Figure S3.1). Therefore, we decided to use a methanol percentage of 80 % in the sampling for bioaccumulation assessments.

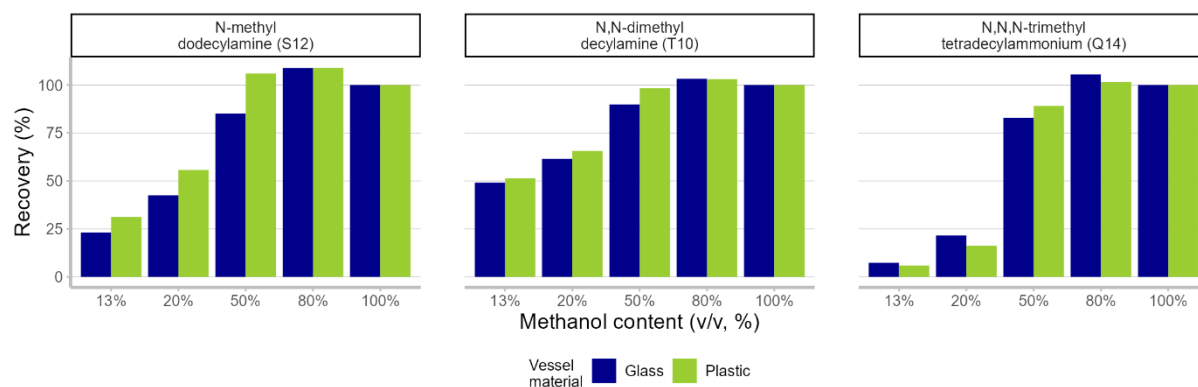


**Figure S3.1: Absorption experiment of test compounds to glass or plastic vials in varying water-methanol mixtures.**

### S3.8 Optimal seeding density for bioaccumulation assessment

We tested two different cell densities of RTgill-W1 in cell culture flasks (25 cm<sup>2</sup> growth area), to ensure minimal variability in cell numbers over the experimental duration of bioaccumulation experiments (Figure S3.2). We assumed a negligible difference between the 48 h and 72 h experimental duration. The cell density of  $4.6 \times 10^6$  cells/flask was chosen as the seeding density for all bioaccumulation experiments with RTgill-W1, since the variability was smaller than in the higher cell density of  $5.6 \times 10^6$  cells/flask.



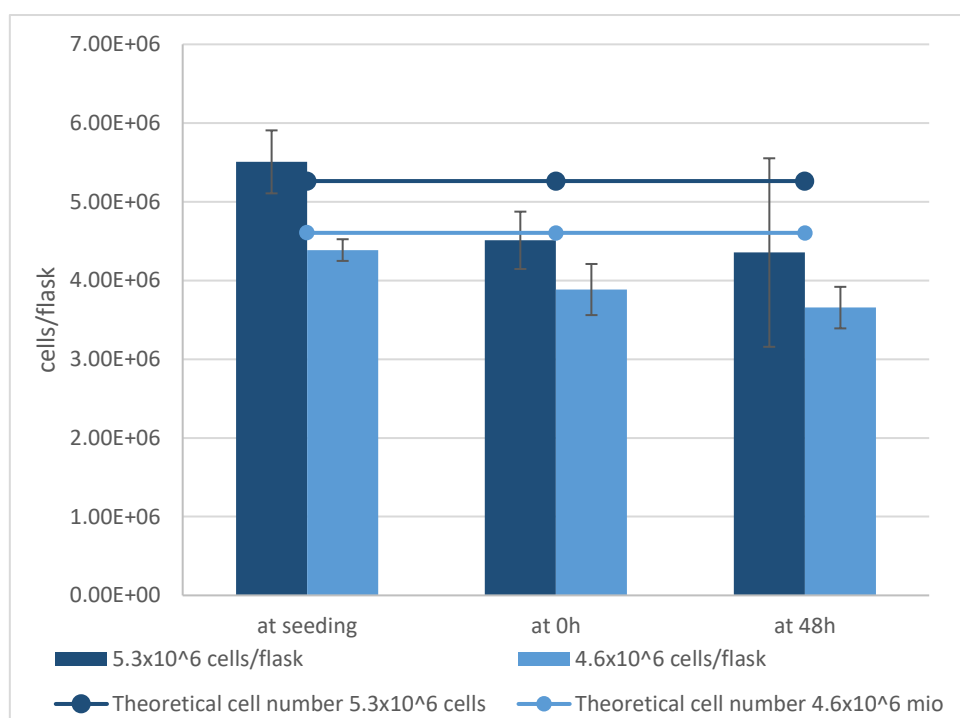


**Figure S3.2: Cell numbers of RTgill-W1 in two tested densities over 48 h.** We assumed a negligible difference of the cell numbers between 48 h and 72 h experimental duration. Each density was measured in three biological replicates. Error bars are standard deviations, while the horizontal lines mark the intended seeding density.

In each experiment, the exposed cells were counted at experimental onset and termination. The cell numbers are documented in Table S3.6. They were used for calculation of cell internal concentrations of the test compounds according to the method by Stadnicka-Michalak et al.<sup>35</sup> and Balk et al.<sup>176</sup>.

**Table S3.6: Cell numbers per test compound and cell line.** Besides the cell numbers, the following metrics were needed for accumulation predictions. RTL-W1 cell diameter: 16.6  $\mu\text{m}$ , volume:  $2.4 \times 10^{-12}$  L cell<sup>-1</sup>, weight:  $2.4 \times 10^{-9}$  g cell<sup>-1</sup>; RTgill-W1 cell diameter: 15.1  $\mu\text{m}$ , volume:  $1.8 \times 10^{-12}$  L cell<sup>-1</sup>, weight:  $1.8 \times 10^{-9}$  g cell<sup>-1</sup>

Compound	Experiment	Cell	Mean cell number (0 h and 72 h)	Standard deviation
S12	bioaccumulation experiment	RTgill-W1	6400200	1742245
S12	bioaccumulation experiment	RTL-W1	3715200	279050
T10	bioaccumulation experiment	RTgill-W1	6471867	1787199
T10	bioaccumulation experiment	RTL-W1	3766720	688284
Q14	bioaccumulation experiment+ re-equilibration phase	RTL-W1	3041675	666557
Q14	bioaccumulation experiment	RTgill-W1	7050000	400327
T10	bioaccumulation experiment+ re-equilibration phase	RTL-W1	3023600	1049162

### S3.9 Cytotoxicity data

The concentration-response curves presented in Figure S3.3 and the concurrent measured exposure concentrations in Table S3.7 were used to derive EC<sub>50</sub> values and non-toxic exposure concentrations for later bioaccumulation experiments.

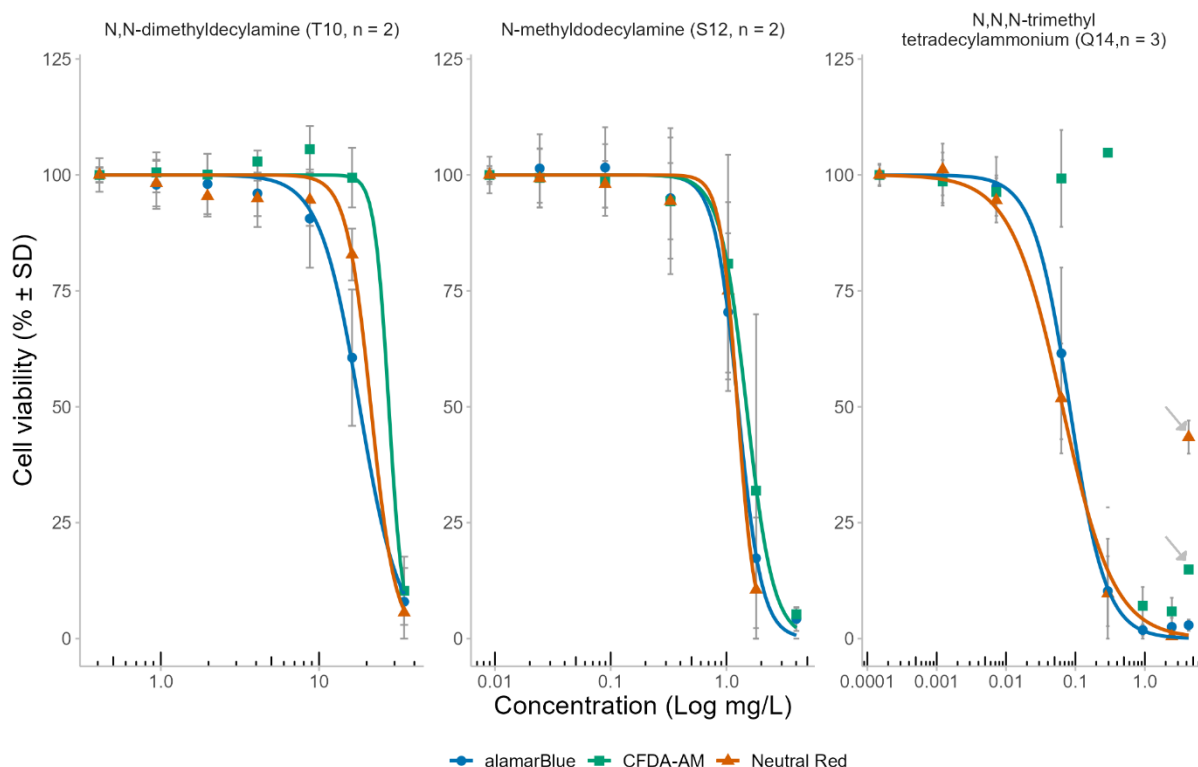


**Figure S3.3: Percent cell viability relative to unexposed control as measured by alamarBlue™, CFDA-AM and Neutral Red upon 24 h exposure of the test compounds to RTgill-W1.** The highest concentration of *N,N,N*-trimethyltetradecylammonium caused a fluorescence interference with Neutral Red and CFDA-AM (indicated by arrows) and the concentration-response curve of the CFDA-AM could not be fitted. The comparisons of nominal and measured exposure concentrations are presented in Table S3.7. Error bars are the standard deviation across all biological replicates. n = number of biological replicates, CFDA-AM = 5-carboxyfluorescein diacetate acetoxy methyl ester

**Table S3.7: Nominal and measured exposure concentrations of the acute cytotoxicity assays.**  
The measured geometric mean based on all biological replicates and their medium samples taken at 0h and 24h of exposure.

Test compound	Nominal concentration (mg L <sup>-1</sup> )	Measured concentration (±SD, 0 h)	Measured concentration (±SD, 24 h)	Measured geometric mean (mg L <sup>-1</sup> )	Measured vs. nominal concentration (%)
S12	0.125	0.03 ± 0.00	0.003 ± 0.000	0.009 ± 0.01	7
S12	0.25	0.07 ± 0.00	0.008 ± 0.000	0.02 ± 0.04	10
S12	0.5	0.2 ± 0.1	0.04 ± 0.02	0.09 ± 0.09	18
S12	1	0.56 ± 0.10	0.2 ± 0.0	0.33 ± 0.20	33
S12	2	1.4 ± 0.4	0.8 ± 0.1	1 ± 0.4	52
S12	3	2.2 ± 0.4	1.5 ± 0.3	1.8 ± 0.5	60
S12	6	4.6 ± 0.7	3.6 ± 0.6	4 ± 0.8	67
T10	1.125	0.5 ± 0.1	0.32 ± 0.04	0.4 ± 0.1	36
T10	2.25	1.2 ± 0.2	0.8 ± 0.1	0.9 ± 0.3	42
T10	4.5	2.3 ± 0.4	1.7 ± 0.1	2 ± 0.4	44
T10	9	4.8 ± 1	3.5 ± 0.3	4.1 ± 0.1	45
T10	18	10.7 ± 0.6	7.2 ± 0.6	8.7 ± 2.1	49
T10	36	19 ± 2.2	13.8 ± 0.5	16.2 ± 3.3	45
T10	74	41 ± 5.3	29 ± 0.5	34.5 ± 7.8	47
Q14	0.06	0.0002 ± 0.000	0.0002 ± 0.000	0.0002 ± 0.000	0
Q14	0.11	0.005 ± 0.004	0.0009 ± 0.0010	0.001 ± 0.004	1
Q14	0.22	0.02 ± 0.01	0.003 ± 0.001	0.007 ± 0.01	3
Q14	0.44	0.13 ± 0.07	0.03 ± 0.01	0.1 ± 0.1	14
Q14	0.88	0.6 ± 0.4	0.17 ± 0.02	0.3 ± 0.3	33
Q14	1.75	1.6 ± 1.0	0.6 ± 0.2	0.9 ± 0.8	53
Q14	3.5	3.7 ± 2.1	1.8 ± 0.4	2.5 ± 1.7	70
Q14	7	4.9*	3.7*	4.3 ± 0.8	61

\*only one replicate tested at this concentration

**Table S3.8: Percent cell viability and corresponding nominal exposure concentrations of the acute cytotoxicity assays after 24 h exposure.** AB = alamarBlue™ (metabolic activity), CFDA-AM = 5-carboxyfluorescein diacetate acetoxymethyl ester (cell membrane integrity), NR = Neutral Red (lysosomal membrane integrity), SD = Standard Deviation

Test compound	Nominal concentration (mg L <sup>-1</sup> )	AB (± SD, %)	CFDA-AM (± SD, %)	Neutral Red (± SD, %)
S12	0	100	100	100
S12	0.125	100 ± 2	100 ± 4	100 ± 1
S12	0.25	101 ± 7	99 ± 6	99 ± 6
S12	0.5	102 ± 9	99 ± 8	98 ± 5
S12	1	95 ± 13	94 ± 8	94 ± 16
S12	2	70 ± 17	81 ± 24	75 ± 19
S12	3	17 ± 15	32 ± 38	11 ± 16
S12	6	4 ± 3	5 ± 1	0 ± 2
T10	0	100	100	100
T10	1.125	100 ± 4	100 ± 2	100 ± 1
T10	2.25	98 ± 5	101 ± 4	98 ± 5
T10	4.5	98 ± 7	100 ± 4	95 ± 4
T10	9	98 ± 7	103 ± 2	95 ± 4
T10	18	91 ± 11	106 ± 5	95 ± 6
T10	36	61 ± 15	99 ± 6	83 ± 6
T10	74	8 ± 3	10 ± 7	6 ± 10
Q14	0	100	100	100
Q14	0.06	100 ± 2	100 ± 2	100 ± 2
Q14	0.11	99 ± 6	99 ± 5	101 ± 6
Q14	0.22	98 ± 6	96 ± 4	95 ± 5
Q14	0.44	62 ± 19	99 ± 10	52 ± 12
Q14	0.88	10 ± 8	105 ± 77	10 ± 12
Q14	1.75	2 ± 1	7 ± 4	0 ± 3
Q14	3.5	3 ± 2	6 ± 3	0 ± 2
Q14	7	2.9 ± 1	15 ± 0.3	43 ± 3

### S3.10 Cell viability on test compound exposure for bioaccumulation experiments

Figure S3.4 shows the viability (%) after exposure to the test compound concentrations intended for the bioaccumulation experiments relative to the test compound-free control. Q14 was initially tested at 100  $\mu\text{g L}^{-1}$  in the absence of fetal bovine serum (FBS) in the L15/ex medium as a worst case-scenario, which resulted in approximately 30 to 40% toxicity in RTgill-W1 after 72 h of exposure. When instead 20  $\mu\text{g L}^{-1}$  of Q14 and L15/ex medium with FBS was used, percent viability in the exposed cells remained comparable to the control.

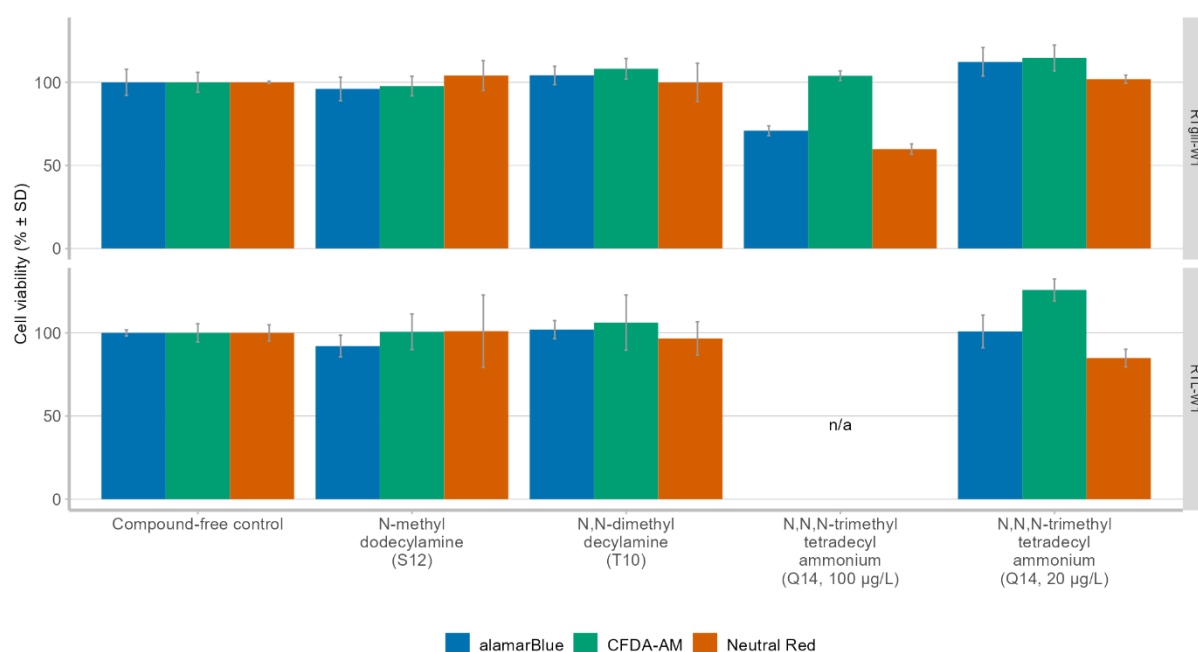


**Figure S3.4: Impact on cell viability of the exposure concentrations used in bioaccumulation assessments after 72 h.** alamarBlue™ indicates metabolic activity, CFDA-AM cell membrane integrity and Neutral Red lysosomal membrane integrity. Error bars indicate the standard deviation of the two biological replicates. Please note that the first and second replicate of *N,N,N*-trimethyltetradecylammonium are presented separately due to the use of different exposure concentrations in experiments with RTgill-W1 (error bars represent technical replicates in this case). n/a = not applicable, since 20  $\mu\text{g L}^{-1}$  exposures of Q14 were not used in RTL-W1 cell cultures.

Table S3.9 shows the compound concentrations measured in the cytotoxicity assay (Figure S3.4). It was observed that the exposure concentration was consistently lower than the nominal concentration. The test compounds likely were taken up by the cells as well as adsorbed to the plastic in the cytotoxicity assay, which lowered the measured medium concentrations relative to the nominal exposure concentration. This effect can be seen most clearly for the second replicate of Q14 (Q14R2, Table S3.9).

**Table S3.9: Measured concentrations ( $C_{0h}$  and  $C_{72h}$ ) of the cytotoxicity assay with final exposure concentrations for bioaccumulation experiments.** Shown are the measured medium concentrations (geometric mean of experimental start,  $C_{0h}$ , and termination,  $C_{72h}$ ) of the two biological replicates of each cell line and the cell-free control. S12 = *N*-methyldodecylamine, T10 = *N,N*-dimethyldodecylamine, Q14 = *N,N,N*-trimethyltetradecylammonium, R1 = replicate 1, R2 = replicate 2, SD = Standard deviation

Compound	Cell line	Nominal concentration ( $\mu\text{g L}^{-1}$ )	Concentration ( $\pm$ SD, 0h)	Concentration ( $\pm$ SD, 72h)	Geometric mean(measured, $\mu\text{g L}^{-1}$ )	SD (measured, $\mu\text{g L}^{-1}$ )	Percent of nominal
S12	cell-free	200	274 $\pm$ 50	243 $\pm$ 34	257	44	129
S12	RTgill-W1	200	237 $\pm$ 20	42 $\pm$ 12	100	103	50
S12	RTL-W1	200	255 $\pm$ 24	86 $\pm$ 14	148	90	74
T10	cell-free	185	171 $\pm$ 30	158 $\pm$ 38	164	34	89
T10	RTgill-W1	185	166 $\pm$ 34	133 $\pm$ 29	149	35	80
T10	RTL-W1	185	168 $\pm$ 31	141 $\pm$ 38	154	36	83
Q14R1	cell-free	100	144 $\pm$ 29	117 $\pm$ 32	130	31	130
Q14R1	RTgill-W1	100	141 $\pm$ 4	22 $\pm$ 1	56	65	56
Q14R1	RTL-W1	100	136 $\pm$ 14	35 $\pm$ 3	69	56	69
Q14R2	cell-free	20	4 $\pm$ 3	2 $\pm$ 4	3	3	14
Q14R2	RTgill-W1	20	5 $\pm$ 0.4	0.8 $\pm$ 0.02	2	2	12
Q14R2	RTL-W1	20	5 $\pm$ 0.6	0.9 $\pm$ 0.05	2	2	11

### S3.11 pH measurements

Most of the samples were measured with pH indicator strips, which allowed for rough pH measurement in steps of 0.5 pH units (Figure S3.5).

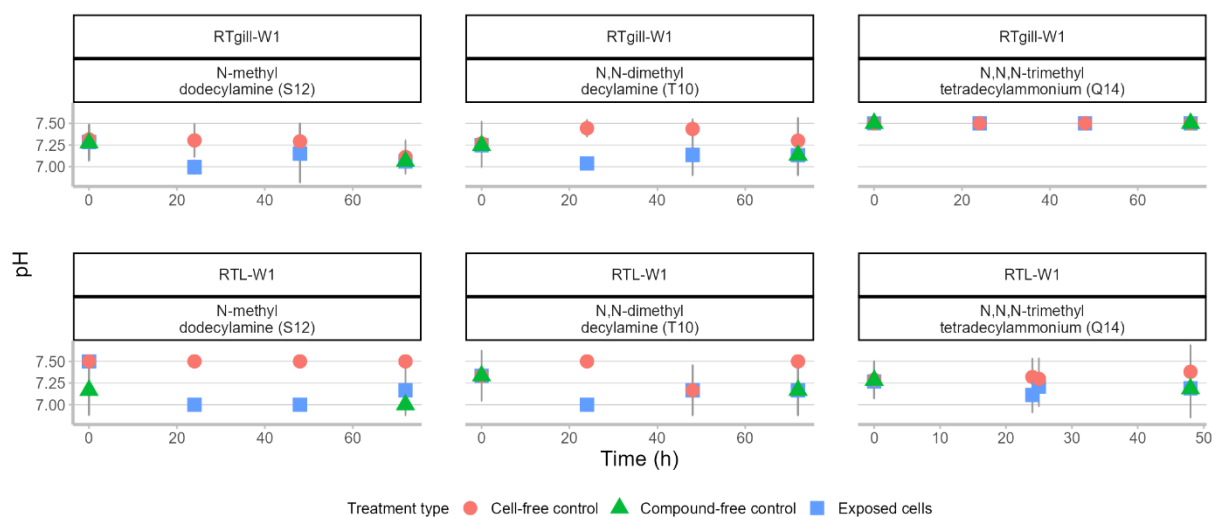


**Figure S3.5: pH measurements of exposed cells and controls over the experimental duration.** The pH was measured every 24 h. Error bars indicate the standard deviation across the biological replicates.

### S3.12 Mass balances

Tables S3.10 to S3.13 show the mass balances of the bioaccumulation experiments. Where no standard deviations are documented, the experiment was conducted only once. Experiments are distinguished as bioaccumulation experiments and bioaccumulation experiments that contain a re-equilibration phase with test compound-free medium (see table captions below). It is possible that the cell surface sampling in the cell-free controls sampled test compound adsorbed to plastic. This explained the partially higher test compound amounts of cell surface samples in the cell-free controls relative to the exposed cells.

**Table S3.10: Mass balances of RTgill-W1 and RTL-W1 cells and cell-free controls exposed to S12 in bioaccumulation experiments.**

Cell line	Sample Type	Timepoint (h)	Absolute amount (exposed cells, ng)	Standard deviation (exposed cells, ng)	Absolute amount (cell-free control, ng)	Standard deviation (cell-free control, ng)
RTgill-W1	CELL	0	204	23	5	2
RTgill-W1	CELL	4	418	69	12	10
RTgill-W1	CELL	8	442	25	3	3
RTgill-W1	CELL	24	375	39	5	1
RTgill-W1	CELL	48	412	34	4	1
RTgill-W1	CELL	72*	465	200	5	1
RTgill-W1	MEDIUM	0	433	164	440	14
RTgill-W1	MEDIUM	4	165	175	434	97
RTgill-W1	MEDIUM	8	55	24	443	95
RTgill-W1	MEDIUM	24	39	12	400	24
RTgill-W1	MEDIUM	48	34	11	391	41
RTgill-W1	MEDIUM	72*	25	7	372	19
RTgill-W1	PLASTIC	0	32	28	130	46
RTgill-W1	PLASTIC	4	74	55	151	52
RTgill-W1	PLASTIC	8	59	49	154	58
RTgill-W1	PLASTIC	24	90	78	161	59
RTgill-W1	PLASTIC	48	67	40	165	49
RTgill-W1	PLASTIC	72*	28	27	172	75
RTgill-W1	SURFACE	0	2	0.20	7	2
RTgill-W1	SURFACE	4	2	0.30	5	1
RTgill-W1	SURFACE	8	2	0.30	5	0.1
RTgill-W1	SURFACE	24	2	0.30	5	1
RTgill-W1	SURFACE	48	1	0.60	5	1



<b>Cell line</b>	<b>Sample Type</b>	<b>Timepoint (h)</b>	<b>Absolute amount (exposed cells, ng)</b>	<b>Standard deviation (exposed cells, ng)</b>	<b>Absolute amount (cell-free control, ng)</b>	<b>Standard deviation (cell-free control, ng)</b>
RTgill-W1	SURFACE	72*	1	0.80	5	2
RTL-W1	CELL	0	162	20	4	4
RTL-W1	CELL	4	354	47	4	3
RTL-W1	CELL	8	369	51	3	3
RTL-W1	CELL	24	365	31	3	2
RTL-W1	CELL	48	370	51	3	2
RTL-W1	CELL	72*	292	50	3	3
RTL-W1	MEDIUM	0	346	54	416	80
RTL-W1	MEDIUM	4	87	10	389	62
RTL-W1	MEDIUM	8	78	7	400	57
RTL-W1	MEDIUM	24	60	8	371	66
RTL-W1	MEDIUM	48	47	1	363	74
RTL-W1	MEDIUM	72*	37	4	349	59
RTL-W1	PLASTIC	0	14	13	106	25
RTL-W1	PLASTIC	4	28	25	108	39
RTL-W1	PLASTIC	8	28	24	116	44
RTL-W1	PLASTIC	24	23	20	118	22
RTL-W1	PLASTIC	48	27	23	123	28
RTL-W1	PLASTIC	72*	13	11	123	33
RTL-W1	SURFACE	0	3	1	5	1
RTL-W1	SURFACE	4	6	1	5	1
RTL-W1	SURFACE	8	4	0.4	4	0.2
RTL-W1	SURFACE	24	2	0.3	3	0.3
RTL-W1	SURFACE	48	2	1	4	0.4
RTL-W1	SURFACE	72*	1	1	4	1

\*At the 72 h time point, samples were spiked to calculate relative recoveries. Consequently, the sample amount was split into a spiked sample and a sample for comparison. This resulted in different dilutions relative to samples from other time points, which we accounted for. However, any differences that occurred for the 72 h samples relative to the other time points are likely an artefact from the different sample dilutions. The spikes were not high enough and no relative recovery could be calculated. Therefore, a separate spike experiment was conducted, see Table S3.5.

**Table S3.11: Mass balances of RTgill-W1 and RTL-W1 cells and cell-free controls exposed to T10 in bioaccumulation experiments.**

Cell line	Sample Type	Timepoint (h)	Absolute amount (exposed cells, ng)	Standard deviation (exposed cells, ng)	Absolute amount (cell-free control, ng)	Standard deviation (cell-free control, ng)
RTgill-W1	CELL	0	215	76	3	5
RTgill-W1	CELL	4	322	104	4	7
RTgill-W1	CELL	8	312	61	4	6
RTgill-W1	CELL	24	364	110	17	22
RTgill-W1	CELL	48	338	78	4	5
RTgill-W1	CELL	72*	196	197	2	4
RTgill-W1	MEDIUM	0	800	512	1099	588
RTgill-W1	MEDIUM	4	724	470	1065	543
RTgill-W1	MEDIUM	8	713	450	1042	545
RTgill-W1	MEDIUM	24	622	472	945	572
RTgill-W1	MEDIUM	48	578	464	890	573
RTgill-W1	MEDIUM	72*	433	321	855	551
RTgill-W1	PLASTIC	0	55	17	114	34
RTgill-W1	PLASTIC	4	110	17	169	31
RTgill-W1	PLASTIC	8	114	38	192	40
RTgill-W1	PLASTIC	24	125	18	207	7
RTgill-W1	PLASTIC	48	140	16	221	52
RTgill-W1	PLASTIC	72*	62	22	211	24
RTgill-W1	SURFACE	0	22	18	6	11
RTgill-W1	SURFACE	4	30	26	8	15
RTgill-W1	SURFACE	8	28	27	7	11
RTgill-W1	SURFACE	24	18	21	17	30
RTgill-W1	SURFACE	48	14	22	6	11
RTgill-W1	SURFACE	72*	37	61	7	12
RTL-W1	CELL	0	230	65	6	5
RTL-W1	CELL	4	289	77	7	6
RTL-W1	CELL	8	289	80	6	5
RTL-W1	CELL	24	344	105	5	5
RTL-W1	CELL	48	349	54	8	9

<b>Cell line</b>	<b>Sample Type</b>	<b>Timepoint (h)</b>	<b>Absolute amount (exposed cells, ng)</b>	<b>Standard deviation (exposed cells, ng)</b>	<b>Absolute amount (cell-free control, ng)</b>	<b>Standard deviation (cell-free control, ng)</b>
RTL-W1	CELL	72*	286	63	0	0
RTL-W1	MEDIUM	0	898	118	1141	181
RTL-W1	MEDIUM	4	876	182	1124	211
RTL-W1	MEDIUM	8	875	166	1092	189
RTL-W1	MEDIUM	24	706	112	1032	187
RTL-W1	MEDIUM	48	635	152	921	198
RTL-W1	MEDIUM	72*	475	137	808	200
RTL-W1	PLASTIC	0	28	13	91	31
RTL-W1	PLASTIC	4	77	12	156	19
RTL-W1	PLASTIC	8	100	29	165	48
RTL-W1	PLASTIC	24	88	27	181	40
RTL-W1	PLASTIC	48	138	21	203	24
RTL-W1	PLASTIC	72*	46*	1	239	14
RTL-W1	SURFACE	0	34	15	17	16
RTL-W1	SURFACE	4	40	18	18	15
RTL-W1	SURFACE	8	37	16	17	16
RTL-W1	SURFACE	24	30	15	16	17
RTL-W1	SURFACE	48	21	24	15	17
RTL-W1	SURFACE	72*	47	29	17	17

\*At the 72 h time point, samples were spiked to calculate relative recoveries. Consequently, the sample amount was split into a spiked sample and a sample for comparison. This resulted in different dilutions relative to samples from other time points, which we accounted for. However, any differences that occurred for the 72 h samples relative to the other time points are likely an artefact from the different sample dilutions. The spikes were not high enough and no relative recovery could be calculated. Therefore, a separate spike experiment was conducted, see Table S3.5.

**Table S3.12: Mass balances of RTgill-W1 cells and cell-free controls exposed to Q14 in one bioaccumulation experiment.**

<b>Sample Type</b>	<b>Timepoint (h)</b>	<b>Absolute amount (exposed cells, ng)</b>	<b>Absolute amount (cell-free control, ng)</b>
CELL	0	20	0
CELL	4	208	0
CELL	8	258	0
CELL	24	259	0
CELL	48	266	0
CELL	72	202	0
MEDIUM	0	228	198
MEDIUM	4	45	168
MEDIUM	8	16	163
MEDIUM	24	9	167
MEDIUM	48	5	164
MEDIUM	72	4	145
PLASTIC	0	8	67
PLASTIC	4	23	87
PLASTIC	8	17	90
PLASTIC	24	14	94
PLASTIC	48	17	89
PLASTIC	72	19	85
SURFACE	0	1	1
SURFACE	4	0.2	1
SURFACE	8	0.2	1
SURFACE	24	0.1	1
SURFACE	48	0.1	1
SURFACE	72	0.2	1

**Table S3.13: Mass balances of RTL-W1 cells and cell-free controls exposed to Q14 in bioaccumulation experiments containing a re-equilibration phase.**

<b>Sample Type</b>	<b>Timepoint (h)</b>	<b>Absolute amount (exposed cells, ng)</b>	<b>Standard deviation (exposed cells, ng)</b>	<b>Absolute amount (cell-free control, ng)</b>	<b>Standard deviation (cell-free control, ng)</b>
CELL	0	36	36	0	0
CELL	24	47	55	0	0
CELL	25	73	13	0	0
CELL	27	75	12	0	0
CELL	30	72	9	0	0
CELL	48	74	13	0	0
MEDIUM	0	56	2	45	10
MEDIUM	24	1.4	2	30	0
MEDIUM	25	1	1	9	0
MEDIUM	27	1	1	5	7
MEDIUM	30	<LOQ*	-	11	6
MEDIUM	48	<LOQ*	-	11	2
PLASTIC	0	3	0.4	28	1
PLASTIC	24	5	0.2	42	6
PLASTIC	25	4	1	33	5
PLASTIC	27	4	0	31	5
PLASTIC	30	4	1	29	5
PLASTIC	48	3	1	26	5
SURFACE	0	0	0	0	0
SURFACE	24	0	0	0	0
SURFACE	25	0	0	0	0
SURFACE	27	0	0	0	0
SURFACE	30	0	0	0	0
SURFACE	48	0	0	0	0

\*Samples were corrected for Q14-free controls, which were close to measured concentrations in the medium samples of the re-equilibration phase. Therefore, it is possible that it appeared here like a decreasing medium concentration over time rather than variabilities in medium concentrations, which were lower than background concentrations of the Q 14-free controls.

### S3. 13 *In vivo*, *in vitro* and partition coefficient-based BCF

Table S3.14 shows the BCF calculation using different approaches to understand the observed *in vitro* and *in vivo* bioaccumulations of the test compounds. The  $K_{OW}$ -,  $D_{OW}$ - and  $D_{MLW}$ -based approaches applied the partition coefficient to predict the accumulation in the cells. RTgill-W1 and RTL-W1 BCF are calculated from the observed mass balances and the measured cell numbers and represent the *in vitro* BCFs. The rainbow trout BCF represents the *in vivo* BCF for reference.

**Table S3.14: Predicted and measured BCFs of the test compounds.** If applicable, the mean of a BCF value is presented. Since Q14 is permanently charged, no  $K_{OW}$  could be calculated and consequently no  $D_{OW}$ . The assumed lipid volume fraction in the cells for  $K_{OW}$  and  $D_{OW}$ -based calculations was 0.04, as for whole fish (subtracting 1 % phospholipid of initially 5 % lipid volume fraction) <sup>41, 179</sup>.

Compound	BCF type	Value (log)
T10	$K_{OW}$ -based <sup>1</sup>	4.81
T10	$D_{OW}$ -based <sup>2</sup>	1.21
T10	$D_{MLW}$ -based <sup>3</sup>	1.64
T10	RTgill-W1	2.36
T10	RTL-W1	2.27
T10	Rainbow trout <sup>4</sup>	2.2
S12	$K_{OW}$ -based <sup>1</sup>	5.25
S12	$D_{OW}$ -based <sup>2</sup>	3.45
S12	$D_{MLW}$ -based <sup>3</sup>	3.15
S12	RTgill-W1	3.57
S12	RTL-W1	3.43
S12	Rainbow trout <sup>4</sup>	2.96
Q14	$K_{OW}$ -based <sup>1</sup>	not available
Q14	$D_{OW}$ -based <sup>2</sup>	not available
Q14	$D_{MLW}$ -based <sup>3</sup>	3.53
Q14	RTgill-W1	3.94
Q14	RTL-W1	4.14
Q14	Rainbow trout <sup>4</sup>	1.75

<sup>1</sup> $K_{OW}$ -driven partitioning into cells, <sup>2</sup> $D_{OW}$ -driven partitioning into cells, <sup>3</sup> $D_{MLW}$ -driven partitioning into cells

Figure S3.6 visualizes the  $K_{OW}$  and  $D_{OW}$ -based BCF prediction in the cells compared to the observed *in vitro* BCFs. The comparison was used to assess whether  $K_{OW}$  and  $D_{OW}$  were

suitable descriptors for the *in vitro* observed accumulation. Since no  $K_{OW}$  or  $D_{OW}$  was available for Q14 (fully ionized), the  $K_{OW}$  and  $D_{OW}$ -based predictions could not be performed.

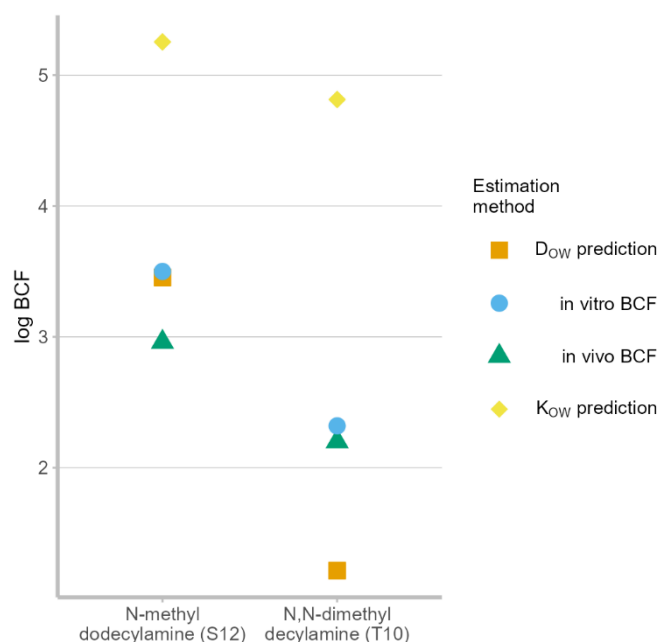


**Figure S3.6: Comparison of *in vitro* BCF with  $K_{OW}$ - and  $D_{OW}$ -based BCF predictions in the cells.** *In vitro* BCF represent the mean of experiments with RTgil-W1 and RTL-W1, while *in vivo* BCF were taken from Kierkegaard et al.<sup>167</sup>.

### S3.14 Biotransformation analysis following OECD TG319A and 319B

OECD TG319<sup>23, 24</sup> criteria were applied to the mass balances to see if a clearance rate could be calculated. The results are shown in Table S3.15 to S3.17.

**Table S3.15: Analysis for biotransformation activity of the experiments with S12 following OECD TG criteria in RTL-W1 (top) and RTgill-W1 (bottom) cell lines.**

N-methyldodecylamine (S12) in RTL-W1		
	Cell-free control	Exposed Cells
R squared	0.06484	0.4517
Is slope significantly non-zero?		
F	1.109	13.18
P value	0.3078	0.0022
Deviation from zero?	Not Significant	Significant
Equation	$Y = -0.0005241 \cdot X + 5.265$	$Y = -0.001796 \cdot X + 5.282$
N-methyldodecylamine (S12) in RTgill-W1		
	Cell-free control	Exposed Cells

R squared	0.03102	0.1706
Is slope significantly non-zero?		
F	0.5122	3.29
P value	0.4845	0.0885
Deviation from zero?	Not Significant	Not Significant
Equation	$Y = -0.0004272 \cdot X + 5.321$	$Y = -0.001429 \cdot X + 5.369$

**Table S3.16: Analysis for biotransformation activity of the experiments with T10 following OECD TG criteria in RTL-W1 (top) and RTgill-W1 (bottom) cell lines.**

<b>N,N-dimethyldecylamine (T10) in RTL-W1</b>		
	Cell-free control	Exposed Cells
R squared	0.2717	0.3426
Is slope significantly non-zero?		
F	5.968	8.338
P value	0.0265	0.0107
Deviation from zero?	Significant	Significant
Equation	$Y = -0.003935 \cdot X + 5.643$	$Y = -0.004492 \cdot X + 5.643$
<b>N,N-dimethyldecylamine (T10) in RTgill-W1</b>		
	Cell-free control	Exposed Cells
R squared	0.01773	0.006749
Is slope significantly non-zero?		
F	0.2887	0.1087
P value	0.5984	0.7459
Deviation from zero?	Not Significant	Not Significant
Equation	$Y = -0.0009844 \cdot X + 5.564$	$Y = -0.0006712 \cdot X + 5.538$

**Table S3.17: Analysis for biotransformation activity of the experiments with Q14 following OECD TG criteria in RTL-W1 (top) cell lines.**

<b>N,N,N-trimethyltetradecylammonium (Q14) in RTL-W1</b>		
	Cell-free control	Exposed Cells
R squared	0.09055	0.003213



Is slope significantly non-zero?		
F	0.5974	0.01934
P value	0.4689	0.8939
Deviation from zero?	Not Significant	Not Significant
Equation	$Y = -0.001199 \cdot X + 4.164$	$Y = -0.0001936 \cdot X + 5.056$

### S3.15 Biotransformation product of T10 in RTL-W1 cells

We conducted screenings for biotransformation products and only experiments with RTL-W1 exposed to T10 indicated biotransformation activity. The screening resulted in the detection of one biotransformation product as shown in Figures S3.7 to S3.9. However, the detections were small and the amounts could not be quantified.

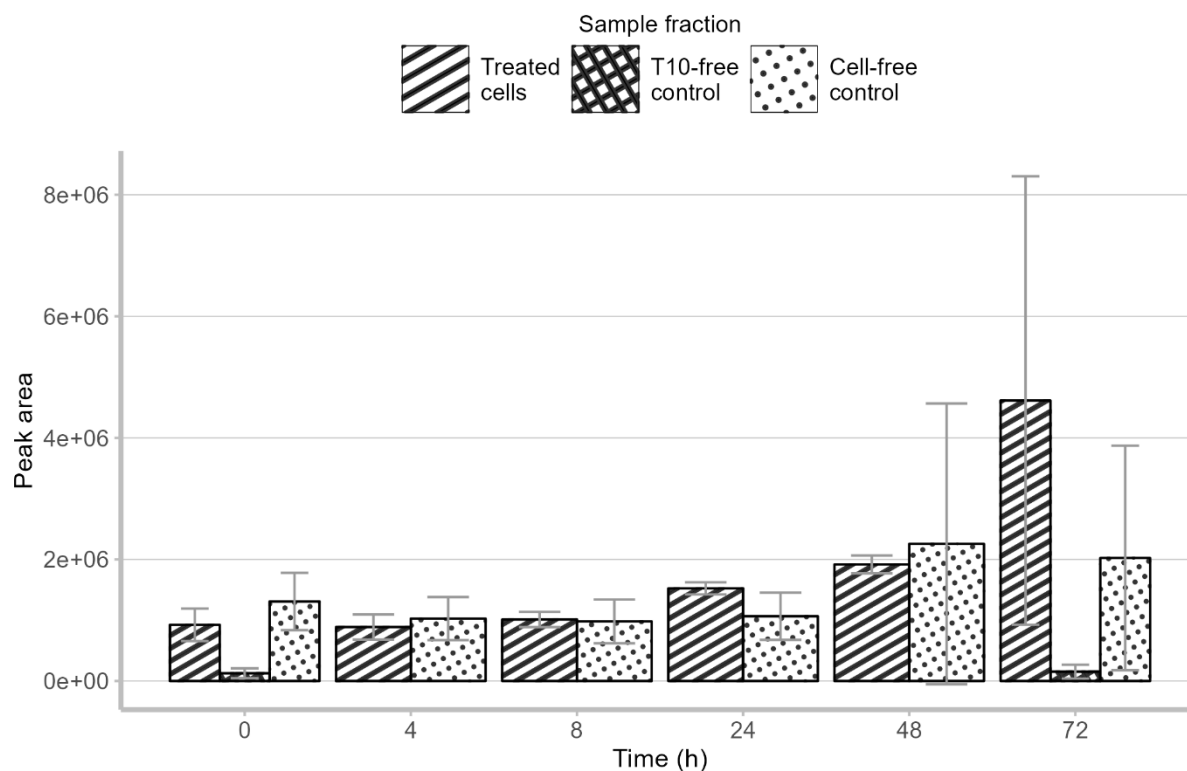


**Figure S3.7: Detection of demethylated T10 in medium samples.** Error bars mark the standard deviations.

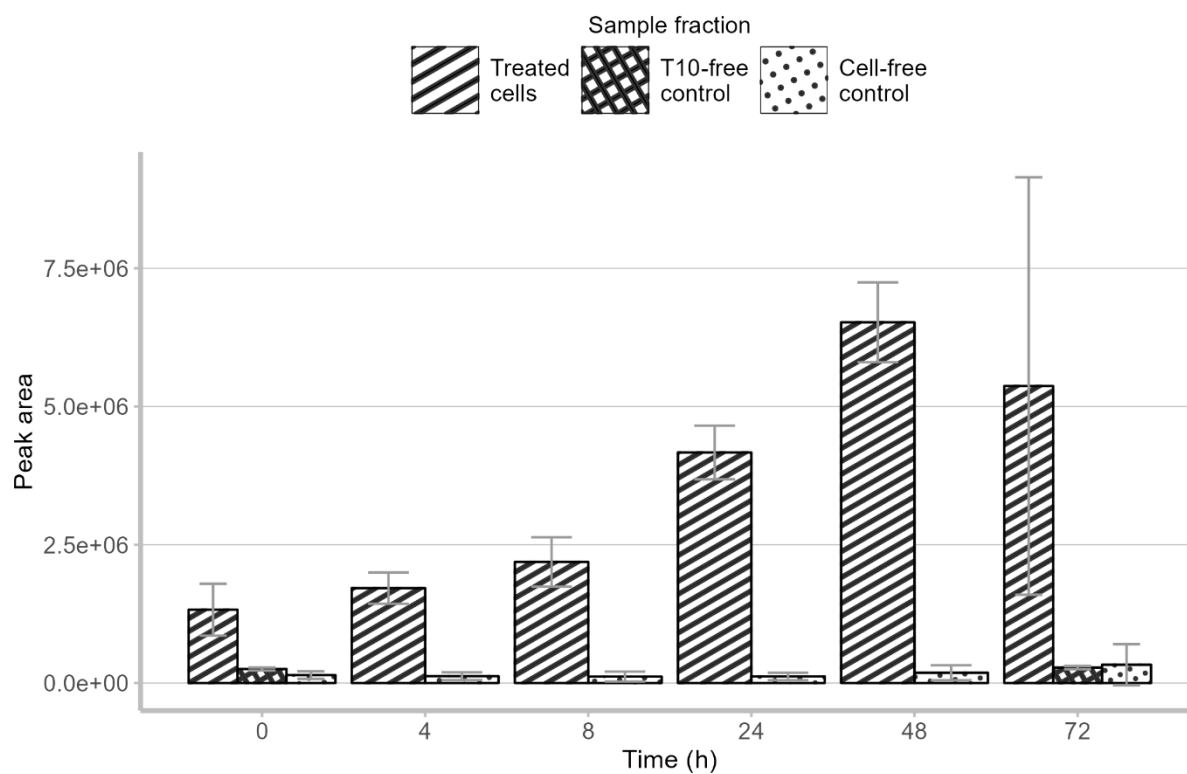


**Figure S3.8: Detection of demethylated T10 in cell samples.** Error bars mark the standard deviations.

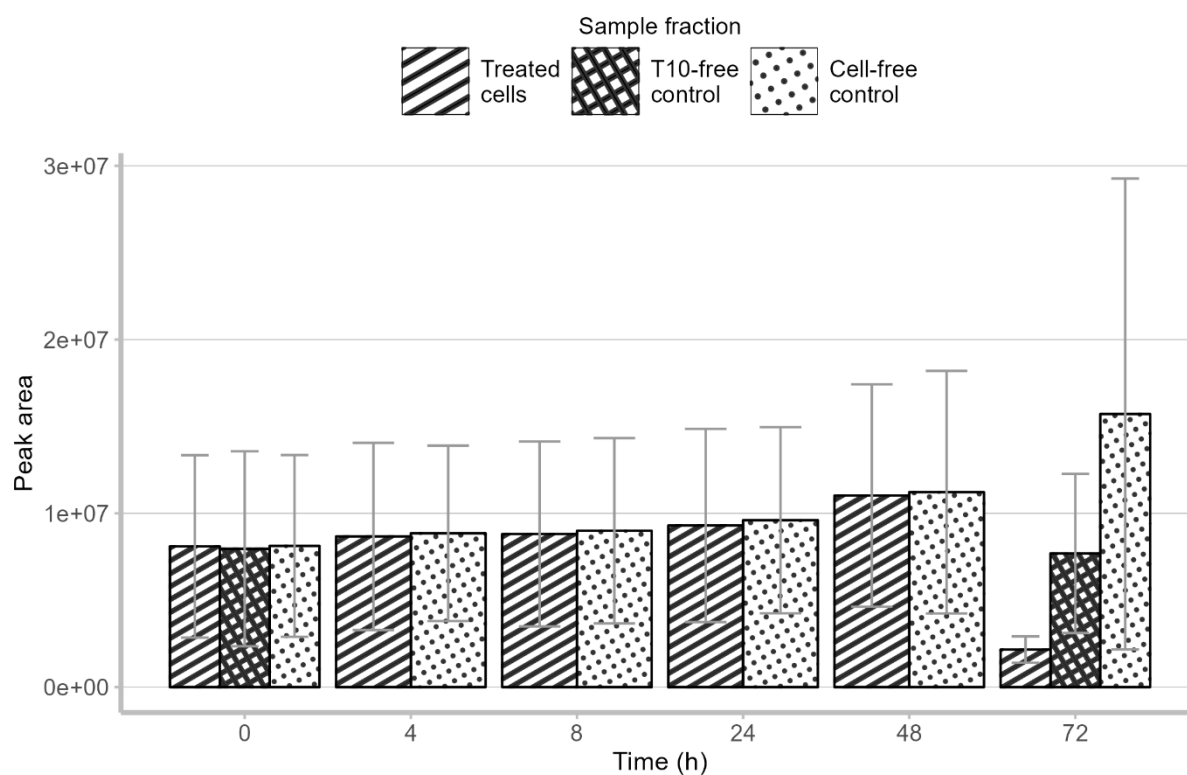


**Figure S3.9: Detection of demethylated T10 in plastic samples.** Error bars mark the standard deviations.

## Supporting Information Chapter 4

**Table S4.1: Substance descriptors of the neutral test compounds.** The partition coefficient estimations are based on these descriptors, following the same approach as outlined in Henneberger et al.<sup>60</sup>. The equations by Abraham et al. were used to calculate the substance descriptors of the ionic compounds<sup>240 241</sup>. The pp-LFER for partition coefficient prediction were taken from Endo et al.<sup>206 87</sup> for the neutral compounds and Henneberger et al.<sup>60</sup> and Bittermann et al.<sup>207</sup> for the ionic compounds. E = excess molar refraction, A = acidity, B = basicity, S = polarizability, V = molar volume, ACD/Labs = Predicted with the ABSOLV module (Percepta v14.50.0)<sup>209</sup>, UFZ LSER = predicted with the UFZ LSER database<sup>208</sup>

Compound	SMILES	E	A	B	S	V	Source
Benzotriazol-propanoic acid	<chem>CC(C)(C)C1=C(C(=CC(=C1)CCC(=O)O)N2N=C3C=CC=CC3=N2)O</chem>	2.59	0.64	1.27	2.64	2.59	ACD/Labs
Diclofenac	<chem>C1=CC=C(C(=C1)CC(=O)[O])NC2=C(C(=CC=C2Cl)Cl</chem>	2.03	0.70	0.67	1.81	2.03	ACD/Labs
N,N,N-trimethyl-1-tetradecylammonium	<chem>CCCCCCCCCCCCCCC[N+](C)(C)C</chem>	-0.23	0.00	0.10	0.15	2.63	ACD/Labs
N,N-dimethyldodecylamine	<chem>N(CCCCCCCCCCCC)(C)C</chem>	0.16	0.00	0.55	0.40	1.90	ACD/Labs
N-Ethyl-N-(2-hydroxyethyl)perfluorooctyl sulfonamide	<chem>CCN(CCO)S(=O)(=O)C(C(C(C(C(C(C(F)(F)F)(F)F)(F)F)(F)F)(F)F)(F)F)(F)F</chem>	2.54	0.33	0.82	- 0.60	2.54	UFZ LSER
N-Ethylperfluorooctane sulfonamidoacetic acid	<chem>CCN(CC(=O)O)S(=O)(=O)C(C(C(C(C(C(C(F)(F)F)(F)F)(F)F)(F)F)(F)F)(F)F)(F)F</chem>	2.56	0.46	0.76	- 0.64	2.56	UFZ LSER
N-Ethylperfluorooctane sulfonamide	<chem>CCNS(=O)(=O)C(C(C(C(C(C(C(F)(F)F)(F)F)(F)F)(F)F)(F)F)(F)F)(F)F</chem>	2.20	0.01	0.88	- 0.79	2.20	UFZ LSER
N-methyldodecylamine	<chem>N(CCCCCCCCCCCCC)C</chem>	0.14	0.13	0.50	0.39	2.04	ACD/Labs
Perfluorooctanesulfonamide	<chem>C(C(C(C(C(F)(F)S(=O)(=O)N)(F)F)(F)F)(F)F)(C(C(C(F)(F)F)(F)F)(F)F)(F)F</chem>	1.92	0.51	0.72	- 0.69	1.92	UFZ LSER
Perfluorooctanesulfonic acid	<chem>C(C(C(C(C(F)(F)S(=O)(=O)O)(F)F)(F)F)(F)F)(C(C(C(F)(F)F)(F)F)(F)F)(F)F</chem>	-0.94	0.31	0.71	0.24	1.87	ACD/Labs
Perfluorooctanoic acid	<chem>C(=O)(C(C(C(C(C(C(C(F)(F)F)(F)F)(F)F)(F)F)(F)F)(F)F)O</chem>	-0.90	0.84	0.29	- 0.34	1.57	ACD/Labs
Pentachlorophenol	<chem>Oc(c(c(c(c1Cl)Cl)Cl)Cl)c1Cl</chem>	1.27	0.70	0.00	1.13	1.39	ACD/Labs
Tecloftalam	<chem>C1=CC(=C(C(=C1)Cl)Cl)NC(=O)C2=C(C(=C(C(=C2Cl)Cl)Cl)Cl)C(=O)O</chem>	2.53	1.22	0.85	2.40	2.53	ACD/Labs

**Table S4.2:  $V_D$  derivation from literature.** The tissue weights in Table S4.3 were taken to calculate fish  $V_D$ . None of the fish studies measured all tissue concentrations in tested fish. Therefore, the measured tissues had to be assumed as representatives for other, not measured, tissues. For example, if muscle tissue was measured, but none of the viscera was, the muscle concentration was taken as representative for viscera concentrations. The available tissue concentrations are listed in brackets in the “comment fish  $V_D$ ” column.

Compound	CASRN	Compound species	$V_D$ (human, L kg <sup>-1</sup> )	Reference human $V_D$	$V_D$ (fish, L kg <sup>-1</sup> )	Reference fish $V_D$	Comment $V_D$	$K_{BW}$	Reference $K_{BW}$	$K_{BW}$ comment
Diclofenac	15307796	Acid	0.22	Willis et al. 1979 <sup>242</sup>	0.82	Memmert et al. 2013 <sup>102</sup>	derived from BCF and $K_{BW}$ in rainbow trout ( <i>Oncorhynchus mykiss</i> ) (each from different studies)	4.98	Lahti et al. 2011 <sup>149</sup> Cuklev et al. 2011 <sup>213</sup>	Mean from two studies in rainbow trout taken (plasma concentrations divided by water concentration)
Diphenhydramine	58731	Base	6.5	Meredith et al. 1984 <sup>243</sup>	3.00	Nichols et al. 2015 <sup>200</sup>	in fathead minnow ( <i>Pimephales promelas</i> ) (approximated as BCF x $K_{BW}^{-1}$ )	9.17	Nichols et al. 2015 <sup>200</sup>	$K_{BW}$ in fathead minnow (noted as plasma-water partitioning)
Ibuprofen	15687271	Acid	0.15	Martin et al. 1990 <sup>244</sup>	0.09	Nallani et al. 2011 <sup>245</sup>	from tissue BCF in catfish ( <i>Ictalurus punctatus</i> ) (muscle, gill, liver, kidney, plasma), weight fraction taken from catfish (Table S4.3)	3.8	Lahti et al. 2011 <sup>149</sup>	in rainbow trout, no value available for catfish
Perfluorooctanesulfonic acid	1763231	Acid	0.23	Thompson et al. 2010 <sup>246</sup>	0.38	Martin et al. 2003 <sup>103</sup>	derived from BCF in rainbow trout (blood, liver, carcass) (Consoer et al. 2016 <sup>220</sup> found a $V_D$ of 0.277 L/kg in rainbow trout)	3100	Martin et al. 2003 <sup>103</sup>	accumulation ratio of blood/water in rainbow trout taken
Perfluorooctanoic acid	335671	Acid	0.17	Thompson et al. 2010 <sup>246</sup>	0.17	Martin et al. 2003 <sup>103</sup>	derived from BCF in rainbow trout (blood, liver, carcass)	25	Martin et al. 2003 <sup>103</sup>	accumulation ratio of blood/water in rainbow trout taken
Methamphetamine	537462	Base	4.3	Harris et al. 2003 <sup>247</sup>	64.81	Sancho Santos et al. 2020 <sup>248</sup>	Derived from BCF in brown trout ( <i>Salmo trutta</i> ) (plasma, muscle, brain, liver and kidney) weight fraction taken from rainbow trout (Table S4.3)	0.115	Sancho Santos et al. 2020 <sup>248</sup>	in brown trout, BCF <sub>plasma</sub> taken
Venlafaxine	93413695	Base	4.4	Patat et al. 1998 <sup>249</sup>	0.83	Grabicova et al. 2014 <sup>250</sup>	derived from BCF in rainbow trout (liver, brain, plasma, muscle)	8	Grabicova et al. 2014 <sup>250</sup>	in rainbow trout

Compound	CASRN	Compound species	V <sub>D</sub> (human, L kg <sup>-1</sup> )	Reference human V <sub>D</sub>	V <sub>D</sub> (fish, L kg <sup>-1</sup> )	Reference fish V <sub>D</sub>	Comment V <sub>D</sub>	K <sub>BW</sub>	Reference K <sub>BW</sub>	K <sub>BW</sub> comment
Atenolol	29122687	Base	0.95	Mason et al. 1979 <sup>251</sup>	23.07	Steinbach et al. 2014 <sup>252</sup>	derived from BCF in rainbow trout (plasma = 0.5*LOQ, liver, kidney, muscle)	0.00087	Steinbach et al. 2014 <sup>252</sup>	in rainbow trout, semi quantitative since Plasma <LOQ, therefore LOQ/2 taken
Carbamazepine	298464	Base	1	Marino et al. 2012 <sup>253</sup>	0.23	Garcia et al. 2012 <sup>254</sup>	derived from BCF in catfish ( <i>I. punctatus</i> ) (muscle, liver, plasma, brain), weight fraction taken from catfish (Table S4.3)	7.1	Garcia et al. 2012 <sup>254</sup>	in <i>Ictalurus punctatus</i> , BCF <sub>plasma</sub> taken
Pentachlorophenol	87865	Acid	2.30	Geyer et al. 1987 <sup>255</sup> , Pearce et al. 2017 <sup>217</sup>	1.95	McKim et al. 1986 <sup>108</sup>	human V <sub>D</sub> calculated from human tissue measurements <sup>255</sup> and composition assumed as in Pearce et al. 2017 <sup>217</sup>	125	McKim et al. 1986 <sup>108</sup>	BCF <sub>blood</sub> taken as K <sub>BW</sub>

**Table S4.3: Weight-based tissue composition in rainbow trout and catfish.** Tissue weights taken from mean values in Kierkegaard et al. 2020 <sup>74</sup> for rainbow trout and in Nichols et al. 1993 for catfish <sup>256</sup>.

<b>Tissue</b>	<b>Weight percent (rainbow trout, total weight 723 g)</b>	<b>Weight percent (catfish, total weight 1 kg)</b>
liver	1.1	1.5
gills	3.4	n/a
viscera	8.8	4.8
blood	0.9	n/a
muscle	80.8	88.1
skin	5.2	n/a

**Table S4.4: Variations in  $BCF_{cell\ model}$  dependent on the volume fraction of phospholipid in cells.** Volume fractions of phospholipid were assumed to be equivalent to Fischer et al.'s measured lipid fractions in mammalian cell lines <sup>89</sup>, mean phospholipid fraction = 0.0213, SD (standard deviation) = 0.011

<b>Compound</b>	<b>log <math>BCF_{cell\ model}</math> (mean)</b>	<b>Log <math>BCF_{cell\ model}</math> (SD)</b>
Benzotriazol-tert-butyl-hydroxyl-phenyl propanoic acid	1.35	0.20
Diclofenac	1.30	0.22
N,N,N-trimethyl-1-tetradecylammonium	5.51	0.25
N,N-dimethyldodecylamine	2.11	0.25
N-Ethyl-N-(2-hydroxyethyl)perfluorooctylsulphonamide	4.07	0.25
N-Ethylperfluorooctane sulfonamidoacetic acid	1.13	0.25
N-Ethylperfluorooctanesulfonamide	4.08	0.25
N-methyldodecylamine	4.25	0.25
perfluorooctanesulfonamide	3.04	0.25
Perfluorooctanesulfonic acid	1.14	0.25
Perfluorooctanoic acid	-0.21	0.24

Compound	log BCF <sub>cell model</sub> (mean)	Log BCF <sub>cell model</sub> (SD)
Phenol, pentachloro-	2.72	0.25
Tecloftalam	4.79	0.25

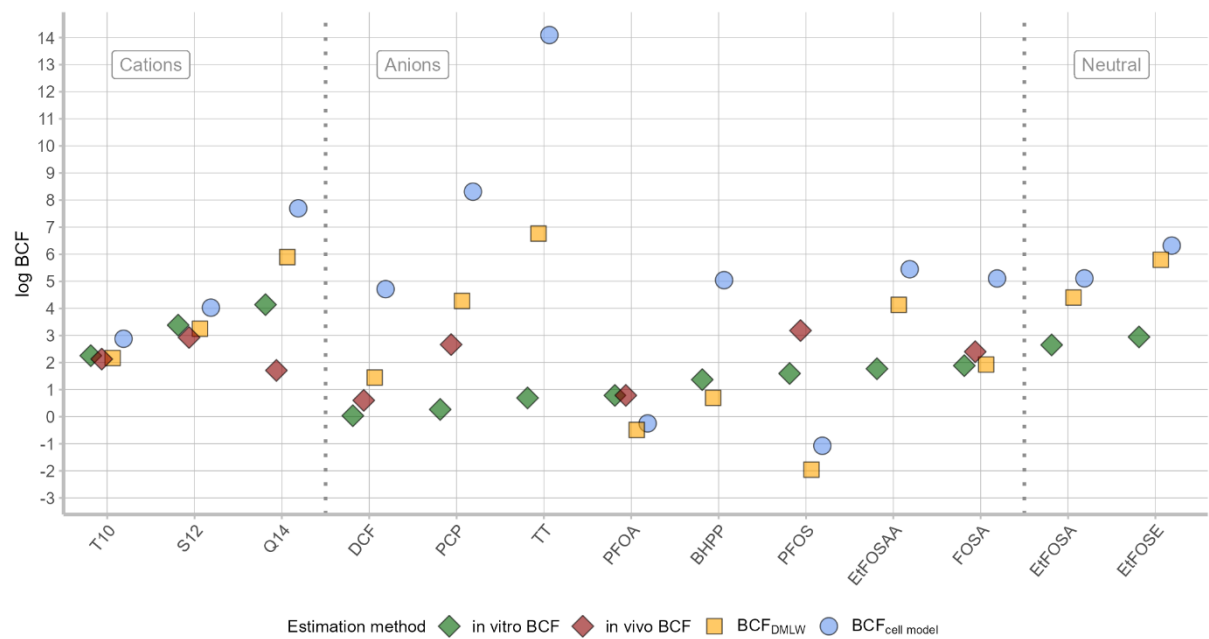


**Figure S4.1: Comparison of predicted BCF and observed *in vivo* and *in vitro* BCF using predicted  $D_{MLW}$  and  $D_{PW}$ .**  $BCF_{DMLW} = f_{ML} \times D_{MLW}$  (Equation 4.4),  $BCF_{cell model}$  = considers kinetics of neutral and ionic species (Equation 4.6)

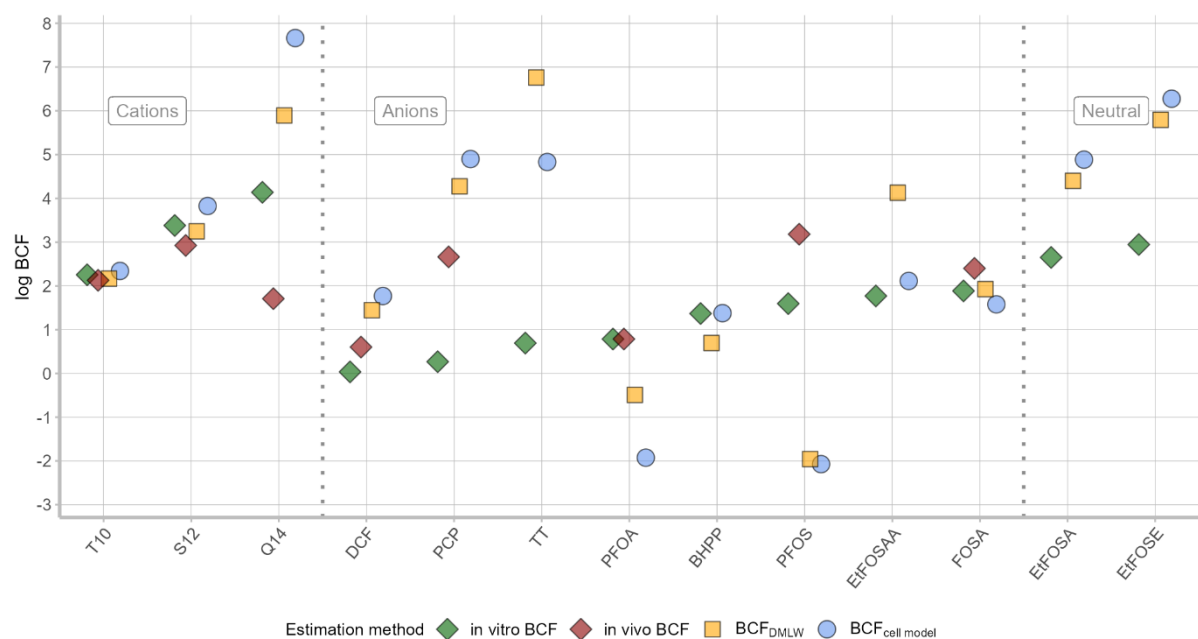


**Figure S4.2: Comparison of predicted BCF and observed *in vivo* and *in vitro* BCF using predicted  $D_{MLW}$ , while protein sorption was excluded.**  $BCF_{DMLW} = f_{PL} \times D_{MLW}$  (Equation 4.4),  $BCF_{cell\ model}$  = considers kinetics of neutral and ionic species (Equation 4.6)



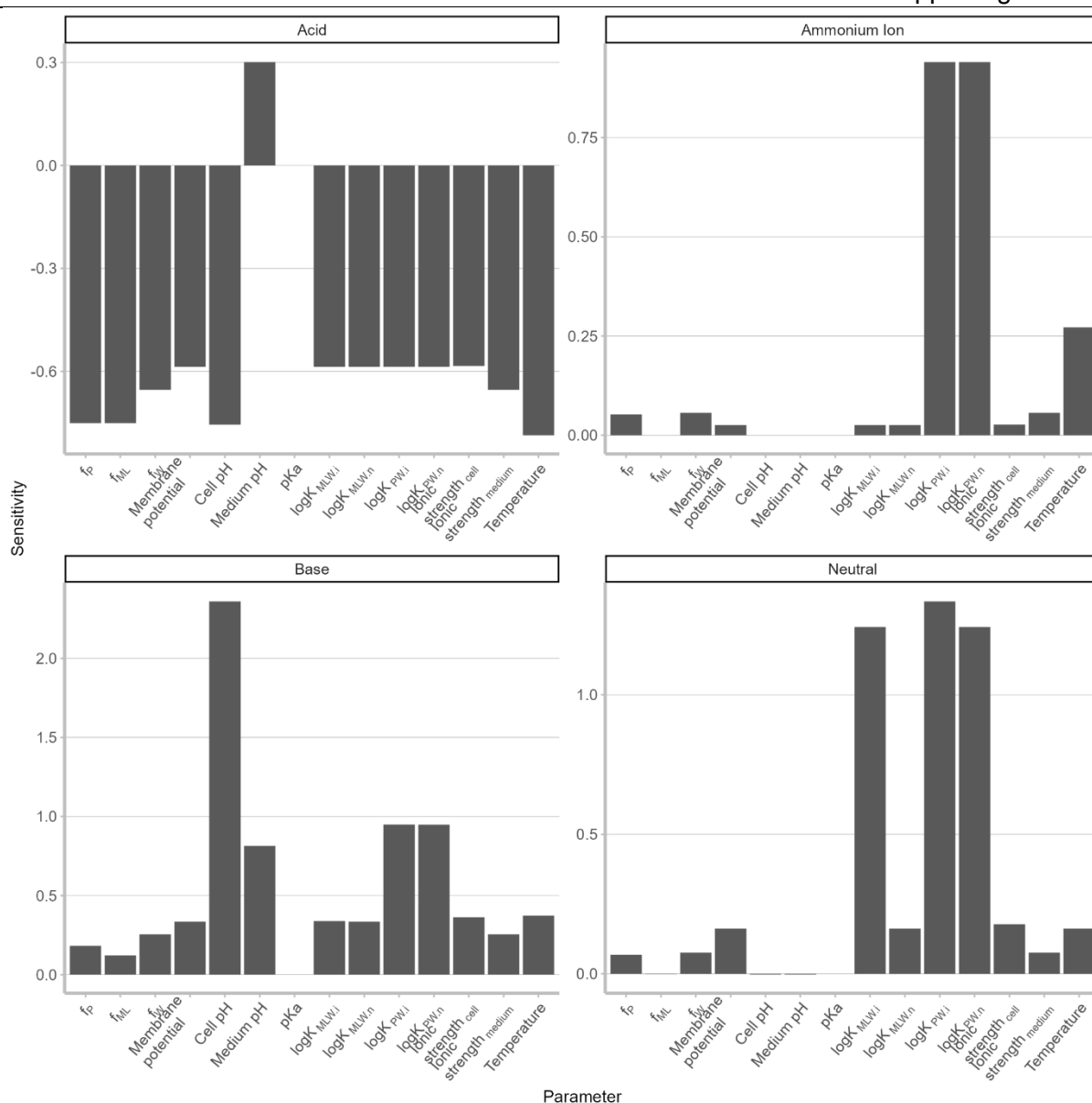


**Figure S4.3: Sensitivity of input parameters of the kinetic cell model.** The ammonium ion stands for the quaternary ammonium ion, for which experimental data (Q14) were available. For the sensitivity analysis, four hypothetical compounds were used, representing mean values of the compound set, for which *in vitro* BCF in RTL-W1 were available. Parameters were each changed by 0.1 % and the resulting output (predicted *in vitro* BCF) was compared to a default scenario to calculate the sensitivity. The resulting sensitivities on the Y axis have to be read in comparison to each other to understand their importance for the model.

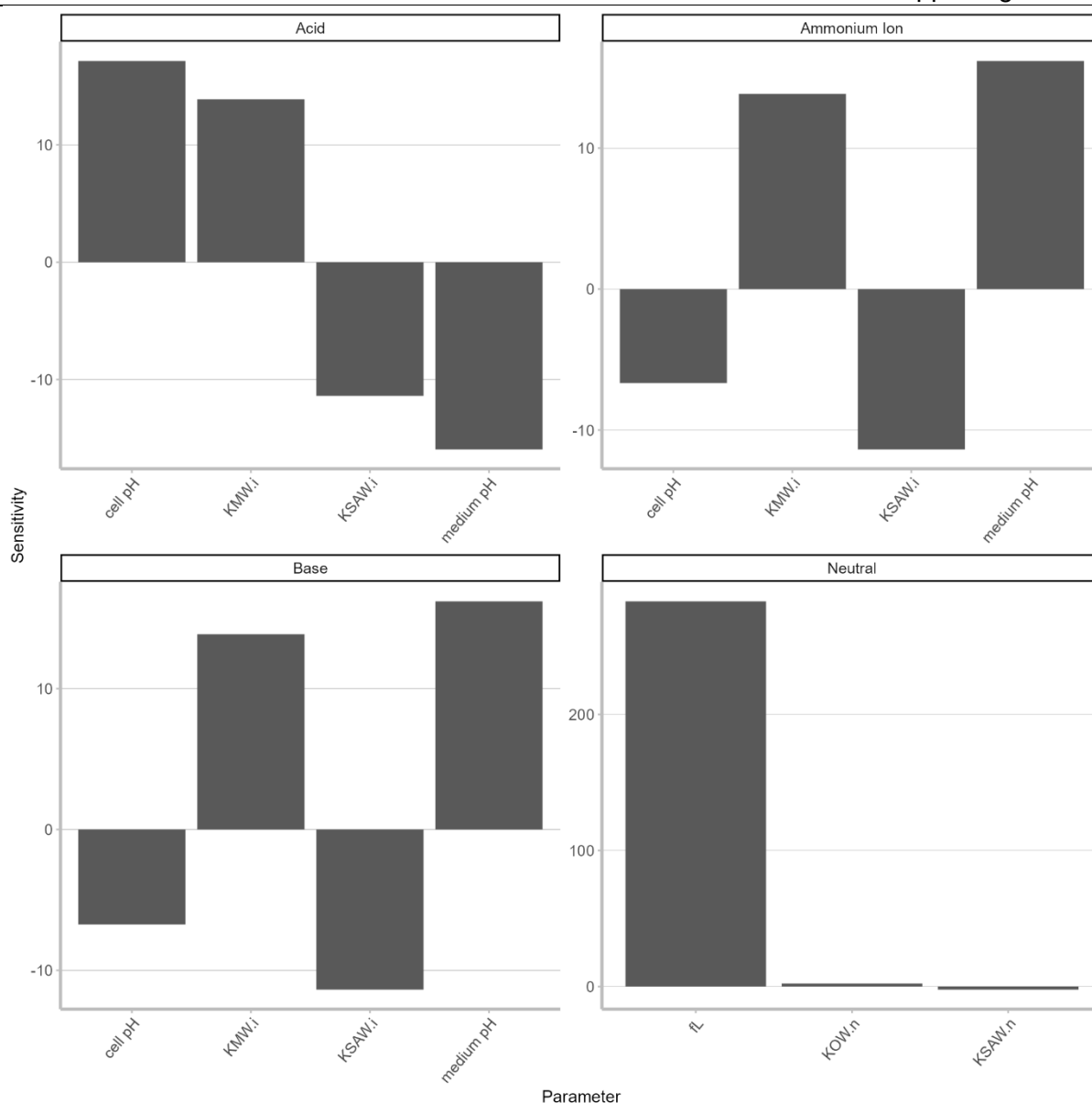


**Figure S4.4: Sensitivity of input parameters of the IV MBM EQP model to predict compound accumulations in the cells.** The ammonium ion stands for the quaternary ammonium ion, for which experimental data (Q14) were available. For the sensitivity analysis, four hypothetical compounds were used, representing mean values of the compound set, for which *in vitro* BCF in RTL-W1 were available. Please note, that only input parameters are shown which have a sensitivity of  $>1$  or  $<-1$ . Parameters were each changed by 0.1 % and the resulting output (predicted *in vitro* BCF) was compared to a default scenario to calculate the sensitivity. The resulting sensitivities on the Y axis have to be read in comparison to each other to understand their importance for the model.  $K_{SAW,i}$  = Serum albumin-water partition coefficient of the charged species

**Table S4.5: Comparison of measured and predicted mass distribution at steady state.** The measured compound mass distribution were taken from the literature <sup>176</sup> or predicted by the IV-MBM EQP model. MF<sub>WAT</sub> is the mass fraction present in the aqueous phase of the exposure medium, also denoted as C<sub>WAT</sub> in Table S4.11, and is part of MF<sub>medium</sub>. MF = Mass fraction (%), n/a = not available

Compound	Measured in experiments with RTL-W1			Predicted by IV-MBM EQP			
	MF medium (%)	MF cell (%)	MF plastic (%)	MF medium (%)	MF C <sub>free</sub> (%)	MF cell (%)	MF plastic (%)
Benzotriazol-tert-butyl-hydroxyl-phenyl propanoic acid	95	4	1	100	1.2	0	0
Diclofenac	100	0.2	0	100	0.5	0	0
N,N,N-trimethyltetradecylamine	<1	96	4	94	0	5.92	0
N,N-dimethyldecylamine	55	34	6	99.3	29.9	0.33	0.4
N-Ethyl-N-(2-hydroxyethyl)perfluorooctylsulphonamide	n/a	n/a	n/a	99.9	0	0.001	0.1
N-Ethylperfluorooctane sulfonamidoacetic acid	n/a	n/a	n/a	100	0	0.0009	0.0
N-Ethylperfluorooctanesulfonamide	n/a	n/a	n/a	69.9	0	0.006	0.3
N-methyldodecylamine	11	85	4	98.4	9.8	1.5	0.1
Perfluorooctanesulfonamide	n/a	n/a	n/a	100	0	0.0002	0
Perfluorooctanesulfonic acid	n/a	n/a	n/a	100	34.6	0.0002	0
Perfluorooctanoic acid	n/a	n/a	n/a	100	6.3	0.0001	0
Pentachlorophenol	100	0.3	0	100	0	0.003	0
Tecloftalam	99	1	0	100	0	0.007	0

**Table S4.6: Comparison of predicted BCF using the *in vitro* mass distribution model IV MDM EQP and measured BCF.** The predicted *in vitro* BCF was derived from the ratio of the cellular concentration over  $C_{free}$ , i.e. " $C_{WAT}$ " Table S4.11<sup>90</sup>. n/a = not available

Compound	predicted log <i>in vitro</i> BCF	log <i>in vitro</i> BCF	log <i>in vivo</i> BCF
Benzotriazol-tert-butyl-hydroxyl-phenyl propanoic acid	1.8	1.4	n/a
Diclofenac	2.5	0.03	0.6
N,N,N-trimethyltetradecylamine	7.7	4.1	1.7
N,N-dimethyldodecylamine	3.6	2.3	2.1
N-Ethyl-N-(2-hydroxyethyl)perfluorooctylsulphonamide	7.7	2.9	n/a
N-Ethylperfluorooctane sulfonamidoacetic acid	6.3	1.8	n/a
N-Ethylperfluorooctanesulfonamide	6.1	2.7	n/a
N-methyldodecylamine	4.8	3.4	2.9
Perfluorooctanesulfonamide	3.5	1.9	2.4
Perfluorooctanesulfonic acid	0.4	1.6	3.2
Perfluorooctanoic acid	0.9	0.8	0.8
Pentachlorophenol	5.4	0.3	2.7
Tecloftalam	7.9	0.7	n/a

#### S4.1 Application of IV MBM EQP in "Model comparison to refine bioconcentration prediction of ionizable organic compounds"

The IV MBM EQP model<sup>90</sup> was applied in one scenario ("PP-LFER"). Scenario "PP-LFER" applied partition coefficients for lipid membrane and serum protein, i.e bovine serum albumin, that were derived by estimation methods (PP-LFER), which are more accurate than the default applied correction terms in the model<sup>257 207 59</sup>. The figures and tables below detail the relevant input data comprising the compound's physicochemical properties (Table S4.7 Input chemical data), test system characteristics (Table S4.8 Input well plate characteristic") and relevant cell and medium constituents (Figure S4.5 Input system parameters). Please note that due to the model design, we could only specify well plate formats. Therefore, we derived the metrics of our test system (cell flask with 25 cm<sup>2</sup> growth area) and adapted it to a well, which would have the same metrics (growth area, headspace volume etc.). The experiments were conducted in commercial Leibovitz's L15 medium, supplemented with 5 % bovine serum albumin, for which the ionic strength was calculated (Table S4.9 Calculation of ionic strength in L15 medium). The results are presented in Table S4.10 and S4.11 and contain the relevant mass fractions and concentrations of the test system at steady state.

**Table S4.7: Input chemical data.** MW = Molecular weight, MP = Melting point (EPI Suite (V1.01)), A = Acid, B = Base, log K<sub>OW</sub> = octanol-water partition coefficient of neutral or ionized form (index “n” or “i”, respectively, estimated using PP-LFER<sup>257</sup>), log K<sub>MW</sub> = membrane lipid-water partition coefficient of neutral or ionized form (index “n” or “i”, respectively), log K<sub>SaW</sub> = Serum albumin-water partition coefficient (index “n” or “i”, respectively, estimated using PP-LFER<sup>59</sup> for neutral species and for ionized species COSMOtherm (version 2022) estimation or correction term -3 subtracted from neutral species<sup>16</sup>), log K<sub>AW,N</sub> = air-water partition coefficient of neutral species (EPI Suite (V1.01)), C<sub>SAT,W,N</sub> = water solubility of neutral species (EPI Suite (V1.01)), EC<sub>x</sub> = Effect concentration in assay

Name	CAS RN	Acronym	MW (g/mol)	MP (°C)	IOC Type	pK <sub>a</sub>	log K <sub>OW,N</sub>	log K <sub>OW,I</sub>	log K <sub>MW,N</sub>	log K <sub>MW,I</sub>	log K <sub>SaW,N</sub>	log K <sub>SaW,I</sub>	log K <sub>AW,N</sub>	C <sub>SAT,W,N</sub> (mg/L)	EC <sub>x</sub> in µM
Benzotriazol-tert-butyl-hydroxyl-phenyl propanoic acid	84268360	BHPP	339.4	224.5	A	4.7	4.1	0.4	4.3	2.3	4.0	4.4	-16.2	212.8	0.025
Diclofenac	15307796	DCF	296.1	174.6	A	4.2	4.5	0.0	4.8	3.1	4.4	4.7	-9.7	10.9	0.7
N,N,N-trimethyltetradecylamine	4574043	Q14	256.5	187.2	B	16.0	9.4	4.7	8.3	7.6	7.3	5.3	-9.4	0.002	0.1
N,N-dimethyldecylamine	1120247	T10	185.35	0.8	B	9.8	5.1	2.5	4.4	3.8	3.8	2.6	-1.7	48.4	2.2
N-Ethyl-N-(2-hydroxyethyl)perfluorooctylsulphonamide	1691992	EtFOSE	571.25	102.1	N	12.5	8.8	5.7	8.0	6.2	6.0	7.6	-1.6	0.0004	0.1
N-Ethylperfluorooctane sulfonamidoacetic acid	2991506	EtFOSA A	585.24	129.0	A	0.1	9.0	-1.6	8.4	6.6	6.3	7.9	-1.1	0.0005	0.10
N-Ethylperfluorooctanesulfonamide	4151502	EtFOSA	527.2	50.5	N	9.5	7.4	4.3	6.6	4.5	4.7	6.6	2.3	0.0002	0.10
N-methyldodecylamine	7311300	S12	199.38	26.5	B	10.8	5.8	2.7	5.0	4.9	4.4	3.3	-1.8	13.6	0.9
Perfluorooctanesulfonamide	754916	FOSA	499.14	42.0	A	3.4	6.5	3.4	6.0	3.9	4.4	6.0	1.9	0.0007	0.1
Perfluorooctanesulfonic acid	1763231	PFOS	500.13	51.9	A	-3.3	4.1	-0.2	3.0	-0.3	3.0	2.7	-0.3	0.05	0.1
Perfluorooctanoic acid	335671	PFOA	414.07	55.0	A	0.3	4.9	-0.6	4.1	1.2	3.9	3.6	0.6	0.002	0.1
Pentachlorophenol	87865	PCP	266.3	106.8	A	4.7	4.7	5.2	5.1	5.9	4.6	6.8	-6.0	45.1	0.02
Tecloftalam	76280916	TT	447.9	246.7	A	1.1	5.4	1.7	5.8	8.4	5.4	8.9	-12.8	0.02	0.1

Table S4.8: Input well plate characteristics.

Unit	mm	mm <sup>2</sup>	μL	μL	μL		mg	ng
Parameter	Well diameter (bottom)	Growth area (bottom)	Total well volume	Typical Working volume	Working volume	Avg. Cell Yield*	Assumed Mass of cells	Single cell weight
Value	56.4	2495	66592.4	2500-6000	3000	3300000	0.008	2.41e-3

TEST SYSTEM PARAMETERS				CELL/BIOLOGICAL/SERUM PARAMETERS			
Test System Type	SER SPECIFIC <--- Scroll over, Click & Select			Proportionality Constants (to octanol)		NOTE:	
System ID	12			Structural Protein	0.035		Denotes USER INPUT
Total well volume	66592.4	uL		DOM*	0.05		Automated or Calculated (do not change)
Bulk Medium	3000	uL		Storage lipid-Octanol	1		
Headspace	63592.4	uL	User-defined	Characteristics of cells/tissues		Serum & DOM Inputs	
Serum albumin	1.86E+00	uL		Storage lipids	0	-	VF <sub>SERUM</sub> 0.050 L/L Typically 2 to 20%
Serum lipids	1.26E-01	uL		Membrane lipids	0.0213	-	C <sub>DOM</sub> 3970.1 mg/l i.e., 0.02 to 0.20
DOM*	1.19E+01	uL		Structural protein (NLOM)	0.09		Density of DOM 1 kg/l
Cells/Tissue	7.95E-03	uL		Density (cells)	1	kg/l	
*DOM = Dissolved organic matter				Mass	0.00795181	mg	
Initial concentration of test chemical				pH	7.4		
Based on user-specified ECx data				Temperature	19	°C	
See Input Chemical Data sheet				Characteristics of Serum			
				Albumin	16.92	g/L	
				Lipids	0.84	g/L	
Initial mass in system				Characteristics of buffer		Quick Check on Cell & Serum lipid volume fraction	
Based on user-specified ECx data				Ionic strength	1.909	M	2.7E-06 L cell per L medium
See Input Chemical Data sheet				pH	7		5.6E-08 L cell lipid per L medium
See Well Plate Characteristics for more details				Option for sorption to vessel wall		4.2E-05 L serum lipid per L medium	
Please make modifications to test system parameters there				Include bottom of well?	FALSCH		6.2E-04 L serum albumin per L medium
				(or assume covered by cells and not accessible)			
				Ignore sorption to plastic	FALSCH		

Figure S4.5: Input system parameters. NLOM= non lipid organic matter, VF<sub>SERUM</sub> = volume fraction of supplemented serum, i.e. fetal bovine serum.

Calculation of ionic strength  $I$  followed Equation S4.1, where  $C_i$  is the concentration of compound  $i$ ,  $x_i$  is the number of atoms of compound  $i$  and  $z_i$  is the charge of adduct in compound  $i$ :

$$\text{Equation S4.1} \quad I = 0.5 \sum_{i=1}^n c_i x_i z_i^2$$

**Table S4.9: Calculation ionic strength in L15 medium.** Medium composition taken from supplier (Thermo Fisher Scientific Inc., CH).

Compound	g/mol	$C_i$ (mg/L)	$C_i$ (Mol/L)	$z_i +$	$z_i -$	$I$ (Mol/L i.e. M)
Choline chloride	140	1	7.143E-05	1	1	7.143E-05
D Calcium pantothenate	477	1	2.096E-05	2	2	6.289E-05
Folic acid	441	1	2.268E-05	0	2	2.268E-05
Pyridoxine Hydrochloride	206	1	4.854E-05	0	1	2.427E-05
Riboflavin 5'- phosphate Na	478	0.1	2.092E-06	1	1	2.092E-06
Thiamine monophosphate	442	1	2.262E-05	1	2	3.394E-05
Calcium chloride (CaCl <sub>2</sub> )	111	140	0.0126126	2	2	0.0378378
Magnesium chloride	95	93.7	0.0098632	2	2	0.0394526
Magnesium sulfate (MgSO <sub>4</sub> )	120	97.67	0.0081392	2	2	0.0325567
Potassium chloride (KCl)	75	400	0.0533333	1	1	0.0533333
Potassium Phosphate monobasic (KH <sub>2</sub> PO <sub>4</sub> )	136	60	0.0044118	1	1	0.0044118
Sodium chloride (NaCl)	58	8000	1.3793103	1	1	1.3793103
Sodium Phosphate dibasic (Na <sub>2</sub> HPO <sub>4</sub> )	142	190	0.0133803	2	2	0.0267606
Sodium pyruvate	110	550	0.05	1	1	0.05

Compound	g/mol	C <sub>i</sub> (mg/L)	C <sub>i</sub> (Mol/L)	z <sub>i</sub> +	Z <sub>i</sub> -	I (Mol/L i.e. M)
Glycine	75	200	0.0266667	1	1	0.0266667
Alanine	89	225	0.0252809	1	1	0.0252809
Arginine	174	500	0.0287356	2	1	0.0431034
Asparagine	132	250	0.0189394	1	1	0.0189394
Cysteine	121	120	0.0099174	1	2	0.014876
Glutamine	146	300	0.0205479	1	1	0.0205479
Histidine	155	250	0.016129	1	1	0.016129
Isoleucin	131	250	0.019084	1	1	0.019084
Leucine	131	125	0.009542	1	1	0.009542
Lysine	146	75	0.005137	2	1	0.0077055
Methionine	149	75	0.0050336	1	1	0.0050336
Phenylalanine	165	125	0.0075758	1	1	0.0075758
Serine	105	200	0.0190476	1	1	0.0190476
Threonine	119	300	0.0252101	1	1	0.0252101
Tryptophan	204	20	0.0009804	1	1	0.0009804
Tyrosine	181	300	0.0165746	1	1	0.0165746
Valine	117	100	0.008547	1	1	0.008547



**Table S4.10: Model output of mass fractions in the test system.** Mass fractions (MF) are presented in air, bulk water (incl. all medium constituents), albumin (ALB), storage lipid (S-Lip), dissolved organic matter (DOM), the pure water phase in the medium (WAT), in cells and plastic.

Name	Acronym	MF <sub>AIR</sub>	MF <sub>BULK WAT</sub>	MF <sub>ALB</sub>	MF <sub>S-LIP</sub>	MF <sub>DOM</sub>	MF <sub>WAT</sub>	MF <sub>Cells</sub>	MF <sub>Plastic</sub>
Benzotriazol-tert-butyl-hydroxyl-phenyl	BHPP	0.0%	100.0%	98.7%	0.0%	0.1%	1.2%	0.000%	0.0%
Diclofenac	DCF	0.0%	100.0%	99.5%	0.0%	0.0%	0.5%	0.000%	0.0%
N,N,N-trimethyl-1-tetradecylammonium	Q14	0.0%	94.0%	72.9%	16.3%	4.8%	0.0%	5.917%	0.0%
N,N-dimethyldodecylamine	T10	0.0%	99.3%	51.7%	1.6%	16.0%	29.9%	0.328%	0.4%
N-Ethyl-N-(2-	EtFOSE	0.0%	99.9%	0.6%	17.3%	81.9%	0.0%	0.0097%	0.1%
N-Ethylperfluorooctane	EtFOSAA	0.0%	100.0%	100.0%	0.0%	0.0%	0.0%	0.0009%	0.0%
N-Ethylperfluorooctanesulfonamide	EtFOSA	29.9%	69.9%	0.5%	12.1%	57.3%	0.0%	0.0059%	0.3%
N-methyldodecylamine	S12	0.0%	98.4%	81.3%	0.7%	6.6%	9.8%	1.4725%	0.1%
Perfluorooctanesulfonamide	FOSA	0.0%	100.0%	99.9%	0.0%	0.1%	0.0%	0.0002%	0.0%
Perfluorooctanesulfonic acid	PFOS	0.0%	100.0%	65.3%	0.0%	0.0%	34.6%	0.0002%	0.0%
Perfluorooctanoic acid	PFOA	0.0%	100.0%	93.6%	0.0%	0.0%	6.3%	0.0001%	0.0%
Pentachlorophenol	PCP	0.0%	100.0%	99.4%	0.0%	0.6%	0.0%	0.0029%	0.0%
Tecloftalam	TT	0.0%	100.0%	100.0%	0.0%	0.0%	0.0%	0.0073%	0.0%

**Table S4.11: Model output of concentrations in the test system.** Concentrations are presented for the initial nominal exposure concentration at 0 h ( $C_{\text{NOM}}$ ), the bulk exposure medium at steady state ( $C_{\text{BULK WAT}}$ ), the pure water phase in the medium ( $C_{\text{WAT}}$ ), in the air ( $C_{\text{AIR}}$ ), in the albumin in the medium ( $C_{\text{ALB}}$ ), in the storage lipid of the medium ( $C_{\text{S-LIP}}$ ), in the dissolved organic matter of the medium ( $C_{\text{DOM}}$ ) and the exposed cells ( $C_{\text{cells}}$ ). From the medium and cell concentrations, the *in vitro* BCF was calculated based on either  $C_{\text{WAT}}$  or  $C_{\text{BULK WAT}}$ .

Name	Acronym	$C_{\text{NOM,initial}}$ ( $\mu\text{mol/L}$ medium)	$C_{\text{BULK WAT}}$ ( $\mu\text{mol/L}$ medium)	$C_{\text{WAT}}$ ( $\mu\text{mol/L}$ water)	$C_{\text{AIR}}$ ( $\mu\text{mol/L}$ air)	$C_{\text{ALB}}$ ( $\mu\text{mol/L}$ alb)	$C_{\text{S-LIP}}$ ( $\mu\text{mol/L}$ lipid)	$C_{\text{DOM}}$ ( $\mu\text{mol/L}$ DOM)	$C_{\text{cells}}$ ( $\mu\text{mol/L}$ cell)	<i>in vitro</i> BCF ( $C_{\text{WAT}}$ )	<i>in vitro</i> BCF ( $C_{\text{BULK WAT}}$ )
Benzotriazol-tert-butyl-hydroxyl-phenyl propanoic acid	BHPP	2.5E-02	2.5E-02	3.0E-04	1.8E-28	3.9E+01	8.0E-02	3.9E-03	1.9E-02	6.22E+01	7.52E-01
Diclofenac	DCF	6.7E-01	6.7E-01	3.4E-03	2.1E-21	1.1E+03	9.0E-01	3.7E-02	1.2E+00	3.50E+02	1.80E+00
N,N,N-trimethyl-1-tetradecylammonium	Q14	8.5E-02	8.0E-02	4.0E-05	9.1E-29	1.0E+02	3.3E+02	1.0E+00	1.9E+03	4.71E+07	2.37E+04
N,N-dimethyldecylamine	T10	2.2E+00	2.2E+00	6.6E-01	5.1E-11	1.8E+03	8.7E+02	8.9E+01	2.7E+03	4.12E+03	1.25E+03
N-Ethyl-N-(2-hydroxyethyl)perfluorooctylsulphonamide	EtFOSE	1.0E-01	1.0E-01	8.1E-08	8.8E-15	9.9E-01	4.1E+02	2.1E+01	3.7E+00	4.56E+07	3.68E+01
N-Ethylperfluorooctane sulfonamidoacetic acid	EtFOSAA	1.0E-01	1.0E-01	1.7E-07	6.8E-21	1.6E+02	5.4E-01	1.0E-05	3.6E-01	2.15E+06	3.58E+00
N-Ethylperfluorooctanesulfonamide	EtFOSA	1.0E-01	7.0E-02	1.7E-06	1.4E-09	7.6E-01	2.9E+02	1.4E+01	2.2E+00	1.27E+06	3.17E+01
N-methyldodecylamine	S12	9.3E-01	9.1E-01	9.1E-02	6.5E-13	1.2E+03	1.6E+02	1.6E+01	5.2E+03	5.64E+04	5.64E+03
Perfluorooctanesulfonamide	FOSA	1.0E-01	1.0E-01	1.8E-05	1.0E-12	1.6E+02	2.1E-01	1.9E-02	6.2E-02	3.42E+03	6.21E-01
Perfluorooctanesulfonic acid	PFOS	1.0E-01	1.0E-01	3.5E-02	1.6E-18	1.1E+02	6.1E-01	4.7E-03	8.6E-02	2.48E+00	8.63E-01
Perfluorooctanoic acid	PFOA	1.0E-01	1.0E-01	6.4E-03	1.1E-14	1.5E+02	7.7E-01	4.2E-04	4.8E-02	7.46E+00	4.75E-01
Pentachlorophenol	PCP	1.7E-02	1.7E-02	7.8E-07	8.5E-21	2.7E+01	8.4E-04	2.6E-02	1.9E-01	2.39E+05	1.09E+01
Tecloftalam	TT	5.7E-02	5.7E-02	1.9E-08	9.5E-33	9.1E+01	7.6E-06	2.2E-07	1.6E+00	8.35E+07	2.74E+01

---

## Bibliography

1. Fent, K., 7 Bioakkumulation, in Ökotoxikologie. 2013, Georg Thieme Verlag KG: Stuttgart.
2. American Chemical Society, CAS Registry. 2023, American Chemical Society: Columbus, Ohio.
3. International Council of Chemical Associations UNEP. Debunking the Myths: Are There More than 100,000 Chemicals in Commerce? . 2020 [13.08.2023]; Available from: [https://icca-chem.org/wpcontent/uploads/2020/05/ICCA\\_DataAvailabilityStudy\\_Infographic.pdf](https://icca-chem.org/wpcontent/uploads/2020/05/ICCA_DataAvailabilityStudy_Infographic.pdf).
4. Fent, K., 1.2 Chemikalien in der Umwelt, in Ökotoxikologie. 2013, Georg Thieme Verlag KG: Stuttgart. p. 5-17.
5. Woodwell, G.M., C.F. Wurster, P.A. Isaacson, DDT Residues in an East Coast Estuary: A Case of Biological Concentration of a Persistent Insecticide. *Science*, 1967. 156(3776): p. 821-824.
6. EU, Regulation (EC) No 1907/2006 of the European Parliament and of the Council of 18 December 2006 concerning the Registration, Evaluation, Authorisation and Restriction of Chemicals (REACH). OJ European Union L396. 2006. p. 1-849.
7. ECHA, Guidance on Information Requirements and Chemical Safety Assessment Chapter R.11: PBT/vPvB Assessment, E.C. Agency, Editor. 2017, European Chemicals Agency: Helsinki Finland.
8. Gobas, F.A.P.C., W. de Wolf, L.P. Burkhard, E. Verbruggen, K. Plotzke, Revisiting Bioaccumulation Criteria for POPs and PBT Assessments. *Integrated Environmental Assessment and Management*, 2009. 5(4): p. 624-637.
9. OECD, Test No. 305: Bioaccumulation in Fish: Aqueous and Dietary Exposure, in OECD Guidelines for the Testing of Chemicals, Section 3. 2012, OECD Publishing: Paris.
10. Scholz, S., E. Sela, L. Blaha, T. Braunbeck, M. Galay-Burgos, M. García-Franco, J. Guinea, N. Klüver, K. Schirmer, K. Tanneberger, M. Tobor-Kapłon, H. Witters, S. Belanger, E. Benfenati, S. Creton, M.T.D. Cronin, R.I.L. Eggen, M. Embry, D. Ekman, A. Gourmelon, M. Halder, B. Hardy, T. Hartung, B. Hubesch, D. Jungmann, M.A. Lampi, L. Lee, M. Léonard, E. Küster, A. Lillicrap, T. Luckenbach, A.J. Murk, J.M. Navas, W. Peijnenburg, G. Repetto, E. Salinas, G. Schüürmann, H. Spielmann, K.E. Tollefsen, S. Walter-Rohde, G. Whale, J.R. Wheeler, M.J. Winter, A European perspective on alternatives to animal testing for environmental hazard identification and risk assessment. *Regulatory Toxicology and Pharmacology*, 2013. 67(3): p. 506-530.
11. Nichols, J.W., J.M. McKim, M.E. Andersen, M.L. Gargas, H.J. Clewell, R.J. Erickson, A physiologically based toxicokinetic model for the uptake and disposition of waterborne organic chemicals in fish. *Toxicology and Applied Pharmacology*, 1990. 106(3): p. 433-447.
12. Wang, Z., G.W. Walker, D.C.G. Muir, K. Nagatani-Yoshida, Toward a Global Understanding of Chemical Pollution: A First Comprehensive Analysis of National and Regional Chemical Inventories. *Environmental Science & Technology*, 2020. 54(5): p. 2575-2584.

13. Meylan, W.M., P.H. Howard, R.S. Boethling, D. Aronson, H. Printup, S. Gouchie, Improved method for estimating bioconcentration/bioaccumulation factor from octanol/water partition coefficient. *Environmental Toxicology and Chemistry*, 1999. 18(4): p. 664-672.
14. Fu, W., A. Franco, S. Trapp, Methods for estimating the bioconcentration factor of ionizable organic chemicals. *Environmental Toxicology and Chemistry*, 2009. 28(7): p. 1372-1379.
15. Bittner, L., N. Klüver, L. Henneberger, M. Mühlenbrink, C. Zarfl, B.I. Escher, Combined Ion-Trapping and Mass Balance Models To Describe the pH-Dependent Uptake and Toxicity of Acidic and Basic Pharmaceuticals in Zebrafish Embryos (*Danio rerio*). *Environmental Science & Technology*, 2019. 53(13): p. 7877-7886.
16. Armitage, J.M., J.A. Arnot, F. Wania, D. Mackay, Development and evaluation of a mechanistic bioconcentration model for ionogenic organic chemicals in fish. *Environmental Toxicology and Chemistry*, 2013. 32(1): p. 115-128.
17. Goss, K.-U., K. Bittermann, L. Henneberger, L. Linden, Equilibrium biopartitioning of organic anions – A case study for humans and fish. *Chemosphere*, 2018. 199: p. 174-181.
18. Nichols, J.W., D.B. Huggett, J.A. Arnot, P.N. Fitzsimmons, C.E. Cowan-Ellsberry, Toward improved models for predicting bioconcentration of well-metabolized compounds by rainbow trout using measured rates of in vitro intrinsic clearance. *Environmental Toxicology and Chemistry*, 2013. 32(7): p. 1611-1622.
19. Mackay, D., Applications of Fugacity Models, in *Multimedia Environmental Models: The Fugacity Approach*. 2001, CRC Press.
20. Treu, G., W. Drost, U. Jöhncke, C. Rauert, C. Schlechtriem, The Dessau workshop on bioaccumulation: state of the art, challenges and regulatory implications. *Environmental Sciences Europe*, 2015. 27(1): p. 34.
21. Henneberger, L., K.-U. Goss, Environmental Sorption Behavior of Ionic and Ionizable Organic Chemicals, in *Reviews of Environmental Contamination and Toxicology Volume 253*, P. de Voogt, Editor. 2021, Springer International Publishing: Cham. p. 43-64.
22. Arnot, J.A., F.A.P.C. Gobas, A Generic QSAR for Assessing the Bioaccumulation Potential of Organic Chemicals in Aquatic Food Webs. *QSAR & Combinatorial Science*, 2003. 22(3): p. 337-345.
23. OECD, Test No. 319A: Determination of in vitro intrinsic clearance using cryopreserved rainbow trout hepatocytes (RT-HEP), in *OECD Guidelines for the Testing of Chemicals, Section 3 2018a*, OECD Publishing: Paris.
24. OECD, Test No. 319B: Determination of in vitro intrinsic clearance using rainbow trout liver S9 sub-cellular fraction (RT-S9), in *OECD Guidelines for the Testing of Chemicals, Section 3 2018b*, OECD Publishing: Paris.
25. Droge, S.T.J., J.M. Armitage, J.A. Arnot, P.N. Fitzsimmons, J.W. Nichols, Biotransformation Potential of Cationic Surfactants in Fish Assessed with Rainbow Trout Liver S9 Fractions. *Environmental Toxicology and Chemistry*, 2021. 40(11): p. 3123-3136.
26. Ribbenstedt, A., J.M. Armitage, F. Günther, J.A. Arnot, S.T.J. Droge, M.S. McLachlan, In Vivo Bioconcentration of 10 Anionic Surfactants in Rainbow Trout Explained by In

- Vitro Data on Partitioning and S9 Clearance. *Environmental Science & Technology*, 2022. 56(10): p. 6305-6314.
27. Han, X., D.L. Nabb, C.-H. Yang, S.I. Snajdr, R.T. Mingoia, Liver microsomes and S9 from rainbow trout (*Oncorhynchus mykiss*): Comparison of basal-level enzyme activities with rat and determination of xenobiotic intrinsic clearance in support of bioaccumulation assessment. *Environmental Toxicology and Chemistry*, 2009. 28(3): p. 481-488.
  28. Nichols, J., K. Fay, M.J. Bernhard, I. Bischof, J. Davis, M. Halder, J. Hu, K. Johanning, H. Laue, D. Nabb, C. Schlechtriem, H. Segner, J. Swintek, J. Weeks, M. Embry, Reliability of In Vitro Methods Used to Measure Intrinsic Clearance of Hydrophobic Organic Chemicals by Rainbow Trout: Results of an International Ring Trial. *Toxicological Sciences*, 2018. 164(2): p. 563-575.
  29. Lee, L.E.J., J.H. Clemons, D.G. Bechtel, S.J. Caldwell, K.-B. Han, M. Pasitschniak-Arts, D.D. Mosser, N.C. Bols, Development and characterization of a rainbow trout liver cell line expressing cytochrome P450-dependent monooxygenase activity. *Cell Biology and Toxicology*, 1993. 9(3): p. 279-294.
  30. Bols, N.C., A. Barlian, M. Chirino-Trejo, S.J. Caldwell, P. Goegan, L.E.J. Lee, Development of a cell line from primary cultures of rainbow trout, *Oncorhynchus mykiss* (Walbaum), gills. *Journal of Fish Diseases*, 1994. 17(6): p. 601-611.
  31. Kawano, A., C. Haiduk, K. Schirmer, R. Hanner, L.E.J. Lee, B. Dixon, N.C. Bols, Development of a rainbow trout intestinal epithelial cell line and its response to lipopolysaccharide. *Aquaculture Nutrition*, 2011. 17(2): p. e241-e252.
  32. Fischer, S., J. Loncar, R. Zaja, S. Schnell, K. Schirmer, T. Smital, T. Luckenbach, Constitutive mRNA expression and protein activity levels of nine ABC efflux transporters in seven permanent cell lines derived from different tissues of rainbow trout (*Oncorhynchus mykiss*). *Aquatic Toxicology*, 2011. 101(2): p. 438-446.
  33. Nehls, S., H. Segner, Detection of DNA damage in two cell lines from rainbow trout, RTG-2 and RTL-W1, using the comet assay. *Environmental Toxicology*, 2001. 16(4): p. 321-329.
  34. Thibaut, R., S. Schnell, C. Porte, Assessment of metabolic capabilities of PLHC-1 and RTL-W1 fish liver cell lines. *Cell Biology and Toxicology*, 2009. 25(6): p. 611-622.
  35. Stadnicka-Michalak, J., F.T. Weiss, M. Fischer, K. Tanneberger, K. Schirmer, Biotransformation of Benzo[a]pyrene by Three Rainbow Trout (*Onchorhynchus mykiss*) Cell Lines and Extrapolation To Derive a Fish Bioconcentration Factor. *Environmental Science & Technology*, 2018b. 52(5): p. 3091-3100.
  36. Geppert, M., L. Sigg, K. Schirmer, A novel two-compartment barrier model for investigating nanoparticle transport in fish intestinal epithelial cells. *Environmental Science: Nano*, 2016. 3(2): p. 388-395.
  37. Minghetti, M., C. Drieschner, N. Bramaz, H. Schug, K. Schirmer, A fish intestinal epithelial barrier model established from the rainbow trout (*Oncorhynchus mykiss*) cell line, RTgutGC. *Cell Biology and Toxicology*, 2017. 33(6): p. 539-555.
  38. Schug, H., F. Begnaud, C. Debonneville, F. Berthaud, S. Gimeno, K. Schirmer, TransFER: a new device to measure the transfer of volatile and hydrophobic organic chemicals across an in vitro intestinal fish cell barrier. *Analytical Methods*, 2018. 10(36): p. 4394-4403.

39. Schug, H., J. Maner, F. Begnaud, F. Berthaud, S. Gimeno, K. Schirmer, A. Županič, Intestinal Fish Cell Barrier Model to Assess Transfer of Organic Chemicals in Vitro: An Experimental and Computational Study. *Environmental Science & Technology*, 2019. 53(20): p. 12062-12070.
40. Tanneberger, K., M. Knöbel, F.J.M. Busser, T.L. Sinnige, J.L.M. Hermens, K. Schirmer, Predicting Fish Acute Toxicity Using a Fish Gill Cell Line-Based Toxicity Assay. *Environmental Science & Technology*, 2013. 47(2): p. 1110-1119.
41. Stadnicka-Michalak, J., K. Tanneberger, K. Schirmer, R. Ashauer, Measured and Modeled Toxicokinetics in Cultured Fish Cells and Application to In Vitro - In Vivo Toxicity Extrapolation. *PLOS ONE*, 2014. 9(3): p. e92303.
42. Fischer, M., S.E. Belanger, P. Berckmans, M.J. Bernhard, L. Bláha, D.E. Coman Schmid, S.D. Dyer, T. Haupt, J.L.M. Hermens, M.T. Hultman, H. Laue, A. Lillicrap, M. Mlnářiková, A. Natsch, J. Novák, T.L. Sinnige, K.E. Tollefsen, V. von Niederhäusern, H. Witters, A. Županič, K. Schirmer, Repeatability and Reproducibility of the RTgill-W1 Cell Line Assay for Predicting Fish Acute Toxicity. *Toxicological Sciences*, 2019. 169(2): p. 353-364.
43. OECD, Test No. 249: Fish Cell Line Acute Toxicity - The RTgill-W1 cell line assay. OECD Guidelines for the Testing of Chemicals, Section 3 2021, Paris: OECD Publishing.
44. OECD, Test No. 203: Fish, Acute Toxicity Test. OECD Guidelines for the Testing of Chemicals, Section 2. 2019, Paris: OECD Publishing.
45. Stadnicka-Michalak, J., M. Knöbel, A. Županič, K. Schirmer, A validated algorithm for selecting non-toxic chemical concentrations. *ALTEX - Alternatives to animal experimentation*, 2018a. 35(1): p. 37-50.
46. Armitage, J.M., R.J. Erickson, T. Luckenbach, C.A. Ng, R.S. Prosser, J.A. Arnot, K. Schirmer, J.W. Nichols, Assessing the bioaccumulation potential of ionizable organic compounds: Current knowledge and research priorities. *Environmental Toxicology and Chemistry*, 2017. 36(4): p. 882-897.
47. Carter, L.J., J.M. Armitage, B.W. Brooks, J.W. Nichols, S. Trapp, Predicting the Accumulation of Ionizable Pharmaceuticals and Personal Care Products in Aquatic and Terrestrial Organisms. *Environmental Toxicology and Chemistry*, 2022. n/a(n/a).
48. Franco, A., A. Ferranti, C. Davidsen, S. Trapp, An unexpected challenge: ionizable compounds in the REACH chemical space. *The International Journal of Life Cycle Assessment*, 2010. 15(4): p. 321-325.
49. Manallack, D.T., The acid–base profile of a contemporary set of drugs: implications for drug discovery. *SAR and QSAR in Environmental Research*, 2009. 20(7-8): p. 611-655.
50. ChemsSketch, version 2021.1.2, Advanced Chemsitry Development, Inc. (ACD/Labs). 2021, Toronto, ON, Canada, [www.acdlabs.com](http://www.acdlabs.com).
51. UNESCO. Water in a changing world. The United Nations World Water Development Report 3: Water in a Changing World 2009 [18.10.2022]; Available from: <https://unesdoc.unesco.org/ark:/48223/pf0000181993/PDF/181993eng.pdf.multi>.
52. Sánchez-Bayo, F., K.A.G. Wyckhuys, Worldwide decline of the entomofauna: A review of its drivers. *Biological Conservation*, 2019. 232: p. 8-27.
53. Trombini, C., J. Blasco, M. Hampel, Ibuprofen and Diclofenac: Effects on Freshwater and Marine Aquatic Organisms – Are They at Risk?, in *Non-Steroidal Anti-Inflammatory*

- Drugs in Water: Emerging Contaminants and Ecological Impact, L.M. Gómez-Oliván, Editor. 2020, Springer International Publishing: Cham. p. 161-189.
54. Schmitt, W., General approach for the calculation of tissue to plasma partition coefficients. *Toxicology in Vitro*, 2008. 22(2): p. 457-467.
  55. Jafvert, C.T., J.C. Westall, E. Grieder, R.P. Schwarzenbach, Distribution of hydrophobic ionogenic organic compounds between octanol and water: organic acids. *Environmental science & technology*, 1990. 24(12): p. 1795-1803.
  56. Johnson, C.A., J.C. Westall, Effect of pH and potassium chloride concentration on the octanol-water distribution of methylanilines. *Environmental Science & Technology*, 1990. 24(12): p. 1869-1875.
  57. Escher, B.I., R.P. Schwarzenbach, Partitioning of Substituted Phenols in Liposome–Water, Biomembrane–Water, and Octanol–Water Systems. *Environmental Science & Technology*, 1996. 30(1): p. 260-270.
  58. Trainor, G.L., The importance of plasma protein binding in drug discovery. *Expert Opinion on Drug Discovery*, 2007. 2(1): p. 51-64.
  59. Henneberger, L., K.-U. Goss, S. Endo, Equilibrium Sorption of Structurally Diverse Organic Ions to Bovine Serum Albumin. *Environmental Science & Technology*, 2016a. 50(10): p. 5119-5126.
  60. Henneberger, L., K.-U. Goss, S. Endo, Partitioning of Organic Ions to Muscle Protein: Experimental Data, Modeling, and Implications for in Vivo Distribution of Organic Ions. *Environmental Science & Technology*, 2016b. 50(13): p. 7029-7036.
  61. Avdeef, A., K.J. Box, J.E.A. Comer, C. Hibbert, K.Y. Tam, pH-Metric logP 10. Determination of Liposomal Membrane–Water Partition Coefficients of Ionizable Drugs. *Pharmaceutical Research*, 1998. 15(2): p. 209-215.
  62. Escher, B.I., M. Berg, J. Mühlemann, M.A.A. Schwarz, J.L.M. Hermens, W.H.J. Vaes, R.P. Schwarzenbach, Determination of liposome/water partition coefficients of organic acids and bases by solid-phase microextraction. *Analyst*, 2002. 127(1): p. 42-48.
  63. Timmer, N., S.T.J. Droge, Sorption of Cationic Surfactants to Artificial Cell Membranes: Comparing Phospholipid Bilayers with Monolayer Coatings and Molecular Simulations. *Environmental Science & Technology*, 2017. 51(5): p. 2890-2898.
  64. Droge, S.T.J., Membrane–Water Partition Coefficients to Aid Risk Assessment of Perfluoroalkyl Anions and Alkyl Sulfates. *Environmental Science & Technology*, 2019. 53(2): p. 760-770.
  65. Droge, S.T.J., P. Scherpenisse, J.A. Arnot, J.M. Armitage, M.S. McLachlan, P.C. von der Ohe, G. Hodges, Screening the baseline fish bioconcentration factor of various types of surfactants using phospholipid binding data. *Environmental Science: Processes & Impacts*, 2021. 23(12): p. 1930-1948.
  66. Bittermann, K., S. Spycher, S. Endo, L. Pohler, U. Huniar, K.-U. Goss, A. Klamt, Prediction of Phospholipid–Water Partition Coefficients of Ionic Organic Chemicals Using the Mechanistic Model COSMOmic. *The Journal of Physical Chemistry B*, 2014. 118(51): p. 14833-14842.
  67. Luebker, D.J., K.J. Hansen, N.M. Bass, J.L. Butenhoff, A.M. Seacat, Interactions of fluorochemicals with rat liver fatty acid-binding protein. *Toxicology*, 2002. 176(3): p. 175-185.

68. Ghuman, J., P.A. Zunszain, I. Petitpas, A.A. Bhattacharya, M. Otagiri, S. Curry, Structural Basis of the Drug-binding Specificity of Human Serum Albumin. *Journal of Molecular Biology*, 2005. 353(1): p. 38-52.
69. Balaz, S., Modeling Kinetics of Subcellular Disposition of Chemicals. *Chemical Reviews*, 2009. 109(5): p. 1793-1899.
70. Zhang, L., X.-M. Ren, L.-H. Guo, Structure-Based Investigation on the Interaction of Perfluorinated Compounds with Human Liver Fatty Acid Binding Protein. *Environmental Science & Technology*, 2013. 47(19): p. 11293-11301.
71. Han, X., T.A. Snow, R.A. Kemper, G.W. Jepson, Binding of Perfluorooctanoic Acid to Rat and Human Plasma Proteins. *Chemical Research in Toxicology*, 2003. 16(6): p. 775-781.
72. Proença, S., B.I. Escher, F.C. Fischer, C. Fisher, S. Grégoire, N.J. Hewitt, B. Nicol, A. Paini, N.I. Kramer, Effective exposure of chemicals in in vitro cell systems: A review of chemical distribution models. *Toxicology in Vitro*, 2021. 73: p. 105133.
73. Endo, S., Applicability Domain of Polyparameter Linear Free Energy Relationship Models Evaluated by Leverage and Prediction Interval Calculation. *Environmental Science & Technology*, 2022. 56(9): p. 5572-5579.
74. Kierkegaard, A., C. Chen, J.M. Armitage, J.A. Arnot, S. Droge, M.S. McLachlan, Tissue Distribution of Several Series of Cationic Surfactants in Rainbow Trout (*Oncorhynchus mykiss*) Following Exposure via Water. *Environmental Science & Technology*, 2020. 54(7): p. 4190-4199.
75. Leslie, E.M., R.G. Deeley, S.P.C. Cole, Multidrug resistance proteins: role of P-glycoprotein, MRP1, MRP2, and BCRP (ABCG2) in tissue defense. *Toxicology and Applied Pharmacology*, 2005. 204(3): p. 216-237.
76. Deeley, R.G., C. Westlake, S.P.C. Cole, Transmembrane Transport of Endo- and Xenobiotics by Mammalian ATP-Binding Cassette Multidrug Resistance Proteins. *Physiological Reviews*, 2006. 86(3): p. 849-899.
77. Roth, M., A. Obaidat, B. Hagenbuch, OATPs, OATs and OCTs: the organic anion and cation transporters of the SLCO and SLC22A gene superfamilies. *British Journal of Pharmacology*, 2012. 165(5): p. 1260-1287.
78. Luckenbach, T., S. Fischer, A. Sturm, Current advances on ABC drug transporters in fish. *Comparative Biochemistry and Physiology Part C: Toxicology & Pharmacology*, 2014. 165: p. 28-52.
79. McLachlan, M.S., A. Ebert, J.M. Armitage, J.A. Arnot, S.T.J. Droge, A framework for understanding the bioconcentration of surfactants in fish. *Environmental Science: Processes & Impacts*, 2023. 25(7): p. 1238-1251.
80. Heringa, M.B., R.H.M.M. Schreurs, F. Busser, P.T. Van Der Saag, B. Van Der Burg, J.L.M. Hermens, Toward More Useful In Vitro Toxicity Data with Measured Free Concentrations. *Environmental Science & Technology*, 2004. 38(23): p. 6263-6270.
81. Chen, Y., M. Geurts, S.B. Sjollema, N.I. Kramer, J.L.M. Hermens, S.T.J. Droge, Acute toxicity of the cationic surfactant C12-benzalkonium in different bioassays: How test design affects bioavailability and effect concentrations. *Environmental Toxicology and Chemistry*, 2014. 33(3): p. 606-615.
82. Krause, S., N. Ulrich, K.-U. Goss, Desorption kinetics of organic chemicals from albumin. *Archives of Toxicology*, 2018. 92(3): p. 1065-1074.



83. Fischer, F.C., L. Henneberger, R. Schlichting, B.I. Escher, How To Improve the Dosing of Chemicals in High-Throughput in Vitro Mammalian Cell Assays. *Chemical Research in Toxicology*, 2019. 32(8): p. 1462-1468.
84. Price, P.J., E.A. Gregory, Relationship between in vitro growth promotion and biophysical and biochemical properties of the serum supplement. *In Vitro*, 1982. 18(6): p. 576-584.
85. Colmenarejo, G., In silico prediction of drug-binding strengths to human serum albumin. *Medicinal Research Reviews*, 2003. 23(3): p. 275-301.
86. Bischel, H.N., L.A. MacManus-Spencer, C. Zhang, R.G. Luthy, Strong associations of short-chain perfluoroalkyl acids with serum albumin and investigation of binding mechanisms. *Environmental Toxicology and Chemistry*, 2011. 30(11): p. 2423-2430.
87. Endo, S., J. Bauerfeind, K.-U. Goss, Partitioning of Neutral Organic Compounds to Structural Proteins. *Environmental Science & Technology*, 2012. 46(22): p. 12697-12703.
88. van der Heijden, S.A., J.L.M. Hermens, T.L. Sinnige, P. Mayer, D. Gilbert, M.T.O. Jonker, Determining High-Quality Critical Body Residues for Multiple Species and Chemicals by Applying Improved Experimental Design and Data Interpretation Concepts. *Environmental Science & Technology*, 2015. 49(3): p. 1879-1887.
89. Fischer, F.C., L. Henneberger, M. König, K. Bittermann, L. Linden, K.-U. Goss, B.I. Escher, Modeling Exposure in the Tox21 in Vitro Bioassays. *Chemical Research in Toxicology*, 2017. 30(5): p. 1197-1208.
90. Armitage, J.M., A. Sangion, R. Parmar, A.B. Looky, J.A. Arnot Update and Evaluation of a High-Throughput In Vitro Mass Balance Distribution Model: IV-MBM EQP v2.0. *Toxics*, 2021. 9, DOI: 10.3390/toxics9110315.
91. Laue, H., L. Hostettler, R.P. Badertscher, K.J. Jenner, G. Sanders, J.A. Arnot, A. Natsch, Examining Uncertainty in In Vitro–In Vivo Extrapolation Applied in Fish Bioconcentration Models. *Environmental Science & Technology*, 2020. 54(15): p. 9483-9494.
92. Stadnicka-Michalak, J., K. Schirmer, In Vitro-In Vivo Extrapolation to Predict Bioaccumulation and Toxicity of Chemicals in Fish Using Physiologically Based Toxicokinetic Models, in *In Situ Bioavailability and Toxicity of Organic Chemicals in Aquatic Systems*, T.-B. Seiler and M. Brinkmann, Editors. 2022, Springer US: New York, NY. p. 229-258.
93. Pietsch, C., J. Hollender, F. Dorusch, P. Burkhardt-Holm, Cytotoxic effects of pentachlorophenol (PCP) and its metabolite tetrachlorohydroquinone (TCHQ) on liver cells are modulated by antioxidants. *Cell Biology and Toxicology*, 2014. 30(4): p. 233-252.
94. Mahoney, H., F.C. da Silva Junior, C. Roberts, M. Schultz, X. Ji, A.J. Alcaraz, D. Montgomery, S. Selinger, J.K. Challis, J.P. Giesy, L. Weber, D. Janz, S. Wiseman, M. Hecker, M. Brinkmann, Exposure to the Tire Rubber-Derived Contaminant 6PPD-Quinone Causes Mitochondrial Dysfunction In Vitro. *Environmental Science & Technology Letters*, 2022. 9(9): p. 765-771.
95. Arp, H.P.H., T.N. Brown, U. Berger, S.E. Hale, Ranking REACH registered neutral, ionizable and ionic organic chemicals based on their aquatic persistency and mobility. *Environmental Science: Processes & Impacts*, 2017. 19(7): p. 939-955.

96. Fredell, D.L., Biological Properties and Applications of Cationic Surfactants. 1 ed. Cationic Surfactants - Analytical and Biological Evaluation. Vol. 53. 1994, Boca Raton: CRC Press.
97. Cowan-Ellsberry, C., S. Belanger, P. Dorn, S. Dyer, D. McAvoy, H. Sanderson, D. Versteeg, D. Ferrer, K. Stanton, Environmental Safety of the Use of Major Surfactant Classes in North America. Critical Reviews in Environmental Science and Technology, 2014. 44(17): p. 1893-1993.
98. Kahrilas, G.A., J. Blotvogel, P.S. Stewart, T. Borch, Biocides in Hydraulic Fracturing Fluids: A Critical Review of Their Usage, Mobility, Degradation, and Toxicity. Environmental Science & Technology, 2015. 49(1): p. 16-32.
99. Manallack, D.T., The pK(a) Distribution of Drugs: Application to Drug Discovery. Perspect Medicin Chem, 2007. 1: p. 25-38.
100. Fawcett, R.S., B.R. Christensen, D.P. Tierney, The impact of conservation tillage on pesticide runoff into surface water: A review and analysis. Journal of Soil and Water Conservation, 1994. 49(2): p. 126-135.
101. Schwaiger, J., H. Ferling, U. Mallow, H. Wintermayr, R.D. Negele, Toxic effects of the non-steroidal anti-inflammatory drug diclofenac: Part I: histopathological alterations and bioaccumulation in rainbow trout. Aquatic Toxicology, 2004. 68(2): p. 141-150.
102. Memmert, U., A. Peither, R. Burri, K. Weber, T. Schmidt, J.P. Sumpter, A. Hartmann, Diclofenac: New data on chronic toxicity and bioconcentration in fish. Environmental Toxicology and Chemistry, 2013. 32(2): p. 442-452.
103. Martin, J.W., S.A. Mabury, K.R. Solomon, D.C.G. Muir, Bioconcentration and tissue distribution of perfluorinated acids in rainbow trout (*Oncorhynchus mykiss*). Environmental Toxicology and Chemistry, 2003. 22(1): p. 196-204.
104. Inoue, Y., N. Hashizume, N. Yakata, H. Murakami, Y. Suzuki, E. Kikushima, M. Otsuka, Unique Physicochemical Properties of Perfluorinated Compounds and Their Bioconcentration in Common Carp *Cyprinus carpio* L. Archives of Environmental Contamination and Toxicology, 2012. 62(4): p. 672-680.
105. Tolls, J., M.P. Lehmann, D.T.H.M. Sijm, Quantification of in vivo biotransformation of the anionic surfactant C12-2-linear alkylbenzene sulfonate in fathead minnows. Environmental Toxicology and Chemistry, 2000. 19(10): p. 2394-2400.
106. Könnecker, G., J. Regelman, S. Belanger, K. Gamon, R. Sedlak, Environmental properties and aquatic hazard assessment of anionic surfactants: Physico-chemical, environmental fate and ecotoxicity properties. Ecotoxicology and Environmental Safety, 2011. 74(6): p. 1445-1460.
107. Mueller, C., S. Trapp, F. Polesel, S. Kuehr, C. Schlechtriem, Biomagnification of ionizable organic compounds in rainbow trout *Oncorhynchus mykiss*. Environmental Sciences Europe, 2020. 32(1): p. 159.
108. McKim, J.M., P.K. Schmieder, R.J. Erickson, Toxicokinetic modeling of [14C]pentachlorophenol in the rainbow trout (*Salmo gairdneri*). Aquatic Toxicology, 1986. 9(1): p. 59-80.
109. Poulin, P., F.P. Theil, A Priori Prediction of Tissue:Plasma Partition Coefficients of Drugs to Facilitate the Use of Physiologically-Based Pharmacokinetic Models in Drug Discovery. Journal of Pharmaceutical Sciences, 2000. 89(1): p. 16-35.

110. Rodgers, T., D. Leahy, M. Rowland, Physiologically Based Pharmacokinetic Modeling 1: Predicting the Tissue Distribution of Moderate-to-Strong Bases. *Journal of Pharmaceutical Sciences*, 2005. 94(6): p. 1259-1276.
111. Rodgers, T., M. Rowland, Physiologically based pharmacokinetic modelling 2: Predicting the tissue distribution of acids, very weak bases, neutrals and zwitterions. *Journal of Pharmaceutical Sciences*, 2006. 95(6): p. 1238-1257.
112. Crawford, J.C., 2(2-hydroxyphenyl)2H-benzotriazole ultraviolet stabilizers. *Progress in Polymer Science*, 1999. 24(1): p. 7-43.
113. Himmelsbach, M., W. Buchberger, E. Reingruber, Determination of polymer additives by liquid chromatography coupled with mass spectrometry. A comparison of atmospheric pressure photoionization (APPI), atmospheric pressure chemical ionization (APCI), and electrospray ionization (ESI). *Polymer Degradation and Stability*, 2009. 94(8): p. 1213-1219.
114. Maddrey, W.C., Chapter 14 - Clinical Manifestations and Management of Drug-Induced Liver Diseases, in *Drug-Induced Liver Disease (Third Edition)*, N. Kaplowitz and L.D. DeLeve, Editors. 2013, Academic Press: Boston. p. 229-240.
115. NHS. [05.08.2022]; Available from: <https://www.nhs.uk/medicines/diclofenac/>.
116. Kobayashi, K., Metabolism of Pentachlorophenol in Fish, in *Pesticide and Xenobiotic Metabolism in Aquatic Organisms*. 1979, American Chemical Society. p. 131-143.
117. Convention, S. Pesticide POPs, PCP, Overview. [05.08.2022]; Available from: <http://chm.pops.int/Implementation/PesticidePOPs/PCP/Overview/tabid/7983/Default.aspx>.
118. Kirkpatrick, D., S.R. Biggs, B. Conway, C.M. Finn, D.R. Hawkins, T. Honda, M. Ishida, G.P. Powell, Metabolism of N-(2,3-dichlorophenyl)-3,4,5,6-tetrachlorophthalamic acid (techlofthalam) in paddy soil and rice. *Journal of Agricultural and Food Chemistry*, 1981. 29(6): p. 1149-1153.
119. Ngo, H.-P.-T., T.-H. Ho, I. Lee, H.-T. Tran, B. Sur, S. Kim, J.-G. Kim, Y.-J. Ahn, S.-S. Cha, L.-W. Kang, Crystal Structures of Peptide Deformylase from Rice Pathogen *Xanthomonas oryzae* pv. *oryzae* in Complex with Substrate Peptides, Actinonin, and Fragment Chemical Compounds. *Journal of Agricultural and Food Chemistry*, 2016. 64(39): p. 7307-7314.
120. Holmbom, B. A procedure for analysis of toxic compounds in pulp and paper mill waste. 1980 [05.08.2022]; Available from: [https://www.researchgate.net/profile/Bjarne-Holmbom-2/publication/259623225\\_A\\_procedure\\_for\\_analysis\\_of\\_toxic\\_compounds\\_in\\_pulp\\_and\\_paper\\_mill\\_waste\\_waters/links/0a85e52d6cceb67ad9000000/A-procedure-for-analysis-of-toxic-compounds-in-pulp-and-paper-mill-waste-waters.pdf](https://www.researchgate.net/profile/Bjarne-Holmbom-2/publication/259623225_A_procedure_for_analysis_of_toxic_compounds_in_pulp_and_paper_mill_waste_waters/links/0a85e52d6cceb67ad9000000/A-procedure-for-analysis-of-toxic-compounds-in-pulp-and-paper-mill-waste-waters.pdf).
121. Oikari, A., T. Kunnamo-Ojala, Tracing of xenobiotic contamination in water with the aid of fish bile metabolites: a field study with caged rainbow trout (*Salmo gairdneri*). *Aquatic Toxicology*, 1987. 9(6): p. 327-341.
122. Loos, R., B.M. Gawlik, G. Locoro, E. Rimaviciute, S. Contini, G. Bidoglio, EU-wide survey of polar organic persistent pollutants in European river waters. *Environmental Pollution*, 2009. 157(2): p. 561-568.
123. Lu, Z., A.O. De Silva, W. Zhou, G.R. Tetreault, S.R. de Solla, P.A. Fair, M. Houde, G. Bossart, D.C.G. Muir, Substituted diphenylamine antioxidants and benzotriazole UV

- stabilizers in blood plasma of fish, turtles, birds and dolphins from North America. *Science of The Total Environment*, 2019. 647: p. 182-190.
124. Larisch, W., K.-U. Goss, Uptake, distribution and elimination of chemicals in fish – Which physiological parameters are the most relevant for toxicokinetics? *Chemosphere*, 2018. 210: p. 1108-1114.
  125. Schug, H., J. Maner, M. Hülskamp, F. Begnaud, C. Debonneville, F. Berthaud, S. Gimeno, K. Schirmer, Extending the concept of predicting fish acute toxicity in vitro to the intestinal cell line RTgutGC. *ALTEX - Alternatives to animal experimentation*, 2020. 37(1): p. 37-46.
  126. Stadnicka-Michalak, J. Determination of chemical Non-toxic Concentrations (NtC). 2018 [24.10.2022]; Available from: [https://utox.shinyapps.io/NtC\\_NtC/](https://utox.shinyapps.io/NtC_NtC/).
  127. Bruijn, J.D., B. Hansen, S. Johansson, M. Luotamo, S. Munn, C. Musset, S. Olsen, H. Olsson, A. Paya-Perez, F. Pedersen, K. Rasmussen, B. Sokull-Kluttgen, Technical Guidance Document on Risk Assessment. 2022.
  128. Lauper, B.B., E. Anthamatten, J. Raths, M. Arlos, J. Hollender, Systematic Underestimation of Pesticide Burden for Invertebrates under Field Conditions: Comparing the Influence of Dietary Uptake and Aquatic Exposure Dynamics. *ACS Environmental Au*, 2022. 2(2): p. 166-175.
  129. Core Team, R., R: A language and environment for statistical computing. R Foundation for Statistical Computing. 2022: Vienna, Austria.
  130. Wickham, H., D. Navarro, T.L. Pedersen, *ggplot2: Elegant Graphics for Data Analysis*. 2016, New York: Springer-Verlag.
  131. Pedersen, T., *patchwork: The Composer of Plots*. 2022.
  132. Schauburger, P., A. Walker, *openxlsx: Read, Write and Edit xlsx Files*. 2022.
  133. Wickham, H., G. M., *tidyr: Tidy Messy Data*. 2022.
  134. Wickham, H., R. François, L. Henry, K. Müller, *dplyr: A Grammar of Data Manipulation*. 2022.
  135. Natsch, A., H. Laue, T. Haupt, V. von Niederhäusern, G. Sanders, Accurate prediction of acute fish toxicity of fragrance chemicals with the RTgill-W1 cell assay. *Environmental Toxicology and Chemistry*, 2018. 37(3): p. 931-941.
  136. Praskova, E., E. Voslarova, Z. Siroka, L. Plhalova, S. Macova, P. Marsalek, V. Pistekova, Z. Svobodova, Assessment of diclofenac LC50 reference values in juvenile and embryonic stages of the zebrafish (*Danio rerio*). *Pol J Vet Sci*, 2011. 14(4): p. 545-549.
  137. Wassenaar, P.N.H., E.M.J. Verbruggen, E. Cieraad, W.J.G.M. Peijnenburg, M.G. Vijver, Variability in fish bioconcentration factors: Influences of study design and consequences for regulation. *Chemosphere*, 2020. 239: p. 124731.
  138. van den Brandhof, E.-J., M. Montforts, Fish embryo toxicity of carbamazepine, diclofenac and metoprolol. *Ecotoxicology and Environmental Safety*, 2010. 73(8): p. 1862-1866.
  139. Lewis, K.A., J. Tzilivakis, D. Warner, A. Green, An international database for pesticide risk assessments and management. *Human and Ecological Risk Assessment: An International Journal*, 2016. 22(4): p. 1050-1064.

140. Gates, V.L., R.S. Tjeerdema, Disposition and Biotransformation of Pentachlorophenol in the Striped Bass (*Morone saxatilis*). *Pesticide Biochemistry and Physiology*, 1993. 46(2): p. 161-170.
141. Schlenk, D., M.C. Celander, E.P. Gallagher, S.G. George, M.O. James, S.W. Kullman, P.v.d. Hurk, K. Willett. *Biotransformation in Fishes*. 2008.
142. Mehinto, A.C., E.M. Hill, C.R. Tyler, Uptake and Biological Effects of Environmentally Relevant Concentrations of the Nonsteroidal Anti-inflammatory Pharmaceutical Diclofenac in Rainbow Trout (*Oncorhynchus mykiss*). *Environmental Science & Technology*, 2010. 44(6): p. 2176-2182.
143. Kobayashi, K., S. Kimura, H. Akitake, Studies on the Metabolism of Chlorophenols in Fish-VII Sulfate Conjugation of Phenol and PCP by Fish Livers. *NIPPON SUISAN GAKKAISHI*, 1976. 42(2): p. 171-177.
144. Renner, G., W. Mücke, Transformations of pentachlorophenol. *Toxicological & Environmental Chemistry*, 1986. 11(1): p. 9-29.
145. Stehly, G.R., W.L. Hayton, Metabolism of pentachlorophenol by fish. *Xenobiotica*, 1989. 19(1): p. 75-81.
146. Frankovic, L., M.A.Q. Khan, S.M.A. Ghais, Metabolism of hexachlorobenzene in the fry of steelhead trout, *Salmo gairdneri* (*Oncorhynchus mykiss*). *Archives of Environmental Contamination and Toxicology*, 1995. 28(2): p. 209-214.
147. Cravedi, J.P., A. Lafuente, M. Baradat, A. Hillenweck, E. Perdu-Durand, Biotransformation of pentachlorophenol, aniline and biphenyl in isolated rainbow trout (*Oncorhynchus mykiss*) hepatocytes: comparison with in vivo metabolism. *Xenobiotica*, 1999. 29(5): p. 499-509.
148. Kallio, J.-M., M. Lahti, A. Oikari, L. Kronberg, Metabolites of the Aquatic Pollutant Diclofenac in Fish Bile. *Environmental Science & Technology*, 2010. 44(19): p. 7213-7219.
149. Lahti, M., J.-M. Brozinski, A. Jylhä, L. Kronberg, A. Oikari, Uptake from water, biotransformation, and biliary excretion of pharmaceuticals by rainbow trout. *Environmental Toxicology and Chemistry*, 2011. 30(6): p. 1403-1411.
150. Fu, Q., D. Fedrizzi, V. Kosfeld, C. Schlechtriem, V. Ganz, S. Derrer, D. Rentsch, J. Hollender, Biotransformation Changes Bioaccumulation and Toxicity of Diclofenac in Aquatic Organisms. *Environmental Science & Technology*, 2020. 54(7): p. 4400-4408.
151. Kosfeld, V., Q. Fu, I. Ebersbach, D. Esser, A. Schauerte, I. Bischof, J. Hollender, C. Schlechtriem, Comparison of Alternative Methods for Bioaccumulation Assessment: Scope and Limitations of In Vitro Depletion Assays with Rainbow Trout and Bioconcentration Tests in the Freshwater Amphipod *Hyalella azteca*. *Environmental Toxicology and Chemistry*, 2020. 39(9): p. 1813-1825.
152. Connors, K.A., B. Du, P.N. Fitzsimmons, A.D. Hoffman, C.K. Chambliss, J.W. Nichols, B.W. Brooks, Comparative pharmaceutical metabolism by rainbow trout (*Oncorhynchus mykiss*) liver S9 fractions. *Environmental Toxicology and Chemistry*, 2013. 32(8): p. 1810-1818.
153. Baron, M.G., K.S. Mintram, S.F. Owen, M.J. Hetheridge, A.J. Moody, W.M. Purcell, S.K. Jackson, A.N. Jha, Pharmaceutical Metabolism in Fish: Using a 3-D Hepatic In Vitro Model to Assess Clearance. *PLoS ONE*, 2017. 12(1): p. e0168837.
154. Dobson, P.D., D.B. Kell, Carrier-mediated cellular uptake of pharmaceutical drugs: an exception or the rule? *Nature Reviews Drug Discovery*, 2008. 7(3): p. 205-220.

155. Sugano, K., M. Kansy, P. Artursson, A. Avdeef, S. Bendels, L. Di, G.F. Ecker, B. Faller, H. Fischer, G. Gerebtzoff, H. Lennernaes, F. Senner, Coexistence of passive and carrier-mediated processes in drug transport. *Nature Reviews Drug Discovery*, 2010. 9(8): p. 597-614.
156. Hagenbuch, B., B. Stieger, The SLCO (former SLC21) superfamily of transporters. *Molecular Aspects of Medicine*, 2013. 34(2): p. 396-412.
157. Steiner, K., B. Hagenbuch, D.R. Dietrich, Molecular cloning and functional characterization of a rainbow trout liver Oatp. *Toxicology and Applied Pharmacology*, 2014. 280(3): p. 534-542.
158. Kropf, C., H. Segner, K. Fent, ABC transporters and xenobiotic defense systems in early life stages of rainbow trout (*Oncorhynchus mykiss*). *Comparative Biochemistry and Physiology Part C: Toxicology & Pharmacology*, 2016. 185-186: p. 45-56.
159. Ebert, A., F. Allendorf, U. Berger, K.-U. Goss, N. Ulrich, Membrane/Water Partitioning and Permeabilities of Perfluoroalkyl Acids and Four of their Alternatives and the Effects on Toxicokinetic Behavior. *Environmental Science & Technology*, 2020. 54(8): p. 5051-5061.
160. Watson, H., Biological membranes. *Essays in Biochemistry*, 2015. 59: p. 43-69.
161. Dayeh, V.R., K. Schirmer, N.C. Bols, Ammonia-containing Industrial Effluents, Lethal to Rainbow Trout, Induce Vacuolisation and Neutral Red Uptake in the Rainbow Trout Gill Cell Line, RTgill-W1. *Alternatives to Laboratory Animals*, 2009. 37(1): p. 77-87.
162. Yue, Y., R. Behra, L. Sigg, P. Fernández Freire, S. Pillai, K. Schirmer, Toxicity of silver nanoparticles to a fish gill cell line: Role of medium composition. *Nanotoxicology*, 2015. 9(1): p. 54-63.
163. Erickson, R.J., J.M. McKim, G.J. Lien, A.D. Hoffman, S.L. Batterman, Uptake and elimination of ionizable organic chemicals at fish gills: I. Model formulation, parameterization, and behavior. *Environmental Toxicology and Chemistry*, 2006. 25(6): p. 1512-1521.
164. Stott, L.C., S. Schnell, C. Hogstrand, S.F. Owen, N.R. Bury, A primary fish gill cell culture model to assess pharmaceutical uptake and efflux: Evidence for passive and facilitated transport. *Aquatic Toxicology*, 2015. 159: p. 127-137.
165. Chang, E.D., R.M. Town, S.F. Owen, C. Hogstrand, N.R. Bury, Effect of Water pH on the Uptake of Acidic (Ibuprofen) and Basic (Propranolol) Drugs in a Fish Gill Cell Culture Model. *Environmental Science & Technology*, 2021. 55(10): p. 6848-6856.
166. Fuchylo, U., H.A. Alharbi, A.J. Alcaraz, P.D. Jones, J.P. Giesy, M. Hecker, M. Brinkmann, Inflammation of Gill Epithelia in Fish Causes Increased Permeation of Petrogenic Polar Organic Chemicals via Disruption of Tight Junctions. *Environmental Science & Technology*, 2022. 56(3): p. 1820-1829.
167. Kierkegaard, A., M. Sundbom, B. Yuan, J.M. Armitage, J.A. Arnot, S.T.J. Droge, M.S. McLachlan, Bioconcentration of Several Series of Cationic Surfactants in Rainbow Trout. *Environmental Science & Technology*, 2021. 55(13): p. 8888-8897.
168. Crookes, M., D. Brooke, Estimation of fish bioconcentration factor (BCF) from depuration data, E. Agency, Editor. 2011, Environment Agency: Bristol.
169. Sijm, D.T.H.M., M.E. Verberne, W.J. Dejonge, P. Part, A. Opperhuizen, Allometry in the Uptake of Hydrophobic Chemicals Determined in Vivo and in Isolated Perfused Gills. *Toxicology and Applied Pharmacology*, 1995. 131(1): p. 130-135.

170. Arnot, J.A., F.A.P.C. Gobas, A food web bioaccumulation model for organic chemicals in aquatic ecosystems. *Environmental Toxicology and Chemistry*, 2004. 23(10): p. 2343-2355.
171. Giolando, S.T., R.A. Rapaport, R.J. Larson, T.W. Federle, M. Stalmans, P. Masscheleyn, Environmental fate and effects of DEEDMAC: A new rapidly biodegradable cationic surfactant for use in fabric softeners. *Chemosphere*, 1995. 30(6): p. 1067-1083.
172. Myers, D., An Overview of Surfactant Science and Technology, in *Surfactant Science and Technology*, D. Myers, Editor. 2005, John Wiley & Sons Inc.: Hoboken New Jersey. p. 1-28.
173. Schwarzenbach, R.P., P.M. Gschwend, D.M. Imboden, *Environmental Organic Chemistry*. 2 ed. Amazon, USA. 2003, Hoboken, New Jersey: John Wiley & Sons.
174. Hodges, G., C. Eadsforth, B. Bossuyt, A. Bouvy, M.-H. Enrici, M. Geurts, M. Kotthoff, E. Michie, D. Miller, J. Müller, G. Oetter, J. Roberts, D. Schowanek, P. Sun, J. Venzmer, A comparison of log K<sub>ow</sub> (n-octanol–water partition coefficient) values for non-ionic, anionic, cationic and amphoteric surfactants determined using predictions and experimental methods. *Environmental Sciences Europe*, 2019. 31(1).
175. Chen, Y., J.L.M. Hermens, M.T.O. Jonker, J.A. Arnot, J.M. Armitage, T. Brown, J.W. Nichols, K.A. Fay, S.T.J. Droge, Which Molecular Features Affect the Intrinsic Hepatic Clearance Rate of Ionizable Organic Chemicals in Fish? *Environmental Science & Technology*, 2016. 50(23): p. 12722-12731.
176. Balk, F., J. Hollender, K. Schirmer, Investigating the bioaccumulation potential of anionic organic compounds using a permanent rainbow trout liver cell line. *Environment International*, 2023. 174: p. 107798.
177. ChemicalBook. Ethylenediaminetetraacetic acid (EDTA)– Physical Properties and Applications. 2020 [13.12.2022]; Available from: <https://www.chemicalbook.com/Article/Ethylenediaminetetraacetic-acid-EDTA-Physical-Properties-and-Applications.htm#:~:text=Physical%20Properties%20of%20EDTA&text=EDTA%20is%20white%20powder%2C%20which,ethanol%20and%20general%20organic%20solvents>.
178. DFG, Ethylendiamintetraessigsäure (EDTA) und ihre Alkalisalze [MAK Value Documentation in German language, 2009], in *The MAK-Collection for Occupational Health and Safety: Annual Thresholds and Classifications for the Workplace*, H. Greim, Editor. 2012, Wiley-VCH Verlag GmbH & Co. p. 1-33.
179. Hendriks, A.J., A. van der Linde, G. Cornelissen, D.T.H.M. Sijm, The power of size. 1. Rate constants and equilibrium ratios for accumulation of organic substances related to octanol-water partition ratio and species weight. *Environmental Toxicology and Chemistry*, 2001. 20(7): p. 1399-1420.
180. ECHA. Assessment Report Decyldimethylamine. [23.01.2023]; Available from: <https://echa.europa.eu/de/regISTRATION-dossier/-/registered-dossier/14493/6/2/1>.
181. Groothuis, F.A., N. Timmer, E. Opsahl, B. Nicol, S.T.J. Droge, B.J. Blaauboer, N.I. Kramer, Influence of in Vitro Assay Setup on the Apparent Cytotoxic Potency of Benzalkonium Chlorides. *Chemical Research in Toxicology*, 2019. 32(6): p. 1103-1114.
182. Bernhard, M.J., S.D. Dyer, Fish critical cellular residues for surfactants and surfactant mixtures. *Environmental Toxicology and Chemistry*, 2009. 24(7): p. 1738-1744.

183. Sandbacka, M., I. Christianson, B. Isomaa, The acute toxicity of surfactants on fish cells, *Daphnia magna* and fish—A comparative study. *Toxicology in Vitro*, 2000. 14(1): p. 61-68.
184. Brinkmann, M., H. Alharbi, U. Fuchylo, S. Wiseman, G. Morandi, H. Peng, J.P. Giesy, P.D. Jones, M. Hecker, Mechanisms of pH-Dependent Uptake of Ionizable Organic Chemicals by Fish from Oil Sands Process-Affected Water (OSPW). *Environmental Science & Technology*, 2020. 54(15): p. 9547-9555.
185. Henneberger, L., M. Mühlenbrink, F.C. Fischer, B.I. Escher, C18-Coated Solid-Phase Microextraction Fibers for the Quantification of Partitioning of Organic Acids to Proteins, Lipids, and Cells. *Chemical Research in Toxicology*, 2019. 32(1): p. 168-178.
186. Barron, M.G., Bioconcentration. Will water-borne organic chemicals accumulate in aquatic animals? *Environmental Science & Technology*, 1990. 24(11): p. 1612-1618.
187. Neumann, E.K., T.D. Do, T.J. Comi, J.V. Sweedler, Exploring the Fundamental Structures of Life: Non-Targeted, Chemical Analysis of Single Cells and Subcellular Structures. *Angewandte Chemie International Edition*, 2019. 58(28): p. 9348-9364.
188. Kümmerer, K., Pharmaceuticals in the Environment. *Annual Review of Environment and Resources*, 2010. 35(1): p. 57-75.
189. Benskin, J.P., D.C.G. Muir, B.F. Scott, C. Spencer, A.O. De Silva, H. Kylin, J.W. Martin, A. Morris, R. Lohmann, G. Tomy, B. Rosenberg, S. Taniyasu, N. Yamashita, Perfluoroalkyl Acids in the Atlantic and Canadian Arctic Oceans. *Environmental Science & Technology*, 2012. 46(11): p. 5815-5823.
190. Chiaia-Hernandez, A.C., M. Krauss, J. Hollender, Screening of Lake Sediments for Emerging Contaminants by Liquid Chromatography Atmospheric Pressure Photoionization and Electrospray Ionization Coupled to High Resolution Mass Spectrometry. *Environmental Science & Technology*, 2013. 47(2): p. 976-986.
191. Schlüsener, M.P., U. Kunkel, T.A. Ternes, Quaternary Triphenylphosphonium Compounds: A New Class of Environmental Pollutants. *Environmental Science & Technology*, 2015. 49(24): p. 14282-14291.
192. Munz, N.A., F.J. Burdon, D. de Zwart, M. Junghans, L. Melo, M. Reyes, U. Schönenberger, H.P. Singer, B. Spycher, J. Hollender, C. Stamm, Pesticides drive risk of micropollutants in wastewater-impacted streams during low flow conditions. *Water Research*, 2017. 110: p. 366-377.
193. Balk, F.G.P., B. Hüsser, J. Hollender, K. Schirmer, Bioaccumulation of cationic surfactants in permanent fish cell lines. *Environmental Science & Technology*, 2023: p. (submitted).
194. Fischer, F.C., C. Abele, S.T.J. Droge, L. Henneberger, M. König, R. Schlichting, S. Scholz, B.I. Escher, Cellular Uptake Kinetics of Neutral and Charged Chemicals in in Vitro Assays Measured by Fluorescence Microscopy. *Chemical Research in Toxicology*, 2018. 31(8): p. 646-657.
195. Dupraz, V., S. Stachowski-Haberkorn, J. Wicquart, N. Tapie, H. Budzinski, F. Akcha, Demonstrating the need for chemical exposure characterisation in a microplate test system: toxicity screening of sixteen pesticides on two marine microalgae. *Chemosphere*, 2019. 221: p. 278-291.
196. Huchthausen, J., M. Mühlenbrink, M. König, B.I. Escher, L. Henneberger, Experimental Exposure Assessment of Ionizable Organic Chemicals in In Vitro Cell-Based Bioassays. *Chemical Research in Toxicology*, 2020. 33(7): p. 1845-1854.



197. Spycher, S., P. Smejtek, T.I. Netzeva, B.I. Escher, Toward a Class-Independent Quantitative Structure–Activity Relationship Model for Uncouplers of Oxidative Phosphorylation. *Chemical Research in Toxicology*, 2008. 21(4): p. 911-927.
198. Flewelling, R.F., W.L. Hubbell, The membrane dipole potential in a total membrane potential model. Applications to hydrophobic ion interactions with membranes. *Biophys J*, 1986. 49(2): p. 541-52.
199. Zarfl, C., M. Matthies, J. Klasmeier, A mechanistical model for the uptake of sulfonamides by bacteria. *Chemosphere*, 2008. 70(5): p. 753-760.
200. Nichols, J.W., B. Du, J.P. Berninger, K.A. Connors, C.K. Chambliss, R.J. Erickson, A.D. Hoffman, B.W. Brooks, Observed and modeled effects of pH on bioconcentration of diphenhydramine, a weakly basic pharmaceutical, in fathead minnows. *Environmental Toxicology and Chemistry*, 2015. 34(6): p. 1425-1435.
201. Zhang, L., B.W. Brooks, F. Liu, Z. Zhou, H. Li, J. You, Human Apparent Volume of Distribution Predicts Bioaccumulation of Ionizable Organic Chemicals in Zebrafish Embryos. *Environmental Science & Technology*, 2022. 56(16): p. 11547-11558.
202. Brooks, B.W., W.B. Steele, Chapter 4 - Ecotoxicological Perspectives on Health Care and the Environment, in *Health Care and Environmental Contamination*, A.B.A. Boxall and R.S. Kookana, Editors. 2018, Elsevier: Amsterdam. p. 41-67.
203. Chen, M., L. Qiang, X. Pan, S. Fang, Y. Han, L. Zhu, In Vivo and in Vitro Isomer-Specific Biotransformation of Perfluorooctane Sulfonamide in Common Carp (*Cyprinus carpio*). *Environmental Science & Technology*, 2015. 49(23): p. 13817-13824.
204. Obach, R.S., L. Franco, J.W. Nigell, Trend Analysis of a Database of Intravenous Pharmacokinetic Parameters in Humans for 670 Drug Compounds. *Drug Metabolism and Disposition*, 2008. 36(7): p. 1385.
205. Franco, L., B. Giuliano, R.S. Obach, Trend Analysis of a Database of Intravenous Pharmacokinetic Parameters in Humans for 1352 Drug Compounds. *Drug Metabolism and Disposition*, 2018. 46(11): p. 1466.
206. Endo, S., B.I. Escher, K.-U. Goss, Capacities of Membrane Lipids to Accumulate Neutral Organic Chemicals. *Environmental Science & Technology*, 2011. 45(14): p. 5912-5921.
207. Bittermann, K., S. Spycher, K.-U. Goss, Comparison of different models predicting the phospholipid-membrane water partition coefficients of charged compounds. *Chemosphere*, 2016. 144: p. 382-391.
208. Ulrich, N., S. Endo, T.N. Brown, N. Watanabe, G. Bronner, M.H. Abraham, K.U. Goss. UFZ-LSER database v 3.2.1 [Internet], Leipzig, Germany, Helmholtz Centre for Environmental Research-UFZ. 2017 [15.05.2023]; Available from: <http://www.ufz.de/lserd>.
209. Percepta, version 14.50.0, Advanced Chemistry Development, Inc. (ACD/Labs). 2020, Toronto, ON, Canada, [www.acdlabs.com](http://www.acdlabs.com).
210. Zilberstein, D., V. Agmon, S. Schuldiner, E. Padan, *Escherichia coli* intracellular pH, membrane potential, and cell growth. *Journal of Bacteriology*, 1984. 158(1): p. 246-252.
211. Alberts, B., A. Johnson, J. Lewis, M. Raff, K. Roberts, P. Walter, Part IV Internal Organization of the Cell: Membrane Structure, in *Molecular Biology of the Cell* 2011, WILEY-VCH Verlag GmbH & Co KGaA: Weinheim.

212. Loidl-Stahlhofen, A., T. Hartmann, M. Schöttner, C. Röhring, H. Brodowsky, J. Schmitt, J. Keldenich, Multilamellar Liposomes and Solid-Supported Lipid Membranes (TRANSIL): Screening of Lipid-Water Partitioning Toward a High-Throughput Scale. *Pharmaceutical Research*, 2001. 18(12): p. 1782-1788.
213. Cuklev, F., E. Kristiansson, J. Fick, N. Asker, L. Förlin, D.G.J. Larsson, Diclofenac in fish: Blood plasma levels similar to human therapeutic levels affect global hepatic gene expression. *Environmental Toxicology and Chemistry*, 2011. 30(9): p. 2126-2134.
214. thermofisher. Media formulation. [22.05.23]; Available from: <https://www.thermofisher.com/ch/en/home/technical-resources/media-formulation.81.html>.
215. MacLeod, M., A.J. Fraser, D. Mackay, Evaluating and expressing the propagation of uncertainty in chemical fate and bioaccumulation models. *Environmental Toxicology and Chemistry*, 2002. 21(4): p. 700-709.
216. Schreiber, R., U. Gündel, S. Franz, A. Küster, B. Rechenberg, R. Altenburger, Using the fish plasma model for comparative hazard identification for pharmaceuticals in the environment by extrapolation from human therapeutic data. *Regulatory Toxicology and Pharmacology*, 2011. 61(3): p. 261-275.
217. Pearce, R.G., R.W. Setzer, J.L. Davis, J.F. Wambaugh, Evaluation and calibration of high-throughput predictions of chemical distribution to tissues. *Journal of Pharmacokinetics and Pharmacodynamics*, 2017. 44(6): p. 549-565.
218. Guy, W.S., D.R. Taves, W.S.J. Brey, Organic Fluorocompounds in Human Plasma: Prevalence and Characterization, in *Biochemistry Involving Carbon-Fluorine Bonds*. 1976, American Chemical Society. p. 117-134.
219. Vanden Heuvel, J.P., B.I. Kuslikis, M.J. Van Rafelghem, R.E. Peterson, Disposition of perfluorodecanoic acid in male and female rats. *Toxicology and Applied Pharmacology*, 1991. 107(3): p. 450-459.
220. Consoer, D.M., A.D. Hoffman, P.N. Fitzsimmons, P.A. Kosian, J.W. Nichols, Toxicokinetics of perfluorooctane sulfonate in rainbow trout (*Oncorhynchus mykiss*). *Environmental Toxicology and Chemistry*, 2016. 35(3): p. 717-727.
221. Chen, Y.M., L.H. Guo, Fluorescence study on site-specific binding of perfluoroalkyl acids to human serum albumin. *Arch Toxicol*, 2009. 83(3): p. 255-61.
222. Allendorf, F., U. Berger, K.-U. Goss, N. Ulrich, Partition coefficients of four perfluoroalkyl acid alternatives between bovine serum albumin (BSA) and water in comparison to ten classical perfluoroalkyl acids. *Environmental Science: Processes & Impacts*, 2019. 21(11): p. 1852-1863.
223. Escher, B.I., L. Sigg, Chemical Speciation of Organics and of Metals at Biological Interphases, in *Physicochemical Kinetics and Transport at Biointerfaces*. 2004. p. 205-269.
224. Hale, S.E., M. Neumann, I. Schliebner, J. Schulze, F.S. Auerbeck, C. Castell-Exner, M. Collard, D. Drmač, J. Hartmann, R. Hofman-Caris, J. Hollender, M. de Jonge, T. Kullick, A. Lennquist, T. Letzel, K. Nödler, S. Pawlowski, N. Reineke, E. Rorije, M. Scheurer, G. Sigmund, H. Timmer, X. Trier, E. Verbruggen, H.P.H. Arp, Getting in control of persistent, mobile and toxic (PMT) and very persistent and very mobile (vPvM) substances to protect water resources: strategies from diverse perspectives. *Environmental Sciences Europe*, 2022. 34(1): p. 22.

225. Creusot, N., F. Brion, B. Piccini, H. Budzinski, J.M. Porcher, S. Aït-Aïssa, BFCOD activity in fish cell lines and zebrafish embryos and its modulation by chemical ligands of human aryl hydrocarbon and nuclear receptors. *Environmental Science and Pollution Research*, 2015. 22(21): p. 16393-16404.
226. Smith, E.M., J.Y. Wilson, Assessment of cytochrome P450 fluorometric substrates with rainbow trout and killifish exposed to dexamethasone, pregnenolone-16 $\alpha$ -carbonitrile, rifampicin, and  $\beta$ -naphthoflavone. *Aquatic Toxicology*, 2010. 97(4): p. 324-333.
227. Franco, M.E., A.J. Ramirez, K.M. Johanning, C.W. Matson, R. Lavado, In vitro-in vivo biotransformation and phase I metabolite profiling of benzo[a]pyrene in Gulf killifish (*Fundulus grandis*) populations with different exposure histories. *Aquatic Toxicology*, 2022. 243: p. 106057.
228. Boaru, D.A., N. Dragoş, K. Schirmer, Microcystin-LR induced cellular effects in mammalian and fish primary hepatocyte cultures and cell lines: A comparative study. *Toxicology*, 2006. 218(2): p. 134-148.
229. Schug, H.I., A fish intestinal barrier model to assess the interaction with chemicals in vitro. 2019, EPFL: Lausanne : Ecole Polytechnique Fédérale de Lausanne. p. 207.
230. Leung, C.M., P. de Haan, K. Ronaldson-Bouchard, G.-A. Kim, J. Ko, H.S. Rho, Z. Chen, P. Habibovic, N.L. Jeon, S. Takayama, M.L. Shuler, G. Vunjak-Novakovic, O. Frey, E. Verpoorte, Y.-C. Toh, A guide to the organ-on-a-chip. *Nature Reviews Methods Primers*, 2022. 2(1): p. 33.
231. Bittermann, K., L. Linden, K.-U. Goss, Screening tools for the bioconcentration potential of monovalent organic ions in fish. *Environmental Science: Processes & Impacts*, 2018. 20(5): p. 845-853.
232. Henneberger, L., N. Klüver, M. Mühlenbrink, B. Escher, Trout and Human Plasma Protein Binding of Selected Pharmaceuticals Informs the Fish Plasma Model. *Environmental Toxicology and Chemistry*, 2022. 41(3): p. 559-568.
233. Lowry, O., N. Rosebrough, A.L. Farr, R. Randall, Protein measurement with the folin phenol reagent. *Journal of Biological Chemistry*, 1951. 193(1): p. 265-275.
234. Smedes, F., Determination of total lipid using non-chlorinated solvents. *Analyst*, 1999. 124(11): p. 1711-1718.
235. Frings, C.S., R.T. Dunn, A Colorimetric Method for Determination of Total Serum Lipids Based on the Sulfo-phospho-vanillin Reaction. *American Journal of Clinical Pathology*, 1970. 53(1): p. 89-91.
236. Armitage, J.M., F. Wania, J.A. Arnot, Application of Mass Balance Models and the Chemical Activity Concept To Facilitate the Use of in Vitro Toxicity Data for Risk Assessment. *Environmental Science & Technology*, 2014. 48(16): p. 9770-9779.
237. Ali, R., S. Trump, I. Lehmann, T. Hanke, Live cell imaging of the intracellular compartmentalization of the contaminate benzo[a]pyrene. *Journal of Biophotonics*, 2015. 8(5): p. 361-371.
238. Johnson, S.M., N. Buttress, The osmotic insensitivity of sonicated liposomes and the density of phospholipid-cholesterol mixtures. *Biochimica et Biophysica Acta (BBA) - Biomembranes*, 1973. 307(1): p. 20-26.
239. Haynes, W.M., *CRC Handbook of Chemistry and Physics*. 2014, Boca Raton: CRC Press.

240. Abraham, M.H., W.E. Acree, Jr., Equations for the Transfer of Neutral Molecules and Ionic Species from Water to Organic phases. *The Journal of Organic Chemistry*, 2010. 75(4): p. 1006-1015.
241. Abraham, M.H., The Permeation of Neutral Molecules, Ions, and Ionic Species Through Membranes: Brain Permeation as an Example. *Journal of Pharmaceutical Sciences*, 2011. 100(5): p. 1690-1701.
242. Willis, J.V., M.J. Kendall, R.M. Flinn, D.P. Thornhill, P.G. Welling, The pharmacokinetics of diclofenac sodium following intravenous and oral administration. *European Journal of Clinical Pharmacology*, 1979. 16(6): p. 405-410.
243. Meredith, C.G., C.D. Christian Jr, R.F. Johnson, S.V. Madhavan, S. Schenker, Diphenhydramine disposition in chronic liver disease. *Clinical Pharmacology & Therapeutics*, 1984. 35(4): p. 474-479.
244. Martin, W., G. Koselowske, H. Töberich, T. Kerkmann, B. Mangold, J. Augustin, Pharmacokinetics and absolute bioavailability of ibuprofen after oral administration of ibuprofen lysine in man. *Biopharmaceutics & Drug Disposition*, 1990. 11(3): p. 265-278.
245. Nallani, G.C., P.M. Paulos, L.A. Constantine, B.J. Venables, D.B. Huggett, Bioconcentration of ibuprofen in fathead minnow (*Pimephales promelas*) and channel catfish (*Ictalurus punctatus*). *Chemosphere*, 2011. 84(10): p. 1371-1377.
246. Thompson, J., M. Lorber, L.-M.L. Toms, K. Kato, A.M. Calafat, J.F. Mueller, Use of simple pharmacokinetic modeling to characterize exposure of Australians to perfluorooctanoic acid and perfluorooctane sulfonic acid. *Environment International*, 2010. 36(4): p. 390-397.
247. Harris, D.S., H. Boxenbaum, E.T. Everhart, G. Sequeira, J.E. Mendelson, R.T. Jones, The bioavailability of intranasal and smoked methamphetamine. *Clinical pharmacology and therapeutics*, 2003. 74(5): p. 475-486.
248. Sancho Santos, M.E., K. Grabicová, C. Steinbach, H. Schmidt-Posthaus, E. Šálková, J. Kolářová, A. Vojs Staňová, R. Grabic, T. Randák, Environmental concentration of methamphetamine induces pathological changes in brown trout (*Salmo trutta fario*). *Chemosphere*, 2020. 254: p. 126882.
249. Patat, A., S. Troy, J. Burke, S. Trocherie, P. Danjou, F. Le Coz, H. Allain, J.M. Gandon, Absolute bioavailability and electroencephalographic effects of conventional and extended-release formulations of venlafaxine in healthy subjects. *Journal of clinical pharmacology*, 1998. 38(3): p. 256-267.
250. Grabicova, K., R.H. Lindberg, M. Östman, R. Grabic, T. Randak, D.G. Joakim Larsson, J. Fick, Tissue-specific bioconcentration of antidepressants in fish exposed to effluent from a municipal sewage treatment plant. *Science of The Total Environment*, 2014. 488-489: p. 46-50.
251. Mason, W.D., N. Winer, G. Kochak, I. Cohen, R. Bell, Kinetics and absolute bioavailability of atenolol. *Clinical Pharmacology & Therapeutics*, 1979. 25(4): p. 408-415.
252. Steinbach, C., V. Burkina, G. Fedorova, K. Grabicova, A. Stara, J. Velisek, V. Zlabek, H. Schmidt-Posthaus, R. Grabic, H. Kocour Kroupova, The sub-lethal effects and tissue concentration of the human pharmaceutical atenolol in rainbow trout (*Oncorhynchus mykiss*). *Science of The Total Environment*, 2014. 497-498: p. 209-218.

- 
253. Marino, S.E., A.K. Birnbaum, I.E. Leppik, J.M. Conway, L.C. Musib, R.C. Brundage, R.E. Ramsay, P.B. Pennell, J.R. White, C.R. Gross, J.O. Rarick, U. Mishra, J.C. Cloyd, Steady-State Carbamazepine Pharmacokinetics Following Oral and Stable-Labeled Intravenous Administration in Epilepsy Patients: Effects of Race and Sex. *Clinical Pharmacology & Therapeutics*, 2012. 91(3): p. 483-488.
  254. Garcia, S.N., M. Foster, L.A. Constantine, D.B. Huggett, Field and laboratory fish tissue accumulation of the anti-convulsant drug carbamazepine. *Ecotoxicology and Environmental Safety*, 2012. 84: p. 207-211.
  255. Geyer, H.J., I. Scheunert, F. Korte, Distribution and bioconcentration potential of the environmental chemical pentachlorophenol (PCP) in different tissues of humans. *Chemosphere*, 1987. 16(4): p. 887-899.
  256. Nichols, J.W., J.M. McKim, G.J. Lien, A.D. Hoffman, S.L. Bertelsen, C.A. Gallinat, Physiologically-based toxicokinetic modeling of three waterborne chloroethanes in channel catfish, *Ictalurus punctatus*. *Aquatic Toxicology*, 1993. 27(1): p. 83-111.
  257. Endo, S., T.N. Brown, K.-U. Goss, General Model for Estimating Partition Coefficients to Organisms and Their Tissues Using the Biological Compositions and Polyparameter Linear Free Energy Relationships. *Environmental Science & Technology*, 2013. 47(12): p. 6630-6639.

---

## Glossary

AB	Alamar Blue
ABC	transporter ATP binding-cassette transporter
BCF	Bioconcentration factor
$BCF_{bulk}$	predicted BCF based on total medium concentration
$BCF_{DMLW}$	$D_{MLW}$ based BCF prediction
$BCF_{cell\ model}$	predicted BCF by kinetic cell model
$BCF_{C_{free}}$	predicted BCF based on bioavailable medium concentration $C_{free}$
$BCF_{V_{D}^{fish\ or\ human}}$	$V_D$ based BCF prediction using fish or human $V_D$
BHPP	Benzotriazol-tert-butyl hydroxyl-phenyl propanoic acid
BMF	Biomagnification factor
CFDA	5-carboxyfluorescein diacetate acetoxy methyl ester
$C_{free}$	freely dissolved aqueous concentration
DCF	Diclofenac
$D_{MLW}$	pH-dependent membrane lipid water partition coefficient
$D_{OW}$	pH-dependent octanol-water partition coefficient
$D_{PW}$	Protein-water partition coefficient
EC <sub>50</sub> 50 %	effective concentration affecting cells
EDTA	ethylenediaminetetraacetic acid
EtFOSA	N-Ethylperfluorooctane sulfonamide
EtFOSAA	N-Ethylperfluorooctanesulfonamide acetic acid
EtFOSE	N-Ethyl-N-(2-hydroxyethyl) perfluorooctylsulphonamide
FBS	Fetal Bovine Serum
FOSA	Perfluorooctanesulfonamide
HPLC	HRMS/MS High pressure liquid chromatography high resolution tandem mass spectrometry

---

<i>in vitro</i> BCF	cell-based BCF
<i>in vivo</i> BCF	BCF in fish
IOC	ionizable organic compound
IVIVE	In vitro-In vivo extrapolation
K <sub>BW</sub>	blood-water partition coefficient
K <sub>MLWi</sub>	membrane lipid-water partition coefficient of the charged compound species
K <sub>MLWn</sub>	membrane lipid-water partition coefficient of the neutral compound species
K <sub>OW</sub>	Octanol-water partition coefficient
K <sub>PWi</sub>	protein-water partition coefficient of the charged compound species
K <sub>PWn</sub>	protein-water partition coefficient of the neutral compound species
LC <sub>50</sub>	Lethal concentration killing 50 % of exposed fish
NR	Neutral Red
OECD	Organisation for Economic Co-operation and Development
PCP	Pentachlorophenol
PFAS	Perfluoroalkyl substances
PFOA	Perfluorooctanoic acid
PFOS	Perfluorooctanesulfonic acid
pK <sub>a</sub>	acid dissociation constant
PBTK	physiology-based toxicokinetic
PP-LFER	poly parameter-linear free energy relationship
Q14	N,N,N-trimethyltetradecylamine
REACH	Registration, Evaluation, Authorization and Restriction of Chemicals
SPME	Solid-phase microextraction
S12	N-methyldodecylamine
TG	Test Guideline

---

TT	Tecloftalam
T10	N,N-dimethyldecylamine
$V_D$	Volume of distribution
$\alpha_n$	fraction of neutral compound species
$\alpha_i$	fraction of charged compound species
$F_{w.cell}$	substance fraction in the water phase of the cell
$f_P$	protein volume fraction
$f_{PL}$	phospholipid volume fraction
$f_w$	water volume fraction
S	Sensitivity
O	<i>Output</i>
I	<i>Input</i>
$\gamma_{medium\ or\ cell.i}$	activity coefficient of the charged compound in the medium or cell
$\gamma_{medium\ or\ cell.n}$	activity coefficient of the neutral compound in the medium or cell



---

## Curriculum Vitae

### Personal information

<b>Name</b>	Fabian Balk
<b>Address</b>	Schuppisstrasse 2, 8057 Zürich
<b>Date of Birth</b>	09.12.1991
<b>Place of Birth</b>	Munich, Germany
<b>Nationality</b>	German
<b>Email</b>	fabian.balk@eawag.ch

### Education

2019-2023	<b>PhD Candidate, Eawag, Dübendorf and EPF, Lausanne</b> Thesis “The Bioaccumulation of ionizable organic compounds in fish cell lines” Focus areas: Cell biology, Computer-based Modelling, Chemical Analysis, Teaching in Ecotoxicology Courses at EPFL and ETHZ Supervision: Kristin Schirmer, Juliane Hollender
2016-2018	<b>Master of Science Environmental Science, Stockholm University, Sweden</b> Specialization: Environmental Chemistry Master thesis: Children’s exposure to perfluoroalkyl acids – a modelling approach Supervision: Kerstin Pütz, Anton Ribbenstedt, Ian Cousins Grade: A (Excellent) Overall grade: Very good
2012-2015	<b>Bachelor of Science Biology, RWTH Aachen University, Germany</b> Specialization: Environmental Sciences Bachelor Thesis: Agonistic and antagonistic steroidal activity of surface water fractions using reporter gene cell-based bioassays Supervision: Carolina di Paolo, Thomas Seiler Grade: 1,0 Overall grade: 1,6
2011	<b>Abitur, Gymnasium Lüneburger Heide, Melbeck</b> Overall grade: 1,6

## Experience

- Sep 2021-  
Apr2022 **Supervision of master thesis**  
Practical training of student (cell-based assays, chemical analysis),  
experimental planning
- Feb 2021 **Organization and Coordination of the YES2021 conference (SETAC)**  
Organization of online platform & workshops, sponsor recruiting & fund  
applications, member of scientific committee and session chair
- 2019-2022 **Teaching in Student courses at EPFL and ETHZ**  
Introduction to mixture toxicity concepts, supervision and correction of student  
exercises
- Nov-Jan  
2018 **Internship at NIRAS Sweden AB, Stockholm**  
Literature review on aerobic degradation of fluorinated substances in  
environmental matrices, visualization of degradation pathways  
Supervision: Marko Filipovic
- Mar-Jul 2016 **Internship at the Netherlands Institute of Ecology (NIOO-KNAW)**  
Experimental work on stoichiometric ecology, GC-MS analyses,  
cyanobacteria and green algae cultivation  
Supervision: Lisette de Senerpont Domis
- Sep 2013 **Entomological internship at Wageningen University and Research Centre**  
Project on Insects as potential food source for humans, experimentation with  
*Locusta migratoria*  
Supervision: Dennis Oonincx

## Honors

- Nov 2019 **Selection as HOT article in Environmental Science: Processes & Impacts**  
Article "Children's exposure to perfluoroalkyl acids – a modelling approach"  
selected as one of the top 10% of relevant papers published in Environmental  
Science: Processes & Impacts in 2019
- Jan 2016 **Dean's List entry for excellent results**  
In recognition of outstanding academic achievement as one among the best 5  
percent of the graduate students in Bachelor of Science Biology at the RWTH  
in 2014/2015

## Scientific Publications

F. Balk; B. Hüsser, J. Hollender; K. Schirmer, Bioaccumulation of cationic surfactants in permanent fish cell lines. Environmental Science & Technology 2023, (submitted).

F. Balk, J. Hollender and K. Schirmer, Investigating the bioaccumulation potential of anionic organic compounds using a permanent rainbow trout liver cell line, Environment International, 2023, DOI:10.1016/j.envint.2023.107798

F. Balk, K. W. Pütz, A. Ribbenstedt, M. I. Gomis, M. Filipovic and I. T. Cousins, Children's exposure to perfluoroalkyl acids—a modelling approach, Environmental Science: Processes & Impacts, 2019, DOI:10.1039/C9EM00323A, 21, 1875-1886

C. Di Paolo, K. Kirchner, F. Balk, M. Muschket, W. Brack, H. Hollert and T.-B. Seiler, Downscaling procedures reduce chemical use in androgen receptor reporter gene assay, Science of The Total Environment, 2016, DOI:10.1016/j.scitotenv.2016.07.059, 571, 826-833

## Scientific Contributions

April 2023	<b>Invited speaker at several PBT-Expert Meetings of the European</b>
May 2022	<b>Chemicals Agency ECHA</b> (PBT = Persistent, Bioaccumulative, Toxic)
Sep 2020	Presented on the accumulation of ionizable organic compounds in fish cell lines
May 2022	<b>Platform Presentation at the SETAC Europe 32nd Annual Meeting (first author)</b>
	Title: Anionic and Cationic Organic Compounds Show Distinct Bioaccumulation in Rainbow Trout Cell Cultures
Aug/Sep 2021	<b>Platform Presentation at the World Congress on Alternatives and Animal Use in the Life Sciences 2021 (first author)</b>
	Title: The Biotransformation and Bioaccumulation of Ionizable Organic Compounds in Rainbow Trout Cell Lines
May 2019	<b>Poster at the SETAC 29th Annual Meeting (first author)</b>
	Title: Understanding children's exposure to perfluoroalkyl acids - a modelling approach
Feb 2017	<b>Poster at the SETAC Young Environmental Scientists Meeting (first author)</b>
	Title: Perfluoroalkyl acids in Stockholm sediments

## Languages

German	Native
English	Full working proficiency
Dutch	Fluent
Swedish	Elementary proficiency
French	Elementary proficiency